

Model Uncertainty and Performance Analysis for Precision Controlled Space Structures

by

Frederic Bourgault

B.Eng., Mechanical Engineering (Aeronautics)
Ecole Polytechnique de Montreal, 1996

SUBMITTED TO THE DEPARTMENT OF AERONAUTICS AND ASTRONAUTICS
IN PARTIAL FULFILLMENT OF THE DEGREE OF

MASTER OF SCIENCE

at the

MASSACHUSETTS INSTITUTE OF TECHNOLOGY

May 2000

© 2000 Massachusetts Institute of Technology
All rights reserved

Signature of Author

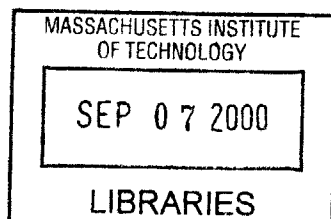
Department of Aeronautics and Astronautics
May 24, 2000

Certified by

Professor David W. Miller
Thesis Supervisor

Accepted by

Professor Nesbitt W. Hagood
Chairman, Department Graduate Committee





Room 14-0551
77 Massachusetts Avenue
Cambridge, MA 02139
Ph: 617.253.2800
Email: docs@mit.edu
<http://libraries.mit.edu/docs>

DISCLAIMER

MISSING PAGE(S)

Chapter 8 (pages 181-184) has been omitted from both the Library, and Archives copy due to pagination error. The "Conclusions" section is included in Chapter 7.

ABSTRACT

The purpose of this thesis is to provide confidence for the designer that a concept of a future space-based telescope will meet its very stringent requirements. More specifically, our goal is to predict the amount of uncertainty in the performance prediction made through out the design process. Also, given a statistical database for structural uncertainty, the methodology presented will establish the probability of success of a particular architecture.

The traditional design process starts by evaluating and comparing the performance of different concepts by using simplified structural and disturbance models. As the process progresses the different solutions are evaluated and the most promising concept is retained and refined. Eventually, some preliminary structural testing is performed, and the model is updated to reflect the reality more accurately. Eventually, when the production of the system is nearly complete, the model performance predictions should converge to the actual system performance.

Large flexible space structures present a problem in using this approach because they are often too flexible to support their own weight and/or too large to fit inside any laboratory facilities to be tested fully assembled. For example, it would be impractical to test the whole assembly of the International Space Station or SIM on the ground. Also, during the preliminary design phase, no test data are available to update the models. Even when the model is very mature and has been updated after experimental testing, a discrepancy remains between the predicted and actual performance of the system. These uncertainties are due to various sources of variability in the system: variable noises (sources and levels), testing conditions and environmental factors, assembly/reassembly, shipset, disturbance levels, and others. How then, can we have confidence that a particular concept will meet the requirements if the only tool we have are finite element models that may not be accurate? The solution is to try to estimate the range of uncertainty around our nominal model performances. Since in the early design phase no test data are available, our best bet will

ABSTRACT

be to use past experience to predict the expected uncertainty range on the performances of our new design. Statistical uncertainty for the modal mass and stiffness parameters, [Hasselman & Chrostowski, 1991], as well as for the modal damping ratios [Simonian, 1987], can be obtained.

ACKNOWLEDGEMENTS

Funding for this research was provided by the Jet Propulsion Laboratory under JPL contract #961123 (Modeling and Optimization of Dynamics and Control for the NASA Space Interferometry Mission and the Micro-Precision Interferometer Testbed), with Dr. Robert Laskin as Technical/Scientific Officer, Dr. Sanjay Joshi as Contract Monitor, and Ms. SharonLeah Brown as MIT Technical Officer. Professor David Miller from the MIT Space Systems Laboratory supervised the research described in this report. Further financial support was provided in the form of a fellowship from le Fonds pour la Formation de Chercheurs et l'Aide a la Recherche (Government of Quebec).

I am indebted to Dr. Homero Gutierrez for his great support and guidance, and whose work formed the foundation on which the research presented in this document was built upon. I wish to thank Dr. Gregory Mallory and Olivier de Weck for their support and advice, which was always useful and greatly appreciated. Special thanks also goes to Brett DeBlonk, Michel Ingham, Alice Liu and Alexei Makarenko for their time commitment in proof-reading this document, and whose help and comments were also greatly appreciated.

ACKNOWLEDGEMENTS

Abstract	3
Acknowledgements	5
List of Figures	11
List of Tables	13
Nomenclature	15
Chapter 1. Introduction	19
1.1 Background	19
1.2 Thesis Research Objectives	21
1.3 Uncertainty Analysis and the DOCS-Framework	23
1.4 Definitions, Literature Review and Previous Work	25
1.4.1 What is Uncertainty?	25
1.4.2 Sources of Uncertainty	26
1.4.3 Lessons from the MACE Program	28
1.5 Thesis Overview and Contributions	29
Chapter 2. Integrated Modeling and Performance Evaluation	33
2.1 Integrated Modeling Description	33
2.1.1 Structural Dynamics Modeling	34
2.1.2 Control Modeling	40
2.1.3 Dynamic Disturbance Modeling	42
2.2 Initial Performance Assessment	45
2.2.1 Performance Modeling	46
2.2.2 Frequency-domain Analysis	46
2.2.3 Lyapunov Approach	48
2.3 Summary	50
Chapter 3. Mass, Stiffness and Damping Uncertainty	51
3.1 Mass and Stiffness Uncertainty	52
3.1.1 Methodology	52
3.1.2 Database	61
3.2 Damping Estimation and Uncertainty	71
3.2.1 Damping Modeling Problem	71
3.2.2 Sources of Damping Uncertainty	73

3.2.3 Damping Uncertainty Estimation	74
3.2.4 Database	81
3.3 Summary	85
Chapter 4. Sensitivity Analysis	87
4.1 First Order Derivatives (Sensitivities)	87
4.1.1 Eigenderivatives	88
4.1.2 Frequency Response Function Derivative	99
4.1.3 Performance RMS Derivative	108
4.2 Second Order Derivatives (curvatures)	111
4.2.1 FRF Second Order Derivative	113
4.2.2 RMS Second Order Derivative	114
4.3 Summary	118
Chapter 5. Uncertainty Analysis	119
5.1 Current Design Practice	120
5.2 Monte Carlo Simulation	122
5.3 Linear Approximation Method	122
5.4 Linear Covariance Propagation	123
5.4.1 Database Scaling	124
5.4.2 Covariance Propagation	125
5.5 Vertex Method	129
5.5.1 Corner Search	129
5.5.2 Included Maxima and Minima	133
5.6 Hybrid Method for the FRF Bounds	134
5.7 Monte Carlo Simulation	135
5.8 Constrained Optimization	135
Chapter 6. Sample Problem	137
6.1 Model Description	138
6.1.1 Physical Description	138
6.1.2 Modeling	141
6.2 Initial Performance Evaluation	143
6.2.1 Frequency Response Function (FRF)	144
6.2.2 Nominal Performance RMS	146
6.3 Database Generation	149

6.3.1	Structural Database	149
6.3.2	Damping Database	152
6.4	Sensitivity Analysis	152
6.4.1	Performance RMS Sensitivity	153
6.4.2	FRF Sensitivity	157
6.5	Uncertainty Analysis	159
6.5.1	Performance RMS Uncertainty	159
6.5.2	FRF Uncertainty	166
6.6	Summary	166
Chapter 7.	Applications	167
7.1	Challenges of large order models	167
7.1.1	Database size	167
7.1.2	Numerical conditioning issues	169
7.2	Origins Program: NGST/SIM Description	169
7.2.1	SIM	178
7.2.2	NGST	179
7.2.3	Modes of Operations	180
7.2.4	FEM	180
7.2.5	Control	180
7.2.6	Disturbances	180
7.3	Initial Performance Assessment for NGST/SIM	180
7.3.1	Frequency-domain	180
7.3.2	Lyapunov	180
7.4	Uncertainty Assessment	180
7.4.1	Frequency-domain (Hybrid)	180
7.4.2	Lyapunov	180
7.4.3	Optimization	180
7.4.4	Interpretation	180
Chapter 8.	Conclusions	181
8.1	Thesis Summary and Contributions	181
8.2	Conclusions for NGST/SIM	181
8.3	Recommendations for Future Work	181
8.4	Uncertainty Management in Flight Programs	181
References		185

Appendix A. Some Probability and Random Variables Fundamentals	193
A.1 Probability for continuous Random Variables	193
A.2 Probability Density Function (PDF)	200
A.2.1 Uniform Probability Density Function	200
A.2.2 Gaussian Probability Density Function	201
A.2.3 Lognormal Probability Density Function	205
A.3 Random Processes	206
Appendix B. Hasselman's databases	209
B.1 LSS database (research models)	210
B.2 CSS database (for pretest and posttest models)	212
B.2.1 Pretest Models Database (CSS I)	213
B.2.2 Posttest Models Database (CSS II)	215
B.3 Combined LSS and CSS Database (COMB)	217
B.4 Database comparison	219
Appendix C. Simonian's Damping Compilation	221
Appendix D. Chain Rules	223
D.1 Derivatives and Differentials of Composite Functions	223
D.2 The General Chain Rule	227
Appendix E. Integral of Transfer functions	233

LIST OF FIGURES

Figure 1.1	Sources of Modeling Uncertainty	27
Figure 1.2	Physical Sources of Uncertainty	27
Figure 1.3	Example of MACE shipset variation	29
Figure 1.4	Thesis Flow: Integral Performance Assessment for Spaceborne Telescope . 31	
Figure 2.1	Open-loop plant block diagram	39
Figure 2.2	Controller block diagram	40
Figure 2.3	Closed-loop plant	41
Figure 2.4	General plant model	42
Figure 2.5	Disturbances filter block diagram	43
Figure 2.6	Disturbance model and general plant model	44
Figure 2.7	Integrated plant model	45
Figure 5.1	Example of uncertainty bounds for different designs.	121
Figure 5.2	Gaussian distribution of the output parameter u	126
Figure 5.3	Distribution of the performance RMS (left), and the corresponding probabilit- ity of success (right)	127
Figure 5.4	Probability of failure	128
Figure 5.5	Two-dimensional corner space	129
Figure 5.6	Uniform 2-D search grid	134
Figure 6.1	Two degree of freedom oscillator	138
Figure 6.2	Distribution for M and K	140
Figure 6.3	Distributions for the damping ratios: Lognormal PDF for the 's (left), and corresponding Gaussian PDF for the 's(right)	141
Figure 6.4	2-DOF oscillator Frequency Response Function.	145
Figure 6.5	2-DOF oscillator cumulative RMS plot (top), and PSD plot (bottom) .	148
Figure 6.6	Covariance matrix estimation error vs. standard derivative multiplicative factor. 151	
Figure 6.7	Frequency response derivatives (1st and 2nd order) evaluated at . . .	158
Figure 6.8	Histograms of the sampled physical mass (left) and stiffness (right) ele- ments distributions compared with their theoretical Gaussian PDF's. .	162

Figure 6.9	Histogram of the "sampled" transformed modal damping parameters compared with their theoretical Gaussian PDF's.	162
Figure 6.10	Histogram of the performance RMS distribution (w/ analytical curve) from the Monte Carlo simulation	162
Figure 6.11	163
Figure A.1	Uniform Probability Density Function	200
Figure A.2	Normal Probability Density Function	202
Figure A.3	Lognormal Probability Density Function	206

LIST OF TABLES

TABLE 3.1	Damping Enhancement Devices	74
TABLE 3.2	Sources of damping uncertainty in damping estimate	75
TABLE 3.3	Extracted Damping Statistics	83
TABLE 6.1	Nominal Structural Element and their Uncertainty	142
TABLE 6.2	Maximum allowable perturbation size	157
TABLE 6.3	Frequency range of validity of the linear approxi.	158
TABLE 6.4	RMS Uncertainty Analysis Results	165
TABLE A.1	CDF for the unit normal PDF	203
TABLE B.1	Structures in LSS Database.	210
TABLE B.2	Structures in CSS Database.	213
TABLE B.3	Eigenvalues of Covariance Matrices.	220
TABLE C.1	Satellites Surveyed	221
TABLE C.2	Summary of Spacecraft Measured Damping Statistics	222

NOMENCLATURE

Abbreviations

<i>BS</i>	beam shear
<i>COMB</i>	combined structures
<i>CSS</i>	conventional space structure
<i>CSS-I</i>	conventional space structure (pretest models)
<i>CSS-II</i>	conventional space structure (posttest models)
<i>dB</i>	decibel
<i>DOF</i>	degree of freedom
<i>DPL</i>	differential pathlength
<i>FEM</i>	finite element method
<i>FFT</i>	fast Fourier transform
<i>FRF</i>	frequency response function, or transfer function
<i>H.O.T.</i>	higher order terms
<i>HST</i>	Hubble Space Telescope
<i>Hz</i>	Hertz (sec^{-1})
<i>i/o</i>	input/output
<i>JPL</i>	Jet Propulsion Laboratory
<i>LOS</i>	line of sight
<i>LSS</i>	large space structure
<i>LTI</i>	linear time-invariant
<i>MIMO</i>	multiple-input multiple-output
<i>NGST</i>	Next Generation Space Telescope
<i>ODL</i>	optical delay line
<i>RMS</i>	root mean square
<i>RWA</i>	reaction wheel assembly
<i>SIM</i>	Space Interferometer Mission
<i>SISO</i>	single-input single-output
<i>SRTM</i>	Shuttle Radar Topography Mission
<i>ST</i>	star tracker
<i>SVD</i>	singular value decomposition
<i>s.v.</i>	singular value
<i>VC</i>	voice coil
<i>WFT</i>	wave front tilt

Symbols

A_c	compensator dynamics matrix
-------	-----------------------------

A_d	disturbance filter dynamics matrix
A_{zd}	augmented disturbance/plant/control dynamics matrix
B_c	compensator input matrix
B_d	disturbance filter input matrix
B_u	plant control input matrix
B_w	plant disturbance input matrix
B_{zd}	augmented disturbance/plant/control input matrix
C_c	compensator output matrix
C_d	disturbance filter output matrix
C_{yx}	plant sensor output matrix
C_{zd}	augmented disturbance/plant/control output matrix
C_{zx}	plant performance output matrix
D_c	compensator feedthrough matrix
D_d	disturbance filter feedthrough matrix
D_{zd}	augmented disturbance/plant/control feedthrough matrix
G	transfer function
K	stiffness matrix of the true (actual) system
L	global Lagrange multiplier
M	mass matrix of the true (actual) system
N	
R	
S	intensity
d	
e	
j	$\sqrt{-1}$
k	
m	
n	
p	vector of modal parameters (modal mass, stiffness, damping)
q	
u	controller inputs
w	disturbance inputs
x	physical generalized coordinates (positions and angles)
y	sensor measurement
z	performance outputs
Δ	change in quantity
Ξ	
Σ	covariance matrix
Φ	mode shape matrix
Ψ	
Ω	modal frequency matrix
α	coefficient in definition of proportional damping
β	coefficient in definition of proportional damping
β_u	plant control influence matrix
β_w	plant disturbance influence matrix

η	modal coordinate vector
λ	eigenvalue
ρ	
σ	standard deviation; ??
ζ	modal damping ratio
ϕ	mode shape vector
ψ	
ω	natural frequency

Subscripts and Superscripts

$(\cdot)_i$	i^{th} entry of a vector
$(\cdot)_{i,j}, (\cdot)_{ij}$	(i, j) entry of a matrix
$(\cdot)^L$	Lagrangian
$(\cdot)^T$	transpose
$\tilde{(\cdot)}$	nominal
$\hat{(\cdot)}$	frequency normalized
$^\circ(\cdot)$	mass normalized

Chapter 1

INTRODUCTION

1.1 Background

The National Aeronautics and Space Administration (NASA) is currently developing the next generation of space based observatories, which are poised to succeed the Hubble Space Telescope (HST) within a decade. They are expected to provide orders of magnitude improvement in angular resolution, spectral resolution and sensitivity. Figure 1 shows a representation of the Space Interferometry Mission (SIM), scheduled for launch in 2006, and the Next Generation Space Telescope (NGST) which is planned for 2009. Motivated by the work done in the past on Large Space Structures (LSS), such as the NASA Voyager spacecraft (1977) and Hubble Space Telescope (1990), the next generation of space-based observatories will require breakthrough technology and unprecedented control performance to meet the very stringent stability criterion required by their science instruments. Elements of the optical train on these large space telescopes will have to maintain relative stability to within a fraction of a wavelength of light [Joshi, 1999]. For example, SIM consists of a series of light collectors and other optical elements placed on top of a flexible light space structure of 10m span. Such a configuration will nearly approximate the light-gathering capability of a single continuous 10-m diameter telescope. Optical elements on the structure will have to maintain relative positions and orientations to within a few nanometers. For reference, 1 nanometer (10^{-9} meters) corresponds to about 15 hydrogen atoms¹ lined up side by side. Furthermore, such extreme requirements must be met despite

the presence of external and internal disturbances such as reaction wheel disturbances, solar pressure, thermally induced microdynamics (snaps or creaks), and other mechanical and electronic disturbance sources.

SIM-2006Faint Star Interferometer
Precision Astrometry**NGST-2009**Lightweight 8m-Optics
IR Deep Field Observations

Although the design process is an iterative procedure, critical design decisions must sometimes be made at an early stage. Typically, these early decisions are made based on simplified models and simulations. Before committing too many resources to a particular architecture, it is paramount to validate these models through integrated analysis. The performance assessment techniques of a system are mostly based on structural finite element modeling to which disturbance models and optical sensitivity matrices are appended [Gutierrez, 1999]. These techniques are not perfectly accurate. Modal frequency predictions can be 5 to 10 percent off when compared to the actual test data. This error is compounded by the fact that the available disturbance models are uncertain. The performance predictions yielded by current state-of-the-art modeling techniques are thus held in doubt. The central question addressed by this research is how to use preliminary design models, which we know are not very accurate, to build confidence that a given preliminary design will meet the stringent performance requirements. It is important to have a means to judge

1. Note: the radius of the hydrogen atom is 30 pm [DMK/DPK, 1984]

the size of the errors made by the model. This entails the evaluation of uncertainty bounds around the nominal performance prediction to make sure that the system will effectively meet the requirements. Furthermore, the controller must remain stable and still meet the requirements in the presence of the plant uncertainties.

1.2 Thesis Research Objectives

The fundamental objective of this research is to assess the amount of uncertainty in the performance predictions of the current state of the art modeling technology in order to reduce the level of risk and to assure suitable flight performance for space-based telescopes.

There are two compelling reasons for conducting an uncertainty analysis early in the design of a complex, integrated opto-mechanical system. The first reason is related to control design. Since it will not be possible to test the next generation of Large Space Structures (LSS) fully in the 0-g or microgravity operating environment, it will be necessary to design the operating software and the control systems based on 1-g component and scaled tests, and on full-scale modeling and simulation. The uncertainty of the structural behavior of the system needs to be taken into account. It is well known in the field of robust control design that there is an inherent trade-off between a controller's robustness to uncertainty and the achievable disturbance rejection or tracking capability. Thus, performing a rigorous uncertainty analysis on the system will provide the engineer useful uncertainty bounds for controller design. If uncertainty is overestimated, resulting controllers might not succeed in meeting the performance requirements. On the other hand, if the uncertainties are underestimated, what seems to be a good controller on paper might not satisfy the target performance or might even become unstable once implemented on the real structure [Joshi, 1999]. In applying multivariable robust control techniques to linear, time-invariant systems, a particular set of plant models described by a nominal model, uncertainty structure, and norm bounds on the model uncertainty and exogenous input is required a priori (for example, see the μ -Synthesis Toolbox in [Balas & al., 1994]). In typical setting, a

controls engineer selects or develops a best possible model either from first principles and/or from system identification or parameter estimation. In situations where the physical conditions are either not accurately known or not reliable, the engineer selects a model uncertainty structure around a best possible nominal model to represent a set of plant models so that the robustness of the system can be analyzed and optimized through feedback control, [Lim & Giesy, 2000]. Where measurements are available, the engineer can check to see if the given set of plants is consistent with the available measurement data. The lack of such measurements is the source of the performance prediction problem.

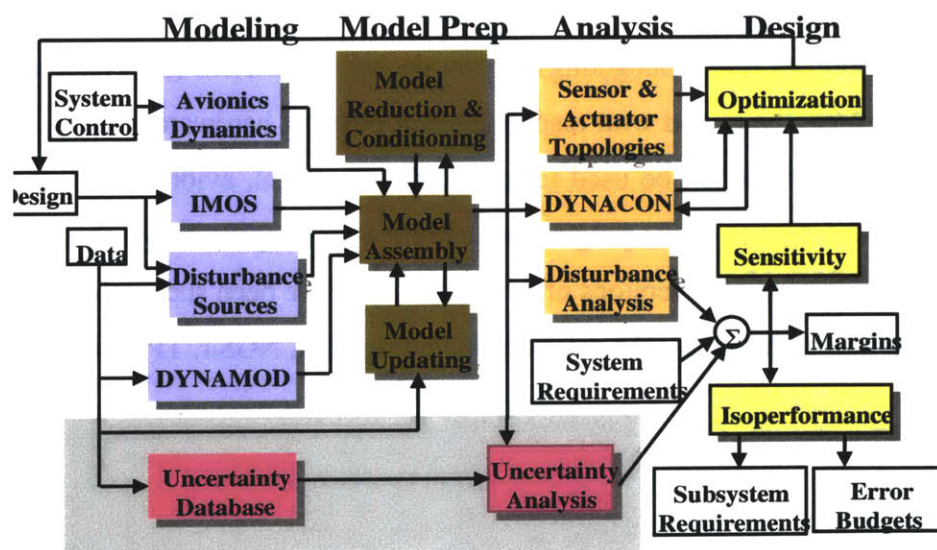
The second reason for conducting an uncertainty analysis is related to performance prediction. It is essential that not only the nominal dynamics and controls performance (e.g. RMS line-of-sight jitter) of the spacecraft be predicted, but that reasonable error bounds be placed on the nominal performance values. Alternatively the uncertainty analysis should provide the likelihood of achieving a required RMS performance, given an integrated model of the system and reasonable uncertainty bounds on the structural parameters. Performance predictions using integrated models (multidisciplinary) are somewhat uncertain due to modeling approximations and assumptions, components uncertainties, model reduction, and discretization. As a result, system designers tend to over-design system components to account for these uncertainties. Such overly conservative design decisions (e.g.: stiffer structure, less noisy sensors, smoother optical surfaces -- all more than necessary) lead to overly expensive systems [Joshi, 1999]. It is, therefore, necessary to have a method to predict the uncertainty bounds around the nominal performance predictions in order to assess the suitability of a particular system concept that will then meet the performance requirements.

The problem can be summarized as follows. Given a model of the plant $G(s)$, the controller $K(s)$ and an uncertainty database, we want to know if the system is stable, and is performing well within the required uncertainty bounds. Specifically, this thesis should answer the following questions:

1. What are the different methods for propagating uncertainty in the structural parameters of the system to the opto-mechanical performance metrics of interest?
2. How can mass, stiffness and uncertainty database information from previous ground- and test- flight experience be used and updated in the most effective way?
3. What is the probability (likelihood) that a system will meet the required performance (expressed as an RMS metric) level given uncertainty bounds?
4. How do the propagation methods used in 1) make the answers more or less conservative?
5. What are the key numerical and computational challenges in implementing a structural uncertainty algorithm for large order integrated models such as SIM or NGST?

1.3 Uncertainty Analysis and the DOCS-Framework

A Dynamics-Optics-Controls-Structures (DOCS) framework is being developed at the M.I.T. Space Systems Laboratory in support of integrated modeling and simulation of spaceborne telescopes during the conceptual and preliminary design phase. This subsection explains the main features of the DOCS framework and how the uncertainty analysis is embedded in it.



The DOCS (Dynamics-Optics-Controls-Structures) framework discussed here is a powerful framework for the modeling and analysis of precision opto-mechanical space systems. Within the MATLAB environment, an integrated model of the spacecraft can be created to simulate the dynamic behavior of the structure, the optical train, the control systems and the expected disturbance sources. The existing toolboxes are compatible with the existing programs IMOS (version 4.0), MSC/NASTRAN, DynaMod, and DynaCon. Once an initial model has been created and numerically conditioned, the root-mean-square (RMS) values of scientific and opto-mechanical performance metrics of the system (e.g. path length difference, pointing jitter, fringe visibility, null depth) can be predicted. The exact performance sensitivities of the RMS with respect to modal or physical design parameters can be computed. These sensitivities are essential for conducting gradient-based optimization, redesign or uncertainty analyses. The goal of the uncertainty analysis, the subject of this thesis, is to associate error bars with the predicted RMS performance based upon an uncertainty database resulting from past ground and flight experience. The gray shaded box (lower left corner) in the above figure corresponds to the modules of the DOCS framework that are related to uncertainty analysis. The actuator-sensor topology of the system can be analyzed numerically to ensure that the control system uses the actuator-sensor pairs that will, in turn, assure maximum disturbance rejection or tracking performance. Once a design has been found that meets all requirements with sufficient margins, an isoperformance analysis can be conducted. Treating the performance as a constraint, the expected error sources (error budgeting) or key design parameters (subsystems requirements definition) can be traded with respect to each other. If hardware exists, the experimental transfer functions can be used to update the structural, avionics and uncertainty models throughout the life of the program to achieve a convergent design that will render mission success. Preliminary versions of the framework have been successfully applied to conceptual designs of future NASA missions including SIM, NGST, TPF and Nexus.

1.4 Definitions, Literature Review and Previous Work

1.4.1 What is Uncertainty?

When a model is created, there will undoubtedly be errors between the model and the actual physical system. In the most general sense, a model uncertainty represents an unknown error in a model of a physical system. We broadly divide model uncertainty into parametric and non-parametric uncertainties. A parametric uncertainty is an uncertainty in a parameter used to generate the model. Either the parameter can appear explicitly in the state-space matrices, or the matrices can be implicit functions of the parameter. For example, a physical parameter such as a stiffness may not appear explicitly in the model state-space matrices; however, uncertainty in this parameter does have an effect on the modes and frequencies, which do appear in the matrices. Non-parametric uncertainty cannot be captured by an uncertainty in one or more parameters. For example, uncertainty in the model order implies that the number of states might be incorrect. This type of uncertainty can capture modeling errors such as modal truncation, lack of fidelity, and incorrect finite-element types. However, the form of this uncertainty is difficult to specify. The error of representing a nonlinear system with a linear model is another example of a non-parametric uncertainty.

The following definitions of uncertainty will be assumed in this thesis:

- **Nominal model** refers to the analytical model evaluated for the nominal values of its parameters. It will also be referred to as the **analytical model**.
- **Physical model** corresponds to the model obtained from the measurement of the actual structure. In the perturbation analysis, we will refer to it as the perturbed model. It will also be referred to indistinctly as the **actual, measurement, or test model**.
- **Performance uncertainty** is a measure of the variation of the actual performance about the predicted nominal performance point. For example, the nominal predicted RMS DPL (differential path length) of a system is 22.7 nm (+ 3.4 nm, - 2.8 nm). The +/- values are the uncertainty bounds on the nominal prediction.

- **Parametric Uncertainty** is the variation of model parameters about their nominal values. The parameters describe the physical plant, on-board and off-board disturbances, and the optics-controls design. The uncertain parameters appear explicitly in the state space matrices or in the mass, stiffness, damping or other system matrices. Examples include material and structural properties, dimensions, and harmonics of RWA disturbances.
- **Non-Parametric Uncertainty** is the variation of the assumed model from physical reality based on modeling assumptions which do not explicitly appear in any system matrices. Examples include missing poles, friction, slip, other non-linearities, insufficient model order, use of inappropriate finite element types.
- **Modeling Error** is the difference between the analytical model and the physical system in modal (w , z , m) parameters by variations in assumed physical parameters (E , r , n) or by non-linearities in the system. The modeling error is the mean of the stochastic errors.
- **Modeling Uncertainty** is the range of error differences across repeated experiments, or the variance of the stochastic errors.
- **Error Management** implies understanding the causes of errors as well as the resulting uncertainties to produce more accurate structural models and to derive realistic requirement bounds on spacecraft performance

The purpose of this thesis is to predict performance uncertainty based on assumptions and database information on parametric uncertainty.

1.4.2 Sources of Uncertainty

As illustrated in Figure 1.1, there are essentially three sources of uncertainty. The first type is related to mismodeling, where there is a discrepancy between the physical reality of the system and the virtual model used for control design and/or performance prediction. The second source of uncertainty is related to the evolution of the design. Design decisions for complex structures have to be made by several organizations in a short time frame and may not be communicated effectively. Thus, it is likely that not all versions of a model reflect the current design accurately. Finally, uncertainty arises from unknown environmental factors. The solar flux, for example, is often assumed to be a constant at 1400 W/m^2 at 1 AU. This value however is subject to the 11 year solar cycle and daily fluctuations, which can only be captured stochastically.

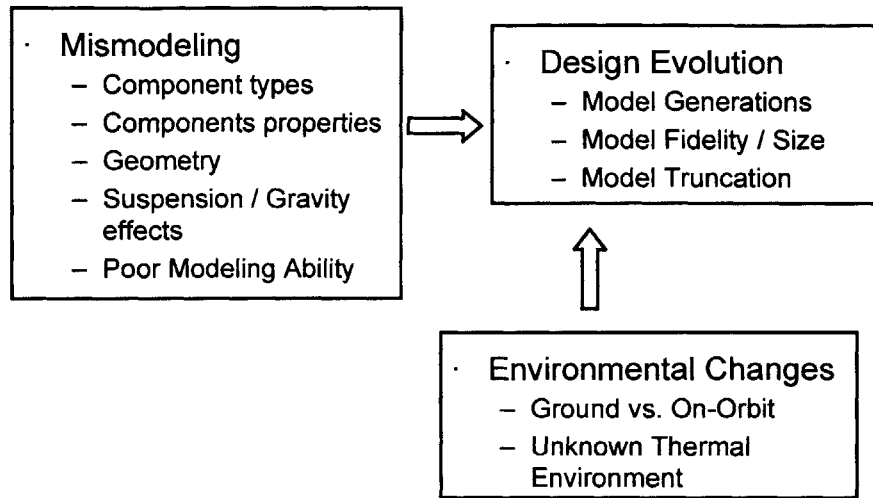


Figure 1.1 Sources of Modeling Uncertainty

Figure 1.2 shows the different physical sources of uncertainty that have to be taken into account.

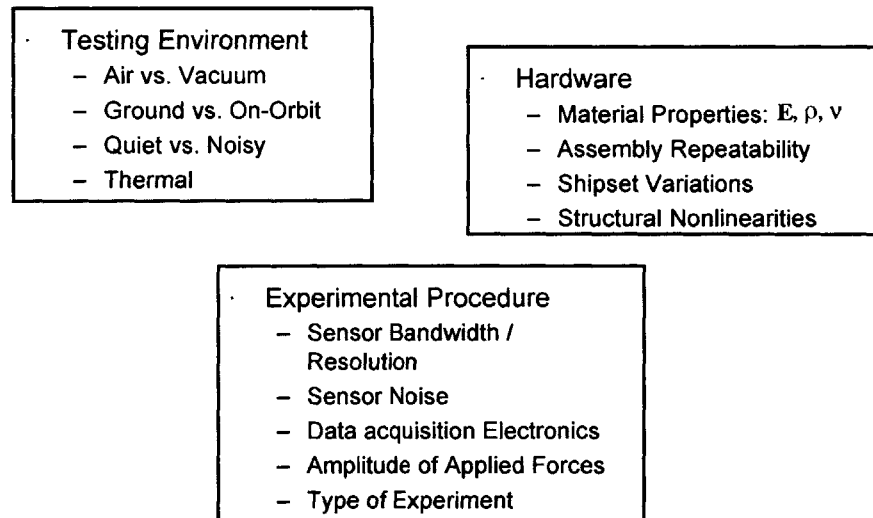


Figure 1.2 Physical Sources of Uncertainty

MIT has investigated a number model/data variations for ground and flight test programs. [Bourgault & Ubelhart, 1999]. These variations were found to be due to the following factors:

- **Hardware:** Manufacturing tolerances and material variations between supposedly identical components (shipset variations). Also, the residual stresses in a single piece of hardware can vary between seemingly identical assemblies.
- **Environment:** Variability in the environmental parameters accounts for variability in the hardware performance. For example, testing and validating a model on the ground (1-g environment) leads to error in predicting the 0-g behavior. In addition, damping is greatly affected by temperature.
- **Nonlinearities:** Small nonlinearities in a structure joints account for the damping sensitivity to the vibrations amplitude.
- **Testing Method:** Excitation amplitude, acquisition electronics, accuracy of the instruments used, and choice of sensor/actuator placement (controllability/observability) affect the accuracy of the results.
- **Model Generations:** Differences between 1st, 2nd, 3rd generation of model. An un-updated model contains larger errors than a model that has been updated after structural identification testing.

Figure 1.3 shows an example from MACE shipset variations.

1.4.3 Lessons from the MACE Program

The following remarks about uncertainty pertain to real life flight programs and are based on experiences from the MACE (Middeck Active Control Experiment -1995) program:

We cannot eliminate uncertainty (= risk) but can manage it by gradually reducing the size of the error bars.

A two pronged approach is recommended by reducing the sensitivity of the design to uncertainty and by reducing the parameter uncertainty space Δp . This can be seen by looking at the first order term of the a Taylor series expansion of the multivariable performance function:

$$\Delta\sigma_z = \frac{\partial\sigma_z}{\partial p_k}\Delta p_k$$

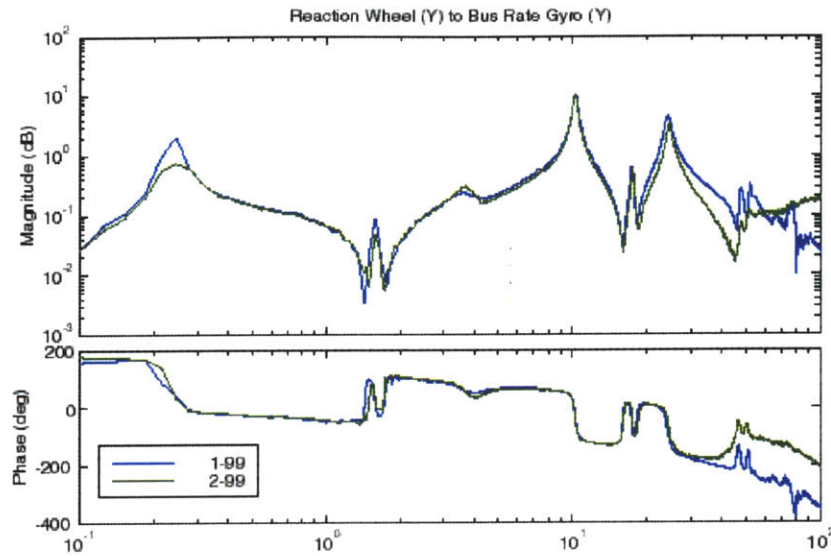


Figure 1.3 Example of MACE shipset variation

Redesign affects the nominal performance point, testing affects the size of the error bars

Uncertainty results from one phase of the program need to be passed on to the next phase (traceability, converging process). Only in this way will the design converge and a successful mission be achieved.

The design uncertainty is largest in the beginning and relates mainly to the hardware; later-on, uncertainty is reduced but the ability to change the design is reduced as well. On-orbit only software changes are possible (e.g. PID-gains).

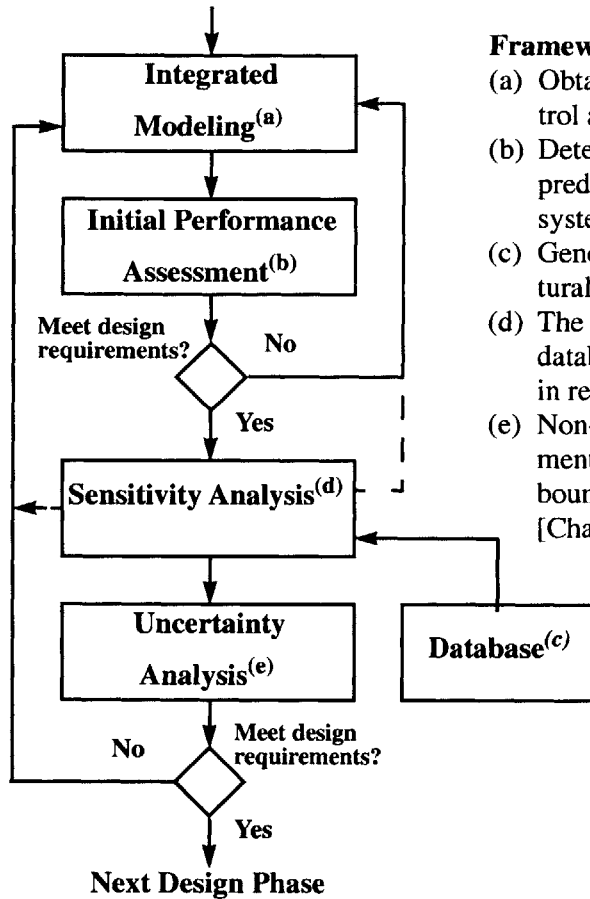
The “evening before launch” uncertainty remaining in the system should only be due to the magnitude of the external disturbances. Plant uncertainties should have been eliminated via rigorous testing/modeling.

1.5 Thesis Overview and Contributions

The organization of the chapters in this thesis, as it is summarized in Figure 1.4, goes as follows. First, in Chapter 2, we describe the integrated modeling framework [Gutierrez,

1999], the corresponding notation, and the non-deterministic performance prediction techniques used throughout this document. In Chapter 3, we describe how to generate a structural modal uncertainty database, as well as a damping uncertainty database. Then, the sensitivity expressions necessary to propagate the uncertainties through the model are derived in Chapter 4. The different uncertainty analysis techniques, described in Chapter 5, are demonstrated and validated on a 2-DOF sample problem in Chapter 6. The most promising techniques are then implemented on a space telescope model in Chapter 7 to assess the uncertainty in the performance predictions based on past experience. One very interesting result from this analysis is the error budget probability curve from which we can assess the risk and the suitability of a particular concept to meet the design requirements. Finally, the conclusions and a summary of the possible extensions of this research work is presented in Chapter 8.

Integral Analysis Framework



Framework Description:

- (a) Obtain a model integrating structure, control and disturbance models [Chapter 2].
- (b) Deterministic performance analysis to predict the nominal performance of the system (disturbance analysis) [Chapter 2].
- (c) Generation of database including structural and damping parameters [Chapter 3].
- (d) The sensitivities are used to propagate the database uncertainty [Chapter 4] and aid in redesign.
- (e) Non-deterministic performance assessment to determine statistical uncertainty bounds and worst-case performance [Chapter 5].

Demonstration/Validation of the Method:

- (f) Complete demonstration of the integral analysis framework on a sample problem [Chapter 6].
- (g) Implementation of the uncertainty analysis on the SIM Classic model to obtain uncertainty bounds, error budget probability curve, and worst-case performance [Chapter 7].
- (h) Conclusions on the analysis and future work description [Chapter 8].

Demonstration

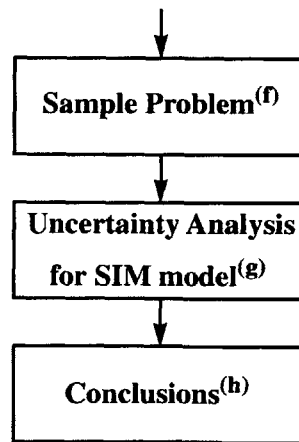


Figure 1.4 Thesis Flow: Integral Performance Assessment for Spaceborne Telescope

Chapter 2

INTEGRATED MODELING AND PERFORMANCE EVALUATION

The basics of a general integrated modeling technique for high precision space systems will be briefly presented in this chapter (Section 2.1). We will also present the tools needed for the initial performance assessment on such systems (Section 2.2). Although the contributions of this thesis are primarily related to the development and application of structural uncertainty analysis tools, it is important to understand the underlying assumptions of the model as well as the type of inputs and outputs. A more thorough discussion of these techniques is presented in [Gutierrez, 1999] from where we borrowed the modeling notation. Complete descriptions of the application of these techniques on large-scale systems can be found in [Gutierrez, 1999] for SIM, and in [de Weck, 1999] for NGST, as well as in Chapter 7 of this document, where we will perform the uncertainty analysis for these systems.

2.1 Integrated Modeling Description

Integrated modeling techniques play an essential role in evaluating potential concepts for the future generation of space-based telescopes. These techniques require modeling of every subsystem, including the structure, disturbances, optics and control, and their interactions in order to get to overall end-to-end system performances [Mosier & al., 1998].

2.1.1 Structural Dynamics Modeling

Numerous well developed commercially available software packages exist to perform structural modeling using the finite-element method (FEM). The level of fidelity, the type of elements used, and the discretization can greatly affect the accuracy of the FEM model and contribute to the overall system uncertainty. Also contributing to the uncertainty is the approximate specification of the damping ratios, which are typically specified after taking measurements on the structures, or estimated by the engineer based on experience, when no data is available. The reader is referred to [Meirovitch, 1986] for a thorough discussion on structural dynamics.

Equation of Motion

A linear time-invariant structural system can be discretized and represented by the following standard equation of motion in physical coordinates.

$$M\ddot{x} + C\dot{x} + Kx = \beta_u u(t) + \beta_w w(t) \quad (2.1)$$

where the vector x represents the generalized displacements (translations and/or rotations) in the physical coordinate space, M represents the global mass matrix, C is the equivalent viscous damping matrix, K is the stiffness matrix, β_u and β_w map the control inputs, u , and the disturbances, w , to the physical degrees of freedom. Note that M , C , and $K \in \mathfrak{R}^{n \times n}$, where n is the number of degrees of freedom.

Let us remark here that M and K are the actual “true”, but unknown, mass and stiffness matrices representing a discretization of the actual physical structure. The values of these matrices are subject of the arbitrary discretization done by the designer and constitute an approximation of the real mass and stiffness of the real continuous structure. One could imagine, though, that these two abstract mass and stiffness matrices are a representation that gives us the exact “true” natural frequencies and mode shapes (at least for the lower ones) of the real “actual” structure. For the purpose of this work, since the natural frequencies and the mode shapes obtained by analysis always differ slightly from the ones of the

physical system, we will make a distinction between the actual (exact, true, real) model of the structure and the analytical (nominal) model. The mass and stiffness matrices of the analytical (or nominal) model will be denoted by \tilde{M} and \tilde{K} . In this document, the tilde symbol ($\tilde{\cdot}$) will always be attributed to the nominal system.

The sensor and performance outputs, y and z are typically expressed as linear combinations, determined by the matrices C_{yx} and C_{zx} , of the physical degrees of freedom (displacements and rates).

$$\begin{aligned} y &= C_{yx}x \\ z &= C_{zx}x \end{aligned} \quad (2.2)$$

It is also possible to add the so called feedthrough D terms which directly “feed” the control input u and the disturbances w to the outputs, although these terms are typically zero for structural plants (output of an accelerometer is a notable exception).

Undamped Free-Vibration Equation

To find a solution to Eq. 2.1, we first consider the undamped homogeneous equations of motions:

$$M\ddot{x} + Kx = 0 \quad (2.3)$$

Eigenproblem

Then, the ensuing undamped eigenproblem enables us to obtain the mode shapes and natural frequencies

$$(K - \lambda_r M)\phi_r = 0 \quad (2.4)$$

where λ_r and ϕ_r are the r^{th} eigenvalue and eigenvector, respectively, corresponding to the r^{th} normal mode of the actual structure. The eigenproblem can also be written in matrix form as:

$$(K - \Lambda M)\Phi = 0 \quad (2.5)$$

where the eigenvector matrix Φ consists of the modes shapes ϕ_r , organized column-wise from $r = 1, 2, \dots, n$, and, the eigenvalue matrix Λ contains the squared natural frequencies on its main diagonal.

$$\Lambda = \begin{bmatrix} \ddots & & \\ & \lambda_r & \\ & & \ddots \end{bmatrix} = \begin{bmatrix} \ddots & & \\ & \omega_r^2 & \\ & & \ddots \end{bmatrix} = \Omega^2 \quad (2.6)$$

Orthogonality Principle

The diagonal modal mass matrix m is obtained by pre-multiplying M with the transpose of Φ and by post-multiplying with Φ .

$$\Phi^T M \Phi = m = m^{1/2} \cdot m^{1/2} \quad (2.7)$$

The eigenvectors (mode shapes) form an orthogonal set and we say that they are orthogonal by the mass matrix since they diagonalize the mass matrix M into m . The matrix m contains the modal masses on the main diagonal. Hence, if we pre and post-multiply the left and right sides of the equation (2.7) shown above by $m^{1/2}$ we get

$$\underbrace{(m^{-1/2})^T \Phi^T}_{\circ \Phi^T} M \underbrace{\Phi m^{-1/2}}_{\circ \Phi} = (m^{-1/2})^T m^{1/2} \cdot m^{1/2} m^{-1/2} = I \quad (2.8)$$

where $\circ \Phi = \Phi m^{-1/2}$ contains the “mass normalized” mode shapes.

Similarly, from the analytical eigenproblem in matrix notation (2.5), by pre-multiplying by Φ^T , we get

$$\Phi^T K \Phi = \Lambda \Phi^T M \Phi = \Lambda m \quad (2.9)$$

and as with the mass matrix, we pre- and post-multiply by $m^{1/2}$ and obtain

$$\underbrace{(m^{-1/2})^T \Phi^T}_{\circ \Phi^T} K \underbrace{\Phi m^{-1/2}}_{\circ \Phi} = \Lambda = \circ \Phi^T K \circ \Phi = \Lambda = \Omega^2 \quad (2.10)$$

In the following, we will assume that the mode shapes are mass normalized and use the symbol Φ instead of $\overset{\circ}{\Phi}$ for simplicity. Therefore, assuming mass normalized mode shapes, where ϕ_s and ϕ_r represent respectively the s^{th} and r^{th} (mass normalized) eigenvectors, or the s^{th} and r^{th} column of Φ , we get

$$\begin{aligned}\phi_s^T M \phi_r &= \delta_{sr} = \begin{cases} 1, & \text{if } s = r \\ 0, & \text{if } s \neq r \end{cases} \\ \phi_s^T K \phi_r &= \lambda_r \delta_{sr} = \begin{cases} \lambda_r, & \text{if } s = r \\ 0, & \text{if } s \neq r \end{cases}\end{aligned}\quad (2.11)$$

where $r, s = 1, 2, \dots, n$ and δ_{sr} , the Kroenecker delta function, is equal to one when $s = r$ and zero otherwise. The equations in (2.11) are referred to as the *orthogonality principle* and can also be written in matrix form simply as

$$\begin{aligned}\Phi^T M \Phi &= I \\ \Phi^T K \Phi &= \Lambda = \Omega^2\end{aligned}\quad (2.12)$$

Modal Coordinates

When damping is small, which is typically the case for space structures, it is common practice to treat damping as modal (e.g.: lightly damped structures can have damping ratios in the range of $\zeta = 0.1\%$ to 0.5%). Specifying modal damping for the structure requires to have its model in modal coordinates.

We can change the coordinate system from physical (Eqs. 2.1 and 2.2) to modal by performing the following linear transformation

$$x = \Phi \eta \quad (2.13)$$

where η are the generalized modal coordinates. After pre-multiplying by Φ^T , Eq. 2.1 becomes

$$I \ddot{\eta} + \Xi \dot{\eta} + \Lambda \eta = \Phi^T \beta_u u(t) + \Phi^T \beta_w w(t) \quad (2.14)$$

and Eq. 2.2 becomes

$$\begin{aligned} y &= C_{yx} \Phi \eta \\ z &= C_{zx} \Phi \eta \end{aligned} \quad (2.15)$$

where

$$\Xi = \Phi^T C \Phi \quad (2.16)$$

For our structural problem, we will specify damping in terms of modal damping ratios [Ewins, 1984]. This is done by assuming that the global damping matrix, C , is proportional to the mass and stiffness matrices as follows

$$C = \alpha M + \beta K \quad (2.17)$$

where α and β are constants. This leads to a diagonal damping matrix Ξ calculated in modal coordinates

$$\Xi = 2\Lambda^{\frac{1}{2}} Z = 2\Omega Z \quad (2.18)$$

where Z is a diagonal matrix whose r^{th} diagonal element is the modal damping ratio ζ_r associated with the r^{th} mode in Φ .

$$Z = \begin{bmatrix} \ddots & & \\ & \zeta_r & \\ & & \ddots \end{bmatrix} \quad (2.19)$$

Thus, the modal damping matrix, Ξ , is given by

$$\Xi = \begin{bmatrix} \ddots & & \\ & \xi_r & \\ & & \ddots \end{bmatrix} = \begin{bmatrix} \ddots & & \\ & 2\zeta_r \lambda_r^{1/2} & \\ & & \ddots \end{bmatrix} = \begin{bmatrix} \ddots & & \\ & 2\zeta_r \omega_r & \\ & & \ddots \end{bmatrix} \quad (2.20)$$

Therefore, Eq. 2.14 can be rewritten as following

$$I \ddot{\eta} + 2Z\Omega \dot{\eta} + \Omega^2 \eta = \Phi^T \beta_u u(t) + \Phi^T \beta_w w(t) \quad (2.21)$$

We notice that the assumption of proportional damping has a convenient property of decoupling the equations of motions of the system into n independent equations since I , Z and Λ (or Ω^2) are all diagonal matrices. In general, though, the modal damping matrix is not diagonal, since off-diagonal terms may couple modes when their frequencies are closely spaced [Hasselmann, 1976]. Therefore, our assumption of proportional damping will be valid only for low modal density structures.

State-Space Form

Rewriting (2.14) and (2.15) in state-space form leads to

$$\underbrace{\begin{Bmatrix} \dot{\eta} \\ \dot{\eta} \end{Bmatrix}}_{\dot{q}_p} = \underbrace{\begin{bmatrix} 0 & I \\ -\Lambda & -2Z\Lambda^{1/2} \end{bmatrix}}_{A_p} \underbrace{\begin{Bmatrix} \eta \\ \dot{\eta} \end{Bmatrix}}_{q_p} + \underbrace{\begin{bmatrix} 0 \\ \Phi^T \beta_w \end{bmatrix}}_{B_w} w + \underbrace{\begin{bmatrix} 0 \\ \Phi^T \beta_u \end{bmatrix}}_{B_u} u$$

$$z = \underbrace{C_{zx}[\Phi \ 0]}_{C_z} \begin{Bmatrix} \eta \\ \dot{\eta} \end{Bmatrix} + \underbrace{0}_{D_{zw}} w + \underbrace{0}_{D_{zu}} u \quad (2.22)$$

$$y = \underbrace{C_{yx}[\Phi \ 0]}_{C_y} \begin{Bmatrix} \eta \\ \dot{\eta} \end{Bmatrix} + \underbrace{0}_{D_{yw}} w + \underbrace{0}_{D_{yu}} u$$

All of D terms are generally zeros for structural plants. Figure 2.1 shows the block diagram of the open-loop plant representing Eq. 2.22.

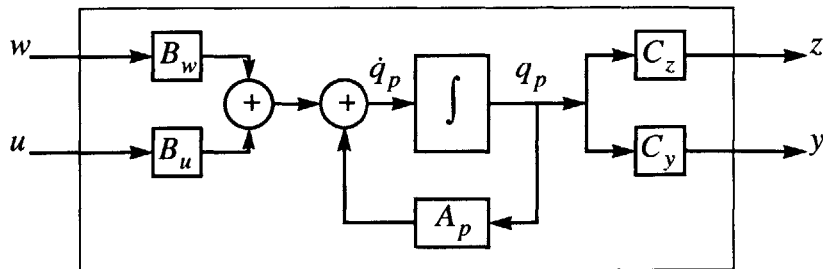


Figure 2.1 Open-loop plant block diagram

In compact form, the open-loop dynamics of the plant are given by

$$\begin{Bmatrix} \dot{q}_p \\ z \\ y \end{Bmatrix} = \begin{bmatrix} A_p & B_w & B_u \\ C_z & D_{zw} & D_{zu} \\ C_y & D_{yw} & D_{yu} \end{bmatrix} \begin{Bmatrix} q_p \\ w \\ u \end{Bmatrix} \quad (2.23)$$

2.1.2 Control Modeling

For the purpose of this work, we will assume the plant to be linear time invariant (LTI) and that it can be a closed-loop system. Taking into account the presence of a dynamic compensator will enable us to use a more general notation. The compensator, also called controller, determines the command signal, u , based on the measurements, y , and is assumed to be linear and strictly proper. The dynamics of the controller can be represented in state space form by the following equation.

$$\begin{aligned} \dot{q}_c &= A_c q_c + B_c y \\ u &= C_c q_c \end{aligned} \quad (2.24)$$

Figure 2.2 shows block diagram representation of the compensator.

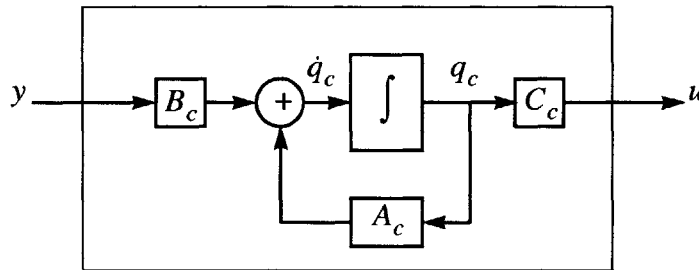


Figure 2.2 Controller block diagram

The general closed-loop plant is obtained by linking the sensor measurements from the structural plant, y , to the controller input, and the controller output to the plant input command, u , as illustrated in Figure 2.3.

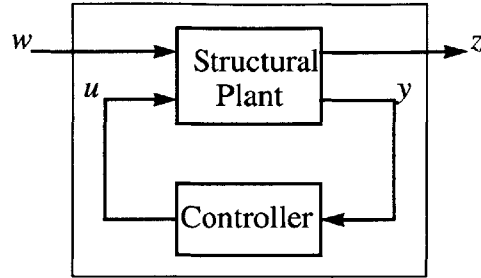


Figure 2.3 Closed-loop plant

The closed-loop dynamics of the plant are obtained by combining Eq. 2.24 with Eq. 2.22.

$$\begin{aligned} \begin{Bmatrix} \dot{q}_p \\ \dot{q}_c \end{Bmatrix} &= \begin{bmatrix} A_p & B_u C_c \\ B_c C_y & A_c + B_c D_{yu} C_c \end{bmatrix} \begin{Bmatrix} q_p \\ q_c \end{Bmatrix} + \begin{bmatrix} B_w \\ B_c D_{yw} \end{bmatrix} w \\ z &= \begin{bmatrix} C_z & D_{zu} C_c \end{bmatrix} \begin{Bmatrix} q_p \\ q_c \end{Bmatrix} + D_{zw} w \end{aligned} \quad (2.25)$$

As mentioned earlier, this notation has the advantage of being more general because it allows for the presence of a compensator, or the absence of it by setting the respective matrices to zero. Also, we can obtain a corresponding transfer function of the plant, also called frequency response function (FRF), by solving the following matrix equation in the s -domain:

$$Z(s) = G_{zw}(s)W(s) \quad \text{where} \quad G_{zw}(s) = C_{zw}[sI - A_{zw}]^{-1}B_{zw} + D_{zw} \quad (2.26)$$

As shown on Figure 2.4, the general plant, including the compensator, can now be represented by a simple box with the physical disturbances, w , as input, and the performance, z , as output.

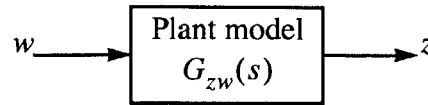


Figure 2.4 General plant model

2.1.3 Dynamic Disturbance Modeling

The disturbances characterization should be given a high priority in the integrated modeling process because mismodeled disturbances can cause the predicted performance to differ substantially from the performance of the actual system in operation. This is especially true for high performance systems where even low disturbance levels can cause the response to exceed the requirements.

The modeling of disturbances is based on the energy perspective since they perform work on the system. The modeling begins with understanding the type and number of energy sources within the system, as well as their magnitude and frequency content. One way to characterize the frequency content of the disturbance energy is to represent it in power spectral density (PSD) form [Wirsching, 1995].

One of the main sources of disturbance on a spaceborne telescope is the attitude control reaction wheel assembly. These wheels, although manufactured to the highest requirements, always have finite static and dynamic imbalances. When spun at high speed, these imbalances cause jittering disturbances that have a considerable impact on a precision space structure. A detailed analysis of wheel disturbances can be found in [Masterson, 1999]. Other mechanical disturbances are produced by thruster impulses, cryocooler pistons and compressor imbalances, propellant sloshing, thermally induced micro-dynamics (thermal snaps), fast steering mirrors, etc. Non-mechanical disturbance sources include sensor and actuator noise, photon noise at the detector, dark current, shot noise, and others. A comprehensive list of spacecraft disturbances is presented in [Gutierrez, 1999].

In this thesis, we will model the physical disturbances into the plant, w , as being the outputs of a shaping filter that has a unit-intensity Gaussian white-noise, d , as input. The power spectral density (PSD) function of the disturbance can be obtained from the following relationship,

$$S_{ww}(\omega) = G_d(j\omega) \cdot S_{dd} \cdot G_d^H(j\omega) \quad (2.27)$$

where $G_d(j\omega)$ is the white noise to disturbance transfer function matrix also referred to as the “shaping” or “pre-whitening” filter, S_{dd} is the intensity of the white-noise (diagonal matrix of constants), and S_{ww} is the cross spectral density matrix of the disturbance w (see Appendix A). For unit-intensity white noise ($S_{dd} = I$), the spectral density of the output reduces to

$$S_{ww}(\omega) = G_d(j\omega)G_d^H(j\omega) \quad (2.28)$$

The dynamics of the disturbance filter is represented in state-space form by the following equation.

$$\begin{aligned} \dot{q}_d &= A_d q_d + B_d d \\ w &= C_d q_d \end{aligned} \quad (2.29)$$

Figure 2.5 illustrates the above state-space representation of the disturbance filter.

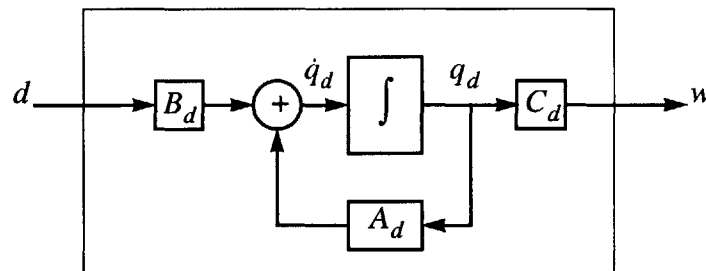


Figure 2.5 Disturbances filter block diagram

Placing the disturbance filter in series with the general plant representation allows us to obtain directly the performance outputs, z , from a simple white-noise input (Figure 2.6).

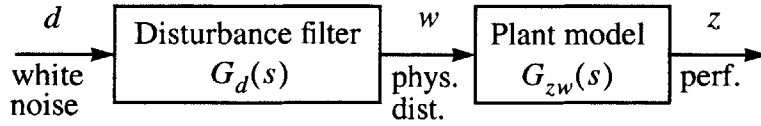


Figure 2.6 Disturbance model and general plant model

Hence, the overall state-space form is obtained by combining Eq. 2.29 with Eq. 2.25.

$$\underbrace{\begin{Bmatrix} \dot{q}_d \\ \dot{q}_p \\ \dot{q}_c \end{Bmatrix}}_{\dot{q}} = \underbrace{\begin{bmatrix} A_d & 0 & 0 \\ \begin{bmatrix} B_w \\ B_c D_{yw} \end{bmatrix} C_d \begin{bmatrix} A_p & B_u C_c \\ B_c C_y & A_c + B_c D_{yu} C_c \end{bmatrix} \end{bmatrix}}_{A_{zd}} \underbrace{\begin{Bmatrix} q_d \\ q_p \\ q_c \end{Bmatrix}}_q + \underbrace{\begin{bmatrix} B_d \\ 0 \\ 0 \end{bmatrix}}_{B_{zd}} d \quad (2.30)$$

$$z = \underbrace{\begin{bmatrix} D_{zw} C_d & C_z & D_{zu} C_c \end{bmatrix}}_{C_{zd}} \begin{Bmatrix} q_d \\ q_p \\ q_c \end{Bmatrix}$$

The equations above can be rewritten in a more compact form

$$\begin{aligned} \dot{q} &= A_{zd}q + B_{zd}d \\ z &= C_{zd}q \end{aligned} \quad (2.31)$$

where, to ensure that the performance has finite energy, D_d must be zero. One interpretation of such notation is that we can consider the assembly of the general plant model in series with the disturbance filter to be nothing else but a filter shaping the white noise

input to the performance output. Hence, the diagram of Figure 2.6 is reduced to the diagram of Figure 2.7.

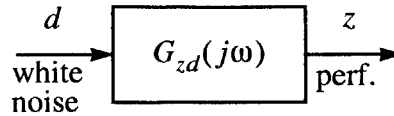


Figure 2.7 Integrated plant model

where the transfer function $G_{zd}(j\omega)$, can be obtained by performing the Laplace transform on (2.31)

$$Z(s) = G_{zd}(s)D(s) \quad \text{where} \quad G_{zd}(s) = C_{zd}[sI - A_{zd}]^{-1}B_{zd} \quad (2.32)$$

and evaluating it for $s = j\omega$ (which correspond to the Fourier transform). This integrated model form will allow us to use statistical tools in order to predict the overall performances of the system (Section 2.2.3).

2.2 Initial Performance Assessment

The objective of a precision controlled structure is to ensure that the *performances* are below some desired level when subjected to a given disturbance. Some of the performance outputs, z , of a spaceborne telescope are, for example, the optical path difference (OPD), the line of sight jitter (LOS), or the wave front error (WFE), and the requirements are generally specified in terms of RMS values in the form of a quadratic cost.

$$J = Tr\{E[zz^T]\} \quad (2.33)$$

As a first step in evaluating the capability of our system to meet the specified requirements, it is necessary to evaluate the performance of the nominal model. To evaluate the stochastic performance z of a linear time invariant (LTI) system, several methods have been developed. For example, three different and complementary techniques to assess the

performance, dubbed as disturbance analyses, are presented in [Gutierrez, 1999]: The time domain, the frequency domain, and the Lyapunov approach. For the purposes of this work, we will describe only the two last methods because they are the tools that we will use to evaluate the performance outputs and to verify whether the nominal models meet the performance specifications.

2.2.1 Performance Modeling

For multiple performance outputs, z is a vector and in order to obtain a scalar performance cost, it is possible to apply a weighting matrix R to z . The matrix R represents the relative importance between the output elements of z in the overall performance cost, but also should take into account the scaling of the units of each performance. For simplicity of notation, it can simply be absorbed into the matrix C_{zx} . Let us denote the weighted performance by z^* ,

$$z^* = Rz \quad (2.34)$$

and define the scalar cost to be its norm as

$$J = \|z^*\| \Rightarrow J = Tr\{RE[zz^T]R^T\} \quad (2.35)$$

For high precision structures, it is common practice to specify the performance requirements in terms of RMS maximum values which are not to be exceeded. In the literature, the RMS values are also referred to as the H_2 norms, and the maximum values as the H_∞ norms.

2.2.2 Frequency-domain Analysis

For linear systems, the advantage of frequency domain analysis (i.e., Laplace domain) is that the output of the system is equal to its transfer function multiplied by the input, while in time domain the output is obtained by a convolution of the input with the impulse-response function of the system. Using linear systems theory, it can be shown that the performance PSD can be obtained by (see [Wirsching, 1995])

$$S_{zz}(\omega) = G_{zw}(j\omega) \cdot S_{ww}(\omega) \cdot G_{zw}^H(j\omega) \quad (2.36)$$

where the disturbance PSD, $S_{ww}(\omega)$, was obtained in (2.28). This implies that Eq. 2.36 can also be written as

$$S_{zz}(\omega) = \underbrace{G_{zw}(j\omega)G_d(j\omega)}_{G_{zd}(j\omega)} \underbrace{G_d^H(j\omega)G_{zw}^H(j\omega)}_{G_{zd}^H(j\omega)} = G_{zd}(j\omega)G_{zd}^H(j\omega) \quad (2.37)$$

where $G_{zd}(j\omega)$ is the global transfer function matrix from the white noise disturbance, d , to the performance outputs, z (see Figure 2.7).

As shown in (A.55), for zero-mean processes, integrating the elements of the spectral density function across the frequency range yields the covariance matrix as follows

$$\Sigma_z = \frac{1}{2\pi} \int_{-\infty}^{\infty} S_{zz}(\omega) d\omega = \int_{-\infty}^{\infty} S_{zz}(f) df \quad (2.38)$$

where ω is the frequency in [rad/s] and $f = \omega/2\pi$ is the frequency in [Hz]. Since the diagonal elements of the covariance matrix are the variances of the different performance outputs, z_i 's (see Eq. A.56)

$$\sigma_{z_i}^2 = (\Sigma_z)_{i,i} = \frac{1}{\pi} \int_0^{\infty} [S_{zz}(\omega)]_{i,i} d\omega = 2 \int_0^{\infty} [S_{zz}(f)]_{i,i} df \quad (2.39)$$

we obtain the root-mean-square (RMS) values of the performance metrics by taking the square root of $(\Sigma_z)_{i,i}$

$$RMS(z_i) = \sigma_{z_i} = \left\{ \frac{1}{\pi} \int_0^{\infty} [S_{zz}(\omega)]_{i,i} d\omega \right\}^{1/2} = \left\{ 2 \int_0^{\infty} [S_{zz}(f)]_{i,i} df \right\}^{1/2} \quad (2.40)$$

which can also be expressed in terms of the transfer function G_{zd} by substituting the identity of Eq. 2.37 into Eq. 2.40.

$$\sigma_{z_i} = \left\{ \frac{1}{\pi} \int_0^{\infty} [S_{zz}(\omega)]_{i,i} d\omega \right\}^{1/2} = \left\{ \frac{1}{\pi} \int_0^{\infty} |G_{zd}(j\omega)|_{i,i}^2 d\omega \right\}^{1/2} \quad (2.41)$$

Equations 2.40 and 2.41 are very useful expressions since they help determine if the RMS requirements for the performance metrics z_i 's are met by the nominal plant. One interpretation of the above expression is that the RMS performance corresponds to the area under the transfer function magnitude curve (scaled by a factor π). Therefore, augmenting the modal damping, thus reducing the height of the modal peaks, has the effect of improving (reducing) the RMS values of the performance outputs by reducing the area under the magnitude curve of the transfer function.

Another very useful expression is the *cumulative RMS function* defined as

$$\sigma_{z_i, c}(f_o) = \left\{ 2 \int_0^{f_o} [S_{zz}(f)]_{i, i} df \right\}^{1/2} \approx \left\{ 2 \int_0^{f_o} [S_{zz}(f)]_{i, i} df \right\}^{1/2} \quad (2.42)$$

where to limit the amount of calculations, we limit ourself to the range where most of the energy is concentrated $f_o \in [f_{min} \dots f_{max}]$. Likewise, $\sigma_{z_i, c}(f_{max})$ should be very close to the correct value of σ_{z_i} . The usefulness of the above expression comes from the fact that, by plotting the function, it becomes very easy to see graphically the contribution of each mode to the RMS value of a particular performance output. The drawback comes from that fact that the accuracy of the method depends on the resolution of the frequency vector (step size) when performing the integration numerically.

2.2.3 Lyapunov Approach

The following Lyapunov approach is valid for a linear time-invariant system driven by white noise. Using the integrated state-space representation of the system from Eq. 2.31, also represented graphically by Figure 2.7, it is possible to obtain the steady-state covariance matrix, Σ_q , by solving the following steady-state Lyapunov equation

$$A_{zd}\Sigma_q + \Sigma_q A_{zd}^T + B_{zd}B_{zd}^T = 0 \quad (2.43)$$

Since the state covariance matrix is symmetric, $\Sigma_q = \Sigma_q^T$. The performance covariance matrix is obtained as follow

$$\begin{aligned}
\Sigma_z &= E[zz^T] = E[C_{zd}qq^T C_{zd}^T] = C_{zd}E[qq^T]C_{zd}^T \\
&= C_{zd}\Sigma_q C_{zd}^T \\
&= \begin{bmatrix} \sigma_{z_1}^2 & \cdots & \sigma_{z_1 z_n} \\ \vdots & \ddots & \vdots \\ \sigma_{z_n z_1} & \cdots & \sigma_{z_n}^2 \end{bmatrix}
\end{aligned} \tag{2.44}$$

where the exact mean-square values of the performance outputs are given by the square roots of the diagonal elements of Σ_z

$$RMS(z_i) = \sigma_{z_i} = \{(\Sigma_z)_{i,i}\}^{1/2} = \left\{ C_{zd_i} \Sigma_q C_{zd_i}^T \right\}^{1/2} \tag{2.45}$$

where C_{zd_i} corresponds to the i^{th} row of C_{zd} . For zero-mean process, the term “mean-square” is synonymous with “variance” and thus the term “RMS”, which we get by taking the square root of the mean-square, is synonymous with “standard deviation”. For the case where the overall performance cost, J , is defined as the sum of all the weighted outputs (Eq. 2.35), we have

$$J = Tr[\Sigma_z] = \sigma_{z_1}^2 + \sigma_{z_2}^2 + \dots + \sigma_{z_n}^2 \tag{2.46}$$

The main advantage of the Lyapunov method is that it provides the exact analytical steady-state performances and does not suffer from poor frequency resolution. The drawback is that it does not provide any insight of the frequency content of the outputs, and that the solution time for the Lyapunov equation increases dramatically for large-order systems. Therefore, the frequency-domain analysis and the Lyapunov approach should be used complementary. For example, the Lyapunov analysis could be used to verify the frequency-domain analysis results and validate the choice of the frequency range and frequency resolution. Both techniques will be demonstrated on sample problems in Chapter 6.

2.3 Summary

We now have described the basic modeling tools and notation for performing integrated modeling and assessing the performance of precision controlled structures. As discussed in the introduction chapter, it is not enough to evaluate only the nominal performance of the system based on the preliminary design models since these preliminary models can be quite crude in early design phase. Although they can provide great qualitative assessment of the performances, their quantitative predictions are not necessarily very accurate. Therefore, in order for the designer to make sure that, once it is built, the system will meet the requirements with a certain degree of confidence, it is a necessity to evaluate the uncertainty range around the performance outputs of the system. The tools to evaluate the uncertainty range around the nominal performances will be presented in the following chapters.

Chapter 3

MASS, STIFFNESS AND DAMPING UNCERTAINTY

The purpose of this thesis is to provide confidence for the designer that a concept of a future space-based telescope will meet its very stringent requirements. The traditional design process starts by evaluating and comparing the performance of different concepts by using simplified structural and disturbance models. As the process progresses the different solutions are evaluated and the most promising concept is retained and refined. Eventually, some preliminary structural testing is performed, and the model is updated to reflect the reality more accurately. Eventually, when the production of the system is nearly complete, the model performance predictions should converge to the actual system performance.

Large flexible space structures present a problem in using this approach because they are often too flexible to support their own weight and/or too large to fit inside any laboratory facilities to be tested fully assembled. For example, it would be impractical to test the whole assembly of the International Space Station or SIM on the ground. Also, during the preliminary design phase, no test data are available to update the models. Even when the model is very mature and has been updated after experimental testing, a discrepancy remains between the predicted and actual performance of the system. These uncertainties are due to various sources of variability in the system: variable noises (sources and levels), testing conditions and environmental factors, assembly/reassembly, shipset, disturbance levels, and others. How then, can we have confidence that a particular concept will meet

the requirements if the only tool we have are finite element models that may not be accurate? The solution is to try to estimate the range of uncertainty around our nominal model performances. Since in the early design phase no test data are available, our best bet will be to use past experience to predict the expected uncertainty range on the performances of our new design. Statistical uncertainty for the modal mass and stiffness parameters, [Hasselman & Chrostowski, 1991], as well as for the modal damping ratios [Simonian, 1987], can be obtained. These methodologies will be presented in Section 3.1 and Section 3.2 respectively.

3.1 Mass and Stiffness Uncertainty

In this section, we will describe the methodology used to express the modal mass and stiffness uncertainties of a structural model as a function of the error in the eigenvalue and mode shape predictions. We will then describe how to use this information to build a statistical database.

First-order perturbation equations for the linear eigenvalue problem can be derived in a variety of ways. The technique presented here is an augmented and more detailed version of the developments presented in [Hasselman & Chrostowski, 1991]. Other similar developments can be found in various references ([Kato, 1966], [Rellich, 1969], [Huag, 1986], [Chen, 1985], [Hasselman, Chrostowski & Ross, 1992]).

3.1.1 Methodology

The methodology will consist of performing a linear perturbation analysis on the equations of motion of the system (Eq. 2.1). For this perturbation analysis, since we have assumed the mass and stiffness to be independent of damping and forcing function (Chapter 2), we will consider only the undamped homogeneous equations of motion (2.3) for which the corresponding undamped eigenproblem (2.4) is reproduced here

$$(K - \lambda_r M)\phi_r = 0 \quad (3.1)$$

where λ_r and ϕ_r are the eigenvalue and eigenvector, respectively, corresponding to the r^{th} normal mode of the structure, and M and K are the actual mass and stiffness matrices.

Linear Perturbation Analysis

The advantage provided by the perturbation analysis is that the changes in the modal properties can be expressed entirely in terms of the eigenproperties of the original system and the changes in the system mass and stiffness. This means that the natural frequencies, loss factors, and mode shapes of the perturbed system can be obtained directly, without the need to re-solve the eigenvalue problem, as long as we know that the size of the perturbation is small enough such that linearity is preserved.

The physical and modal parameters of the analytical, or nominal, model are related to those of the actual structure as follows:

$$M = \tilde{M} + \Delta M \quad (3.2)$$

$$K = \tilde{K} + \Delta K \quad (3.3)$$

$$\lambda_r = \tilde{\lambda}_r + \Delta\lambda_r \quad (3.4)$$

$$\phi_r = \tilde{\phi}_r + \Delta\phi_r \quad (3.5)$$

In matrix form, equation (3.4) becomes

$$\Lambda = \tilde{\Lambda} + \Delta\Lambda \quad (3.6)$$

where the eigenvalue matrices Λ and $\tilde{\Lambda}$ are diagonal matrices containing respectively the measured actual eigenvalues λ_r and the analytical eigenvalues $\tilde{\lambda}_r$ along their diagonals. The matrix $\Delta\Lambda$ is the difference between the actual and the analytical eigenvalue matrices ($\Lambda - \tilde{\Lambda}$).

Equation (3.5) can also be expressed in matrix form as follows

$$\Phi = \tilde{\Phi} + \Delta\Phi \quad (3.7)$$

where the matrices Φ and $\tilde{\Phi}$ contain respectively the actual and analytical eigenvectors organized column-wise from $r = 1, 2, \dots, n$, and similarly, $\Delta\Phi$ is organized as follows

$$\Delta\Phi = [\Delta\phi_1 \dots \Delta\phi_2] \quad (3.8)$$

It is always possible to express the vector $\Delta\phi_r$ as a linear combination of the original eigenvectors since they span the vector space of all the possible displacements:

$$\Delta\phi_r = \tilde{\Phi}\Delta\psi_r \quad (3.9)$$

where the matrix $\tilde{\Phi}$ consists of the analytical modes shapes $\tilde{\phi}_r$ organized column-wise from $r = 1, 2, \dots, n$, and $\Delta\psi_r$ is the vector of linear combination coefficients. In matrix notation, Eq. 3.9 becomes

$$\Delta\Phi = \tilde{\Phi}\Delta\Psi \quad (3.10)$$

where $\Delta\Psi$ is organized as follows

$$\Delta\Psi = [\Delta\psi_1 \dots \Delta\psi_2] \quad (3.11)$$

Substitution of equations (3.2) through (3.5) into the eigenproblem (3.1) gives:

$$[\tilde{K} + \Delta K - (\tilde{\lambda}_r + \Delta\lambda_r)(\tilde{M} + \Delta M)](\tilde{\phi}_r + \Delta\phi_r) = 0 \quad (3.12)$$

After multiplying out the factors we get

$$\begin{aligned} &(\tilde{K} + \Delta K - \tilde{\lambda}_r\tilde{M} - \tilde{\lambda}_r\Delta M - \Delta\lambda_r\tilde{M} - \Delta\lambda_r\Delta M)\tilde{\phi}_r \\ &+ (\tilde{K} + \Delta K - \tilde{\lambda}_r\tilde{M} - \tilde{\lambda}_r\Delta M - \Delta\lambda_r\tilde{M} - \Delta\lambda_r\Delta M)\Delta\phi_r = 0 \end{aligned} \quad (3.13)$$

This expression contains second order terms $(-\Delta\lambda_r\Delta M\tilde{\phi}_r + \Delta K\Delta\phi_r - \tilde{\lambda}_r\Delta M\Delta\phi_r - \Delta\lambda_r\tilde{M}\Delta\phi_r)$ and third order terms $(-\Delta\lambda_r\Delta M\Delta\phi_r)$. Ignoring these terms is equivalent to the “small numbers” or “first order” approximation

which is valid as long as the perturbation is not “too large”. In Chapter 4 we will discuss the range of validity for the approximation.

Caution: One must keep in mind that the following developments will only be valid if the mass and stiffness uncertainties, ΔM and ΔK , (or frequency and mode shape uncertainties, $\Delta\lambda_r$ and $\Delta\phi_r$) are small compared to the nominal analytical quantities \tilde{M} , \tilde{K} , $\tilde{\lambda}_r$, $\tilde{\phi}_r$. For good structural modeling, however, we expect this assumption will hold. For example, the natural frequencies are typically off by less than 10 or even 5 percent.

Hence, neglecting second and third order terms in Eq. 3.13, we get:

$$(\tilde{K} - \tilde{\lambda}_r \tilde{M}) \Delta\phi_r + (\tilde{K} + \Delta K - \tilde{\lambda}_r \tilde{M} - \tilde{\lambda}_r \Delta M - \Delta\lambda_r \tilde{M}) \tilde{\phi}_r = 0 \quad (3.14)$$

where $(\tilde{K} - \tilde{\lambda}_r \tilde{M}) \tilde{\phi}_r = 0$ is the eigenproblem for the analytical (nominal) model (correspond Eq. 3.1 evaluated for the nominal parameters). Thus, reducing equation (3.14) to:

$$(\tilde{K} - \tilde{\lambda}_r \tilde{M}) \Delta\phi_r + (\Delta K - \tilde{\lambda}_r \Delta M - \Delta\lambda_r \tilde{M}) \tilde{\phi}_r = 0 \quad (3.15)$$

This equation will be used extensively in the following developments to first obtain an expression of the uncertainty on the eigenvalues based on the uncertainty in the mass and stiffness matrices, and then to find approximate expressions for the mass and stiffness based on the difference between the modal mass and stiffness of the test model and the analytical model.

Firstly, pre-multiplying (3.15) by $\tilde{\phi}_r^T$ gives

$$\underbrace{\tilde{\phi}_r^T (\tilde{K} - \tilde{\lambda}_r \tilde{M})}_{0} \Delta\phi_r + \tilde{\phi}_r^T (\Delta K - \tilde{\lambda}_r \Delta M - \Delta\lambda_r \tilde{M}) \tilde{\phi}_r = 0 \quad (3.16)$$

where $(\tilde{\phi}_r^T (\tilde{K} - \tilde{\lambda}_r \tilde{M}) = 0)$ since it is the transposed of the analytical eigenproblem (Eq. 3.1) \tilde{K} and \tilde{M} are symmetric ($\tilde{K} = \tilde{K}^T$, $\tilde{M} = \tilde{M}^T$). That leaves us with:

$$\tilde{\phi}_r^T (\Delta K - \tilde{\lambda}_r \Delta M) \tilde{\phi}_r = \tilde{\phi}_r^T (\Delta\lambda_r \tilde{M}) \tilde{\phi}_r = \Delta\lambda_r \tilde{\phi}_r^T \tilde{M} \tilde{\phi}_r \quad (3.17)$$

Applying the orthogonality principle (see Eqs. 2.11 in Section 2.1.1) on equation (3.17) leaves us with the following approximate expression for the perturbation in the r^{th} eigenvalue caused by perturbations in the original mass and stiffness matrices:

$$\boxed{\Delta\lambda_r = \tilde{\phi}_r^T (\Delta K - \tilde{\lambda}_r \Delta M) \tilde{\phi}_r = \Delta k_{rr} - \tilde{\lambda}_r \Delta m_{rr}} \quad (3.18)$$

where $\Delta k_{rr} = \tilde{\phi}_r^T \Delta K \tilde{\phi}_r$ and $\Delta m_{rr} = \tilde{\phi}_r^T \Delta M \tilde{\phi}_r$. The above expression was first obtained in [Nelson, 1976] and is important because it relates perturbations or uncertainties in the physical space (ΔM , ΔK) to perturbations or uncertainties on the eigenvalues in the modal space. It will be used in Chapter 4 to obtain the eigenvalue derivatives. The expressions for Δm_{rr} and Δk_{rr} are obtained later in Eq. 3.38 and 3.39, respectively.

Secondly, pre-multiplying (3.15) by $\tilde{\phi}_s^T$, where $s \neq r$, gives:

$$\tilde{\phi}_s^T (\tilde{K} - \tilde{\lambda}_r \tilde{M}) \Delta \tilde{\phi}_r + \tilde{\phi}_s^T (\Delta K - \tilde{\lambda}_r \Delta M - \Delta \lambda_r \tilde{M}) \tilde{\phi}_r = 0 \quad (3.19)$$

Substitution of the expression for $\Delta \tilde{\phi}_r$ from (3.9) into (3.19) gives

$$\tilde{\phi}_s^T (\tilde{K} - \tilde{\lambda}_r \tilde{M}) \tilde{\Phi} \Delta \psi_r + \tilde{\phi}_s^T (\Delta K - \tilde{\lambda}_r \Delta M - \Delta \lambda_r \tilde{M}) \tilde{\phi}_r = 0 \quad (3.20)$$

$$\Leftrightarrow (\tilde{\phi}_s^T \tilde{K} \tilde{\Phi} - \tilde{\lambda}_r \tilde{\phi}_s^T \tilde{M} \tilde{\Phi}) \Delta \psi_r + \tilde{\phi}_s^T (\Delta K - \tilde{\lambda}_r \Delta M) \tilde{\phi}_r - \Delta \lambda_r \tilde{\phi}_s^T \tilde{M} \tilde{\phi}_r = 0 \quad (3.21)$$

Applying the orthogonality principle (Eqs. 2.11), we obtain:

$$(\tilde{\lambda}_s \cdot e_s^T - \tilde{\lambda}_r \cdot e_s^T) \Delta \psi_r + \tilde{\phi}_s^T (\Delta K - \tilde{\lambda}_r \Delta M) \tilde{\phi}_r = 0 \quad (3.22)$$

where e_s is a column vector with a 1 at the s^{th} entry and zeros elsewhere. Since $\Delta \psi_r$ is also a column vector, then the product of e_s^T and $\Delta \psi_r$ reduces to a single element $\Delta \psi_{sr}$ which is the s^{th} element of the vector $\Delta \psi_r$, (or as seen later, the element of the $\Delta \Psi$ corresponding to the s^{th} row and r^{th} column) yielding

$$\begin{aligned} & (\tilde{\lambda}_s - \tilde{\lambda}_r) \Delta \psi_{sr} + \tilde{\phi}_s^T (\Delta K - \tilde{\lambda}_r \Delta M) \tilde{\phi}_r = 0 \\ \Leftrightarrow & (\tilde{\lambda}_r - \tilde{\lambda}_s) \Delta \psi_{sr} = \tilde{\phi}_s^T (\Delta K - \tilde{\lambda}_r \Delta M) \tilde{\phi}_r \end{aligned} \quad (3.23)$$

For convenience, the following notation is defined:

$$\begin{aligned}
m &= \tilde{\Phi}^T M \tilde{\Phi} = \text{true modal mass matrix in } \tilde{\Phi}\text{-coordinates} \\
k &= \tilde{\Phi}^T K \tilde{\Phi} = \text{true modal stiffness matrix in } \tilde{\Phi}\text{-coordinates} \\
\tilde{m} &= \tilde{\Phi}^T \tilde{M} \tilde{\Phi} = I \text{ (identity matrix)} \\
\tilde{k} &= \tilde{\Phi}^T \tilde{K} \tilde{\Phi} = \tilde{\Lambda} \text{ (diagonal matrix of analytical eigenvalues = } \tilde{\Omega}^2) \\
\Delta m &= \tilde{\Phi}^T \Delta M \tilde{\Phi} = m - I \text{ (modal mass matrix uncertainty in } \tilde{\Phi}\text{-coordinates)} \\
\Delta k &= \tilde{\Phi}^T \Delta K \tilde{\Phi} = k - \tilde{\Lambda} \text{ (modal stiffness matrix uncertainty in } \tilde{\Phi}\text{-coordinates)}
\end{aligned} \tag{3.24}$$

where by “ $\tilde{\Phi}$ -coordinates” we mean the analytical modal coordinates. By applying the above notation to (3.23), we can get:

$$(\tilde{\lambda}_r - \tilde{\lambda}_s) \Delta \psi_{sr} = \Delta k_{sr} - \tilde{\lambda}_r \Delta m_{sr} \tag{3.25}$$

where Δk_{sr} and Δm_{sr} are the elements of Δm and Δk corresponding to the s^{th} row and r^{th} column. Since Δm and Δk are symmetric, we can write

$$(\tilde{\lambda}_s - \tilde{\lambda}_r) \Delta \psi_{rs} = \Delta k_{rs} - \tilde{\lambda}_s \Delta m_{rs} = \Delta k_{sr} - \tilde{\lambda}_s \Delta m_{sr} \tag{3.26}$$

The difference of (3.25) and (3.26) gives:

$$\begin{aligned}
(\tilde{\lambda}_r - \tilde{\lambda}_s) \Delta \psi_{sr} - (\tilde{\lambda}_s - \tilde{\lambda}_r) \Delta \psi_{rs} &= \Delta k_{sr} - \tilde{\lambda}_r \Delta m_{sr} - (\Delta k_{sr} - \tilde{\lambda}_s \Delta m_{sr}) \\
\Leftrightarrow (\tilde{\lambda}_r - \tilde{\lambda}_s) (\Delta \psi_{sr} + \Delta \psi_{rs}) &= -(\tilde{\lambda}_r - \tilde{\lambda}_s) \Delta m_{sr}
\end{aligned} \tag{3.27}$$

$$\Rightarrow \Delta m_{sr} = -(\Delta \psi_{sr} + \Delta \psi_{rs}) \quad \text{for } (r \neq s) \tag{3.28}$$

The sum of equations (3.25) and (3.26) gives:

$$\begin{aligned}
(\tilde{\lambda}_r - \tilde{\lambda}_s) \Delta \psi_{sr} + (\tilde{\lambda}_s - \tilde{\lambda}_r) \Delta \psi_{rs} &= \Delta k_{sr} - \tilde{\lambda}_r \Delta m_{sr} + \Delta k_{sr} - \tilde{\lambda}_s \Delta m_{sr} \\
\Leftrightarrow (\tilde{\lambda}_r - \tilde{\lambda}_s) (\Delta \psi_{sr} - \Delta \psi_{rs}) &= 2\Delta k_{sr} - (\tilde{\lambda}_r + \tilde{\lambda}_s) \Delta m_{sr}
\end{aligned} \tag{3.29}$$

where by substituting in (3.29) the newly found expression for Δm_{sr} (Eq. 3.28) yields

$$\begin{aligned}
(\tilde{\lambda}_r - \tilde{\lambda}_s)(\Delta\psi_{sr} - \Delta\psi_{rs}) &= 2\Delta k_{sr} + (\tilde{\lambda}_r + \tilde{\lambda}_s)(\Delta\psi_{sr} + \Delta\psi_{rs}) \\
\Leftrightarrow 2\Delta k_{sr} &= -2(\tilde{\lambda}_s\Delta\psi_{sr} + \tilde{\lambda}_r\Delta\psi_{rs})
\end{aligned} \tag{3.30}$$

$$\Rightarrow \Delta k_{sr} = -(\tilde{\lambda}_s\Delta\psi_{sr} + \tilde{\lambda}_r\Delta\psi_{rs}) \quad \text{for } (r \neq s) \tag{3.31}$$

In (3.28) and (3.31) we have obtained the expressions for the off-diagonal terms of the mass and stiffness uncertainty matrices expressed in analytical modal coordinates (Δm and Δk). We should now find the expressions for the diagonal terms Δk_{rr} and Δm_{rr} for every mode r .

First, to obtain the term Δm_{rr} we start with the normalization condition on the actual mode ϕ_r (2.11).

$$\phi_r^T M \phi_r = 1 \tag{3.32}$$

Substituting (3.2) and (3.5) into (3.32) gives:

$$(\tilde{\phi}_r + \Delta\phi_r)^T (\tilde{M} + \Delta M) (\tilde{\phi}_r + \Delta\phi_r) = 1 \tag{3.33}$$

Multiplying term by term and neglecting second and third order terms leaves

$$\tilde{\phi}_r^T \tilde{M} \tilde{\phi}_r + \tilde{\phi}_r^T \tilde{M} \Delta\phi_r + \Delta\phi_r^T \tilde{M} \tilde{\phi}_r + \tilde{\phi}_r^T \Delta M \tilde{\phi}_r = 1 \tag{3.34}$$

where substituting the expression for $\Delta\tilde{\phi}_r$ from (3.9) gives

$$\tilde{\phi}_r^T \tilde{M} \tilde{\phi}_r + \tilde{\phi}_r^T \tilde{M} \tilde{\Phi} \Delta\psi_r + \Delta\psi_r^T \tilde{\Phi}^T \tilde{M} \tilde{\phi}_r + \tilde{\phi}_r^T \Delta M \tilde{\phi}_r = 1 \tag{3.35}$$

and applying the orthogonality principle (Eqs. 2.11) reduces (3.35) to

$$1 + e_r^T \cdot \Delta\psi_r + \Delta\psi_r^T \cdot e_r + \Delta m_{rr} = 1 \tag{3.36}$$

where, just like in Eq. 3.22, e_r is a column vector with a 1 at the r^{th} entry and zeros elsewhere. Since $\Delta\psi_r$ is also a column vector, then the product of e_r^T and $\Delta\psi_r$ reduces to a

single element $\Delta\psi_{rr}$ which is the r^{th} element of the vector $\Delta\psi_r$, (or the element of the $\Delta\Psi$ matrix corresponding to the r^{th} row and r^{th} column) yielding

$$1 + \Delta\psi_{rr} + \Delta\psi_{rr}^T + \Delta m_{rr} = 1 \quad (3.37)$$

$$\Leftrightarrow \Delta m_{rr} = -2\Delta\psi_{rr} \quad (3.38)$$

Now, to obtain the Δk_{rr} , term we substitute (3.38) into (3.18) and get:

$$\Delta k_{rr} = \Delta\lambda_r + \tilde{\lambda}_r \Delta m_{rr} = \Delta\lambda_r - 2\tilde{\lambda}_r \Delta\psi_{rr} \quad (3.39)$$

It can be easily shown that combining equations (3.28) and (3.38) for the elements of Δm , and equations (3.31) and (3.39) for the elements of Δk yields

$$\begin{aligned} \Delta m &= -(\Delta\Psi + \Delta\Psi^T) \\ \Delta k &= \Delta\Lambda - \tilde{\Lambda}\Delta\Psi - \Delta\Psi^T\tilde{\Lambda} \end{aligned} \quad (3.40)$$

where $\Delta\Lambda$ is the eigenvalues difference matrix (Eq. 3.6), and $\Delta\Psi$ is the matrix that combines linearly the analytical mode shapes to obtain the modes shapes difference matrix $\Delta\Phi$ (Eq. 3.10). The two above expressions are very useful because they give us an approximate (H.O.T. neglected) way to express the difference between the analytical modal mass and stiffness matrices versus the mass and stiffness matrices corresponding to the experimental test data, expressed in the analytical model modal coordinates system. The usefulness of these expressions comes, firstly, from the fact that it would be impractical to measure the mass and stiffness elements on a real structure in order to get the uncertainty matrices Δm and Δk . Secondly, because these first order perturbations are expressed in the analytical modal coordinates, they can be readily applied to the analytic (nominal) model to obtain the actual (experimental) model matrices as follows

$$\begin{aligned} m &= \tilde{m} + \Delta m \\ k &= \tilde{k} + \Delta k \end{aligned} \quad (3.41)$$

where we recall that the matrices m and k are the modal mass and stiffness matrices of the actual structure expressed in the modal coordinates of the analytical model as defined in (3.24).

To obtain the matrix $\Delta\Psi$, we must first find the cross-orthogonality matrix, Ψ , from the following cross-orthogonality test between the analysis modes, $\tilde{\Phi}$, and the actual test modes, Φ :

$$\tilde{\Phi} \tilde{M} \Phi = \tilde{\Phi} \tilde{M} (\tilde{\Phi} \Psi) = I \Psi = \Psi \quad (3.42)$$

where we assume that the test mode shapes, Φ , can be expressed as a linear combination of the analytical mode shapes, $\tilde{\Phi}$, by the following expression

$$\Phi = \tilde{\Phi} \Psi \quad (3.43)$$

To obtain the explicit relationship between Ψ and $\Delta\Psi$, we plug in the expression (3.43) for Φ and expression (3.10) for $\Delta\Phi$ into equation (3.7), and get

$$\tilde{\Phi} \Psi = \tilde{\Phi} + \tilde{\Phi} \Delta\Psi \quad (3.44)$$

which by pre-multiplying by $\tilde{\Phi}^T$ reduces to

$$\begin{aligned} \Psi &= I + \Delta\Psi \\ \Leftrightarrow \Delta\Psi &= \Psi - I \end{aligned} \quad (3.45)$$

When there is no modeling error, meaning that there is no difference between the analytical and the actual eigenvalues and modes shapes ($\Delta\Lambda = 0$ and $\Delta\Phi = 0$), it means that $\Delta\Psi$ in Eq. 3.7 is also equal to zero. In this case, we can see from Eq 3.45 that the cross-orthogonality matrix is then equal to the identity matrix ($\Psi = I$). This is consistent with the definition of the cross-orthogonality matrix in (3.42) where it is obvious that, if the analytical mode shapes and the actual mode shapes obtained experimentally are the same, the left hand side of the equation reduces to the identity by the orthogonality principle.

Lastly, substitution of (3.45) into the equations of (3.40) gives us the final expressions for Δm and Δk , the difference between the modal stiffness and modal mass matrices of the actual (test) model expressed in the analytical modal ($\tilde{\Phi}$) coordinates (see Eq. 3.24) and the modal mass and stiffness matrices from the analytical model.

$$\begin{aligned} \Delta m &= (I - \Psi) + (I - \Psi)^T \\ \Delta k &= \Delta \Lambda + \tilde{\Lambda}(I - \Psi) + (I - \Psi)^T \tilde{\Lambda} \end{aligned} \quad (3.46)$$

The above equations are very important since they give us a measure of the error made in the analytical modal mass and stiffness matrices based on the measured errors in the eigenvalues and the cross-orthogonality matrix (Eq. 3.42). Let us notice that even though the modal mass and stiffness matrices are diagonal, this is generally not the case for Δm and Δk . Studying statistically the size of these modal errors for different structures will help us to build knowledge about the amount of uncertainty involved in modeling real structures. The fact that these errors are expressed in modal form is a very useful property because they can be readily applied to the modal model of a new structural system to estimate its uncertainty.

3.1.2 Database

In order to estimate the range of uncertainty around our nominal model performance predictions, and thus build confidence that a particular concept will meet the requirements, we have to rely on data from past experience. Performing a statistical analysis of the modal mass and stiffness parameters will provide such data.

Statistical Analysis

Statistical analysis of the modal mass and stiffness variability involves averaging the elements of Δk and Δm over a family of similar structure/model pairs. It is possible to statistically analyze together all sorts of structures that could be very different topologically. The knowledge gained from the statistical data of such structures would give us a very general idea of the amount of uncertainty involved in a broad variety of structural models.

For high-precision space structures with very tight requirements a lot of design effort is usually expended to achieve models with higher accuracy. Therefore looking at the statistical modeling errors for such structures would be more appropriate to estimate the uncertainty on a space telescope model. This statement is even more true if the structures are topologically similar (trusses, flexible appendages, etc...) since one can reasonably assume that the same kind of modeling discrepancies are repeated for the same type of structures. Also, as the design process progresses, the fidelity of the model increases over the different generations (unupdated vs. updated models). To estimate the uncertainty of a preliminary design model, it is appropriate to use data from the unupdated models. Thus, “generically similar” structures could refer to a more restricted set of structures with the same kind of topology, function, and model generation altogether. Another criterion could be that the structures have the same modal content (modal density and transition frequency from global to local modes).

The Δk and Δm matrices are found by comparing the measurements on the actual structure with the modal properties of the analytical model (Eq. 3.46). Data can be compiled over multiple structure/model pairs. To perform a statistical analysis of the Δk and Δm data, we first normalize Δk to remove its inherent frequency dependence.

$$\begin{aligned}\Delta \hat{k} &= \tilde{\Lambda}^{-1/2} \Delta k \tilde{\Lambda}^{-1/2} \\ &= \tilde{\Omega}^{-1} \Delta k \tilde{\Omega}^{-1}\end{aligned}\tag{3.47}$$

At this point, the non-dimensional matrices Δm and $\Delta \hat{k}$ are vectorized. Since those matrices are generally fully populated but symmetric, we can keep only the upper triangular meaningful elements and obtain:

$$V_{\Delta m} = \begin{bmatrix} \Delta m_{11} \\ \Delta m_{12} \\ \vdots \\ \Delta m_{22} \\ \Delta m_{23} \\ \vdots \\ \Delta m_{nn} \end{bmatrix} \quad \text{and} \quad V_{\Delta \hat{k}} = \begin{bmatrix} \Delta \hat{k}_{11} \\ \Delta \hat{k}_{12} \\ \vdots \\ \Delta \hat{k}_{22} \\ \Delta \hat{k}_{23} \\ \vdots \\ \Delta \hat{k}_{nn} \end{bmatrix} \quad (3.48)$$

Then, the vector of modal parameter errors representing the difference between the nominal (analysis) parameters and the test parameters (assumed to be the “truth”) is formed:

$$\Delta \hat{p} = \begin{bmatrix} V_{\Delta m} \\ V_{\Delta \hat{k}} \end{bmatrix} \quad (3.49)$$

The length of $\Delta \hat{p}$ is given by $(n^2 + n)$ where n is the number of modes in the system. In this vector, the modeling errors are expressed with respect to the analytical modal coordinates. It is reasonable to define the uncertainty in terms of the difference between the predicted and observed behavior even if the observations are not perfect. Thus, both measurement and modeling inaccuracies are included in the parameter uncertainties.

If we also define the frequency normalized modal parameter vector, \hat{p} , that contains the actual vectorized upper triangular modal mass and normalized stiffness matrix elements, m_{ij} and \hat{k}_{ij} , (just like we have done for $\Delta \hat{p}$ in (3.48)), then the covariance matrix of \hat{p} is given by (see Section A.1)

$$\Sigma_{\hat{p}\hat{p}} = E[(\hat{p} - \underline{\hat{p}})(\hat{p} - \underline{\hat{p}})^T] = E[\Delta \hat{p} \Delta \hat{p}^T] = \frac{1}{N} \sum_{i=1}^N [\Delta \hat{p} \Delta \hat{p}^T]_i \quad (3.50)$$

where E is the expectation operator (Appendix A), $\underline{\hat{p}}$ is the normalized nominal modal parameter vector (notice that we assume that the nominal values of \hat{p} correspond to their mean), and N is the overall number of comparisons (analytical models vs. experimental

measurements). The unbiased version of the estimator in Eq. 3.50 would be normalized by $(N - 1)$ instead of N , but for a small number of samples, it is more accurate as is. Also, the dimension of $\Sigma_{\hat{p}\hat{p}}$ is equal to $n^2 + n$, where n is the number of modes modeled in the system.

The covariance matrix of the modal mass matrix elements and the normalized modal stiffness elements, $\Sigma_{\hat{p}\hat{p}}$, as expressed in equation (3.50), is a very important result. The non-dimensionality of its elements (variances and covariances of the modal mass and stiffness matrix elements) makes it very suitable for use as a database as it can be readily propagated to any analytical model in modal form (see Chapter 5). Also, $\Sigma_{\hat{p}\hat{p}}$ can be written in terms of its correlation matrix (Section A.1) as follows

$$\Sigma_{\hat{p}\hat{p}} = \sigma_{\hat{p}} \rho_{\hat{p}\hat{p}} \sigma_{\hat{p}} \quad (3.51)$$

where $\sigma_{\hat{p}}$ is a diagonal (square) matrix containing the standard deviations of the normalized modal parameters (which correspond to the square roots of the diagonal elements of the covariance matrix), and $\rho_{\hat{p}\hat{p}}$ is their correlation matrix:

$$\rho_{\hat{p}\hat{p}} = \begin{bmatrix} \rho_{mm} & \rho_{m\hat{k}} \\ \rho_{m\hat{k}}^T & \rho_{\hat{k}\hat{k}} \end{bmatrix} \quad (3.52)$$

where ρ_{mm} is the correlation matrix of the modal mass matrix elements, $\rho_{\hat{k}\hat{k}}$ is the correlation matrix of the normalized modal stiffness matrix elements, and $\rho_{m\hat{k}}$ is the cross-correlation matrix of modal mass and normalized modal stiffness matrix elements.

Generation of the database

The covariance matrix of the normalized modal parameters (mass and stiffness), \hat{p} , (Eq 3.50) can be used as a database when it is obtained for a set of generically similar structures. The data required to generate these covariance matrices consists of the following:

1. A set of frequencies and mode shapes normalized to unit modal mass obtained from testing (Λ and Φ);

2. A corresponding set of analytical frequencies and mode shapes normalized to unit modal mass ($\tilde{\Lambda}$ and $\tilde{\Phi}$);
3. The analytical mass matrix, \tilde{M} , to compute the cross-orthogonality matrix.

In order to compute the cross-orthogonality matrix (Eq. 3.42), the analytical model must be reduced to the test degrees of freedom (sometimes referred to as a “Test Analysis Model”), or alternatively, the test modes may be expanded to match the original analytical model. The description of model manipulation techniques is beyond the scope of this thesis. If the cross-orthogonality matrix is available, then all that is needed to compute the covariance matrix, $\Sigma_{\hat{p}\hat{p}}$, which constitutes an uncertainty database, are the analysis and test frequencies ($\tilde{\Lambda}$ and Λ). For the purpose of the uncertainty analysis in this document, we will use the databases compiled by Hasselman in [Hasselman & Chrostowski, 1991] and described in the next subsection.

Description of Hasselman’s databases (see also appendix B)

The objective of this thesis is to evaluate the amount of uncertainty involved in the performance predictions for large high-precision controlled structures. Assessment of the performance uncertainty of these structures will be based on past experience. To do so, it is important to have an uncertainty database, $\Sigma_{\hat{p}\hat{p}}$, that reflects the amount of modeling error usually involved with these type of space systems. In other words, the database must have been obtained for structures “generically similar” to the one been evaluated. It is also important that for a particular design phase, the database reflects the uncertainty involved with the appropriate model generation. For example, early preliminary design phase corresponds to unupdated low fidelity models (usually stick models with tabulated property values), and flight testing or operations should correspond to updated high fidelity models.

Data has been compiled for several “similar” space structures and corresponding databases have been extracted [Hasselman & Chrostowski, 1991]. The data came from various military, governmental and commercial sources and corresponds to different generations of models. Two separate structural databases have been proposed: one for large truss-type space structures (LSS); and one for conventional space structures (CSS). The data for the

CSS database is segregated into pre-test models (CSS-I), which have not had the benefit of experimental verification, and post-test models (CSS-II), which have been updated to match test data as closely as possible. The models in the LSS database are considered to be neither pre-test nor post-test models. They are not pre-test models in the strict sense because all of them have been adjusted to some extent to resolve differences between the pre-test models and test data. However, the models were not “fine-tuned” as required on models of flight hardware. The models are therefore not considered post-test models in the sense as those of CSS. Hence, the LSS models are referred to as “research models” for the purpose of this text. Also, a combined database (COMB) was proposed by combining all of the compiled structures. For the rest of this document, we will refer to these four databases as Hasselman’s databases.

Research Models of Large Space Structures (LSS):

LSS refers to large truss-type space structures currently being used for research purposes. Compared to the CSS structures, these structures tend to have relatively low non-structural mass. For example, JPL Micro-Precision Instrument (MPI) testbed would fit into this category. The seven structures from which the data sets were obtained to compile the database are listed in Table B.1. Since only four modes of data were available for the third structure (LSS 3), it was omitted, leaving only 6 structures for the computation of the covariance matrix, $\Sigma_{\hat{p}\hat{p}}$, presented in Appendix B.1.

Pre-test and Post-test Models of the Conventional Space Structures (CSS):

A conventional space structure is defined as a stiff bus with flexible appendages stowed in the launch configuration. As designers minimize their structural weight to maximize payload, these structures tend to have a large proportion of non-structural mass, especially when compared to the LSS structures. The eleven structures used to compile the CSS database are listed in Table B.2. We can see from the table that data sets for pre-test and post-test models were available. Therefore, two generic categories were created. For some cases, both pre-test and post-test models were available, and for other cases, either cate-

gory of models were available, but not both. A combination of seven structures were used for the computation of the pre-test database (CSS-I) reproduced in Appendix B.2.1, and eight for the post-test database (CSS-II) shown in Appendix B.2.2. One would expect the covariance matrix of modeling error to be smaller for post-test models. Although, looking at the databases in Appendix B.2.1 and Appendix B.2.2, it is not immediately apparent that this is the case. The individual standard deviations appear to be roughly equivalent. However, they are not as discussed in the following comparison subsection.

Combined Database (COMB):

The five mode covariance matrix for the combined LSS, and CSS pretest and posttest models is reproduced in Appendix B.3. Again, no significant differences are immediately apparent between the combined database and the three separate databases.

Database Comparison

As stated earlier, in order to assess the uncertainty of the performance predictions of a system, it is important to use a database obtained from a set of structures of the same generic category. Although, these categories can have a rather broad definition as they are largely dictated by the availability of data.

For evaluating the uncertainty of the model predictions, a database obtained from unupdated (pretest) models should be used during the preliminary design phase, while a database obtained from updated models should be used as the model of the system is refined and as the modeling errors are expected to become smaller. Hence, for the latter, one would expect the covariance matrix to reflect the smaller uncertainty of the modeling errors. As we mentioned before, by looking at the database matrices listed in Appendix B, it is not very obvious that it is the case. Although, the difference becomes more apparent when comparing the eigenvalues of these covariance matrices which provide a measure of their uncertainty. In fact, taking the trace of a covariance matrix or alternatively the sum of

its eigenvalues, provides a scalar measure of uncertainty which in turn can be used to compare the relative degrees of uncertainty represented by different databases.

Table B.3 compares the singular values of the four covariance matrices obtained by singular value decomposition (SVD). We can see from the table that the pretest models reflect the largest uncertainty, while posttest models reflect the smallest uncertainty which is consistent with our intuition. Furthermore, the uncertainty of the LSS database, involving partially updated models, lies between the two extremes, while the combined database reflects an average of the three. Notice that the uncertainty of the pretest CSS models is approximately twice that of the posttest models, while that of the combined database is slightly less than that of the LSS models.

We notice all four covariance matrices are singular. This is due to the fact that their rank, which is governed by the number of structures in the database, is less than the dimension of the matrices. The covariance matrices are of dimension 30×30 , where basically 30 corresponds to the 15 upper triangular mass matrix elements and the 15 upper triangular stiffness matrix elements of a five modes model.

Limitations of the database

The database uncertainty propagation method uses past experience to provide us with a realistic way to quantify the amount of uncertainty on the FRF and the performance RMS from an analytical model before any structural testing has been done. Once testing data is available, the model can be updated and then one can still use the uncertainty propagation method with a database for updated structural models to obtain the uncertainty on the outputs that reflects the variability in the structure due to testing conditions, assembly/reassembly, and shipset variability.

One of the problem with the databases is that, often, few structures are available to generate a statistically valid generic database. Also, the only data one has available to generate a database could be from very disparate set of structures breaking the generic structures assumption. As we discussed earlier, the more similar (with respect to geometry, modal

frequency range, modal density) the structures in the database are to the current analytical model, the more confidence one will have in the uncertainty propagation results. Also, the method offers no guarantees on the modeling ability of the designer, implying that the actual error on the performance predictions might be worse, for a poor model, than the range of uncertainty one would usually expect from models in the same class of generic structures.

One other major problem we might encounter is to be faced with a database that contains less modes than the structure for which we are trying to evaluate the uncertainty. For example, the databases from [Hasselmann & Chrostowski, 1991], presented in the above subsection, contain the information for only five modes. However it would be easy to use either the posttest CSS database (which has five structures with nine or more modes), or a combination of the posttest CSS and LSS databases (see Table B.1 and Table B.2), which would give us eight structures with nine modes of uncertainty data, to construct a larger database containing nine modes. Also, it is worth mentioning that a beta version of UAI/NASTRAN software Version 20.2 is now available with a predictive accuracy capability that uses a more complete version of Hasselmann's databases containing up to nine modes. This is a slight improvement over the current five-mode database, but seems of marginal importance when we are faced with large models containing tens to hundreds of modes.

Expansion of the database

For large space structures such as SIM and NGST that contain many modes (much more than the five available in Hasselmann's databases) it would probably be more appropriate to construct a new dedicated database from more recent and more generically similar structures (e.g., HST, Chandra X-ray Observatory, or SRTM). The problem is that the necessary data might be scarce or unavailable. Using the LSS, or the CSS databases, despite their too few modes, seems at least to be a reasonable option. One can think of ways to get around the problem of having too few modes in the database:

- 1) by expanding the database by extrapolation, or
- 2) by reducing the model by selecting only a few "significant" modes.

Database Expansion by Extrapolation

The idea of significantly augmenting the size of the available databases by somehow extrapolating values for extra rows and columns of the covariance matrices $\Sigma_{\hat{p}\hat{p}}$ seems very appealing. However, further research would have to be conducted to determine how to properly extrapolate these databases and to verify the validity of such method. The derivation of such extrapolation techniques is beyond the scope of this work.

Model Reduction by Selection

The selection of “significant” modes will be explained in greater detail in Chapter 7 where one of Hasselman’s databases will be used to perform the uncertainty analysis of the SIM classic model. The idea is to use the fact that it is possible, by looking at the cumulative RMS plot of a system, to identify which of the modes are contributing the most to the total performance RMS [Gutierrez, 1999]. It turns out that, for most systems, even for very large ones, the contributions of only a few modes account for most of the total RMS. For example, a typical structure with 35 modes might have only three modes (not necessary those lowest in frequency, say modes number 8, 12 and 15) contributing to 98% of the total RMS. Also, in general those few “significant” modes are also the most sensitive ones [Gutierrez, 1999], implying that small parameter changes on these modes would create large variations in the RMS outputs. Therefore, we can argue that since the significant modes are the ones that contribute the most to the RMS and that they are also the most sensitive to parameter uncertainty, it is a valid approximation to propagate the uncertainties to the modal parameters of these selected modes only, in order to estimate the uncertainty on the total performance RMS. Doing so reduces greatly the amount of computations involved without losing much of the accuracy. However, one could argue against propagating the modal uncertainties of the database to parameters in the structures corresponding to different mode numbers (e.g.: mode 1 of the database to mode 8 of the model of our “typical” structure, mode 2 to mode 12, and mode 3 to mode 15).

Another equivalent method would be to approximate the system by a reduced model containing only the significant modes, and then perform the uncertainty analysis on the reduced model. This way of looking at the problem would dissipate the reservation mentioned about the first method since in this case, for our imaginary structure, the modes originally numbered 8, 12 and 15 would effectively become the first, second and third modes corresponding to the same mode numbers in the database.

Yet another way to obtain the same results from uncertainty propagation would be to augment the $\Sigma_{\hat{p}\hat{p}}$ matrix with rows and columns of zeros corresponding to the “non-significant” modes. The interpretation in this method would be that since we assumed that the uncertainty contributions of the non-significant modes are negligible, the uncertainty in the associated parameters can also be neglected.

3.2 Damping Estimation and Uncertainty

In this section, we will discuss how damping uncertainty plays a role in the uncertainty analysis problem. We will first go through some background in damping modeling and discuss why it is such a hard problem (Section 3.2.1). Then, we will explain how to model damping uncertainty (Section 3.2.3), and how to obtain a modal damping uncertainty database (Section 3.2.4).

3.2.1 Damping Modeling Problem

Current and future large space-based optical systems require state of the art precision structural designs in order to meet the very stringent pointing requirements. The necessary vibration suppression may be achieved through passive or active means, or a combined passive/active control approach. The enhanced damping is necessary to prevent excessive slew/settle times, unacceptable jitter levels, and harmful controls/structures interactions.

Determination of structural damping is a difficult problem [Barlow, 1992]. Historically, the inherent damping characteristics of actual built-up structures have been and still are

poorly understood and hence not particularly amenable to rational analysis. Although recent studies have improved our ability to model damping for certain types of structures, there are no general tools available for modeling damping as there are for modeling mass and stiffness. Finite element modeling can be used to determine natural frequencies, but modal testing is usually needed to provide the damping estimates necessary to predict the realistic response from finite element codes. For further discussion on this topic, see Ewins' work on structural identification [Ewins, 1984].

When no experimental data is available, for example during a preliminary design phase, we are reduced to estimating the modal damping values. The current practice is to adopt overly conservative assumptions and to assign very small damping values to these systems. For instance, values as low as 0.1 percent modal damping are sometimes assumed in early design stage. Such conservative estimates are unacceptable for performance assessment of future spacecraft systems.

Challenges with damping modeling

Sensitivity analysis of the deterministic equations of motion reveals that damping parameters are extremely important to the performance of precision controlled structures [Simonian, 1987]. Furthermore, flexible and actively controlled space structures impose additional requirements for both the precision and nature of ground vibration testing, such as developing an estimate of the on-orbit structural damping [Barlow, 1992], [Bourgault & Ubelhart, 1999]. This is especially true in actively controlled structures where the level of passive structural damping directly influences both the robustness and achievable authority of the active controller [Balas, 1982]. Since these factors influence vehicle performance, preflight knowledge of the structural damping becomes a necessity.

The difficulty of testing the next generation of large flexible space structures on the ground places an emphasis on developing innovative means of validating the predicted dynamic behavior. In some cases, the large size of the structure prohibits testing the full scale spacecraft. In other cases, the gravity-induced loads and deflections are excessive. The

prediction, and even measurement, of damping in such large built-up structures is especially challenging. Although several systematic approaches to damping prediction have been proposed, none has yet been completely verified [Crawley & O'Donnell, 1987].

Background (Modeling techniques)

Some progress has been made in recent years in analytically synthesizing highly damped structures with viscoelastic materials ([Gehling,1987], [Johnson & Kienholz, 1982], [Gilleheany, 1989], [Johnson, 1985]). In addition, emerging technology for damping synthesis can be found in literature describing the experimental design of large space structures [Hasselmann, 1972]. However, for the most part, damping is still estimated from empirical data. Table 3.1 presents a sample reference on damping modeling and design techniques. It is commonly acknowledged that damping must be included in the design as assuming very low modal damping values is too conservative and is not acceptable on high performance structures.

Current and future large space-based optical systems require state of the art precision structural designs in order to meet the very stringent pointing requirements. The necessary vibration suppression may be achieved through passive or active means or through combined passive/active control approach. Enhanced damping is often necessary to prevent excessive slew/settle times, unacceptable jitter levels, and harmful controls/structures interactions. Table 3.1 gives a description of different damping enhancement devices.

3.2.2 Sources of Damping Uncertainty

Modal damping represents the energy dissipation per cycle in a particular mode, assuming that the mode vibrates independently of the other structural modes. The modal damping ratio, ζ_r , is proportional to the ratio of modal dissipative energy, D_r , to modal kinetic energy, K_r , which is constant in the case of linear viscous damping.

$$\zeta_r = \frac{1}{4\pi} \left(\frac{D_r}{K_r} \right) \quad (3.53)$$

TABLE 3.1 Damping Enhancement Devices

damping devices	description	reference
Constrained layer damping technique	Significantly increases the initial amount of damping by replacing some of the struts of a truss structure with members having a constrained layer of viscoelastic material.	[Slater, 1991], [Balas, 1982], [Lim & Giesy, 2000]
Shunted piezoelectric materials	Passive damping	[Gutierrez, Bour-gault & Miller, 1999] and [Hagood, 1989]
Semi-active elements	Combine active and passive isolation (e.g. Honeywell "D-strut" for Hubble Space Telescope Reaction Wheel Assembly isolation),	[Crawley & O'Donnell, 1987]

In general, the ratio of dissipative to kinetic energy is not constant, but depends on other factors including vibration amplitude, frequency and temperature. Nevertheless, in the absence of more accurate models, the equivalent linear viscous damping model is commonly accepted with the understanding that the parameters of that model must be determined experimentally and often with a large degree of uncertainty. Table 3.2 list different sources of damping uncertainty.

3.2.3 Damping Uncertainty Estimation

Since a combination of passive and active damping measures will necessarily be implemented on any future space telescope and will improve the damping by multiple orders of magnitudes, it necessary that these measures be reflected in the model when propagating the damping uncertainty. Otherwise, the variance on the performance predictions of damping uncertainty would be insignificant in comparison to the huge modeling error induced by omitting damping enhancement techniques.

Since we made the proportional damping assumption (Chapter 2), all modes of the system are considered decoupled (diagonal modal damping matrix). Stated differently, each mode vibrates independently of the other structural modes and has its own damping ratio. On a

TABLE 3.2 Sources of damping uncertainty in damping estimate

Sources of Damping Uncertainty	References
Fast Fourier Transform approximations due to leakage, resolution, bias and variance errors (FFTs typically overestimate damping ratio).	[Pandit, 1989]
Nonlinearities in the system introduce dependence on forcing amplitude (e.g. joint deadband).	[Wada, 1988], [Ingham, 1998]
Non-structural sources which are absent in the space environment (e.g. gravity effects, air damping, wiring harnesses).	[Ingham, 1998], [Barlow, 1992]
<p>Linear viscous damping approximation:</p> <ul style="list-style-type: none"> • The ratio of dissipative to kinetic energy is not really constant, but depends on other factors including amplitude, frequency and temperature. • Despite the fact that the off-diagonal elements of the transformed damping matrix are generally of the same order of magnitude as the diagonal elements, they are typically neglected. The diagonal elements are expressed in terms of critical damping ratio consistent with the assumption that the equations of motion are uncoupled in modal coordinates. This assumption is valid for lightly damped, well separated modes. 	[Hasselmann, 1976]

real structure, this is not necessarily the case, and the damping matrix is in general fully populated. This, in addition to the fact that the modal damping ratios, which represent the energy dissipation capacity, are amplitude, frequency and temperature dependent, partially accounts for the large degree of the uncertainty in damping.

In the previous subsection, we have seen that although there have been improvements in the ability to model structural damping, it remains a challenging task. General tools for modeling damping are not yet available. Thus, damping ratios must be estimated from experimental measurements. If no measurements are available, the modal damping ratios must be estimated based on past experience. Therefore, the rationale for quantifying the

uncertainty based on the variability between the analytical and test model parameters over a family of similar structures is not valid for the damping. Instead, we will define the damping uncertainty in terms of the variability of the experimental modal damping estimates. In this case, we can think of several ways to obtain a measure of the damping uncertainty depending on the availability of the data and the current generation (maturity) of our structural model. We present here three different methods of building a damping database, (later referred to as databases of type 1, 2, and 3) which correspond to an increasing need for accuracy in the uncertainty predictions:

1. If the available statistical data is rare, and/or the model is in an early stage, insofar as we do not have a good feel for the damping values, we could statistically analyze the experimental values of the damping ratios obtained for one particular structure. The single global mean, μ , and the variance, σ^2 , obtained for the ensemble of damping ratios could be used as a first cut estimate for all the nominal damping ratios ($\tilde{\zeta}_r = \mu$), and their variability ($\sigma_{\tilde{\zeta}_r}^2 = \sigma^2$). The same type of database could also be obtained from the statistical analysis of the experimental damping values from more than one structure at the time. The advantages of this method are that it is very cost-efficient to perform and it provides us with both an estimate for the uncertainty and the nominal parameter values. Alternatively, we could decide to arbitrarily set the nominal values at more conservative levels. The high level of uncertainty of our estimates is captured by the large value of σ , which comes from the high variability of the experimental damping values from mode to mode.
2. If more data is available, and we want to increase the accuracy of our uncertainty predictions, we could perform the statistical analysis for each mode from the data of multiple structures. This way, multiple modal mean values $[\mu_1, \dots, \mu_n]$ and variances $[\sigma_1^2, \dots, \sigma_n^2]$ are obtained. While providing us with estimates of the nominal parameters ($\tilde{\zeta}_r = \mu_r$) and their uncertainty ($\sigma_{\tilde{\zeta}_r}^2 = \sigma_r^2$), this method also reveals the fact that the modal damping ratios,

and their variability, are different for each mode. In this way, the estimates are more accurate as they reflect the acknowledged fact of the modal dependence of the damping values. Here too, rather than using the mean values provided by the statistical analysis, we could decide to use our own arbitrary modal damping ratio estimates, yet still use the variances from the statistical analysis to estimate their uncertainty.

3. If our damping model is very accurate (for example, if it is updated from experimental measurements), then we can assume that the damping errors depend only on the variability of the environmental factors affecting the damping (noises, perturbations, temperature). In this case, in order to have a more accurate estimate of the uncertainty, we could statistically compute the variance and mean values of each modal damping ratios from multiple measurements of the same structure taken on different days. In so doing, we would have a fairly accurate model of the uncertainty (and the nominal value of the damping ratios). To get an uncertainty model for shipset variability, the same procedure could be implemented where the multiple measurements would come from different representatives of the same type of structure.

Other variations of the same methodology could be appropriate as well.

Methodology

For the purpose of this work, we will assume the modal damping ratios to have lognormal distributions. This assumption is based on the results presented in [Simonian, 1987]. Lognormal distributions are not symmetric (see Figure A.3), but it is possible to transform them into Gaussian distributions -- a rather useful characteristic. Linear systems have the property of preserving "Gaussianness" (or normality) [Gelb & al., 1974]. To use this property for the uncertainty propagation of the damping, the first step will be to transform the damping ratio distributions from the logarithmic space (ζ_r) to the gaussian space (γ_r)

$$\zeta_r \rightarrow \gamma_r = \ln \zeta_r \quad (3.54)$$

where ζ_r is the modal damping ratio as defined in Chapter 2, and γ_r is the transformed modal damping ratio. The reciprocal of equation (3.54) is given by

$$\zeta_r = e^{\gamma_r} \quad (3.55)$$

This means that the modal damping matrix, Z , as defined in equation (2.19), becomes

$$Z = \begin{bmatrix} \ddots & & \\ & \zeta_r & \\ & & \ddots \end{bmatrix} = \begin{bmatrix} \ddots & & \\ & e^{\gamma_r} & \\ & & \ddots \end{bmatrix} = Z_\gamma \quad (3.56)$$

where even though the matrices Z and Z_γ are equal, we will use through out this document the notation Z_γ to distinguish the transformed matrix Z . The Gaussian PDF is obtained from the lognormal PDF as follows

$$f_{\gamma_r}(\gamma_{r0}) = f_{\zeta_r}(\zeta_{r0}) \left| \frac{d\zeta_{r0}}{d\gamma_{r0}} \right| \quad (3.57)$$

where the Jacobian of the transformation is given by

$$\left| \frac{d\zeta_{r0}}{d\gamma_{r0}} \right| = e^{\gamma_r} \quad (3.58)$$

Using the lognormal distribution as defined in equation (A.44) and replacing in (3.57) yields the normal distribution

$$\begin{aligned} f_{\gamma_r}(\gamma_{r0}) &= \frac{1}{\sqrt{2\pi}\zeta_{r0}d} e^{-(\ln(\zeta_{r0})-c)^2/2d^2} \cdot e^{\gamma_r} \\ &= \frac{1}{\sqrt{2\pi}d} e^{-(\gamma_{r0}-c)^2/2d^2} \end{aligned} \quad (3.59)$$

where the mean and variance of the gaussian distribution correspond to the parameters c and d of the lognormal

$$\begin{aligned}\mu_{\gamma_r} &= c \\ \sigma_{\gamma_r}^2 &= d^2\end{aligned}\quad (3.60)$$

and where c and d are obtained from the statistical analysis of the modal damping ratio ζ_r from equation (A.45)

$$c = \ln\left(\frac{\mu_{\zeta_r}}{\sqrt{\rho_{\zeta_r}^2 + 1}}\right), \quad d = \sqrt{\ln(\rho_{\zeta_r}^2 + 1)} \quad (3.61)$$

where $\rho_{\zeta_r}^2$ is the covariance and is given by

$$\rho_{\zeta_r}^2 = \left(\frac{\sigma_{\zeta_r}}{\mu_{\zeta_r}}\right)^2 \quad (3.62)$$

Therefore, once we have μ_{ζ_r} and σ_{ζ_r} for each mode from statistical analysis of the data (using one of the three above) the gaussian distribution parameters for each mode (μ_{γ_r} and σ_{γ_r}) are very easy to obtain using equations (3.60) and (3.61).

Linear Perturbation Analysis

We will relate the analytical transformed modal damping parameters to the parameters of the actual structure as follows

$$\gamma_r = \tilde{\gamma}_r + \Delta\gamma_r \quad (3.63)$$

or in matrix notation

$$\Gamma = \tilde{\Gamma} + \Delta\Gamma \quad (3.64)$$

where, due to our assumption of proportional damping, the parameters are decoupled, and the matrices Γ and $\tilde{\Gamma}$ are diagonal. They contain, respectively, the actual transformed modal damping ratios γ_r and the nominal transformed damping ratios $\tilde{\gamma}_r$. The matrix $\Delta\Gamma$ is the difference between the actual and the nominal transformed modal damping ratio matrices ($\Gamma - \tilde{\Gamma}$).

Statistical Analysis

At this point, we vectorize the matrix $\Delta\Gamma$ as follows

$$V_{\Delta\gamma} = \Delta\gamma = \begin{bmatrix} \Delta\gamma_1 \\ \vdots \\ \Delta\gamma_n \end{bmatrix} \quad (3.65)$$

where n corresponds to the number of modes in the system. Just like we did for the modal mass and stiffness parameters (Eq. 3.50), we can define a covariance matrix for the transformed modal damping ratios, $\Sigma_{\gamma\gamma}$, as follows

$$\Sigma_{\gamma\gamma} = E[\Delta\gamma\Delta\gamma^T] \quad (3.66)$$

which is a diagonal matrix since, based on our assumption that all damping parameters are independent. The diagonal elements correspond to the variance of every transformed modal damping parameter. Therefore, $\Sigma_{\gamma\gamma}$ can be constructed directly from the transformed variances obtained after the statistical analysis (Eq. 3.60)

$$\Sigma_{\gamma\gamma} = \begin{bmatrix} \ddots & & \\ & \sigma_{\gamma_r}^2 & \\ & & \ddots \end{bmatrix} = \begin{bmatrix} \ddots & & \\ & d_r^2 & \\ & & \ddots \end{bmatrix} \quad (3.67)$$

We extend our definition of the uncertain modal parameters, as defined in equation (3.49), by appending to the normalized vector of modeling errors $\Delta\hat{p}$, the vector of transformed modal damping parameters errors $V_{\Delta\gamma}$, as follows:

$$\Delta\hat{p} = \begin{bmatrix} V_{\Delta m} \\ V_{\Delta\hat{k}} \\ V_{\Delta\gamma} \end{bmatrix} \quad (3.68)$$

where, for a system with n modes, the length of \hat{p} becomes equal to $(n^2 + n + n = n^2 + 2n)$. The augmented covariance matrix is given by

$$\Sigma_{\hat{p}\hat{p}} = E[\Delta\hat{p}\Delta\hat{p}^T] = \begin{bmatrix} \Sigma_{mm} & \Sigma_{m\hat{k}} & 0 \\ \Sigma_{\hat{k}m} & \Sigma_{\hat{k}\hat{k}} & 0 \\ 0 & 0 & \Sigma_{\gamma\gamma} \end{bmatrix} \quad (3.69)$$

which is block diagonal since the damping uncertainty is estimated independently from the mass and stiffness uncertainty.

3.2.4 Database

To fulfill the objective of determining jitter amplitude uncertainty for spaceborne telescopes, it is critical to evaluate the damping uncertainty, as it has great impact on the overall performance of the system. Damping being hard to model, one must look at past experience data for similar types of structures to determine its statistical characteristics. In the previous subsection, we described three different approaches to obtain a damping database. All these approaches were based on statistical analysis of measured damping data. For the purpose of this research we will use the damping measurement data compiled by Simonian [Simonian, 1987]. After describing Simonian's damping compilation, we will give an example of how to generate a database of *Type 1*.

Description of Simonian's damping compilation

Simonian has gathered and compiled measured damping values for a multitude of spacecraft structures. His results include published data from on-orbit damping measurements and results from ground modal testing of spacecraft. Since damping is amplitude dependent, satellite data measured at higher vibration amplitudes were removed from the survey. The damping data compiled is comprised of results taken from 23 different spacecraft (Table C.1) with a total of 290 sample measurements spanning the frequency range from 0.15 through 195 Hz.

The results of the statistical analysis are summarized in Table C.2. This analysis was performed for various combinations of the data, grouped by frequency bandwidth (identified

by letter A through G in the table). For each group of data analyzed, a histogram was constructed, and the probability density functions (PDF) were obtained by fitting the data.

The most interesting result of the study is perhaps the fact that, for each frequency group, it appears that the disturbances at the damping ratios ζ_r fit well to a lognormal probability density function (PDF). The parameters for this type of fitted PDF are presented in Table C.2. It is also very interesting to note that measured building damping factors also fit well with these types of PDF ([Haviland, 1976], [Hasselmann & Simonian, 1980]). The fact that the damping ratios for structures from very different fields (buildings vs. light spacecraft) have the same kind of distribution supports the validity of the approach.

Generation of the database

In this subsection, we give an example of how to generate a damping uncertainty database using Simonian's statistical data. The database generated will be of *Type 1*, as described in Section 3.2.3. This exercise will be particularly useful for the application in Chapter 7 where we will perform the uncertainty analysis on the old SIM Classic model which, though quite detailed, constitutes an early stage model for which it is fair to say that its damping model is very uncertain. To match the number of modes contained in Hasselmann's database (see Section 3.1.2), we will build a five mode damping database.

Database of Type 1:

In this case, we use the broadband (group A) statistical data from the Simonian's compilation (Table C.2). From the table, we get the lognormal parameter $d = 0.680$ which, using the identity, translates to a variance in the Gaussian-space of $\sigma_{\gamma_r}^2 = d^2 = (0.680)^2$. Hence, in this case, the covariance matrix is constant for all the modal damping ratios.

$$\Sigma_{\gamma\gamma} = \begin{bmatrix} \ddots & & \\ & d^2 & \\ & & \ddots \end{bmatrix} = d^2 I \quad (3.70)$$

It should be noted that the ζ values used to construct the tables in Appendix C are in percent (%). It has been shown experimentally that the amount of damping varies for each mode [Ewins, 1984], actual damping measurements on various spacecraft have given values between 0.02 and 0.005.

Database of Type 1 (variant):

In this variant of the *Type 1* method, in an attempt to increase the accuracy of the uncertainty analysis, we want the covariance matrix to reflect the modal dependency of the damping uncertainty. With this in mind, we assume that the first five modes of the SIM model are spread such that each of them is included in the frequency range of a different group. Hence, we have associated the mode numbers 1 to 5 to the frequency bins B to F in Table C.2. The pertinent data, extracted from Table C.2, are reproduced here in Table 3.3.

TABLE 3.3 Extracted Damping Statistics

Frequency Interval (Hz)	c	d
B: 0.14 - 9.99	0.379	0.725
C: 10.00 - 19.99	-0.218	0.560
D: 20.00 - 29.99	-0.0475	0.653
E: 30.00 - 39.99	-0.108	0.623
F: 40.00 - 49.99	0.0755	0.572
Gaussian Parameters	μ_{γ_r}	σ_{γ_r}

Using the data from Table 3.3 we construct the damping covariance matrix as follows

$$\Sigma_{\gamma\gamma} = \begin{bmatrix} (0.725)^2 & & & & \\ & (0.560)^2 & & & \\ & & (0.653)^2 & & \\ & & & (0.623)^2 & \\ & & & & (0.572)^2 \end{bmatrix} \quad (3.71)$$

This is the covariance matrix that we will use to demonstrate the methodology of the uncertainty analysis in Chapter 7.

Although the nominal values for the ζ_r 's have already been set up in the SIM model, we could also use the data from the table to obtain an estimate of the nominal transformed damping ratios by setting the nominal values equal to the mean ($\tilde{\gamma}_r = \mu_{\gamma_r} = c_r$).

We would like to remark at this point that because of the way the data was analyzed in Simonian's compilation, the above transformed modal damping database (Eq. 3.71) represents more of a frequency dependent damping uncertainty than one that is dependent on the modal number. Indeed, for each frequency bin in Table C.2, the statistical parameters presented were computed over a range of disparate modes. This is due to the fact that different structures have different modal frequency spacing. Hence, in the frequency range responding to group B, (Table C.2) for example, it is possible that many modes of a particular structure are included in the bandwidth; for another structure, the first mode could be at a higher frequency than the range and not even be included; while a few of the intermediate modes of yet another structure could be in the middle of the range, and so on. Therefore, it is the author's belief that in order to remove the frequency dependence from the uncertainty database, and better represent the modal dependence of the uncertainty, future damping uncertainty data analysis should be performed by evaluating the statistical parameters either for a single mode at a time or by grouping the data using modal bins rather than frequency bins. Such an analysis would correspond to a *Type 2* method.

3.3 Summary

In this chapter, we have presented methodologies for computing uncertainties for the modal mass, stiffness and transformed damping. Modal mass and stiffness uncertainties for a structural model are expressed as a function of the error in the eigenvalue and mode shape predictions (cross-orthogonality). The methodology for obtaining modal mass and stiffness uncertainties is based on linear perturbation analysis of the eigen-problem. A database consisting of a covariance matrix of the normalized modal parameters (m and k), constructed from statistical analysis of families of structure/model pairs was presented [Hasselmann & Chrostowski, 1991]. The main limitations of the database are the limited sources of data available for statistical validity, and the limited number of modes documented for each sampled structure. Damping uncertainty for a structural model is defined in terms of the variability in experimental modal damping estimates. A methodology for obtaining damping uncertainties was outlined, assuming lognormal distributions for the modal damping data. The damping parameters were transformed from the lognormal space to the Gaussian space, in order to propagate their corresponding uncertainties. Three methods for generating damping uncertainty database were introduced, corresponding to different levels of accuracy (from model generation) in the uncertainty predictions.

Chapter 4

SENSITIVITY ANALYSIS

In order to propagate the uncertainties from the databases presented in Chapter 3, we will need to first perform a sensitivity analysis. In this chapter, we derive the first order derivatives (sensitivities) of the RMS metrics and FRF (magnitude and phase) with respect to the database parameters, p (Section 4.1). Also, in order to establish the range of validity for these sensitivities, it is necessary to evaluate their curvature (second order derivatives) (Section 4.2). These curvatures will help us determine the range of perturbation for which the linearity of the system is preserved.

In a broader perspective, the sensitivity analysis can be used to identify which of the system design parameters (modal or physical) have the strongest influence on the performance of the integrated system, and use this knowledge to modify the design and improve the performances. This will not be the subject of the present document as it is well discussed in [Gutierrez, 1999].

4.1 First Order Derivatives (Sensitivities)

As we mentioned in Chapter 5, the derivatives, $\partial u / \partial p$, are particularly easy to derive whenever u represents an eigenvalue or eigenvector and p represents a modal mass or stiffness parameter (Section 4.1.1). Also, $\partial u / \partial p = 0$ when u represents an undamped eigenvalue or an eigenvector and p represents modal damping.

4.1.1 Eigenderivatives

In this section, we derive the expressions for the eigenvalue and the eigenvector first order derivatives with respect to the modal mass and stiffness matrix elements m and k (expressed in the analytical modal coordinates). A similar development can be found in [Hasselmann & Chrostowski, 1991]. Other references include [Kato, 1966], [Rellich, 1969], [Huag, 1986], and [Chen, 1985]. The resulting expressions will be used to propagate the uncertainties in the modal mass and stiffness matrices and, ultimately, into the FRF and the RMS response of the system.

Eigenvalue derivatives

We start with the undamped eigenproblem seen in Eq. 2.4 and reproduced below

$$(K - \lambda_r M)\phi_r = 0 \quad (4.1)$$

Taking the derivative with respect to the modal parameter p_k , the k^{th} element of the vector of modal parameters p , gives

$$\frac{\partial}{\partial p_k}[(K - \lambda_r M)\phi_r] = 0 \quad (4.2)$$

$$\Leftrightarrow (K - \lambda_r M)\frac{\partial \phi_r}{\partial p_k} + \left(\frac{\partial K}{\partial p_k} - \lambda_r \frac{\partial M}{\partial p_k}\right)\phi_r - \frac{\partial \lambda_r}{\partial p_k} M\phi_r = 0 \quad (4.3)$$

Pre-multiplying equation 4.3 by ϕ_r^T gives

$$\phi_r^T (K - \lambda_r M)\frac{\partial \phi_r}{\partial p_k} + \phi_r^T \left(\frac{\partial K}{\partial p_k} - \lambda_r \frac{\partial M}{\partial p_k}\right)\phi_r - \frac{\partial \lambda_r}{\partial p_k} \phi_r^T M\phi_r = 0 \quad (4.4)$$

Using the transpose of Eq. 4.1, $\phi_r^T (K - \lambda_r M) = 0$ with K and M symmetric ($K = K^T$ and $M = M^T$), and the orthogonality principle ($\phi_r^T M\phi_r = 1$), we get the following expression

$$\frac{\partial \lambda_r}{\partial p_k} = \phi_r^T \left(\frac{\partial K}{\partial p_k} - \lambda_r \frac{\partial M}{\partial p_k} \right) \phi_r \quad (4.5)$$

After post-multiplication by Δp_k , the uncertainty on modal parameter p_k , we obtain

$$\frac{\partial \lambda_r}{\partial p_k} \Delta p_k = \phi_r^T \left(\frac{\partial K}{\partial p_k} \Delta p_k - \lambda_r \frac{\partial M}{\partial p_k} \Delta p_k \right) \phi_r \quad (4.6)$$

The above expression can be rewritten as follow

$$\frac{\partial \lambda_r}{\partial p_k} \Delta p_k = \phi_r^T (\Delta K_k - \lambda_r \Delta M_k) \phi_r \quad (4.7)$$

where ΔK_k and ΔM_k are the uncertainty contributions to the stiffness and mass matrix respectively, due to the uncertainty on the parameter p_k and are elements of matrices ΔK and ΔM , defined as follows

$$\begin{aligned} \sum_k \Delta M_k &= \sum_k \frac{\partial M}{\partial p_k} \Delta p_k = \Delta M \\ \sum_k \Delta K_k &= \sum_k \frac{\partial K}{\partial p_k} \Delta p_k = \Delta K \end{aligned} \quad (4.8)$$

Substituting equation 3.5, for ϕ_r , in equation 4.7, we get

$$\frac{\partial \lambda_r}{\partial p_k} \Delta p_k = (\tilde{\phi}_r + \Delta \phi_r)^T (\Delta K_k - \lambda_r \Delta M_k) (\tilde{\phi}_r + \Delta \phi_r) \quad (4.9)$$

which after performing the multiplication gives

$$\begin{aligned} \frac{\partial \lambda_r}{\partial p_k} \Delta p_k &= \tilde{\phi}_r^T (\Delta K_k - \lambda_r \Delta M_k) \tilde{\phi}_r + \tilde{\phi}_r^T (\Delta K_k - \lambda_r \Delta M_k) \Delta \phi_r \\ &\quad + \Delta \phi_r^T (\Delta K_k - \lambda_r \Delta M_k) \tilde{\phi}_r + \Delta \phi_r^T (\Delta K_k - \lambda_r \Delta M_k) \Delta \phi_r \end{aligned} \quad (4.10)$$

Neglecting second and third order terms, and replacing λ_r in the above equation with the expression given in (3.4), we get

$$\frac{\partial \lambda_r}{\partial p_k} \Delta p_k = \tilde{\phi}_r^T (\Delta K_k - (\tilde{\lambda}_r + \Delta \lambda_r) \Delta M_k) \tilde{\phi}_r \quad (4.11)$$

Again, we neglect the second order term and obtain the following expression

$$\frac{\partial \lambda_r}{\partial p_k} \Delta p_k = \tilde{\phi}_r^T (\Delta K_k - \tilde{\lambda}_r \Delta M_k) \tilde{\phi}_r \quad (4.12)$$

Summing over all k^{th} derivatives we find

$$\begin{aligned} \sum_k \frac{\partial \lambda_r}{\partial p_k} \Delta p_k &= \sum_k \tilde{\phi}_r^T (\Delta K_k - \lambda_r \Delta M_k) \tilde{\phi}_r = \tilde{\phi}_r^T \left(\sum_k \Delta K_k - \lambda_r \sum_k \Delta M_k \right) \tilde{\phi}_r \\ &= \tilde{\phi}_r^T (\Delta K - \lambda_r \Delta M) \tilde{\phi}_r = \Delta \lambda_r \end{aligned} \quad (4.13)$$

If we divide both sides of equation (4.12) by Δp_k and take the limit as Δp_k approaches zero, and use the definitions in (4.8), we get an expression of the sensitivity of the r^{th} eigenvalue with respect to the k^{th} modal parameter

$$\frac{\partial \lambda_r}{\partial p_k} = \tilde{\phi}_r^T \left(\frac{\partial K}{\partial p_k} - \tilde{\lambda}_r \frac{\partial M}{\partial p_k} \right) \tilde{\phi}_r \quad (4.14)$$

It is important to remember that the above sensitivity expression is for the nominal plant (i.e., it is evaluated at the nominal parameters) and should in fact be designated $(\partial \lambda_r / \partial p_k) \big|_{\tilde{p}_k}$ to be precise. Since, for the purposes of uncertainty propagation, we always evaluate the sensitivities for the nominal plant, it will be assumed through out this document that the sensitivity as noted in (4.14) are always evaluated at the nominal parameter.

Equation (4.14) can be rewritten as following

$$\frac{\partial \lambda_r}{\partial p_k} = \tilde{\phi}_r^T \frac{\partial K}{\partial p_k} \tilde{\phi}_r - \tilde{\lambda}_r \tilde{\phi}_r^T \frac{\partial M}{\partial p_k} \tilde{\phi}_r \quad (4.15)$$

where we will compute $\tilde{\phi}_r^T \frac{\partial K}{\partial p_k} \tilde{\phi}_r$ and $\tilde{\phi}_r^T \frac{\partial M}{\partial p_k} \tilde{\phi}_r$ separately.

First, let us calculate the part containing the mass matrix, M . We have defined the true modal mass expressed in the nominal modal coordinates in equation (3.24) as

$$m = \tilde{\Phi}^T M \tilde{\Phi} \quad (4.16)$$

Differentiating with respect to p_k gives

$$\frac{\partial m}{\partial p_k} = \frac{\partial \tilde{\Phi}^T}{\partial p_k} M \tilde{\Phi} + \tilde{\Phi}^T \frac{\partial M}{\partial p_k} \tilde{\Phi} + \tilde{\Phi}^T M \frac{\partial \tilde{\Phi}}{\partial p_k} \quad (4.17)$$

where $\frac{\partial \tilde{\Phi}}{\partial p_k} = \frac{\partial \tilde{\Phi}^T}{\partial p_k} = 0$ since the nominal mode shapes are constant. This leaves us with

$$\tilde{\Phi}^T \frac{\partial M}{\partial p_k} \tilde{\Phi} = \frac{\partial m}{\partial p_k} \quad (4.18)$$

or

$$\tilde{\Phi}_r^T \frac{\partial M}{\partial p_k} \tilde{\Phi}_s = e_r^T \frac{\partial m}{\partial p_k} e_s = \frac{\partial m_{rs}}{\partial p_k} = \begin{cases} 1, & \text{if } p_k = m_{rs} \\ 0, & \text{otherwise} \end{cases} \quad (4.19)$$

where e_r and e_s are unitary vectors containing one at the r^{th} and s^{th} entry respectively and zeros everywhere else.

Then, using a similar approach for the part with the stiffness matrix, K , we obtain

$$\tilde{\Phi}_r^T \frac{\partial K}{\partial p_k} \tilde{\Phi}_s = e_r^T \frac{\partial k}{\partial p_k} e_s = \frac{\partial k_{rs}}{\partial p_k} = \begin{cases} 1, & \text{if } p_k = k_{rs} \\ 0, & \text{otherwise} \end{cases} \quad (4.20)$$

where as defined in (3.24), k is the true modal stiffness expressed in analytical modal coordinates. Substituting equations (4.19) and (4.20) into (4.15) gives us the final expression for the eigenvalues sensitivity expression

$$\boxed{\frac{\partial \lambda_r}{\partial p_k} = \frac{\partial k_{rr}}{\partial p_k} - \tilde{\lambda}_r \frac{\partial m_{rr}}{\partial p_k} = \begin{cases} -\tilde{\lambda}_r, & \text{if } p_k = m_{rr} \\ 1, & \text{if } p_k = k_{rr} \\ 0, & \text{otherwise} \end{cases}} \quad (4.21)$$

Eigenvector derivatives

Let us now attack the derivation of the mode shape sensitivities. Starting with equation (4.3) and substituting the expressions for K , M , λ_r and ϕ_r from equations (3.2), (3.3), (3.4) and (3.5), we get

$$(\bar{K} + \Delta K - (\tilde{\lambda}_r + \Delta\lambda_r)(\tilde{M} + \Delta M)) \frac{\partial \phi_r}{\partial p_k} + \left(\frac{\partial K}{\partial p_k} - (\tilde{\lambda}_r + \Delta\lambda_r) \frac{\partial M}{\partial p_k} \right) (\tilde{\phi}_r + \Delta\phi_r) - \frac{\partial \lambda_r}{\partial p_k} (\tilde{M} + \Delta M) (\tilde{\phi}_r + \Delta\phi_r) = 0 \quad (4.22)$$

Expanding and neglecting second and third order terms gives

$$(\tilde{K} - \tilde{\lambda}_r \tilde{M}) \frac{\partial \phi_r}{\partial p_k} + \left(\frac{\partial K}{\partial p_k} - \tilde{\lambda}_r \frac{\partial M}{\partial p_k} \right) \tilde{\phi}_r - \frac{\partial \lambda_r}{\partial p_k} \tilde{M} \tilde{\phi}_r = 0 \quad (4.23)$$

It is interesting to mention here that in the same way that we have demonstrated the equivalence of equations (4.12) and (3.18) by performing the summation over the “k” parameters, we could show that the newly obtained equation (4.23) is also consistent with equation (3.15). In order to compute equation (4.23), we start by rearranging it as the following

$$\begin{aligned} (\tilde{K} - \tilde{\lambda}_r \tilde{M}) \frac{\partial \phi_r}{\partial p_k} &= \frac{\partial \lambda_r}{\partial p_k} \tilde{M} \tilde{\phi}_r - \left(\frac{\partial K}{\partial p_k} - \tilde{\lambda}_r \frac{\partial M}{\partial p_k} \right) \tilde{\phi}_r \\ &= F_r \end{aligned} \quad (4.24)$$

where F_r is a $(n \times 1)$ vector. The problem with solving equation (4.24) comes from the rank deficiency of $(\tilde{K} - \tilde{\lambda}_r \tilde{M})$. For example, we can express the eigenvector derivative as a linear combination of all nominal eigenvectors

$$\frac{\partial \phi_r}{\partial p_k} = \sum_{i=1}^n \tilde{\phi}_i a_i = \tilde{\Phi} a \quad (4.25)$$

where a is a vector of arbitrary constants that we have to find. If we plug in this expression as is into equation (4.24) and pre-multiply by $\tilde{\Phi}^T$, we get the following

$$\tilde{\Phi}^T (\tilde{K} - \tilde{\lambda}_r \tilde{M}) \tilde{\Phi} a = [\tilde{\Lambda} - \tilde{\lambda}_r I] a = \tilde{\Phi}^T F_r \quad (4.26)$$

which in detail looks like

$$\begin{bmatrix} \tilde{\lambda}_1 & & & \\ & \ddots & & \\ & & \tilde{\lambda}_r & \\ & & & \ddots \\ & & & & \tilde{\lambda}_n \end{bmatrix} - \tilde{\lambda}_r \begin{bmatrix} 1 & & & \\ & \ddots & & \\ & & 1 & \\ & & & \ddots \\ & & & & 1 \end{bmatrix} \begin{Bmatrix} a_1 \\ \vdots \\ a_r \\ \vdots \\ a_n \end{Bmatrix} = \begin{bmatrix} (\tilde{\lambda}_1 - \tilde{\lambda}_r) & & & \\ & \ddots & & \\ & & (\tilde{\lambda}_r - \tilde{\lambda}_r) & \\ & & & \ddots \\ & & & & (\tilde{\lambda}_n - \tilde{\lambda}_r) \end{bmatrix} \begin{Bmatrix} a_1 \\ \vdots \\ a_r \\ \vdots \\ a_n \end{Bmatrix} = \tilde{\Phi}^T F_r \quad (4.27)$$

where we notice that the r^{th} element on the diagonal is equal to zero ($\tilde{\lambda}_r - \tilde{\lambda}_r = 0$). From (4.27), we can see that the i^{th} element of the vector a can be express as

$$a_i = \frac{\tilde{\Phi}_i^T F_r}{(\tilde{\lambda}_i - \tilde{\lambda}_r)}, \quad \text{for } i \neq r \quad (4.28)$$

where F_r was defined in (4.24). So, all the elements of vector a can be found except a_r , since when we write explicitly F_r in (4.28) and apply the orthogonality principle and the definition for $\partial\lambda_r/\partial p_k$ from (4.14) we get

$$a_r = \frac{\tilde{\Phi}_r^T F_r}{(\tilde{\lambda}_r - \tilde{\lambda}_r)} = \frac{\frac{\partial\lambda_r}{\partial p_k} \tilde{\Phi}_r^T M \tilde{\Phi}_r - \tilde{\Phi}_r^T \left(\frac{\partial K}{\partial p_k} - \tilde{\lambda}_r \frac{\partial M}{\partial p_k} \right) \tilde{\Phi}_r}{(\tilde{\lambda}_r - \tilde{\lambda}_r)} = \frac{\frac{\partial\lambda_r}{\partial p_k} - \frac{\partial\lambda_r}{\partial p_k}}{(\tilde{\lambda}_r - \tilde{\lambda}_r)} = \frac{0}{0} \quad (4.29)$$

which constitutes an indeterminate situation. Hence, we need an extra procedure to find the term a_r .

To resolve this problem, we can rewrite equation (4.25) as a linear combination of $(n - 1)$ nominal eigenvectors, for which we can find the associated coefficients, a_i 's, plus the product of an indeterminate constant, a_r , and the remaining eigenvector as follows

$$\frac{\partial\Phi_r}{\partial p_k} = \underbrace{\sum_{\substack{i=1 \\ i \neq r}}^n \tilde{\Phi}_i a_i}_{V_r} + \tilde{\Phi}_r a_r = V_r + \tilde{\Phi}_r a_r \quad (4.30)$$

Notice that V_r is orthogonal with $\tilde{\Phi}_r a_r$ with respect to the mass matrix since

$$V_r^T \tilde{M} \tilde{\phi}_r a_r = \left(\sum_{\substack{i=1 \\ i \neq r}}^n \tilde{\phi}_i a_i \right)^T \tilde{M} \tilde{\phi}_r a_r = \sum_{\substack{i=1 \\ i \neq r}}^n a_i a_r \tilde{\phi}_i^T \tilde{M} \tilde{\phi}_r = 0 \quad (4.31)$$

where, by the orthogonality principle, $\tilde{\phi}_i^T \tilde{M} \tilde{\phi}_r$ is always equal to zero for $i \neq r$.

Now, since $\phi_r^T M \phi_r = 1$, we get the following expression after differentiation

$$\frac{\partial(\phi_r^T M \phi_r)}{\partial p_k} = \frac{\partial \phi_r^T}{\partial p_k} M \phi_r + \phi_r^T \frac{\partial M}{\partial p_k} \phi_r + \phi_r^T M \frac{\partial \phi_r}{\partial p_k} = \phi_r^T \frac{\partial M}{\partial p_k} \phi_r + 2 \phi_r^T M \frac{\partial \phi_r}{\partial p_k} = 0 \quad (4.32)$$

By post multiplying the above by Δp_k , it becomes

$$\phi_r^T \frac{\partial M}{\partial p_k} \Delta p_k \phi_r + 2 \phi_r^T M \frac{\partial \phi_r}{\partial p_k} \Delta p_k = 0 \quad (4.33)$$

which can be rewritten as

$$\phi_r^T \Delta M_k \phi_r + 2 \phi_r^T M (\Delta \phi_r)_k = 0 \quad (4.34)$$

where the vector $(\Delta \phi_r)_k$ is the uncertainty contribution (or perturbation) on the r^{th} eigenvector due to the uncertainty (or perturbation) on the parameter p_k and is defined as

$$\sum_k (\Delta \phi_r)_k = \sum_k \frac{\partial \phi_r}{\partial p_k} \Delta p_k = \Delta \phi_r \quad (4.35)$$

Substituting the expression for M from (3.2), and ϕ_r from (3.5) in equation (4.34) produces

$$(\tilde{\phi}_r + \Delta \phi_r)^T \Delta M_k (\tilde{\phi}_r + \Delta \phi_r) + 2(\tilde{\phi}_r + \Delta \phi_r)^T (\tilde{M} + \Delta M) (\Delta \phi_r)_k = 0 \quad (4.36)$$

which after expanding and neglecting second and third order terms becomes

$$\tilde{\phi}_r^T \Delta M_k \tilde{\phi}_r + 2 \tilde{\phi}_r^T \tilde{M} (\Delta \phi_r)_k = 0 \quad (4.37)$$

Dividing by Δp_k , using the definitions for ΔM_k and $(\Delta \phi_r)_k$ from (4.8) and (4.35), yields

$$\tilde{\phi}_r^T \frac{\partial M}{\partial p_k} \tilde{\phi}_r + 2 \tilde{\phi}_r^T \tilde{M} \frac{\partial \phi_r}{\partial p_k} = 0 \quad (4.38)$$

Substituting the expression for $\partial \phi_r / \partial p_k$ from (4.30) into (4.38) gives

$$\tilde{\phi}_r^T \frac{\partial M}{\partial p_k} \tilde{\phi}_r + 2 \tilde{\phi}_r^T \tilde{M} (V_r + \tilde{\phi}_r a_r) = 0 \quad (4.39)$$

which can be reduced by using the orthogonality condition described in (4.31)

$$\tilde{\phi}_r^T \frac{\partial M}{\partial p_k} \tilde{\phi}_r + 2 \underbrace{\tilde{\phi}_r^T \tilde{M} \tilde{\phi}_r}_1 a_r = 0 \quad (4.40)$$

From the above expression, we finally obtain the expression for the indeterminate coefficient a_r

$$a_r = -\frac{1}{2} \tilde{\phi}_r^T \frac{\partial M}{\partial p_k} \tilde{\phi}_r \quad (4.41)$$

After the expressions for all the linear combination coefficients a_i 's in (4.28) and (4.41) have been found, they can be substituted in equation (4.30) to obtain the complete expression for the mode shape derivatives

$$\frac{\partial \phi_r}{\partial p_k} = \sum_{\substack{i=1 \\ i \neq r}}^n \tilde{\phi}_i \frac{\tilde{\phi}_i^T F_r}{(\tilde{\lambda}_i - \tilde{\lambda}_r)} + \tilde{\phi}_r \left(-\frac{1}{2} \tilde{\phi}_r^T \frac{\partial M}{\partial p_k} \tilde{\phi}_r \right) \quad (4.42)$$

where replacing F_r by the expression from (4.24) leaves us with

$$\frac{\partial \phi_r}{\partial p_k} = \sum_{\substack{i=1 \\ i \neq r}}^n \tilde{\phi}_i \frac{\tilde{\phi}_i^T}{\tilde{\lambda}_i - \tilde{\lambda}_r} \left[\frac{\partial \lambda_r}{\partial p_k} \tilde{M} \tilde{\phi}_r - \left(\frac{\partial K}{\partial p_k} - \tilde{\lambda}_r \frac{\partial M}{\partial p_k} \right) \tilde{\phi}_r \right] + \tilde{\phi}_r \left(-\frac{1}{2} \tilde{\phi}_r^T \frac{\partial M}{\partial p_k} \tilde{\phi}_r \right) \quad (4.43)$$

Applying the orthogonality condition reduces the above to

$$\frac{\partial \phi_r}{\partial p_k} = \sum_{\substack{i=1 \\ i \neq r}}^n \tilde{\phi}_i \frac{\tilde{\phi}_i^T}{\tilde{\lambda}_r - \tilde{\lambda}_i} \left(\frac{\partial K}{\partial p_k} - \tilde{\lambda}_r \frac{\partial M}{\partial p_k} \right) \tilde{\phi}_r - \frac{1}{2} \tilde{\phi}_r \tilde{\phi}_r^T \frac{\partial M}{\partial p_k} \tilde{\phi}_r \quad (4.44)$$

Which can be written in a more compact form using the Kroenecker delta function (see 2.11) as follow

$$\frac{\partial \phi_r}{\partial p_k} = \sum_{i=1}^n \tilde{\phi}_i \tilde{\phi}_i^T \left[\frac{1 - \delta_{ir}}{\tilde{\lambda}_r - \tilde{\lambda}_i} \left(\frac{\partial K}{\partial p_k} - \tilde{\lambda}_r \frac{\partial M}{\partial p_k} \right) - \frac{\delta_{ir}}{2} \frac{\partial M}{\partial p_k} \right] \tilde{\phi}_r \quad (4.45)$$

Using equations (4.19) and (4.20) in the above expression, we get the following results for the eigenvector sensitivities evaluated at the nominal parameters

$$\frac{\partial \phi_r}{\partial p_k} = \begin{cases} \frac{\tilde{\phi}_i}{\tilde{\lambda}_r - \tilde{\lambda}_i} \tilde{\lambda}_r, & \text{if } p_k = m_{ir} \\ \frac{\tilde{\phi}_r}{2}, & \text{if } p_k = m_{rr} \\ \frac{\tilde{\phi}_i}{\tilde{\lambda}_r - \tilde{\lambda}_i}, & \text{if } p_k = k_{ir} \\ 0, & \text{otherwise} \end{cases} \quad (4.46)$$

Example

In the two subsections above we have found useful expressions to compute the eigenvalue and eigenvector sensitivities (evaluated at the nominal parameters) with respect to the modal mass and stiffness parameters. The resulting expressions (4.21) and (4.46) are easy to compute as we will see in the following 3-DOF example.

For a 3-DOF system ($n = 3$), Φ , m and k are all 3×3 matrices, and the modal parameter vector p , as defined in Chapter 3, would contain the following elements

$$p = \left[m_{11} \ m_{12} \ m_{13} \ m_{22} \ m_{23} \ m_{33} \ k_{11} \ k_{12} \ k_{13} \ k_{22} \ k_{23} \ k_{33} \ \gamma_1 \ \gamma_2 \ \gamma_3 \right]^T \quad (4.47)$$

We recall that since both modal matrices m and k are symmetric, we only use their upper triangular elements as parameters. Also, since the eigenvalues and eigenvectors are independent of the damping, their derivatives with respect to the γ_i 's are zero. Therefore, for simplicity of notation in this example we will consider only the derivatives with respect to the mass and stiffness parameters. Hence, by applying equation (4.21) we obtain the eigenvalue sensitivity matrix

$$\begin{aligned} \left(\frac{\partial \lambda_r}{\partial p_k} \right) &= \left(\frac{\partial \lambda_i}{\partial p_j} \right) = \begin{bmatrix} \frac{\partial \lambda_1}{\partial m_{11}} & \frac{\partial \lambda_1}{\partial m_{12}} & \frac{\partial \lambda_1}{\partial m_{13}} & \frac{\partial \lambda_1}{\partial m_{22}} & \frac{\partial \lambda_1}{\partial m_{23}} & \frac{\partial \lambda_1}{\partial m_{33}} & \frac{\partial \lambda_1}{\partial k_{11}} & \frac{\partial \lambda_1}{\partial k_{12}} & \frac{\partial \lambda_1}{\partial k_{13}} & \frac{\partial \lambda_1}{\partial k_{22}} & \frac{\partial \lambda_1}{\partial k_{23}} & \frac{\partial \lambda_1}{\partial k_{33}} \\ \frac{\partial \lambda_2}{\partial m_{11}} & \frac{\partial \lambda_2}{\partial m_{12}} & \frac{\partial \lambda_2}{\partial m_{13}} & \frac{\partial \lambda_2}{\partial m_{22}} & \frac{\partial \lambda_2}{\partial m_{23}} & \frac{\partial \lambda_2}{\partial m_{33}} & \frac{\partial \lambda_2}{\partial k_{11}} & \frac{\partial \lambda_2}{\partial k_{12}} & \frac{\partial \lambda_2}{\partial k_{13}} & \frac{\partial \lambda_2}{\partial k_{22}} & \frac{\partial \lambda_2}{\partial k_{23}} & \frac{\partial \lambda_2}{\partial k_{33}} \\ \frac{\partial \lambda_3}{\partial m_{11}} & \frac{\partial \lambda_3}{\partial m_{12}} & \frac{\partial \lambda_3}{\partial m_{13}} & \frac{\partial \lambda_3}{\partial m_{22}} & \frac{\partial \lambda_3}{\partial m_{23}} & \frac{\partial \lambda_3}{\partial m_{33}} & \frac{\partial \lambda_3}{\partial k_{11}} & \frac{\partial \lambda_3}{\partial k_{12}} & \frac{\partial \lambda_3}{\partial k_{13}} & \frac{\partial \lambda_3}{\partial k_{22}} & \frac{\partial \lambda_3}{\partial k_{23}} & \frac{\partial \lambda_3}{\partial k_{33}} \end{bmatrix} \\ &= \begin{bmatrix} -\lambda_1 & 0 & 0 & 0 & 0 & 0 & 1 & 0 & 0 & 0 & 0 & 0 \\ 0 & 0 & 0 & -\lambda_2 & 0 & 0 & 0 & 0 & 0 & 1 & 0 & 0 \\ 0 & 0 & 0 & 0 & 0 & -\lambda_3 & 0 & 0 & 0 & 0 & 0 & 1 \end{bmatrix} \end{aligned} \quad (4.48)$$

where the indices r and k for the r^{th} eigenvalue and k^{th} parameter correspond respectively to the i^{th} row and j^{th} column (Eq. C.11) of the sensitivity matrix ($r = i = 1, \dots, n$ and $k = j = 1, \dots, (n^2 + n)$).

Similarly, the eigenvector sensitivity matrix can be obtained by applying equation (4.46)

$$\begin{aligned} \left(\frac{\partial \phi_r}{\partial p_k} \right) &= \left(\frac{\partial \phi_i}{\partial p_j} \right) = \begin{bmatrix} \frac{\partial \phi_1}{\partial m_{11}} & \frac{\partial \phi_1}{\partial m_{12}} & \frac{\partial \phi_1}{\partial m_{13}} & \frac{\partial \phi_1}{\partial m_{22}} & \frac{\partial \phi_1}{\partial m_{23}} & \frac{\partial \phi_1}{\partial m_{33}} & \frac{\partial \phi_1}{\partial k_{11}} & \frac{\partial \phi_1}{\partial k_{12}} & \frac{\partial \phi_1}{\partial k_{13}} & \frac{\partial \phi_1}{\partial k_{22}} & \frac{\partial \phi_1}{\partial k_{23}} & \frac{\partial \phi_1}{\partial k_{33}} \\ \frac{\partial \phi_2}{\partial m_{11}} & \frac{\partial \phi_2}{\partial m_{12}} & \frac{\partial \phi_2}{\partial m_{13}} & \frac{\partial \phi_2}{\partial m_{22}} & \frac{\partial \phi_2}{\partial m_{23}} & \frac{\partial \phi_2}{\partial m_{33}} & \frac{\partial \phi_2}{\partial k_{11}} & \frac{\partial \phi_2}{\partial k_{12}} & \frac{\partial \phi_2}{\partial k_{13}} & \frac{\partial \phi_2}{\partial k_{22}} & \frac{\partial \phi_2}{\partial k_{23}} & \frac{\partial \phi_2}{\partial k_{33}} \\ \frac{\partial \phi_3}{\partial m_{11}} & \frac{\partial \phi_3}{\partial m_{12}} & \frac{\partial \phi_3}{\partial m_{13}} & \frac{\partial \phi_3}{\partial m_{22}} & \frac{\partial \phi_3}{\partial m_{23}} & \frac{\partial \phi_3}{\partial m_{33}} & \frac{\partial \phi_3}{\partial k_{11}} & \frac{\partial \phi_3}{\partial k_{12}} & \frac{\partial \phi_3}{\partial k_{13}} & \frac{\partial \phi_3}{\partial k_{22}} & \frac{\partial \phi_3}{\partial k_{23}} & \frac{\partial \phi_3}{\partial k_{33}} \end{bmatrix} \\ &= \begin{bmatrix} \frac{\tilde{\phi}_1}{2} & \frac{\tilde{\phi}_2 \tilde{\lambda}_1}{\tilde{\lambda}_1 - \tilde{\lambda}_2} & \frac{\tilde{\phi}_3 \tilde{\lambda}_1}{\tilde{\lambda}_1 - \tilde{\lambda}_3} & 0 & 0 & 0 & 0 & \frac{\tilde{\phi}_2}{\tilde{\lambda}_1 - \tilde{\lambda}_2} & \frac{\tilde{\phi}_3}{\tilde{\lambda}_1 - \tilde{\lambda}_3} & 0 & 0 & 0 \\ 0 & \frac{\tilde{\phi}_1 \tilde{\lambda}_2}{\tilde{\lambda}_2 - \tilde{\lambda}_1} & 0 & \frac{\tilde{\phi}_2}{2} & \frac{\tilde{\phi}_3 \tilde{\lambda}_2}{\tilde{\lambda}_2 - \tilde{\lambda}_3} & 0 & 0 & \frac{\tilde{\phi}_1}{\tilde{\lambda}_2 - \tilde{\lambda}_1} & 0 & 0 & \frac{\tilde{\phi}_3}{\tilde{\lambda}_2 - \tilde{\lambda}_3} & 0 \\ 0 & 0 & \frac{\tilde{\phi}_1 \tilde{\lambda}_3}{\tilde{\lambda}_3 - \tilde{\lambda}_1} & 0 & \frac{\tilde{\phi}_2 \tilde{\lambda}_3}{\tilde{\lambda}_3 - \tilde{\lambda}_2} & \frac{\tilde{\phi}_3}{2} & 0 & 0 & \frac{\tilde{\phi}_1}{\tilde{\lambda}_3 - \tilde{\lambda}_1} & 0 & \frac{\tilde{\phi}_2}{\tilde{\lambda}_3 - \tilde{\lambda}_2} & 0 \end{bmatrix} \end{aligned} \quad (4.49)$$

where we recall that each of the eigenvectors, ϕ_r , has $n = 3$ elements

$$\phi_r = \begin{bmatrix} \phi_{1r} \\ \phi_{2r} \\ \phi_{3r} \end{bmatrix} \quad (4.50)$$

which means that all of the elements in (4.49) are themselves three element vectors

$$\frac{\partial \phi_r}{\partial p_k} = \frac{\partial}{\partial p_k} \begin{bmatrix} \phi_{1r} \\ \phi_{2r} \\ \phi_{3r} \end{bmatrix} = \begin{bmatrix} \partial \phi_{1r} / \partial p_k \\ \partial \phi_{2r} / \partial p_k \\ \partial \phi_{3r} / \partial p_k \end{bmatrix} \quad (4.51)$$

Therefore, the complete expression for the mode shape sensitivities (from Eq. 4.49) would look like

$$\left(\frac{\partial \phi_r}{\partial p_k} \right) = \begin{bmatrix} \frac{\tilde{\Phi}_{11}}{2} & \frac{\tilde{\Phi}_{12}\tilde{\lambda}_1}{\tilde{\lambda}_1 - \tilde{\lambda}_2} & \frac{\tilde{\Phi}_{13}\tilde{\lambda}_1}{\tilde{\lambda}_1 - \tilde{\lambda}_3} & 0 & 0 & 0 & 0 & \frac{\tilde{\Phi}_{12}}{\tilde{\lambda}_1 - \tilde{\lambda}_2} & \frac{\tilde{\Phi}_{13}}{\tilde{\lambda}_1 - \tilde{\lambda}_3} & 0 & 0 & 0 \\ \frac{\tilde{\Phi}_{21}}{2} & \frac{\tilde{\Phi}_{22}\tilde{\lambda}_1}{\tilde{\lambda}_1 - \tilde{\lambda}_2} & \frac{\tilde{\Phi}_{23}\tilde{\lambda}_1}{\tilde{\lambda}_1 - \tilde{\lambda}_3} & 0 & 0 & 0 & 0 & \frac{\tilde{\Phi}_{22}}{\tilde{\lambda}_1 - \tilde{\lambda}_2} & \frac{\tilde{\Phi}_{23}}{\tilde{\lambda}_1 - \tilde{\lambda}_3} & 0 & 0 & 0 \\ \frac{\tilde{\Phi}_{31}}{2} & \frac{\tilde{\Phi}_{32}\tilde{\lambda}_1}{\tilde{\lambda}_1 - \tilde{\lambda}_2} & \frac{\tilde{\Phi}_{33}\tilde{\lambda}_1}{\tilde{\lambda}_1 - \tilde{\lambda}_3} & 0 & 0 & 0 & 0 & \frac{\tilde{\Phi}_{32}}{\tilde{\lambda}_1 - \tilde{\lambda}_2} & \frac{\tilde{\Phi}_{33}}{\tilde{\lambda}_1 - \tilde{\lambda}_3} & 0 & 0 & 0 \\ 0 & \frac{\tilde{\Phi}_{11}\tilde{\lambda}_2}{\tilde{\lambda}_2 - \tilde{\lambda}_1} & 0 & \frac{\tilde{\Phi}_{12}}{2} & \frac{\tilde{\Phi}_{13}\tilde{\lambda}_2}{\tilde{\lambda}_2 - \tilde{\lambda}_3} & 0 & 0 & \frac{\tilde{\Phi}_{11}}{\tilde{\lambda}_2 - \tilde{\lambda}_1} & 0 & 0 & \frac{\tilde{\Phi}_{13}}{\tilde{\lambda}_2 - \tilde{\lambda}_3} & 0 \\ 0 & \frac{\tilde{\Phi}_{21}\tilde{\lambda}_2}{\tilde{\lambda}_2 - \tilde{\lambda}_1} & 0 & \frac{\tilde{\Phi}_{22}}{2} & \frac{\tilde{\Phi}_{23}\tilde{\lambda}_2}{\tilde{\lambda}_2 - \tilde{\lambda}_3} & 0 & 0 & \frac{\tilde{\Phi}_{21}}{\tilde{\lambda}_2 - \tilde{\lambda}_1} & 0 & 0 & \frac{\tilde{\Phi}_{23}}{\tilde{\lambda}_2 - \tilde{\lambda}_3} & 0 \\ 0 & \frac{\tilde{\Phi}_{31}\tilde{\lambda}_2}{\tilde{\lambda}_2 - \tilde{\lambda}_1} & 0 & \frac{\tilde{\Phi}_{32}}{2} & \frac{\tilde{\Phi}_{33}\tilde{\lambda}_2}{\tilde{\lambda}_2 - \tilde{\lambda}_3} & 0 & 0 & \frac{\tilde{\Phi}_{31}}{\tilde{\lambda}_2 - \tilde{\lambda}_1} & 0 & 0 & \frac{\tilde{\Phi}_{33}}{\tilde{\lambda}_2 - \tilde{\lambda}_3} & 0 \\ 0 & 0 & \frac{\tilde{\Phi}_{11}\tilde{\lambda}_3}{\tilde{\lambda}_3 - \tilde{\lambda}_1} & 0 & \frac{\tilde{\Phi}_{12}\tilde{\lambda}_3}{\tilde{\lambda}_3 - \tilde{\lambda}_2} & \frac{\tilde{\Phi}_{13}}{2} & 0 & 0 & \frac{\tilde{\Phi}_{11}}{\tilde{\lambda}_3 - \tilde{\lambda}_1} & 0 & \frac{\tilde{\Phi}_{12}}{\tilde{\lambda}_3 - \tilde{\lambda}_2} & 0 \\ 0 & 0 & \frac{\tilde{\Phi}_{21}\tilde{\lambda}_3}{\tilde{\lambda}_3 - \tilde{\lambda}_1} & 0 & \frac{\tilde{\Phi}_{22}\tilde{\lambda}_3}{\tilde{\lambda}_3 - \tilde{\lambda}_2} & \frac{\tilde{\Phi}_{23}}{2} & 0 & 0 & \frac{\tilde{\Phi}_{21}}{\tilde{\lambda}_3 - \tilde{\lambda}_1} & 0 & \frac{\tilde{\Phi}_{22}}{\tilde{\lambda}_3 - \tilde{\lambda}_2} & 0 \\ 0 & 0 & \frac{\tilde{\Phi}_{31}\tilde{\lambda}_3}{\tilde{\lambda}_3 - \tilde{\lambda}_1} & 0 & \frac{\tilde{\Phi}_{32}\tilde{\lambda}_3}{\tilde{\lambda}_3 - \tilde{\lambda}_2} & \frac{\tilde{\Phi}_{33}}{2} & 0 & 0 & \frac{\tilde{\Phi}_{31}}{\tilde{\lambda}_3 - \tilde{\lambda}_1} & 0 & \frac{\tilde{\Phi}_{32}}{\tilde{\lambda}_3 - \tilde{\lambda}_2} & 0 \end{bmatrix} \quad (4.52)$$

4.1.2 Frequency Response Function Derivative

For control design purposes, it is useful to evaluate the uncertainty range on the magnitude and phase of the frequency response function (FRF). In this section we will derive the FRF sensitivity with respect to the modal parameters, p_k 's directly from the forced equations of motion, as well as from the FRF state-space representation which is more useful from the integrated model framework perspective.

Equations of motion derivative

Assuming zero initial states, the transformation to the frequency domain of the forced equation of motion in modal form (2.14) is given by

$$[(\Lambda - \omega I^2) + j\omega\Xi]N(j\omega) = P(j\omega)N(j\omega) = \Phi^T \beta_u U(j\omega) + \Phi^T \beta_w W(j\omega) \quad (4.53)$$

where

$$P(j\omega) = [(\Lambda - \omega^2 I) + j\omega\Xi] \quad (4.54)$$

and $N(j\omega)$, $U(j\omega)$, and $W(j\omega)$ are respectively the Fourier transforms of the vectors $\eta(t)$, $u(t)$ and $w(t)$. This means that the modal states, N , as a function of complex frequency ($s = j\omega$) are given by

$$N(j\omega) = P^{-1} \Phi^T \beta_u U + P^{-1} \Phi^T \beta_w W \quad (4.55)$$

Since the outputs are given by

$$\begin{aligned} Y(j\omega) &= C_{yx} \Phi N(j\omega) \\ Z(j\omega) &= C_{zx} \Phi N(j\omega) \end{aligned} \quad (4.56)$$

we get the following expression for the FRF

$$\begin{aligned} \begin{Bmatrix} Z \\ Y \end{Bmatrix} &= \begin{bmatrix} C_{zx} \Phi P^{-1} \Phi^T \beta_w & C_{zx} \Phi P^{-1} \Phi^T \beta_u \\ C_{yx} \Phi P^{-1} \Phi^T \beta_w & C_{yx} \Phi P^{-1} \Phi^T \beta_u \end{bmatrix} \begin{Bmatrix} W \\ U \end{Bmatrix} \\ &= \begin{bmatrix} C_{zx} \\ C_{yx} \end{bmatrix} \Phi P^{-1} \Phi^T \begin{bmatrix} \beta_w & \beta_u \end{bmatrix} \begin{Bmatrix} W \\ U \end{Bmatrix} \end{aligned} \quad (4.57)$$

where

$$G(j\omega) = \begin{bmatrix} G_{zw}(j\omega) & G_{zu}(j\omega) \\ G_{yw}(j\omega) & G_{yu}(j\omega) \end{bmatrix} = \begin{bmatrix} C_{zx} \\ C_{yx} \end{bmatrix} \Phi P^{-1}(j\omega) \Phi^T \begin{bmatrix} \beta_w & \beta_u \end{bmatrix} \quad (4.58)$$

The derivatives of the FRF, $G(j\omega)$, with respect to the (scalar) modal parameter, p_k , (assuming that C_{zx} , C_{yx} , β_w , and β_u are not functions of p_k) is

$$\frac{\partial G(j\omega)}{\partial p_k} = \begin{bmatrix} C_{zx} \\ C_{yx} \end{bmatrix} \left[\frac{\partial \Phi^T}{\partial p_k} P^{-1}(j\omega) \Phi + \Phi^T \frac{\partial P^{-1}(j\omega)}{\partial p_k} \Phi + \Phi^T P^{-1}(j\omega) \frac{\partial \Phi}{\partial p_k} \right] \begin{bmatrix} \beta_w & \beta_u \end{bmatrix} \quad (4.59)$$

where $\partial P^{-1}(j\omega)/\partial p_k$ is given by

$$\frac{\partial P^{-1}(j\omega)}{\partial p_k} = -P^{-1}(j\omega) \frac{\partial P(j\omega)}{\partial p_k} P^{-1}(j\omega) \quad (4.60)$$

and $\partial P(j\omega)/\partial p_k$ is obtained from differentiating (4.54)

$$\begin{aligned} \frac{\partial P(j\omega)}{\partial p_k} &= \frac{\partial \Lambda}{\partial p_k} + j\omega \frac{\partial \Xi}{\partial p_k} \\ &= \frac{\partial \Lambda}{\partial p_k} + j\omega \left(\Lambda^{-\frac{1}{2}} Z \frac{\partial \Lambda}{\partial p_k} + 2\Lambda^{\frac{1}{2}} \frac{\partial Z}{\partial p_k} \right) \\ &= \left(1 + j\omega \Lambda^{-\frac{1}{2}} Z \right) \frac{\partial \Lambda}{\partial p_k} + j\omega 2\Lambda^{\frac{1}{2}} \frac{\partial Z}{\partial p_k} \end{aligned} \quad (4.61)$$

where Λ is the eigenvalue matrix, and Z is the modal damping matrix as defined in Chapter 3. Evaluated for the nominal parameters, equation (4.61) becomes

$$\frac{\partial P(j\omega)}{\partial p_k} = \left(1 + j\omega\tilde{\Lambda}^{-\frac{1}{2}}\tilde{Z}\right) \frac{\partial \Lambda}{\partial p_k} + j\omega 2\tilde{\Lambda}^{\frac{1}{2}} \frac{\partial Z}{\partial p_k} \quad (4.62)$$

and equation (4.60) becomes

$$\frac{\partial P^{-1}(j\omega)}{\partial p_k} = -\tilde{P}^{-1}(j\omega) \frac{\partial P(j\omega)}{\partial p_k} \tilde{P}^{-1}(j\omega) \quad (4.63)$$

Therefore, the sensitivity of the nominal structural plant FRF to parameter p_k is obtained by substituting (4.62) and (4.63) into (4.59)

$$\boxed{\frac{\partial G(j\omega)}{\partial p_k} = \begin{bmatrix} C_{zx} \\ C_{yx} \end{bmatrix} \left[\frac{\partial \Phi^T \tilde{P}^{-1} \tilde{\Phi}}{\partial p_k} - \tilde{\Phi}^T \tilde{P}^{-1} \frac{\partial P}{\partial p_k} \tilde{P}^{-1} \tilde{\Phi} + \tilde{\Phi}^T \tilde{P}^{-1} \frac{\partial \Phi}{\partial p_k} \right] \begin{bmatrix} \beta_w & \beta_u \end{bmatrix}} \quad (4.64)$$

with the nominal expression for P given by

$$\tilde{P}(j\omega) = [(\tilde{\Lambda} - \omega^2 I) + j\omega \tilde{\Xi}] = [(\tilde{\Lambda} - \omega^2 I) + j\omega 2\tilde{\Lambda} \tilde{Z}] \quad (4.65)$$

We will not demonstrate it here, but we want the reader to bear in mind that when the structure is base-excited, β_w (or its equivalent) is then a function of p_k , as the disturbance coming into the system depends on the system compliance, and should not be ignored in the derivative terms (Chapter 4 of [Hasselmann & Chrostowski, 1991]).

State-space form derivative

Equation (4.64) is very useful to compute the FRF sensitivities, but in an integrated model framework, it is more useful to use the integrated model notation as was defined in Chapter 2. Thus, in this subsection, we will derive the FRF sensitivity directly from the expression for $G_{zd}(s)$ (Eq. 2.32) reproduced below

$$G_{zd}(s) = C_{zd} [sI - A_{zd}]^{-1} B_{zd} \quad (4.66)$$

where $G_{zd}(s)$ is the integrated plant transfer function from the white noise input signal, d , to the performance outputs, z . The frequency dependent sensitivity of the system FRF with respect to the parameter p_k , noted $T_{G_{zd}p_k}(\omega)$ is obtained as follows (with $s = j\omega$)

$$\begin{aligned} T_{G_{zd}p_k}(\omega) &= \frac{\partial G_{zd}(j\omega)}{\partial p_k} = \frac{\partial(C_{zd}(j\omega I - A_{zd})^{-1}B_{zd})}{\partial p_k} \\ &= \frac{\partial C_{zd}}{\partial p_k}(j\omega I - A_{zd})^{-1}B_{zd} + C_{zd} \frac{\partial(j\omega I - A_{zd})^{-1}}{\partial p_k} B_{zd} \\ &\quad + C_{zd}(j\omega I - A_{zd})^{-1} \frac{\partial B_{zd}}{\partial p_k} \end{aligned} \quad (4.67)$$

where

$$\frac{\partial(j\omega I - A_{zd})^{-1}}{\partial p_k} = (j\omega I - A_{zd})^{-1} \frac{\partial A_{zd}}{\partial p_k} (j\omega I - A_{zd})^{-1} \quad (4.68)$$

Substituting (4.68) into (4.67), and evaluating for the nominal parameters, yields the sensitivity equation for the integrated (nominal) system model

$$T_{G_{zd}p_k}(\omega) = \frac{\partial C_{zd}}{\partial p_k}(j\omega I - \tilde{A}_{zd})^{-1} \tilde{B}_{zd} + \tilde{C}_{zd}(j\omega I - \tilde{A}_{zd})^{-1} \frac{\partial A_{zd}}{\partial p_k} (j\omega I - \tilde{A}_{zd})^{-1} \tilde{B}_{zd} + \tilde{C}_{zd}(j\omega I - \tilde{A}_{zd})^{-1} \frac{\partial B_{zd}}{\partial p_k} \quad (4.69)$$

which, since B_{zd} is independent of p , see equation 2.30 for B_{zd} , reduces to

$$\boxed{T_{G_{zd}p_k}(\omega) = \frac{\partial C_{zd}}{\partial p_k}(j\omega I - \tilde{A}_{zd})^{-1} \tilde{B}_{zd} + \tilde{C}_{zd}(j\omega I - \tilde{A}_{zd})^{-1} \frac{\partial A_{zd}}{\partial p_k} (j\omega I - \tilde{A}_{zd})^{-1} \tilde{B}_{zd}} \quad (4.70)$$

We recall that the parameters in vector p are defined as

$$p_k \in \left[m_{qr} \ k_{qr} \ \gamma_r \right], \quad \text{for } \begin{cases} r = 1, \dots, n \\ q = 1, \dots, r \end{cases} \quad (4.71)$$

where the m_{qr} 's and k_{qr} 's correspond to the upper triangular elements of the modal matrices, and the γ_r 's are the transformed damping parameters. We can see that, except for the

γ_r 's, the parameters p_k do not appear explicitly in the state-space matrices A_{zd} , B_{zd} , or C_{zd} . However, the eigenvalues in Λ and the modes shapes, Φ , appear explicitly in A_{zd} and C_{zd} , and do depend on the p_k 's. This parameter dependence can be expressed in functional notation as

$$\begin{aligned} A_{zd} &\rightarrow A_{zd}(\Lambda(p), \Phi(p), Z(p)) \\ C_{zd} &\rightarrow C_{zd}(\Phi(p)) \end{aligned} \quad (4.72)$$

The matrix derivatives $\frac{\partial A_{zd}}{\partial p_k}$ and $\frac{\partial C_{zd}}{\partial p_k}$ need to be computed. B_{zd} is independent of p . By invoking the chain rule (Appendix C.2) and based on the parameter dependence expressed in (4.72), the derivatives of A_{zd} and C_{zd} can be expressed as

$$\frac{\partial A_{zd}}{\partial p_k} = \sum_{r=1}^N \left(\frac{\partial A_{zd}}{\partial \lambda_r} \frac{\partial \lambda_r}{\partial p_k} + \sum_{q=1}^n \frac{\partial A_{zd}}{\partial \phi_{qr}} \frac{\partial \phi_{qr}}{\partial p_k} + \frac{\partial A_{zd}}{\partial \gamma_r} \frac{\partial \gamma_r}{\partial p_k} \right) \quad (4.73)$$

$$\frac{\partial C_{zd}}{\partial p_k} = \sum_{r=1}^N \sum_{q=1}^n \left[0 \quad \frac{\partial C_z}{\partial \phi_{qr}} \quad 0 \right] \frac{\partial \phi_{qr}}{\partial p_k} \quad (4.74)$$

since, as defined in (2.30), where D_{zw} and D_{zu} are both zero. Also, in the above expres-

$$C_{zd} = \begin{bmatrix} D_{zw} C_d & C_z & D_{zu} C_c \end{bmatrix}$$

sions, N is the number of modes kept in Φ , and n is the number of DOF's. N and n are different in the case where we have truncated some of the modes ($N \leq n$). In order to evaluate expressions (4.73) and (4.74), we will first compute the derivatives with respect to p_k , namely $\frac{\partial \phi_{qr}}{\partial p_k}$, $\frac{\partial \lambda_r}{\partial p_k}$, and $\frac{\partial \gamma_r}{\partial p_k}$, the mode shape, eigenvalue, and damping parameter derivatives. We already have obtained the expressions for the eigenvalue and mode shape derivatives in expressions (4.21) and (4.46), and the expression for the transformed damping ratio derivatives is trivial.

$$\frac{\partial \gamma_r}{\partial p_k} = \begin{cases} 1, & \text{if } p_k = \gamma_r \\ 0, & \text{otherwise} \end{cases} \quad (4.75)$$

We now need to compute the state-space matrix derivatives with respect to eigenvalues, mode shapes and modal damping ratios (i.e.: $\frac{\partial A_{zd}}{\partial \lambda_r}$, $\frac{\partial A_{zd}}{\partial \phi_{qr}}$, $\frac{\partial A_{zd}}{\partial \gamma_r}$, and $\frac{\partial C_z}{\partial \phi_{qr}}$). Before we perform the computations for $\frac{\partial A_{zd}}{\partial \lambda_r}$ and $\frac{\partial A_{zd}}{\partial \gamma_r}$ about the nominal plant, we recall that the integrated model dynamic matrix, A_{zd} , as defined in equation (2.30), is of the following shape

$$A_{zd} = \begin{bmatrix} A_d & 0 & 0 \\ \begin{bmatrix} 0 \\ \Phi^T \beta_w \end{bmatrix} C_d & \begin{bmatrix} 0 & I \\ -\Lambda & -2Z_\gamma \Lambda^{1/2} \end{bmatrix} & \begin{bmatrix} 0 \\ \Phi^T \beta_u \end{bmatrix} C_c \\ 0 & B_c C_{yx} [\Phi \ 0] & A_c \end{bmatrix} \quad (4.76)$$

where $Z = Z_\gamma$ as defined in Chapter 2. Using the above definition, the following derivatives (evaluated for the nominal plant) are easily obtained by inspection.

$$\frac{\partial A_{zd}}{\partial \lambda_r} = \begin{bmatrix} 0 & 0 & 0 \\ 0 & \begin{bmatrix} 0 & 0 \\ \begin{bmatrix} 0 \\ -(1)_r \\ 0 \end{bmatrix} \end{bmatrix} & \begin{bmatrix} 0 \\ \begin{bmatrix} -\tilde{\lambda}_r^{-1/2} e^{\tilde{\gamma}_r} \\ 0 \end{bmatrix} \end{bmatrix} \\ 0 & 0 & 0 \end{bmatrix}, \quad \frac{\partial C_z}{\partial \lambda_r} = [0] \quad (4.77)$$

$$\frac{\partial A_p}{\partial \gamma_r} = \begin{bmatrix} 0 & 0 & 0 \\ 0 & \begin{bmatrix} 0 & 0 \\ 0 & \begin{bmatrix} 0 & \\ -2\tilde{\lambda}_r^{1/2} e^{\tilde{\gamma}_r} & \\ & 0 \end{bmatrix} \\ 0 & 0 & 0 \end{bmatrix}, \quad \frac{\partial C_z}{\partial \gamma_r} = [0] \quad (4.78)$$

Sparse matrix representation may be necessary to use while implementing these computations in order to reduce storage requirements and speed up the code [Gutierrez, 1999]. The derivatives with respect to ϕ_{qr} are also easily obtained by inspection.

$$\frac{\partial A_{zd}}{\partial \phi_{qr}} = \begin{bmatrix} 0 & 0 & 0 \\ \begin{bmatrix} 0 \\ (1_{q,r}^{n \times N})^T \beta_w \end{bmatrix} C_d & \begin{bmatrix} 0 & 0 \\ 0 & 0 \end{bmatrix} & \begin{bmatrix} 0 \\ (1_{q,r}^{n \times N})^T \beta_u \end{bmatrix} C_c \\ 0 & B_c C_{yx} \begin{bmatrix} (1_{q,r}^{n \times N}) & 0 \end{bmatrix} & 0 \end{bmatrix} \quad (4.79)$$

$$\frac{\partial C_z}{\partial \phi_{qr}} = \begin{bmatrix} 0 & C_{zx} \begin{bmatrix} (1_{q,r}^{n \times N}) & 0 \end{bmatrix} & 0 \end{bmatrix} \quad (4.80)$$

where we define the term $(1_{q,r}^{n \times N})$ as an $n \times N$ matrix whose entry corresponding to the q^{th} row and the r^{th} column is 1 and is zero elsewhere.

FRF Magnitude derivative

In order to propagate the uncertainty to the magnitude of the FRF $G_{zd}(j\omega)$, we have to compute explicitly the derivatives for magnitude, H , given by

$$H(\omega) = |G_{zd}(j\omega)| = (G_{zd}(j\omega)G_{zd}(-j\omega))^{\frac{1}{2}} = (G_{zd}\overline{G_{zd}})^{\frac{1}{2}} \quad (4.81)$$

where the notation $\overline{(\cdot)}$ designate the complex conjugate. Taking the derivative of the magnitude with respect to the parameters p_k gives us the magnitude sensitivity

$$T_{H p_k}(\omega) = \frac{\partial H(\omega)}{\partial p_k} = \frac{1}{2(G_{zd} \overline{G_{zd}})^{1/2}} \left[\frac{\partial G_{zd}}{\partial p_k} \overline{G_{zd}} + G_{zd} \frac{\partial \overline{G_{zd}}}{\partial p_k} \right] \quad (4.82)$$

where we already have obtained the expression for $\frac{\partial G_{zd}}{\partial p_k}$ in Eq. (4.70). Often times for plotting purposes (e.g., Bode plot), we like to have the magnitude expressed in decibels [dB]. To propagate the uncertainty on the FRF magnitude in dB, we will have to compute explicitly the sensitivity in dB. A bel¹ is the logarithm of the ratio of two measurements of power. A decibel is one-tenth of a bel and is given by

$$(4.83)$$

$$\text{dB} = 10 \log_{10} \frac{|S_{zz}(\omega)|}{|S_{zx}(\omega)|}$$

Thus, a doubling in the spectral density of a signal for example corresponds to an increase of approximately 3 dB, since $10 \log_{10}(2) \approx 3.01$. For quantities that are not powers, or powerlike in having units of z^2 , the decibel is defined to be 20 times the logarithm of the ratio. A doubling of voltage, for example, corresponds approximately to 6 dB. The magnitude expressed in dB is thus given by

$$H_{dB}(\omega) = 20 \log_{10} |H(\omega)| = \frac{20 \ln H(\omega)}{\ln 10} \quad (4.84)$$

Taking the derivative with respect to p_k produces

1. named after Alexander Graham Bell (1847-1922)

$$\frac{\partial H_{dB}(\omega)}{\partial p_k} = \frac{\partial}{\partial p_k} \left(\frac{20 \ln H(\omega)}{\ln 10} \right) = \frac{20}{\ln 10} \frac{\partial(\ln H)}{\partial p_k} = \frac{20}{\ln 10} \frac{1}{H} \frac{\partial H}{\partial p_k} \quad (4.85)$$

where replacing $\frac{\partial H}{\partial p_k}$ from (4.82) yields the final expression for the magnitude in dB sensitivity

$$T_{H_{dB}p_k}(\omega) = \frac{\partial H_{dB}(\omega)}{\partial p_k} = \frac{10}{\ln 10} \cdot \frac{1}{\underbrace{G_{zd} \overline{G_{zd}}}_{H^2(\omega)}} \left[\frac{\partial G_{zd}}{\partial p_k} \overline{G_{zd}} + G_{zd} \frac{\partial \overline{G_{zd}}}{\partial p_k} \right] \quad (4.86)$$

FRF Phase derivative

The transfer function can be expressed into a real and an imaginary part as follows

$$G_{zd}(j\omega) = \text{Re}\{G_{zd}(j\omega)\} + j\text{Im}\{G_{zd}(j\omega)\} \quad (4.87)$$

where the real and the imaginary parts of G_{zd} are given as

$$\begin{aligned} \text{Re}\{G_{zd}(j\omega)\} &= \frac{1}{2}[G_{zd}(j\omega) + \overline{G_{zd}(j\omega)}] \\ \text{Im}\{G_{zd}(j\omega)\} &= \frac{1}{2j}[G_{zd}(j\omega) - \overline{G_{zd}(j\omega)}] \end{aligned} \quad (4.88)$$

Thus, the argument (phase) of the FRF in [rad] is calculated as

$$\varphi(\omega) = \angle G_{zd}(j\omega) = \text{atan} \left[\frac{\text{Im}\{G_{zd}(j\omega)\}}{\text{Re}\{G_{zd}(j\omega)\}} \right] = \text{atan} \left[\frac{G_{zd} - \overline{G_{zd}}}{j(G_{zd} + \overline{G_{zd}})} \right] \quad (4.89)$$

Taking the derivative with respect to the parameters; p_k , gives

$$\begin{aligned}
\frac{\partial \phi(\omega)}{\partial p_k} &= \frac{1}{1 + \left[\frac{G_{zd} - \overline{G_{zd}}}{j(G_{zd} + \overline{G_{zd}})} \right]^2} \frac{\partial}{\partial p_k} \left[\frac{G_{zd} - \overline{G_{zd}}}{j(G_{zd} + \overline{G_{zd}})} \right] \\
&= \frac{[j(G_{zd} + \overline{G_{zd}})]^2}{[j(G_{zd} + \overline{G_{zd}})]^2 + [G_{zd} - \overline{G_{zd}}]^2} \frac{j(G_{zd} + \overline{G_{zd}}) \left[\frac{\partial G_{zd}}{\partial p_k} - \frac{\partial \overline{G_{zd}}}{\partial p_k} \right] - j(G_{zd} - \overline{G_{zd}}) \left[\frac{\partial G_{zd}}{\partial p_k} + \frac{\partial \overline{G_{zd}}}{\partial p_k} \right]}{[j(G_{zd} + \overline{G_{zd}})]^2} \\
&= \frac{j \left[G_{zd} \frac{\partial G_{zd}}{\partial p_k} - G_{zd} \frac{\partial \overline{G_{zd}}}{\partial p_k} + \overline{G_{zd}} \frac{\partial G_{zd}}{\partial p_k} - \overline{G_{zd}} \frac{\partial \overline{G_{zd}}}{\partial p_k} \right] - j \left[G_{zd} \frac{\partial G_{zd}}{\partial p_k} + G_{zd} \frac{\partial \overline{G_{zd}}}{\partial p_k} - \overline{G_{zd}} \frac{\partial G_{zd}}{\partial p_k} - \overline{G_{zd}} \frac{\partial \overline{G_{zd}}}{\partial p_k} \right]}{-[G_{zd} + \overline{G_{zd}}]^2 + [G_{zd} - \overline{G_{zd}}]^2} \\
&= \frac{j2 \left[\overline{G_{zd}} \frac{\partial G_{zd}}{\partial p_k} - G_{zd} \frac{\partial \overline{G_{zd}}}{\partial p_k} \right]}{-[G_{zd}^2 + 2G_{zd}\overline{G_{zd}} + \overline{G_{zd}}^2] + [G_{zd}^2 - 2G_{zd}\overline{G_{zd}} + \overline{G_{zd}}^2]} = \frac{j2 \left[\overline{G_{zd}} \frac{\partial G_{zd}}{\partial p_k} - G_{zd} \frac{\partial \overline{G_{zd}}}{\partial p_k} \right]}{-4G_{zd}\overline{G_{zd}}}
\end{aligned} \tag{4.90}$$

which reduces to the final expression for phase sensitivity

$$\boxed{T_{\phi_{dB} p_k}(\omega) = \frac{\partial \phi(\omega)}{\partial p_k} = \frac{j \left[\overline{G_{zd}} \frac{\partial G_{zd}}{\partial p_k} - G_{zd} \frac{\partial \overline{G_{zd}}}{\partial p_k} \right]}{2 \underbrace{G_{zd} \overline{G_{zd}}}_{H^2(\omega)}}} \tag{4.91}$$

4.1.3 Performance RMS Derivative

The performance RMS sensitivities are most useful from a structural design point of view. As an important step in the performance uncertainty analysis, they help the designer to build confidence whether or not the design will meet the requirements. (e.g., if the nominal model meets the specifications, what is the probability (range of confidence) that the actual plant will meet these requirements). The sensitivity analysis can also point the designer towards possible performance enhancement alternatives [Gutierrez, Bourgault & Miller, 1999].

From equation (2.45) we can see that it is not possible to obtain a closed form expression for the sensitivities of the individual performance RMS, σ_{z_i} , with respect to our modal parameters, p_k , because they do not depend explicitly on the state covariance matrix, Σ_q ,

which is the solution of the Lyapunov equation (2.43). An alternative way to compute the performance RMS derivatives, $\frac{\partial \sigma_{z_i}}{\partial p_k}$, is to use the so-called Lagrange multiplier with the Lyapunov equation being the constraining equation. Similar developments are presented in [Gutierrez, 1999]. We start by computing the Lagrangian of the variance (RMS squared), $\sigma_{z_i}^2$

$$(\sigma_{z_i}^2)^L = \underbrace{C_{zd_i} \Sigma_q C_{zd_i}^T}_{\sigma_{z_i}^2} + tr \left\{ L_i (A_{zd} \Sigma_q + \Sigma_q A_{zd}^T + B_{zd} B_{zd}^T) \right\} \quad (4.92)$$

where the notation $(.)^L$ denotes the Lagrangian, and L_i is the symmetric Lagrange multiplier matrix for the i^{th} output performance. L_i is obtained by solving the following Lyapunov equation

$$L_i A_{zd} + A_{zd}^T L_i + C_{zd_i}^T C_{zd_i} = 0 \quad (4.93)$$

which is also referred to as the dual form of the Lyapunov equation (2.43) reproduced below

$$A_{zd} \Sigma_q + \Sigma_q A_{zd}^T + B_{zd} B_{zd}^T = 0 \quad (4.94)$$

Taking the derivatives of (4.92) with respect to p_k gives the following expression for the variance sensitivity

$$\frac{\partial \sigma_{z_i}^2}{\partial p_k} = tr \left\{ \Sigma_q \frac{\partial (C_{zd_i}^T C_{zd_i})}{\partial p_k} \right\} + tr \left\{ L_i \left(\frac{\partial A_{zd}}{\partial p_k} \Sigma_q + \Sigma_q \frac{\partial A_{zd}^T}{\partial p_k} + \frac{\partial (B_{zd} B_{zd}^T)}{\partial p_k} \right) \right\} \quad (4.95)$$

The above expression is very general and could be used to perform sensitivity analysis for various parameters p , modal or physical. It requires to solve two Lyapunov equations, namely (4.93) for L_i , and (4.94) for Σ_q (which we had already solved during the nominal performance assessment). The sensitivity for the global cost, J , as defined in (2.46) would be obtained in a very similar fashion with the following equation

$$\frac{\partial J}{\partial p_k} = \text{tr} \left\{ \Sigma_q \frac{\partial (C_{zd}^T C_{zd})}{\partial p_k} \right\} + \text{tr} \left\{ L \left(\frac{\partial A_{zd}}{\partial p_k} \Sigma_q + \Sigma_q \frac{\partial A_{zd}^T}{\partial p_k} + \frac{\partial (B_{zd} B_{zd}^T)}{\partial p_k} \right) \right\} \quad (4.96)$$

where Σ_q is again obtained by solving (4.94), and the global Lagrange multiplier, L , is the solution of

$$L A_{zd} + A_{zd}^T L + C_{zd}^T C_{zd} = 0 \quad (4.97)$$

For the modal parameters p_k 's as we have defined them in Chapter 3, and the state-space notation for the integrated model defined in Chapter 2, equation (4.95) reduces to

$$\begin{aligned} \frac{\partial \sigma_{z_i}^2}{\partial p_k} &= \text{tr} \left\{ \Sigma_q \frac{\partial (C_{zd_i}^T C_{zd_i})}{\partial p_k} + L_i \left(\frac{\partial A_{zd}}{\partial p_k} \Sigma_q + \Sigma_q \frac{\partial A_{zd}^T}{\partial p_k} \right) \right\} \\ &= \text{tr} \left\{ \Sigma_q \left(\frac{\partial C_{zd_i}^T}{\partial p_k} C_{zd_i} + C_{zd_i}^T \frac{\partial C_{zd_i}}{\partial p_k} \right) + L_i \left(\frac{\partial A_{zd}}{\partial p_k} \Sigma_q + \Sigma_q \frac{\partial A_{zd}^T}{\partial p_k} \right) \right\} \end{aligned} \quad (4.98)$$

as B_{zd} is completely independent of the p_k 's. In order to obtain the derivative for the performance RMS, we use the following calculus identity to express how it relates to the variance sensitivity.

$$\frac{\partial}{\partial x} [y^2(x)] = 2y(x) \frac{\partial}{\partial x} [y(x)] \Leftrightarrow \frac{\partial}{\partial x} [y(x)] = \frac{1}{2y(x)} \frac{\partial}{\partial x} [y^2(x)] \quad (4.99)$$

The sensitivity of the RMS value, σ_{z_i} , is computed as follows

$$\frac{\partial RMS(z_i)}{\partial p_k} = \frac{\partial \sigma_{z_i}}{\partial p_k} = \frac{1}{2\sigma_{z_i}} \text{tr} \left\{ \Sigma_q \left(\frac{\partial C_{zd_i}^T}{\partial p_k} C_{zd_i} + C_{zd_i}^T \frac{\partial C_{zd_i}}{\partial p_k} \right) + L_i \left(\frac{\partial A_{zd}}{\partial p_k} \Sigma_q + \Sigma_q \frac{\partial A_{zd}^T}{\partial p_k} \right) \right\} \quad (4.100)$$

which evaluated for the nominal plant is written

$$\boxed{\frac{\partial RMS(z_i)}{\partial p_k} = \frac{1}{2\tilde{\sigma}_{z_i}} \text{tr} \left\{ \Sigma_q \left(\frac{\partial C_{zd_i}^T}{\partial p_k} \tilde{C}_{zd_i} + \tilde{C}_{zd_i}^T \frac{\partial C_{zd_i}}{\partial p_k} \right) + \tilde{L}_i \left(\frac{\partial A_{zd}}{\partial p_k} \tilde{\Sigma}_q + \tilde{\Sigma}_q \frac{\partial A_{zd}^T}{\partial p_k} \right) \right\}} \quad (4.101)$$

where the necessary derivatives $\frac{\partial A_{zd}}{\partial p_k}$ and $\frac{\partial C_{zd_i}}{\partial p_k}$ have already been computed in Section 5.1.2, and the nominal state covariance matrix and the nominal Lagrange multiplier are evaluated from the following (nominal) Lyapunov equations

$$\begin{aligned}\tilde{A}_{zd}\tilde{\Sigma}_q + \tilde{\Sigma}_q\tilde{A}_{zd}^T + \tilde{B}_{zd}\tilde{B}_{zd}^T &= 0 \\ \tilde{L}_i\tilde{A}_{zd} + \tilde{A}_{zd}^T\tilde{L}_i + \tilde{C}_{zd_i}^T\tilde{C}_{zd_i} &= 0\end{aligned}\quad (4.102)$$

4.2 Second Order Derivatives (curvatures)

Most of the uncertainty propagation techniques that we will present in Chapter 5, make use of the linear approximation (Eq. 5.2). For this approximation to be valid, the curvature terms must be small. In other words, the second order terms must be negligible compared to the first order terms. That means that, in the following series expression for a performance output variable u (FRF or performance RMS),

$$u = \tilde{u} + \frac{\partial u}{\partial p_k}\Delta p_k + \frac{1}{2}\frac{\partial^2 u}{\partial p_k^2}\Delta p_k^2 + H.O.T. \quad (4.103)$$

the second order terms must be much smaller than the first order term.

$$\left|\frac{\partial u}{\partial p_k}\Delta p_k\right| \gg \left|\frac{1}{2}\frac{\partial^2 u}{\partial p_k^2}\Delta p_k^2\right| \quad (4.104)$$

In fact, the smaller the ratio, ε , of the second order term over the first order term, the better the approximation. Also, by setting a limit on ε , e.g. 1%,

$$\frac{\left|\frac{1}{2}\frac{\partial^2 u}{\partial p_k^2}\Delta p_k^2\right|}{\left|\frac{\partial u}{\partial p_k}\Delta p_k\right|} \leq \varepsilon = 0.01 \quad (4.105)$$

we can specify the accuracy of the linear approximation. The error bound on the linear approximation provides us with a bound on the k^{th} parameter uncertainty, Δp_k , that must be respected to preserve the linearity of the system (for our accuracy specification).

$$|\Delta p_k| \leq (0.01) \times \frac{\left| 2 \frac{\partial u}{\partial p_k} \right|}{\left| \frac{\partial^2 u}{\partial p_k^2} \right|} \quad (4.106)$$

The above expression can be used in the uncertainty analysis to determine the range of uncertainty in the parameters p_k which is allowed for the linear approximation to be valid. Determining the range of validity of the linear approximation is even more important for the uncertainty propagation. It is well known that linear systems with normally distributed input parameters have outputs that are also normally distributed [Gelb & al., 1974]. The implications of this statement are great for our uncertainty analysis as the uncertainty database presented in Chapter 3 assumed normal, or Gaussian, distributions of the uncertain parameters. This means that the distribution of the performance outputs (RMS and FRF) are also normal as long as the bounds of Eq. 4.106 are respected.

Caution: Notice that the series expansion, as described in equation (4.103), is valid for the case where the function u is dependent on one parameter only. To be accurate, for the case where p contains multiple parameters p_k , mixed derivative terms, $\frac{\partial^2 u}{\partial p_k \partial p_j}$, should appear in the expression as follows

$$u = \tilde{u} + \sum_{k=1}^{N_p} \frac{\partial u}{\partial p_k} \Delta p_k + \frac{1}{2} \sum_{k=1}^{N_p} \sum_{j=1}^{N_p} \Delta p_k \frac{\partial^2 u}{\partial p_k \partial p_j} \Delta p_j + H.O.T. \quad (4.107)$$

where N_p is the number of uncertain parameters in the vector p . This expression can also be written in a more formal way as

$$u = \tilde{u} + \nabla u^T \Delta p + \frac{1}{2} \Delta p^T H \Delta p + H.O.T. \quad (4.108)$$

where ∇u , the gradient of u , and H , the Hessian matrix, are defined as

$$\nabla u = \begin{bmatrix} \frac{\partial u}{\partial p_1} \\ \vdots \\ \frac{\partial u}{\partial p_{N_p}} \end{bmatrix}, \quad H = \begin{bmatrix} \frac{\partial^2 u}{\partial p_1^2} & \cdots & \frac{\partial^2 u}{\partial p_1 \partial p_{N_p}} \\ \vdots & \ddots & \vdots \\ \frac{\partial^2 u}{\partial p_{N_p} \partial p_1} & \cdots & \frac{\partial^2 u}{\partial p_{N_p}^2} \end{bmatrix} \quad (4.109)$$

For the purposes of determining the range of uncertainty in the parameters p_k that preserves the linearity, we assume equation (4.106) is adequate. We have obtained the first order derivatives in Section 4.1. We will now derive the second order derivatives for FRF (magnitude and phase) and performance RMS necessary to evaluate equation (4.106).

4.2.1 FRF Second Order Derivative

The Taylor series for the FRF looks like

$$G_{zd}(s) = \tilde{G}_{zd}(s) + \frac{\partial G_{zd}(s)}{\partial p_k} \Delta p_k + \frac{1}{2} \frac{\partial^2 G_{zd}(s)}{\partial p_k^2} \Delta p_k^2 + \dots \quad (4.110)$$

and based on Eq. 4.106, for a given parameter uncertainty size Δp_k , we can determine if at a certain frequency the linear approximation is valid and therefore, determining the frequency range for which the linear covariance propagation can be used.

$$\left| \frac{1}{2\varepsilon} \frac{\partial^2 G_{zd}(s)}{\partial p_k^2} \right| |\Delta p_k| \leq \left| \frac{\partial G_{zd}(s)}{\partial p_k} \right| \quad (4.111)$$

We have found already found an expression for the first derivative of the FRF in equation (4.69). We now have to find the second order derivative, which is done by differentiating Eq. 4.69 and using the identity of Eq. 4.68.

$$\begin{aligned}
\frac{\partial^2 G_{zd}(s)}{\partial p_k^2} = & \left(\frac{\partial^2 C_{zd}}{\partial p_k^2} F B_{zd} + \frac{\partial C_{zd}}{\partial p_k} F \frac{\partial A_{zd}}{\partial p_k} F B_{zd} + \frac{\partial C}{\partial p_k} F \frac{\partial B_{zd}}{\partial p_k} \right) \\
& + \left(\frac{\partial C_{zd}}{\partial p_k} F \frac{\partial A_{zd}}{\partial p_k} F B_{zd} + C_{zd} F \frac{\partial A_{zd}}{\partial p_k} F \frac{\partial A_{zd}}{\partial p_k} F B_{zd} + C_{zd} F \frac{\partial^2 A_{zd}}{\partial p_k^2} F B_{zd} + C_{zd} F \frac{\partial A_{zd}}{\partial p_k} F \frac{\partial A_{zd}}{\partial p_k} F B_{zd} + C_{zd} F \frac{\partial A_{zd}}{\partial p_k} F \frac{\partial B_{zd}}{\partial p_k} \right) \\
& + \left(\frac{\partial C_{zd}}{\partial p_k} F \frac{\partial B_{zd}}{\partial p_k} + C_{zd} F \frac{\partial A_{zd}}{\partial p_k} F \frac{\partial B_{zd}}{\partial p_k} + C_{zd} F \frac{\partial^2 B_{zd}}{\partial p_k^2} \right)
\end{aligned} \tag{4.112}$$

where $F(s) = (sI - A_p)^{-1}$ is used to simplify the notation. Collecting terms,

$$\begin{aligned}
\frac{\partial^2 G_{zd}(s)}{\partial p_k^2} = & \frac{\partial^2 C_{zd}}{\partial p_k^2} F B_{zd} + 2 \frac{\partial C_{zd}}{\partial p_k} F \frac{\partial A_{zd}}{\partial p_k} F B_{zd} + 2 \frac{\partial C}{\partial p_k} F \frac{\partial B_{zd}}{\partial p_k} + 2 C_{zd} F \frac{\partial A_{zd}}{\partial p_k} F \frac{\partial A_{zd}}{\partial p_k} F B_{zd} \\
& + C_{zd} F \frac{\partial^2 A_{zd}}{\partial p_k^2} F B_{zd} + 2 C_{zd} F \frac{\partial A_{zd}}{\partial p_k} F \frac{\partial B_{zd}}{\partial p_k} + C_{zd} F \frac{\partial^2 B_{zd}}{\partial p_k^2}
\end{aligned} \tag{4.113}$$

Based on our integrated model notation and the definition of the parameters p_k , we find that the matrix B_{zd} is completely independent of the p_k 's which simplifies Eq. 4.113. Therefore, provided that we can obtain the expressions from differentiating Eqs. 4.73 and 4.74, the FRF curvature, evaluated for the nominal parameters, is obtained by

$$\boxed{\frac{\partial^2 G_{zd}(s)}{\partial p_k^2} = \frac{\partial^2 C_{zd}}{\partial p_k^2} F B_{zd} + 2 \frac{\partial C_{zd}}{\partial p_k} F \frac{\partial A_{zd}}{\partial p_k} F B_{zd} + 2 C_{zd} F \frac{\partial A_{zd}}{\partial p_k} F \frac{\partial A_{zd}}{\partial p_k} F B_{zd} + C_{zd} F \frac{\partial^2 A_{zd}}{\partial p_k^2} F B_{zd}} \tag{4.114}$$

where we refer to Section 4.1 for the first order derivatives for A_{zd} and C_{zd} . To obtain the expressions for the second order derivatives $\frac{\partial^2 A_{zd}}{\partial p_k^2}$ and $\frac{\partial^2 C_{zd}}{\partial p_k^2}$, the second order derivatives for the mode shapes and eigenvalues with respect to the modal mass and stiffness elements need to be computed. More research needs to be done to obtain these expressions and their derivation is included in the subsequent future work.

4.2.2 RMS Second Order Derivative

In order to compute the performance RMS second derivative with respect to p_k , we need first to compute the second derivative of the variances, $\sigma_{z_i}^2$ [Gutierrez, 1999]

$$\frac{\partial^2 \sigma_{z_i}^2}{\partial p_k^2} = \frac{\partial}{\partial p_k} \left(\frac{\partial \sigma_{z_i}^2}{\partial p_k} \right) \quad (4.115)$$

where as we have determined in (4.98), $\frac{\partial \sigma_{z_i}^2}{\partial p_k}$ is a function of the state covariance matrix, Σ_q , and the Lagrange multiplier, L_i , both of which do not depend explicitly on p_k as they are solutions to Lyapunov equations. One way to get around this problem would be to use the Lagrange multiplier technique, like we have done in Section 4.1.3, and treat the two Lyapunov equations (i.e., equation (4.93) for L_i , and (4.94) for Σ_q) as constraint equations

$$\begin{aligned} \left(\frac{\partial \sigma_{z_i}^2}{\partial p_k} \right)^L &= \frac{\partial \sigma_{z_i}^2}{\partial p_k} + \text{tr} \left\{ M_{i,k} (L_i A_{zd} + A_{zd}^T L_i + C_{zd_i}^T C_{zd_i}) \right\} \\ &+ \text{tr} \left\{ N_{i,k} (A_{zd} \Sigma_q + \Sigma_q A_{zd}^T + B_{zd} B_{zd}^T) \right\} \end{aligned} \quad (4.116)$$

where the Lagrange multiplier matrices $M_{i,k}$ and $N_{i,k}$ depend on the performance metric of interest, z_i , and the modal parameter of interest, p_k . Another way to obtain $\frac{\partial^2 \sigma_{z_i}^2}{\partial p_k^2}$ is to start directly with the expression for $\frac{\partial \sigma_{z_i}^2}{\partial p_k}$ given in (4.95) and write out the derivative explicitly as

$$\begin{aligned} \frac{\partial^2 \sigma_{z_i}^2}{\partial p_k^2} &= \text{tr} \left\{ \frac{\partial \Sigma_q}{\partial p_k} \left(\frac{\partial C_{zd_i}^T}{\partial p_k} C_{zd_i} + C_{zd_i}^T \frac{\partial C_{zd_i}}{\partial p_k} \right) + \Sigma_q \left(\frac{\partial^2 C_{zd_i}^T}{\partial p_k^2} C_{zd_i} + 2 \frac{\partial C_{zd_i}^T}{\partial p_k} \frac{\partial C_{zd_i}}{\partial p_k} + C_{zd_i}^T \frac{\partial^2 C_{zd_i}}{\partial p_k^2} \right) \right\} \\ &+ \text{tr} \left\{ \frac{\partial L_i}{\partial p_k} \left(\frac{\partial A_{zd}}{\partial p_k} \Sigma_q + \Sigma_q \frac{\partial A_{zd}^T}{\partial p_k} + \frac{\partial B_{zd}}{\partial p_k} B_{zd}^T + B_{zd} \frac{\partial B_{zd}^T}{\partial p_k} \right) \right\} \\ &+ \text{tr} \left\{ L_i \left(\frac{\partial^2 A_{zd}}{\partial p_k^2} \Sigma_q + \frac{\partial A_{zd}}{\partial p_k} \frac{\partial \Sigma_q}{\partial p_k} + \frac{\partial \Sigma_q}{\partial p_k} \frac{\partial A_{zd}^T}{\partial p_k} + \Sigma_q \frac{\partial^2 A_{zd}^T}{\partial p_k^2} \right) \right\} \\ &+ \text{tr} \left\{ L_i \left(\frac{\partial^2 B_{zd}}{\partial p_k^2} B_{zd}^T + 2 \frac{\partial B_{zd}}{\partial p_k} \frac{\partial B_{zd}^T}{\partial p_k} + B_{zd} \frac{\partial^2 B_{zd}^T}{\partial p_k^2} \right) \right\} \end{aligned} \quad (4.117)$$

With our definition of B_{zd} , we have $\frac{\partial B_{zd}}{\partial p_k} = \frac{\partial^2 B_{zd}}{\partial p_k^2} = 0$ and the above expression for the second order derivative of the variance, $\sigma_{z_i}^2$, can be reduced and evaluated for the nominal parameters as follows

$$\begin{aligned} \frac{\partial^2 \sigma_{z_i}^2}{\partial p_k^2} = & \text{tr} \left\{ \frac{\partial \Sigma_q}{\partial p_k} \left(\frac{\partial C_{zd_i}^T}{\partial p_k} \tilde{C}_{zd_i} + \tilde{C}_{zd_i}^T \frac{\partial C_{zd_i}}{\partial p_k} \right) + \tilde{\Sigma}_q \left(\frac{\partial^2 C_{zd_i}^T}{\partial p_k^2} \tilde{C}_{zd_i} + 2 \frac{\partial C_{zd_i}^T}{\partial p_k} \frac{\partial C_{zd_i}}{\partial p_k} + \tilde{C}_{zd_i}^T \frac{\partial^2 C_{zd_i}}{\partial p_k^2} \right) \right\} \\ & + \text{tr} \left\{ \frac{\partial L_i}{\partial p_k} \left(\frac{\partial A_{zd}}{\partial p_k} \tilde{\Sigma}_q + \tilde{\Sigma}_q \frac{\partial A_{zd}^T}{\partial p_k} \right) \right\} \\ & + \text{tr} \left\{ \tilde{L}_i \left(\frac{\partial^2 A_{zd}}{\partial p_k^2} \tilde{\Sigma}_q + \frac{\partial A_{zd}}{\partial p_k} \frac{\partial \Sigma_q}{\partial p_k} + \frac{\partial \Sigma_q}{\partial p_k} \frac{\partial A_{zd}^T}{\partial p_k} + \tilde{\Sigma}_q \frac{\partial^2 A_{zd}^T}{\partial p_k^2} \right) \right\} \end{aligned} \quad (4.118)$$

where, as described in [Mallory, 2000], the derivatives for L_i , and Σ_q can be obtained as follows. First, for the state covariance matrix derivative, we start by differentiating the Lyapunov equation (4.94) with respect to p_k

$$\begin{aligned} \frac{\partial}{\partial p_k} (A_{zd} \Sigma_q + \Sigma_q A_{zd}^T + B_{zd} B_{zd}^T) &= 0 \\ \Rightarrow \frac{\partial A_{zd}}{\partial p_k} \Sigma_q + A_{zd} \frac{\partial \Sigma_q}{\partial p_k} + \frac{\partial \Sigma_q}{\partial p_k} A_{zd}^T + \Sigma_q \frac{\partial A_{zd}^T}{\partial p_k} + \frac{\partial B_{zd}}{\partial p_k} B_{zd}^T + B_{zd} \frac{\partial B_{zd}^T}{\partial p_k} &= 0 \end{aligned} \quad (4.119)$$

which, if we rearrange, we realize that we can obtain $\frac{\partial \Sigma_q}{\partial p_k}$ simply by solving another type of Lyapunov equation.

$$A_{zd} \frac{\partial \Sigma_q}{\partial p_k} + \frac{\partial \Sigma_q}{\partial p_k} A_{zd}^T + \left[\frac{\partial A_{zd}}{\partial p_k} \Sigma_q + \Sigma_q \frac{\partial A_{zd}^T}{\partial p_k} + \frac{\partial B_{zd}}{\partial p_k} B_{zd}^T + B_{zd} \frac{\partial B_{zd}^T}{\partial p_k} \right] = 0 \quad (4.120)$$

which for the nominal parameters (with $\frac{\partial B_{zd}}{\partial p_k} = 0$) is written

$$\tilde{A}_{zd} \frac{\partial \Sigma_q}{\partial p_k} + \frac{\partial \Sigma_q}{\partial p_k} \tilde{A}_{zd}^T + \left[\frac{\partial A_{zd}}{\partial p_k} \tilde{\Sigma}_q + \tilde{\Sigma}_q \frac{\partial A_{zd}^T}{\partial p_k} \right] = 0 \quad (4.121)$$

The derivative for the Lagrange multiplier is also obtained the way by differentiating explicitly the dual Lyapunov equation (4.93)

$$\begin{aligned} \frac{\partial}{\partial p_k}(L_i A_{zd} + A_{zd}^T L_i + C_{zd_i}^T C_{zd_i}) &= 0 \\ \Rightarrow \frac{\partial L_i}{\partial p_k} A_{zd} + L_i \frac{\partial A_{zd}}{\partial p_k} + \frac{\partial A_{zd}^T}{\partial p_k} L_i + A_{zd}^T \frac{\partial L_i}{\partial p_k} + \frac{\partial C_{zd_i}^T}{\partial p_k} C_{zd_i} + C_{zd_i}^T \frac{\partial C_{zd_i}}{\partial p_k} &= 0 \end{aligned} \quad (4.122)$$

By rearranging the above expression we obtain another form of Lyapunov equation for which $\frac{\partial L_i}{\partial p_k}$ is the solution.

$$\frac{\partial L_i}{\partial p_k} A_{zd} + A_{zd}^T \frac{\partial L_i}{\partial p_k} + \left[L_i \frac{\partial A_{zd}}{\partial p_k} + \frac{\partial A_{zd}^T}{\partial p_k} L_i + \frac{\partial C_{zd_i}^T}{\partial p_k} C_{zd_i} + C_{zd_i}^T \frac{\partial C_{zd_i}}{\partial p_k} \right] = 0 \quad (4.123)$$

which evaluated for the nominal parameters is written

$$\boxed{\frac{\partial L_i}{\partial p_k} \tilde{A}_{zd} + \tilde{A}_{zd}^T \frac{\partial L_i}{\partial p_k} + \left[\tilde{L}_i \frac{\partial A_{zd}}{\partial p_k} + \frac{\partial A_{zd}^T}{\partial p_k} \tilde{L}_i + \frac{\partial C_{zd_i}^T}{\partial p_k} \tilde{C}_{zd_i} + \tilde{C}_{zd_i}^T \frac{\partial C_{zd_i}}{\partial p_k} \right]} = 0 \quad (4.124)$$

Now that we have all the elements necessary to evaluate the second derivative of the performance metric variance (Eq. 4.118), we need to find the expression that will tell us how it relates to the second derivative of the performance RMS. First, as we have determined in (4.99), the relation between the variance sensitivity and the RMS sensitivity is described as follows

$$\frac{\partial \sigma_{z_i}^2}{\partial p_k} = 2\sigma_{z_i} \frac{\partial \sigma_{z_i}}{\partial p_k} \quad (4.125)$$

Taking the derivative of the above gives

$$\frac{\partial^2 \sigma_{z_i}^2}{\partial p_k^2} = 2 \left(\frac{\partial \sigma_{z_i}}{\partial p_k} \right)^2 + 2\sigma_{z_i} \frac{\partial^2 \sigma_{z_i}}{\partial p_k^2} \quad (4.126)$$

from which we solve for the second derivative of the RMS and obtain

$$\frac{\partial^2 \sigma_{z_i}}{\partial p_k^2} = \frac{1}{2\sigma_{z_i}} \left[\frac{\partial^2 \sigma_{z_i}^2}{\partial p_k^2} - 2 \left(\frac{\partial \sigma_{z_i}}{\partial p_k} \right)^2 \right] \quad (4.127)$$

an expression that depends only on the sensitivity of the RMS (Eq. 4.101) and the second derivative of the variances (Eq. 4.118). Therefore, we now have everything for computing second order derivatives of the RMS. Using equation (4.106) will tell us the range of uncertainty for which the linearity of the system is preserved and hence the Normal distribution of the performance RMS distribution. Knowing the shape of the probability distribution function is very useful because integrating under the curve will give us the cumulative distribution function (CDF) used to determine the probability that the requirements will be met. These results will be illustrated on two sample problems in Chapter 6.

4.3 Summary

This chapter presented the derivation of first order and second order derivatives of the frequency response function (FRF) matrix and the performance RMS of a linear time invariant system with respect to modal parameters $p = [m, k, \gamma]$. The first order derivatives are necessary for uncertainty propagation as presented in Chapter 5. The second order derivatives are used to establish parameter uncertainty bounds Δp_i within which linearity is preserved. This is essential since the assumed normally distributed uncertainty parameters will lead to a Gaussian distribution of the performance RMS and FRF magnitude and phase.

Chapter 5

UNCERTAINTY ANALYSIS

Parametrized models can be classified as being analysis- or measurement-based [Hagood, 1991]. The *analysis-based* model is developed using assumptions on system properties and the nature of component interactions. The *measurement-based* model is generated based on identification of measured data. That is, the response of the system is measured after a known input is applied. Hence, the measurement model is obtained mathematically by fitting the data [Jacques, 1994]. These two model types are in some sense complementary: measurement-based models provide the accuracy which analysis based models lack, while analysis based models provide more insight into the structure of the system.

The approach for generating a parameterized model depends on whether the model is measurement- or analysis-based. It is important to consider the nature of parametric uncertainty. In general, uncertainty can arise from four sources: errors in the values of system parameters used in the model, unmodeled dynamics, neglected nonlinearities, and neglected disturbances ([Skelton, 1989], [Campbell, 1996]). A key concept for evaluating the merits of a given uncertainty representation is the idea of *conservatism* (i.e., the degree of uncertainty attributed to each parameter). The conservatism of a representation can be reduced by tracking the correlations of the uncertainties in the model rather than modeling correlated uncertainties as statistically independent. Averaging the performance cost over the model set allows it to reflect the effects of parametric uncertainty on the system performance.

In Chapter 3, we expressed the modeling uncertainties in terms of modal parameters (m, k, γ) . One of the advantages of doing so is that it becomes very easy to propagate the uncertainty through the model to evaluate either the eigenvalue and eigenvector uncertainty, the frequency response uncertainty, or the performance cumulative RMS uncertainty.

5.1 Current Design Practice

In the preceding chapters, we have described the different steps involved in deterministic jitter analysis, which summarized the current design practice. In brief, a detailed FEM model is first constructed to generate the mass and stiffness matrices. Then the undamped modal characteristics of the structure are determined (an eigenproblem is solved). It is generally assumed that spacecraft are lightly damped [Ewins, 1984]. Then, based on engineering judgment and past experience, the modal damping ratios are specified. Finally, for a given disturbance (e.g., reaction wheels and their dynamic imbalances [Masterson, 1999]), a closed-form solution is obtained to predict the appropriate dynamic response quantities such as pointing, wave front tilt, optical line difference, or line of sight errors [Gutierrez, 1999]. These initial performance predictions are referred to as the nominal performances. That is where the analysis typically stops if the model predicts that performance requirements are met.

However, preliminary model predictions, although useful for comparing qualitatively competing design architectures, are not suitable for making absolute performance predictions. It is important to perform a disturbance analysis to determine the error bounds around the nominal performance values. Figure 5.1 illustrates the dangers of not meeting the requirements even when the nominal predictions are within the bounds of the requirements.

Given a particular nominal design and uncertainty level, the ultimate question the designer wants to answer is: "What is the worst or best possible performance I can expect from my system, and what is the probability that the actual system will effectively meet the require-

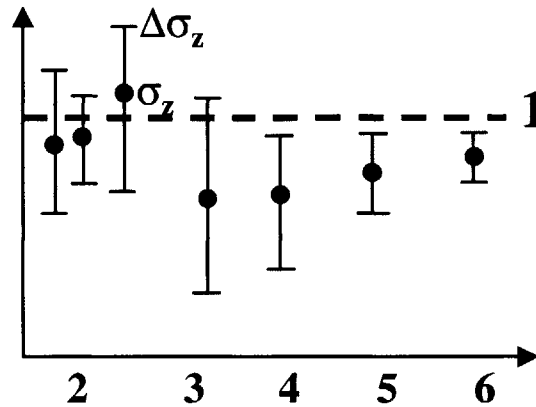


Figure 5.1 Example of uncertainty bounds for different designs.

ments?” For example, a system having its worst case bound outside the acceptable range might still constitute a valid solution if the probability of getting such worst case performance is sufficiently low. Therefore, in addition to determining the worst (and best) case performance, the capability to estimate the non-deterministic performance distribution would be very useful.

Hence, following the initial disturbance analysis, the steps involved in performing the uncertainty analysis are as follows:

1. Perform a parametric sensitivity analysis of the performances due to changes in the calculated modal parameters (modal mass and stiffness matrix elements, and transformed modal damping) as described in Chapter 4.
2. Based on the final sensitivity step in the deterministic analysis, identify parameters which significantly affect the computed magnitude of the output variable of interest. The sensitive parameters can now be identified as “random” parameters or random variables (RV) of the problem at hand.
3. Statistically characterize each chosen RV, e.g., mean, variance, probability density functions (PDF).
4. Formulate and solve the resulting random vibration problem.
5. For a given analysis confidence level (i.e. 2σ , 3σ equivalents), calculate the performance output (e.g., OPD or LOS error RMS).
6. Integrate under the distribution curve to get the probability of failure.

In this chapter, we will describe the following techniques, each having its own merit, to propagate uncertainties through the dynamic model of the system:

- Monte Carlo numerical simulation;
- linear approximation based on Taylor series expansion;
- linear covariance propagation method;
- extensive search of all “corners” of the uncertain parameter space (vertex method) for evaluating functions of interval (fuzzy) variables; and
- constrained optimization.

5.2 Monte Carlo Simulation

For simple systems with a few degrees-of-freedom and only several uncertain parameters, given the probability distributions of these parameters, it is possible to compute the probability distribution of the predicted performance, if not in closed-form then, at least, numerically. For larger models, however, such solutions are not feasible. Therefore, in order to validate a particular uncertainty propagation methodology, it is useful to compare its prediction to the results from an exhaustive random simulation.

The Monte Carlo simulation consists in obtaining the performance distribution by averaging the performance outputs over a large ensemble of random plants. These plants are computed based on randomly generated parameters. The larger the ensemble, the more accurate the uncertainty prediction. For our sample problem in the next chapter, we will perform such a simulation in order to compare the results of the different uncertainty evaluation techniques.

5.3 Linear Approximation Method

Based on the Taylor series expansion, this method is very straightforward. It uses the slope (sensitivity) of a specific output metric versus an uncertain parameters. For a particular perturbation size, the method provides the corresponding variation in the output. The assumption is that the linearity of the system is preserved for the perturbation size.

First, we define the vector u containing the variables of interest. The variables downstream from the modal parameters in the analysis flow are referred to as the “responses variables” and include the RMS performance and the FRF (magnitude and phase).

$$u = u(p) \quad (5.1)$$

The vector, u , which might represent eigenvalues, eigenvectors or frequency responses, are expanded into Taylor series about the nominal vector, \tilde{u} , such that

$$u = \tilde{u} + \left[\frac{\partial u}{\partial p} \right] \Delta p + \text{h.o.t.} \quad (5.2)$$

The matrix, $\partial u / \partial p$, is called the *sensitivity* matrix and is designated T_{up} . The derivatives, $\partial u / \partial p$, are particularly simple to derive when u represents eigenvalues or eigenvectors and r represents modal mass and stiffness parameters (Chapter 4). Also, $\partial u / \partial p$ is zero whenever u represents an eigenvalue (undamped) and/or eigenvector and r represents modal damping.

$$T_{up} \equiv \frac{\partial u}{\partial p} \quad (5.3)$$

Thus, by linear approximation, the vector of uncertainty $\Delta u = u - \tilde{u}$ is given by

$$\Delta u = T_{up} \Delta p \quad (5.4)$$

The sensitivities can be calculated for various structural parameters, not just the modal parameters as defined in Chapter 3. For example, we could compute the sensitivities with respect not only to the physical parameters of the structure such as the physical mass and stiffness of structural elements, but also for parameters such as characteristic length, material density, temperature, etc. The accuracy of this method is very sensitive to the size of the perturbations and is really only valid for small perturbations. Also, it does *not* provide us with statistical information on the distribution of the output parameters, u unlike the approach described in the following section.

5.4 Linear Covariance Propagation

The linear covariance propagation builds on the linear approximation method to propagate statistical uncertainty from a database. Between the database uncertainty propagation methods described below, this is the most straightforward, economical, and generally applicable.

5.4.1 Database Scaling

In order to be able to use the database described in Chapter 3, it must first be scaled appropriately for the particular nominal modal model under consideration. As we recall, the database must be normalized to remove frequency dependence. Hence, the scaled covariance matrix, Σ_{pp} , is obtained from the dimensionless covariance matrix, $\Sigma_{\hat{p}\hat{p}}$, by appropriate frequency scaling. Given, $\Sigma_{\hat{r}\hat{r}}$, in the form

$$\Sigma_{\hat{p}\hat{p}} = \begin{bmatrix} \Sigma_{mm} & \Sigma_{m\bar{k}} & 0 \\ \Sigma_{\bar{k}m} & \Sigma_{\bar{k}\bar{k}} & 0 \\ 0 & 0 & \Sigma_{\gamma\gamma} \end{bmatrix} \quad (5.5)$$

Σ_{pp} is obtained by multiplying the individual elements of $\Sigma_{\hat{p}\hat{p}}$ by the appropriate frequencies to get the following form

$$\Sigma_{pp} = \begin{bmatrix} \Sigma_{mm} & \Sigma_{mk} & 0 \\ \Sigma_{km} & \Sigma_{kk} & 0 \\ 0 & 0 & \Sigma_{\gamma\gamma} \end{bmatrix} \quad (5.6)$$

As stated in Chapter 3, Σ_{pp} represents the covariance matrix of the modal mass, stiffness and transformed damping parameters. It is in block-diagonal form, provided that the damping uncertainty is estimated independently of mass and stiffness uncertainty, as is usually the case in structural dynamic modeling. Therefore, when a particular element of Σ_{mk} corresponds to m_{gh} and k_{ij} , then

$$\Sigma_{m_{gh}k_{ij}} = \tilde{\omega}_i \tilde{\omega}_j \Sigma_{m_{gh}\tilde{k}_{ij}} \quad (5.7)$$

where the $\tilde{\omega}$ are the natural frequencies corresponding to the square roots of the eigenvalues λ . Similarly, when an element of Σ_{kk} corresponds to k_{gh} and k_{ij} , then

$$\Sigma_{k_{gh}k_{ij}} = \tilde{\omega}_g \tilde{\omega}_h \tilde{\omega}_i \tilde{\omega}_j \Sigma_{\tilde{k}_{gh}\tilde{k}_{ij}} \quad (5.8)$$

The corresponding scaling operations of equations 5.6 through 5.8 can be obtained by pre- and post-multiplying the database covariance matrix by a transformation matrix, $T_{p\hat{p}}$

$$\Sigma_{pp} = T_{p\hat{p}} \Sigma_{\hat{p}\hat{p}} T_{p\hat{p}}^T \quad (5.9)$$

where the transformation matrix is given by

$$T_{p\hat{p}} = \begin{bmatrix} I_{N \times N} & & 0 & & 0 \\ & \begin{bmatrix} \tilde{\omega}_1 \tilde{\omega}_1 & 0 & 0 & 0 & 0 & 0 & 0 \\ 0 & \tilde{\omega}_1 \tilde{\omega}_2 & 0 & 0 & 0 & 0 & 0 \\ 0 & 0 & \ddots & 0 & 0 & 0 & 0 \\ 0 & 0 & 0 & \tilde{\omega}_1 \tilde{\omega}_n & 0 & 0 & 0 \\ 0 & 0 & 0 & 0 & \tilde{\omega}_2 \tilde{\omega}_2 & 0 & 0 \\ 0 & 0 & 0 & 0 & 0 & \ddots & 0 \\ 0 & 0 & 0 & 0 & 0 & 0 & \tilde{\omega}_n \tilde{\omega}_n \end{bmatrix} & & 0 \\ & & 0 & & & & I_{n \times n} \end{bmatrix} \quad (5.10)$$

where n is the number of modes in the database, and $N = \frac{1}{2}(n^2 + n)$ corresponds to the number of uncertain modal mass parameters (upper triangular).

5.4.2 Covariance Propagation

The covariance matrix of the output variable uncertainty Δu is defined as

$$\Sigma_{uu} = E[\Delta u \Delta u^T] \quad (5.11)$$

which can be simplified using the linear approximation from equation (5.4).

$$\Sigma_{uu} = T_{up}E[\Delta p\Delta p^T]T_{up}^T = T_{up}\Sigma_{pp}T_{up}^T \quad (5.12)$$

To obtain the covariance matrix of the performance outputs, it is only necessary to pre- and post-multiply the modeling error covariance matrix by the sensitivity matrix. The simplicity and the computational cost efficiency of this method makes it very attractive. The diagonal elements of Σ_{uu} correspond to the variance, σ_u^2 , of the variables contained in the vector u which gives us directly a measure of the uncertainty in the output parameters. The square root of the diagonal elements correspond to the standard deviations of the parameters examined. Hence, it is very easy to propagate the uncertainty through the variables of interest in an analysis as long as we have an expression for their sensitivities.

Since we have assumed Gaussian distributions of the statistical database parameters, we can deduced that the performance outputs also have Gaussian distributions as long as the linearity is preserved. This is a very important result. Stated differently, it means that, inside the range of validity of the linear approximation, the output will be distributed around its nominal value with a standard deviation σ_u as illustrated in Figure 5.2

This has a very strong implication for the uncertainty analysis on the performance RMS. For instance, integrating under the PDF, gives us the cumulative distribution density function (CDF) that tells us, for a particular error budget, with what probability the current design will satisfy that requirement. Figure 5.3 shows the RMS distribution for a system with a nominal prediction of $\mu = 4$ [m rms] and a standard deviation of $\sigma = 1$ [m]. For this example, the performance requirement is 5.5 [m rms] (which corresponds to a 1.5σ bound). The corresponding cumulative RMS plot is shown on the right and shows that even though there is a slight possibility for the system to exceed the specification, there is a 93% probability of success.

From the probability of success curve, it is also possible to compute the probability of failure (which correspond to its complementary probability).

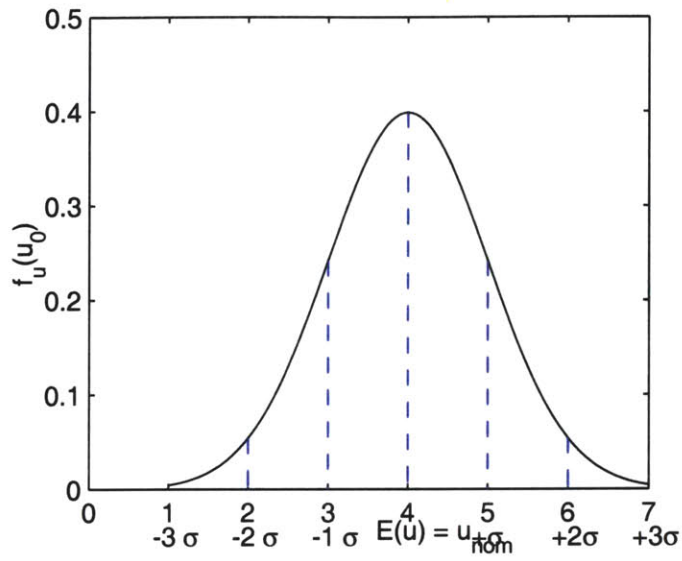


Figure 5.2 Gaussian distribution of the output parameter u

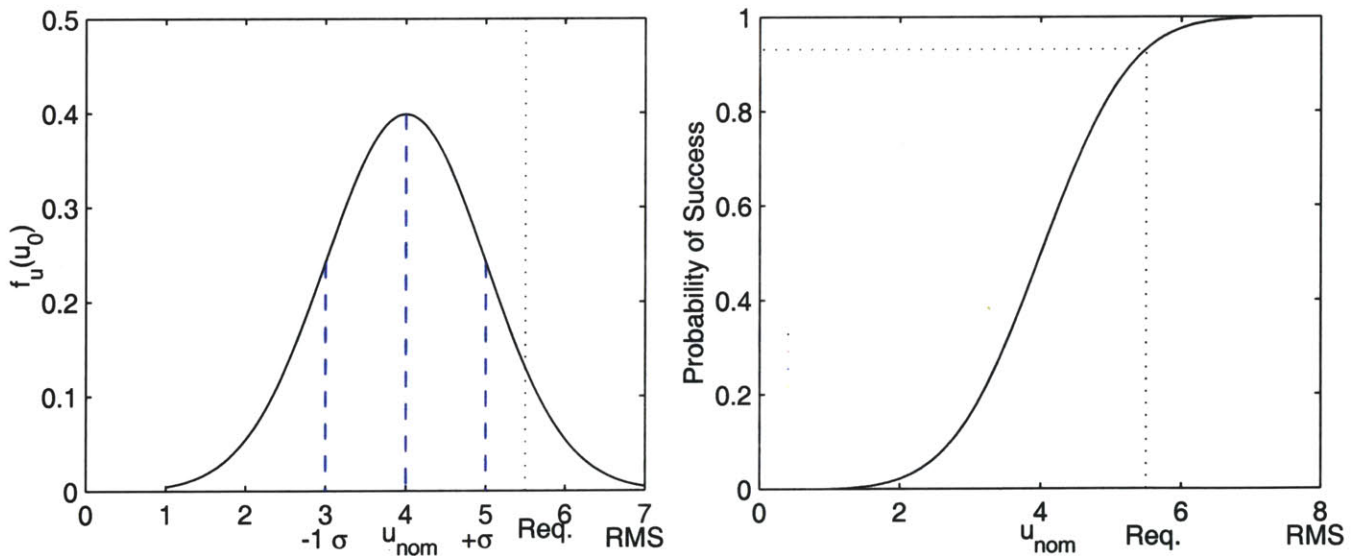


Figure 5.3 Distribution of the performance RMS (left), and the corresponding probability of success (right)

$$P(\text{Failure}) = 1 - P(\text{Success}) \tag{5.13}$$

Figure 5.4 illustrates the probability of failure for the above example, which happens to e

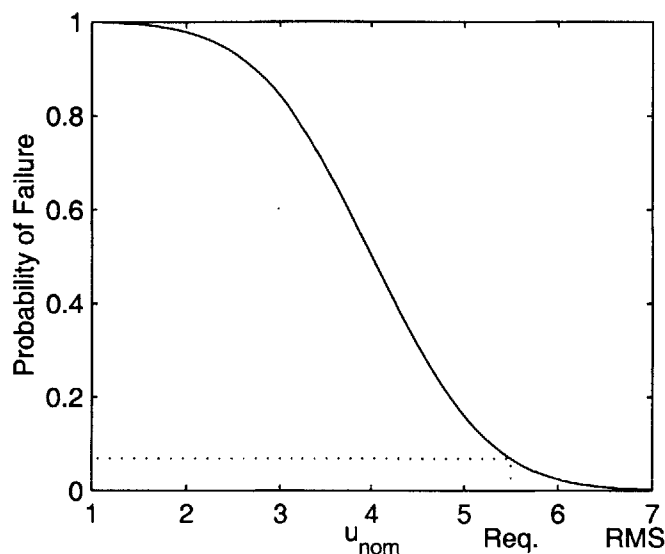


Figure 5.4 Probability of failure

slightly less than 7% for the given requirement. If the RMS requirement is tightened, the probability of failure increases accordingly.

In summary, we use the performance RMS sensitivity to the modal parameters as follows:

1. we propagate the uncertainty covariance matrix Σ_{pp} to obtain the performance covariance matrix Σ_{zz} ;
2. the square roots of the diagonal elements of Σ_{zz} correspond to the standard deviations of the performance RMS metrics;
3. since we assumed that the linearity is preserved and that the uncertain parameters are gaussian, we obtain the normal distribution of the RMS centered around the nominal prediction;
4. integrating under the PDF gives us the probability of success (CDF) for a given error budget;
5. we can also obtain the probability of failure from the complementary probability.

For the FRF magnitude and phase, it is also possible to use the covariance propagation method. The only difference is that the process must be repeated at every frequency point. Using the $\sigma(\omega)$, we can plot the transfer function along with its $\mp n\sigma$ bounds. However, around the poles and zeros, the linear assumption fails and the covariance propagation results are no longer valid. This will be demonstrated in Chapter 6.

5.5 Vertex Method

5.5.1 Corner Search

Another approach to evaluating the bounds on the performance predictions is to perform an extensive search of all the “vertices”, the possible combinations of the upper and lower limits of each parameter. These combinations correspond to the vertices of a rectangular hyperspace. Figure 5.5 illustrates a two-dimension space for the case of two uncertain parameters.

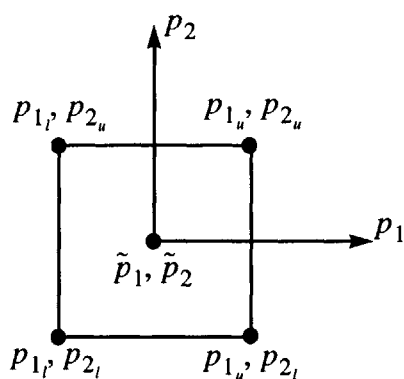


Figure 5.5 Two-dimensional corner space

The upper and lower bounds of the response interval correspond to the largest and smallest response obtained while searching the corner space.

Diagonalization of the Covariance Matrix

Before the method can be applied, it is necessary to uncouple the parameters in the database by transforming them from the original database parameters in vector p to an uncorrelated set of parameters r . Since the covariance matrix Σ_{pp} is symmetric and non-negative definite, it can be diagonalized via a singular values decomposition

$$\Sigma_{pp} = U\Sigma_{rr}U^T \quad (5.14)$$

where the eigenvector matrix U is unique and defines the linear transformation between the database modal parameters, p , and the uncorrelated parameters, r .

$$\Delta p = U\Delta r \quad (5.15)$$

By applying the above transformation to the covariance matrix definition (Eq. 3.50), we recover the expression from (5.14).

$$\begin{aligned} \Sigma_{pp} &= E[\Delta p \Delta p^T] = E[U\Delta r \Delta r^T U^T] = UE[\Delta r \Delta r^T]U^T \\ &= U\Sigma_{rr}U^T \end{aligned} \quad (5.16)$$

where the diagonal covariance matrix of the uncorrelated transformed parameters, r , is expressed as follows

$$\Sigma_{rr} = \begin{bmatrix} \sigma_{r_1}^2 & & \\ & \ddots & \\ & & \sigma_{r_N}^2 \end{bmatrix} = RR \quad (5.17)$$

where $N = (n^2 + 2n)$ is the total number of parameters in the database (n being the number of uncertain modes), $\sigma_{r_i}^2$ are the variance of the uncorrelated transformed parameters r_k and the matrix R is the diagonal matrix of their standard deviations.

$$R = \begin{bmatrix} \sigma_{r_1} & & \\ & \ddots & \\ & & \sigma_{r_N} \end{bmatrix} \quad (5.18)$$

Possibility Intervals

To evaluate the possibility bounds on the output variable u_j corresponding to the $\pm n\sigma_{r_k}$ parameter intervals, we define

$$\Delta r_k = \pm n\sigma_{r_k} \quad (5.19)$$

A particular vertex $\{\Delta r\}_i$ (corner) is obtained by selecting a particular combination, v_i , of perturbation on the parameter r_k , where the corner, for a $n\sigma$ bound, is expressed as

$$\{\Delta r\}_i = nRv_i \quad (5.20)$$

where the combination vector, v_i , contains only (+1)'s and (-1)'s, corresponding to the upper and lower bounds of the parameters, r_k respectively. To recover the corresponding perturbation vector for the original parameters, p_k 's, we use equation (5.15) as follows

$$\{\Delta p\}_i = U\{\Delta r\}_i = UnRv_i \quad (5.21)$$

For a particular vertex, we can reconstruct from $\{\Delta p\}_i$ the corresponding modal mass, stiffness and transformed damping matrix errors ($\{\Delta m\}_i$, $\{\Delta k\}_i$, $\{\Delta \Gamma\}_i$) from which we get

$$\begin{aligned} \{m\}_i &= I + \{\Delta m\}_i \\ \{k\}_i &= \tilde{\Lambda} + \{\Delta k\}_i \\ \{\Gamma\}_i &= \tilde{\Gamma} + \{\Delta \Gamma\}_i \end{aligned} \quad (5.22)$$

From there, two options are available. We can either use the sensitivity equations of the response variable u_j , with respect to the uncertain parameters, to propagate linearly, as described in Section 5.3, the perturbations $\{\Delta p\}_i$ to obtain an approximate value of u_j

for each corner. This is a simple and fast result to obtain. Or, we can compute the response of the system evaluates for the perturbed parameters, $\{p\}_i$, the vertex is given by

$$\{p\}_i = \tilde{p} + \{\Delta p\}_i \quad (5.23)$$

This would be a more accurate, but more costly answer. Notice that for a system with N uncertain parameters, there is 2^N possible combinations to search. This means that the number of corners to search increases very rapidly as the number of degrees of freedom of the system increases. For example, a 1-DOF system has three uncertain parameters (i.e., one modal mass, one modal stiffness, and one transformed modal damping parameter) which corresponds to height vertices. For a 2-DOF system, the number of uncertain parameters goes to $N = (2^2 + 2(2)) = 8$ which corresponds to already 256 combinations! Therefore, for large order models, the method becomes very costly as thousands of vertices have to be searched to find the lower and upper bounds on the response. Furthermore, for the uncertainty on the FRF Bode plot, the procedure must be repeated for every frequency points. The number of calculation, x , is then given by

$$x = N_f N_F (2^{N_p}) \quad (5.24)$$

where N_f is the number of frequency points, N_F is the number of FRF's, and N_p is the number of uncertain parameters.

Improvements

In order to limit the number of corners to be searched and limit the computation time, Gutierrez proposes to use the sensitivity information (sign of the slopes) to identify a priori the “bad” or “good” corners [Gutierrez, 1999]. This method is inspired by the so-called Taguchi Methods which propose ways to reduce the number of corners to search [Taguchi, 1995].

Since, even for large systems, only a few modes contribute for most of the performance RMS [Gutierrez, 1999], we propose to select only these critical modes, and perform the

corner search only for the modal parameters corresponding to these particular modes. This idea is the beneficial result to reduce by orders of magnitude the amount of computation. We will demonstrate this technique in Chapter 7 for the SIM Classic model.

5.5.2 Included Maxima and Minima

One other issue with the vertex method, is that it is assumed that the worst and/or best case will occur at one of the vertices. It is often the case for simple SISO system with flat (white noise) disturbances. In general, it is not the case.

For system with closely spaced modes, there is combinations of incremental perturbation sizes (inside the lower and upper bounds interval of the parameters) for which the poles and zeros of the system will interact in a constructive and/or destructive way increasing the interval of the response (higher RMS when two poles combine together, and smaller RMS for poles zeros cancellation). Gutierrez shows the example of a cantilever beam whose two perpendicular bending modes are very close [Gutierrez, 1999].

Another type of system for which the maxima and minima of the response will not necessarily be at the vertices, even when the modes are widely spaced in frequency is for the case when the disturbance is tinted. For instance, if the disturbance has discrete frequency content, then the poles of the plant will interact with the peaks of the disturbance. The worst case will be when all the poles align with the disturbance frequencies. Vice-versa for the best performance, which will occur when the poles are far away from the disturbance frequencies and/or when the zeros of the plant will attenuate the disturbance effects.

Therefore, in order to increase the accuracy of the worst/best case estimate, it will be necessary to search the whole uncertainty space. Three methods can be implemented to do so:

1. Uniform grid search: compute the response at different interval (Fuzzy analysis)
2. Random search (corresponds to a Monte Carlo simulation inside the parameter bounds)
3. Constrained optimization.

Uniform Grid Search

Performing a uniform grid search, also known as Fuzzy analysis [Dong & Shah, 1987], as illustrated in Figure 5.6 for a 2D's case will improve the accuracy of the estimate of the worst/best response performance, but will also increase significantly the computation cost. The finer the grid, the better the estimates, but the higher the costs.

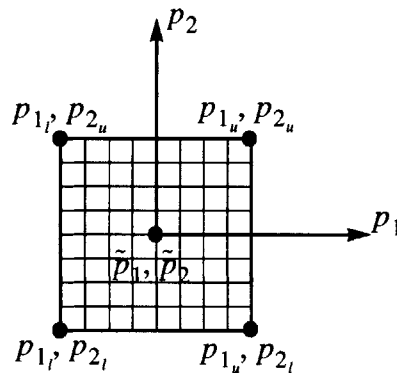


Figure 5.6 Uniform 2-D search grid

Constrained Optimization

This approach has better chance to find a more accurate prediction of the worst/best case estimate of the response. This extra accuracy though comes at a great cost as it is a computational intensive method.

The approach described by Gutierrez in [Gutierrez, 1999] attempts to find a solution to an optimization problem cast as follows

$$\max_p J = \text{trace}(\Sigma_{z^*}), \quad \text{where } p_{LB} \leq p \leq p_{UB} \quad (5.25)$$

where p is the vector of uncertain parameters, and p_{LB} and p_{UB} are the lower and upper bounds, respectively of the parameters.

The contribution of the present work to this method is to provide the constrained optimization with realistic parameter bounds, extracted from a statistical database, for the modal mass and stiffness matrix elements and the transformed damping parameters.

Recapitulation of the Vertex Method

In summary, the vertex method gives us a worst/best case estimate of the response (RMS or FRF). It can become very costly unless measures are taken to reduce the search space. The method suggested in this research is to select the critical modes and perform the corner search only on the parameters of these modes. Also, one inconvenience of the method, is that it does not provide us with a measure of the probability of having the worst/best case to happen. In fact it corresponds more to a “ 3σ ” type event that has very small chance to happen. Therefore, using the vertex bounds for design would be very conservative.

5.6 Hybrid Method for the FRF Bounds

As described in Section 5.4 the linear covariance propagation is not valid to evaluate the uncertainty bounds on the FRF magnitude and phase near the poles and zeros. Hasselman suggests to use the vertex method to limit the uncertainty around these singularities [Hasselman, Chrostowski & Ross, 1994]. Although, the vertex method gives us a worst-case type analysis, it is the most convenient way to evaluate the bounds on the FRF near the poles and zeros. We will show an example of this method in the next chapter.

5.7 Summary

In this chapter we have presented different methods that we use to propagate the uncertainties and evaluate the error bounds around the nominal performance predictions. One contribution of this research work was to obtain the probability distribution of the response and hence evaluate the probability of success of the design given a certain error budget. We have also obtained the complementary probability of failure of the design given an error budget. This is an important result in the context of high profile spacecraft

UNCERTAINTY ANALYSIS

mission such as SIM or NGST as it help the engineer build confidence that a particular architecture is suitable to meet its specific tight requirements in presence of modeling uncertainties. An other contribution was to provide the constrained optimization technique, use to evaluate the worst-case performance, with the necessary bounds on the parameters. These bounds were obtained from the past experience database.

Chapter 6

SAMPLE PROBLEM

In order to build intuition about how the uncertainties propagate through the dynamic model and to validate the uncertainty analysis methods presented in Chapter 5 for the performance RMS and the transfer function (magnitude and phase), we will present a thorough numerical uncertainty analysis of a two-degree-of-freedom oscillator. The uncertainty analysis will be demonstrated for realistic large-scale models on the SIM Classic integrated model in Chapter 7.

Although the two-degree-of-freedom (2-DOF) oscillator is the most simplistic abstraction of a dynamical system and very few structures could realistically be modeled by such a simple system, we will spend time analyzing this 2-DOF oscillator because it will be easier to grasp the implications of the parameter uncertainties with no complications arising from analyzing a realistic structure standing in the way. In fact, the knowledge of the properties of this system will help us build intuition for more complex multi-degree-of-freedom (MDOF) systems. Complex structures can always be represented as a linear superposition of a number of single-degree-of-freedom characteristics [Ewins, 1984]. This is especially true for lightly damped structures with large modal frequency separation.

After describing the model characteristics in the next section, we will go through the steps of evaluating the nominal performance of the system (Section 6.2), describe the uncertainty database (Section 6.3), and computing the sensitivities (Section 6.4). We will then validate the uncertainty analysis methodology by performing the uncertainty analysis

using the methods described in Chapter 5 (Section 6.5) and compare the accuracy of their predictions.

6.1 Model Description

6.1.1 Physical Description

A mechanical implementation of a two-degree-of-freedom oscillator is illustrated in Figure 6.1. It is composed of two mass elements, M_1 and M_2 , linked in series and attached to a fixed wall (fixed boundary condition) by two springs of stiffnesses K_1 and K_2 . The system is driven by a zero-mean unit-intensity white noise disturbance force w applied to the second mass.

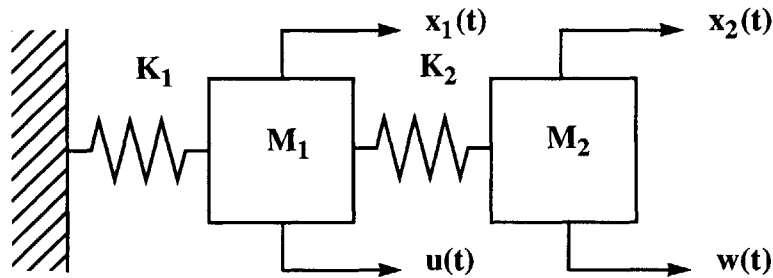


Figure 6.1 Two degree of freedom oscillator

We want to determine the uncertainty on the FRF (magnitude and phase) as well as on the root-mean-square (RMS) value of the displacement response of the second mass x_2 due to a collocated disturbance force w . In order to do so, we will first compute the nominal FRF and the nominal performance RMS. Then we will proceed to compute their sensitivities with respect to the system uncertain parameters. The model of a dynamic system is a mathematical abstraction of a real physical system and is only as good as our estimates of the physical parameters of the system are. Furthermore, for a continuous system, the way the system is discretized also has a great influence on the accuracy of the predictions.

For the purposes of this example, we consider a 2-DOF oscillator designed to vibrate freely at two different specific frequency, ω_1 and ω_2 [rad/s]. The analytical model of this system will be called the *nominal* (also referred to as analytical) model

. The nominal masses, \tilde{M}_1 and \tilde{M}_2 , have values of 3.0 kg and 1.5 kg respectively, and the springs have nominal stiffnesses, \tilde{K}_1 and \tilde{K}_2 , of 8 N/m and 4 N/m respectively. The nominal damping ratios, $\tilde{\zeta}_1$ and $\tilde{\zeta}_2$, as we modeled them, are equal to 1% and 0.5%.

In order to build an intuitive feeling for the uncertainty propagation and also validate the techniques described in Chapter 5, we will imagine that we want to mass produce this oscillator that we have designed. Even if manufactured with great precision, we know that the physical masses and springs, as well as the damping ratios, will have actual values different than the specified ones. Three factors influence the probability distribution of the physical mass and stiffness values:

- tolerances (affect the width of the distribution);
- the manufacturing process (homogeneity of the material characteristic, repeatability and stability of the process);
- and quality control (affects the width of the distribution, but can also influence the shape of the distribution (e.g. by removing the tails of the distribution)).

Therefore, the behavior of any of the oscillators manufactured in presence of disturbances will differ from the predictions made by the nominal model. The mathematical representation of one particular unit will be called the *actual* (also referred to as test, or measured) model. For our example, we will assume that the actual mass and stiffness elements have gaussian distributions ($\mathfrak{N}(\mu, \sigma^2)$) centered around their means which correspond to their nominal values:

$$\begin{aligned}
 M_1 &\sim \mathfrak{N}(3, (0.2)^2) \\
 M_2 &\sim \mathfrak{N}(1.5, (0.1)^2) \\
 K_1 &\sim \mathfrak{N}(8, (0.4)^2) \\
 K_2 &\sim \mathfrak{N}(4, (0.2)^2)
 \end{aligned}
 \tag{6.1}$$

Figure 6.2 illustrates the probability density functions for the mass and stiffness elements as described above.

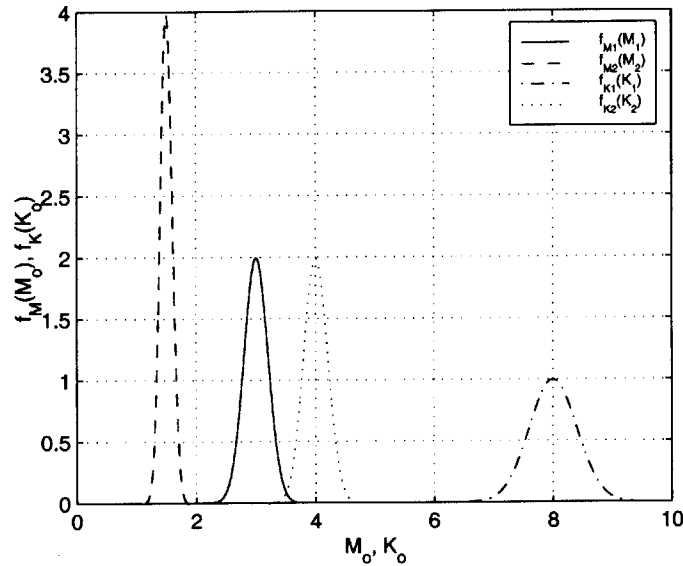


Figure 6.2 Distribution for M and K

The damping ratios, ζ_r , also have values distributed around their mean values (nominal). Unlike the mass and spring distributions, the damping ratios distributions are not symmetric. Typically, they have log-normal distributions, which can also be expressed in terms of the mean and standard deviation (μ_ζ and σ_ζ). For our design, we have set the standard deviations to 0.8% and 0.4% respectively for ζ_1 and ζ_2 . Following equations (3.60) through (3.62), we can transform a log-normal distribution (noted $\aleph_{\log}(\mu_\zeta, \sigma_\zeta^2)$) into a Gaussian distribution (noted $\aleph(\mu_\gamma, \sigma_\gamma^2)$), where γ_1 and γ_2 are the corresponding transformed damping parameters. The damping ratio distributions are transformed as follows

$$\zeta_1 \sim \aleph_{\log}(0.01, (0.008)^2) \Rightarrow \begin{cases} c = -4.8525 \\ d = 0.70335 \end{cases} \Rightarrow \aleph(-4.8525, (0.70335)^2) \sim \gamma_1 \quad (6.2)$$

$$\zeta_2 \sim \aleph_{\log}(0.005, (0.004)^2) \Rightarrow \begin{cases} c = -5.5457 \\ d = 0.70335 \end{cases} \Rightarrow \aleph(-5.5457, (0.70335)^2) \sim \gamma_2$$

Figure 6.3 illustrates the above transformation from the damping ratios log-normal distribution to their corresponding Gaussian distributions.

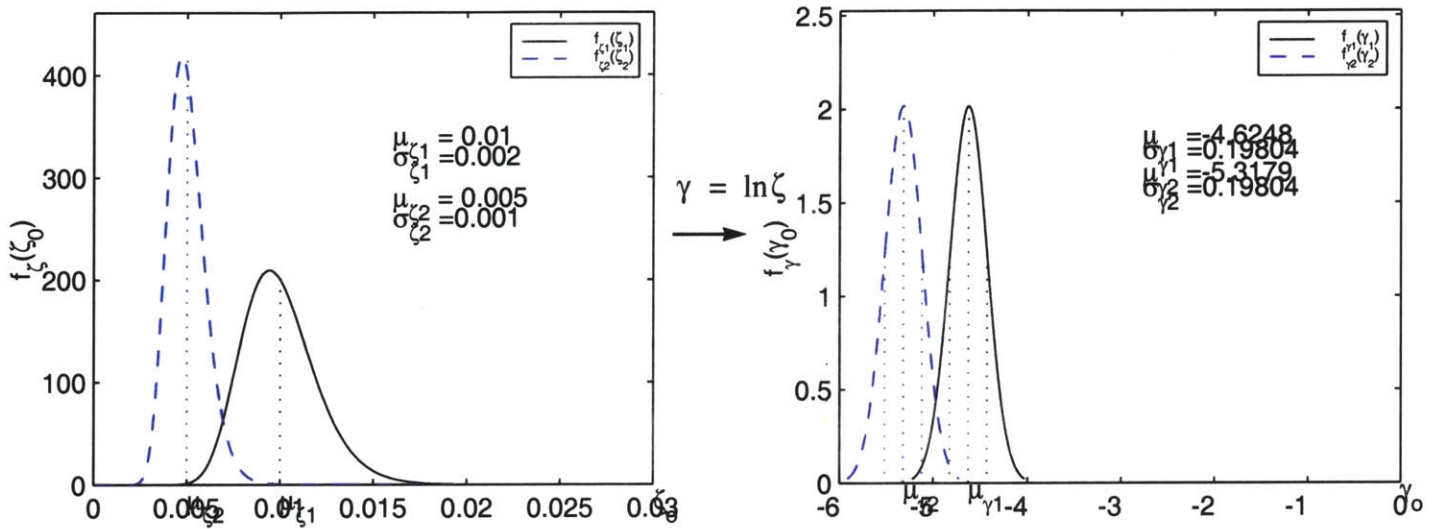


Figure 6.3 Distributions for the damping ratios: Lognormal PDF for the ζ_r 's (left), and corresponding Gaussian PDF for the γ_r 's (right)

Table 6.1 summarizes all nominal parameters values and their standard deviations.

TABLE 6.1 Nominal Structural Element and their Uncertainty

Parameters	Nominal	Units	Uncertainty
	Values $\tilde{p} = \mu_p$		
M_1	3	[kg]	0.2
M_2	1.5	[kg]	0.1
K_1	8	[N/m]	0.4
K_2	4	[N/m]	0.2
γ_1	-4.8525	---	0.70335
γ_2	-5.5457	---	0.70335

6.1.2 Modeling

The equations of motion (see Eq. 2.1) for the 2-DOF system are given by

$$\begin{aligned} M\ddot{x} + C\dot{x} + Kx &= \beta_w w \\ z &= C_{zx}x \end{aligned} \quad (6.3)$$

where C is the equivalent damping matrix, and the performance matrix C_{zx} is an identity matrix. For the two-mass-two spring problem, the mass and stiffness matrices are given by

$$M = \begin{bmatrix} M_1 & 0 \\ 0 & M_2 \end{bmatrix}, \quad K = \begin{bmatrix} K_1 + K_2 & -K_2 \\ -K_2 & K_2 \end{bmatrix} \quad (6.4)$$

Following the procedure described in Chapter 2, the first step in solving the equations of motion is to solve the generalized eigenvalue problem for the undamped case ($C = 0$ and $w = 0$)

$$(K - \lambda_r M)\phi_r = \begin{bmatrix} K_1 + K_2 - \lambda_r M_1 & -K_2 \\ -K_2 & K_2 - \lambda_r M_2 \end{bmatrix} \begin{bmatrix} \phi_{1,r} \\ \phi_{2,r} \end{bmatrix} = 0 \quad (6.5)$$

from which we obtain the eigenvalues

$$\lambda_{1,2} = \omega_{1,2}^2 = \frac{1}{2} \left\{ \frac{K_1}{M_1} + \frac{K_2}{M_2} \left(1 + \frac{M_2}{M_1} \right) \mp \sqrt{\left[\frac{K_1}{M_1} + \frac{K_2}{M_2} \left(1 + \frac{M_2}{M_1} \right) \right]^2 - \frac{4K_1K_2}{M_1M_2}} \right\} \quad (6.6)$$

and the mass normalized mode shapes

$$\Phi = \begin{bmatrix} \phi_{11} & \phi_{12} \\ \phi_{21} & \phi_{22} \end{bmatrix} = \frac{1}{\sqrt{M_1K_2^2 + M_2(K_1 + K_2 - \lambda_1M_1)^2}} \begin{bmatrix} K_2 & K_2 \\ K_1 + K_2 - \lambda_1M_1 & K_1 + K_2 - \lambda_2M_1 \end{bmatrix} \quad (6.7)$$

Performing the following transformation on equation (6.3),

$$x = \Phi\eta \quad (6.8)$$

yields the uncoupled modal equations of motion

$$\begin{aligned}\ddot{\eta} + 2Z\Lambda^{1/2}\dot{\eta} + \Lambda\eta &= \Phi^T\beta_w w \\ z &= C_{zx}\Phi\eta\end{aligned}\quad (6.9)$$

which when written in state-space form (for the nominal plant) gives

$$\begin{aligned}\underbrace{\begin{bmatrix} \dot{\eta} \\ \ddot{\eta} \end{bmatrix}}_{\dot{q}} &= \underbrace{\begin{bmatrix} 0 & I \\ -\tilde{\Lambda} & -2\tilde{Z}\tilde{\Lambda}^{1/2} \end{bmatrix}}_{A_{zw}} \begin{bmatrix} \eta \\ \dot{\eta} \end{bmatrix} + \underbrace{\begin{bmatrix} 0 \\ \tilde{\Phi}^T\beta_w \end{bmatrix}}_{B_{zw}} w \\ z &= \underbrace{\begin{bmatrix} C_{zx}\tilde{\Phi} & 0 \end{bmatrix}}_{C_{zw}} \begin{bmatrix} \eta \\ \dot{\eta} \end{bmatrix} + \underbrace{[0]}_{D_{zw}}\end{aligned}\quad (6.10)$$

For this example $C_{zx} = \begin{bmatrix} 0 & 1 \end{bmatrix}$ and $\beta_w = \begin{bmatrix} 0 \\ 1 \end{bmatrix}$.

After having obtained our system model, the next step of the performance analysis is to evaluate nominal performance.

6.2 Initial Performance Evaluation

For the nominal model described in the previous section, we get the following nominal variables. The nominal eigenvalues are given by

$$\tilde{\Lambda} = \tilde{\Phi}^T \tilde{K} \tilde{\Phi} = \begin{bmatrix} 1.333 & 0 \\ 0 & 5.333 \end{bmatrix}\quad (6.11)$$

and since $\tilde{\Lambda} = \tilde{\Omega}^2$, we can get the natural frequencies

$$\tilde{\Omega} = \sqrt{\tilde{\Lambda}} = \begin{bmatrix} 1.1547 & 0 \\ 0 & 2.3094 \end{bmatrix}\quad (6.12)$$

The mass normalized nominal eigenvector matrix is

$$\tilde{\Phi} = \begin{bmatrix} -0.3333 & -0.4714 \\ -0.6667 & 0.4714 \end{bmatrix} \quad (6.13)$$

and therefore, we get the following values for the state-space matrices

$$\tilde{A}_{zw} = \begin{bmatrix} 0 & 0 & 1 & 0 \\ 0 & 0 & 0 & 1 \\ -1.333 & 0 & -0.023094 & 0 \\ 0 & -5.333 & 0 & -0.023094 \end{bmatrix}, \quad \tilde{B}_{zw} = \begin{bmatrix} 0 \\ 0 \\ -0.6667 \\ -0.4714 \end{bmatrix} \quad (6.14)$$

$$\tilde{C}_{zw} = [-0.6667 \ 0.4714 \ 0 \ 0]$$

We can now proceed to evaluate the nominal performance RMS and the FRF of this deterministic model.

6.2.1 Frequency Response Function (FRF)

The FRF of the disturbance input w to the performance output z , illustrated on Figure 6.4, is given by

$$G_{zw}(s) = C_{zw}(sI - A_{zw})^{-1}B_{zw} \quad (6.15)$$

Because we have assumed proportional damping, the equations of motion, as written in equation (6.9), are decoupled. It can be shown that the above transfer function (also called dynamic response) can also be written in the following modal contribution form

$$\tilde{G}_{zw}(j\omega) = \sum_{r=1}^2 \frac{C_{zx}\tilde{\phi}_r\tilde{\phi}_r^T\beta_w}{(\tilde{\lambda}_r - \omega^2) + j2\tilde{\zeta}_r\tilde{\lambda}_r^{1/2}\omega} \quad (6.16)$$

which for our specific C_{zx} and β_w reduces to

$$\tilde{G}_{zw}(j\omega) = \frac{\tilde{\phi}_{21}\tilde{\phi}_{21}^T}{(\tilde{\lambda}_1 - \omega^2) + j\omega 2\tilde{\zeta}_1\tilde{\lambda}_1^{1/2}} + \frac{\tilde{\phi}_{22}\tilde{\phi}_{22}^T}{(\tilde{\lambda}_2 - \omega^2) + j\omega 2\tilde{\zeta}_2\tilde{\lambda}_2^{1/2}} = \tilde{G}_{zw_1} + \tilde{G}_{zw_2} \quad (6.17)$$

The Bode plot of the magnitude and phase of the above FRF is shown in Figure 6.4.

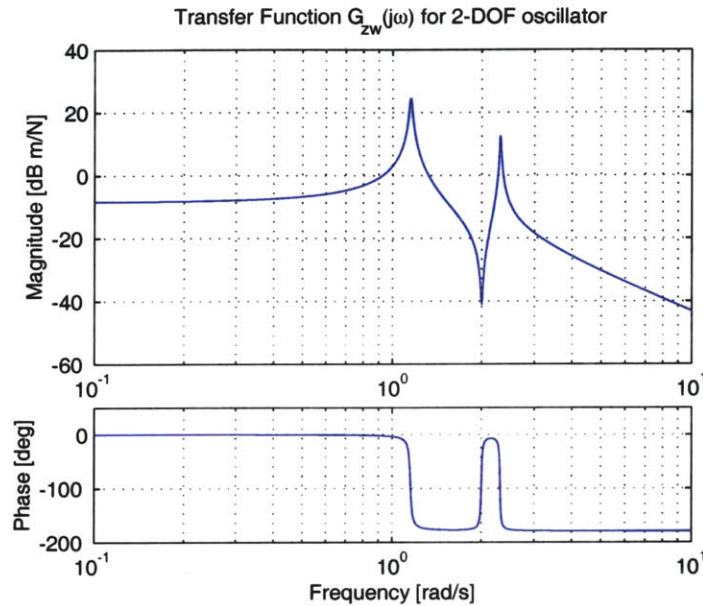


Figure 6.4 2-DOF oscillator Frequency Response Function.

Notice that since the input w and the output z are collocated, the phase of the FRF ($\angle \tilde{G}_{zw}(j\omega)$) is bounded between 0° and -180° . This is always the case for collocated sensors and actuators. Also, we notice that at DC ($\omega = 0$), the slope of the magnitude of the transfer function is zero. In fact, from equation (6.16), we can see that the gain of the FRF reduces to a constant K^{-1} when ω is set to zero. It can be shown (for $C_{zx} = \beta_w = 1$) that this constant gain is equal to

$$K^{-1} = \frac{K_1 + K_2}{K_1 K_2} = \frac{1}{K} \tag{6.18}$$

which is consistent with Hooke's law for springs in series (K being the equivalent stiffness). Explicitly, at DC, we have the displacement x that is proportional to the amplitude of the applied force $W = w(0)$ (i.e., $x = \tilde{G}_{zw}(0) \cdot W = \frac{W}{K}$)

6.2.2 Nominal Performance RMS

We define the output performance as the displacement x_2 of the second mass. We will compute the nominal performance RMS using two methods described in Chapter 2: the power spectral density (PSD) integration and the Lyapunov equation method. The computations for the second method will be carried out explicitly to be used later in sensitivity analysis.

Lyapunov Approach

The first step is to find the 2×2 state covariance matrix by solving the following Lyapunov equation (from Eq. 2.43)

$$A_{zw}\Sigma_q + \Sigma_q A_{zw}^T + B_{zw}B_{zw}^T = 0 \quad (6.19)$$

The performance covariance matrix can then be obtained as

$$\Sigma_z = C_{zw}\Sigma_q C_{zw}^T \quad (6.20)$$

In general, the diagonal terms of Σ_z represent the mean-square values $\sigma_{z_i}^2$, and the root-mean-square (RMS) values are simply σ_{z_i} obtained by taking the square roots of the diagonal elements of Σ_z . Since we only have a single-input-single-output (SISO) system, $\Sigma_z = \sigma_z^2$ and so the RMS is found as

$$\text{RMS} = \sigma_z = (C_{zw}\Sigma_q C_{zw}^T)^{1/2} \quad (6.21)$$

Frequency-domain Analysis

The RMS of the performance output can also be obtained by computing the square root of the area under its PSD curve in the frequency domain as below (from Eq. 2.41):

$$\begin{aligned}\sigma_z &= \left(\frac{1}{2\pi} \int_{-\infty}^{\infty} S_{zz}(\omega) d\omega \right)^{1/2} = \left(\frac{1}{2\pi} \int_{-\infty}^{\infty} G_{zw}(j\omega) \underbrace{S_{ww}(\omega)}_1 G_{zw}(j\omega)^H(d\omega) \right)^{1/2} \\ &= \left(\frac{1}{2\pi} \int_{-\infty}^{\infty} |G_{zw}(j\omega)|^2 d\omega \right)^{1/2}\end{aligned}\quad (6.22)$$

where S_{zz} is the PSD of the performance output, and S_{ww} is the PSD of the disturbance input. Since we have assumed unit-intensity white-noise as the input, S_{ww} is set to 1. Using the modal contribution form defined in Eq. 6.17, the above equation can be rewritten as follows

$$\begin{aligned}\sigma_z &= \left(\frac{1}{2\pi} \int_{-\infty}^{\infty} (|G_{zw_1}|^2 + |G_{zw_2}|^2) d\omega \right)^{1/2} = \left(\frac{1}{2\pi} \int_{-\infty}^{\infty} |G_{zw_1}|^2 d\omega \right)^{1/2} + \frac{1}{2\pi} \int_{-\infty}^{\infty} |G_{zw_2}|^2 d\omega^{1/2} \\ &= \left(\frac{1}{2\pi} (I_{2_a} + I_{2_b}) \right)^{1/2}\end{aligned}\quad (6.23)$$

We compute the I_2 terms, which represents the integral of the magnitudes squared, using the formula in Appendix C. In order to do so, we must first express FRF modal contribution terms, in the following form

$$\begin{aligned}\tilde{G}_{zw_1}(j\omega) &= \frac{(j\omega)^2 b_2 + (j\omega) b_1 + b_0}{(j\omega)^2 a_2 + (j\omega) a_1 + a_0} = \frac{\tilde{\Phi}_{21} \tilde{\Phi}_{21}^T}{-\omega^2 + j\omega 2\tilde{\zeta}_1 \tilde{\lambda}_1^{1/2} + \tilde{\lambda}_1} \\ \tilde{G}_{zw_2}(j\omega) &= \frac{(j\omega)^2 b_2 + (j\omega) b_1 + b_0}{(j\omega)^2 a_2 + (j\omega) a_1 + a_0} = \frac{\tilde{\Phi}_{22} \tilde{\Phi}_{22}^T}{-\omega^2 + j\omega 2\tilde{\zeta}_2 \tilde{\lambda}_2^{1/2} + \tilde{\lambda}_2}\end{aligned}\quad (6.24)$$

By comparing the coefficient in the above expression, we can compute the I_2 values:

$$\begin{aligned}I_{2_a} &= \int_{-\infty}^{\infty} |\tilde{G}_{zw_1}(j\omega)|^2 d\omega = \pi \frac{a_0 b_1^2 + a_2 b_0^2}{a_0 a_1 a_2} = \pi \frac{(\tilde{\Phi}_{21} \tilde{\Phi}_{21}^T)^2}{2\tilde{\zeta}_1 \tilde{\lambda}_1^{3/2}} \\ I_{2_b} &= \int_{-\infty}^{\infty} |\tilde{G}_{zw_2}(j\omega)|^2 d\omega = \pi \frac{a_0 b_1^2 + a_2 b_0^2}{a_0 a_1 a_2} = \pi \frac{(\tilde{\Phi}_{22} \tilde{\Phi}_{22}^T)^2}{2\tilde{\zeta}_2 \tilde{\lambda}_2^{3/2}}\end{aligned}\quad (6.25)$$

Thus, we get a closed form expression for the mass displacement RMS as a function of the parameters of the structure:

$$\tilde{\sigma}_z = \sqrt{\frac{1}{2\pi}(I_{2_a} + I_{2_b})} = \frac{1}{2} \sqrt{\frac{(\tilde{\Phi}_{21}\tilde{\Phi}_{21}^T)^2}{\tilde{\zeta}_1\tilde{\lambda}_1^{3/2}} + \frac{(\tilde{\Phi}_{22}\tilde{\Phi}_{22}^T)^2}{\tilde{\zeta}_2\tilde{\lambda}_2^{3/2}}} \quad (6.26)$$

Substituting in the respective values of the parameters, we obtain a nominal RMS value of $\tilde{\sigma}_z = 1.8462$ [m rms], which is the same value as the one we would obtain using the Lyapunov approach (Eq. 6.21). Also, using the expression for the cumulative RMS (Eq. 2.42) and integrating numerically gives the cumulative RMS curve shown in Figure 6.5.

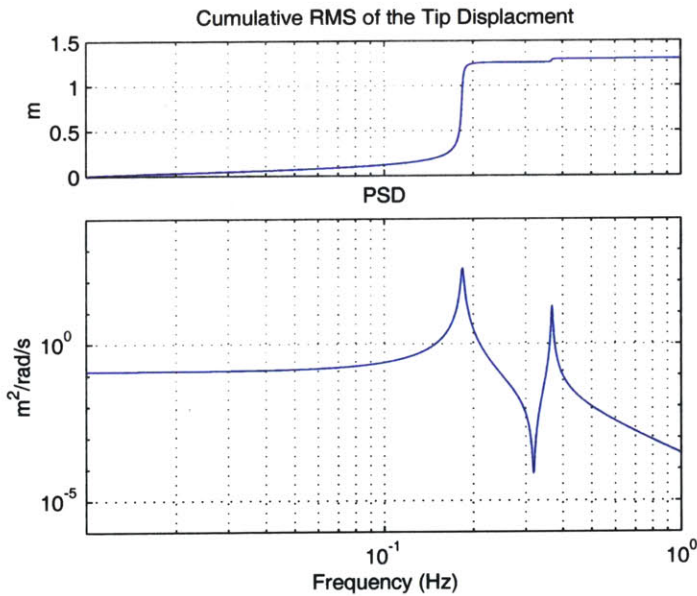


Figure 6.5 2-DOF oscillator cumulative RMS plot (top), and PSD plot (bottom)

We can see from the cumulative RMS curve, that the first mode contribute for almost all of the performance RMS. Figure 6.6, shows the relative modal contribution of each mode to the total RMS..

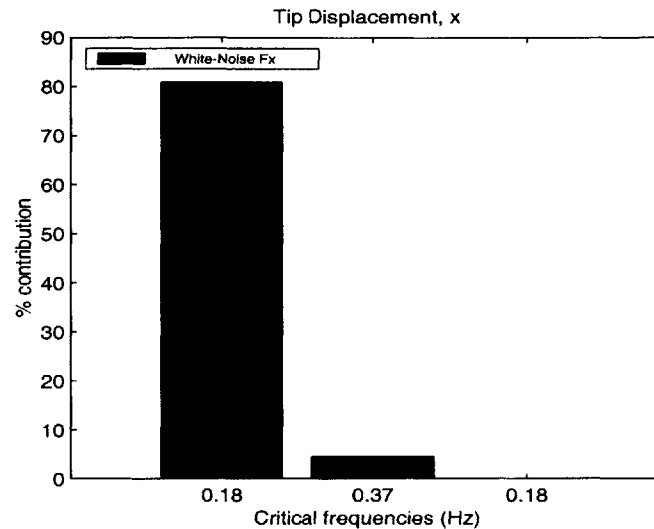


Figure 6.6 Modal contributions to performance RMS

As stated earlier, we can be assured that none of the real oscillators, manufactured under our design specifications (nominal parameters), will perform exactly as predicted. To understand how they will be distributed, we will have to perform an uncertainty analysis. Before we can do this, we will have to generate the uncertainty database.

6.3 Database Generation

In this section, we will generate a structural database and a damping database based on the distributions of the mass and stiffness elements and damping ratios.

6.3.1 Structural Database

In order to generate a database of modal mass and modal stiffness modeling errors, we will simulate the sampling of one thousand 2-DOF oscillator units coming out of the assembly line. We will imagine that the units are assembled by picking up randomly one of each of the components (i.e., one mass of type 1, one mass of type 2, one spring of type 1, and one spring of type 2) from a large batch (ensemble). One thousand units of each component are generated randomly according to their distribution parameters (Table 6.1) and assembled to create the actual units.

Then, each of the sampled oscillator is tested (e.g., hammer test) to get their actual mode shapes and eigen frequencies (Φ and Λ). These values are all that is needed to generate the database. Here are the steps:

1. compute the cross-correlation matrix Ψ using equation (3.42);
2. get $\Delta\Lambda$ simply from the difference between the squares of the measured and the analytical modal frequencies ($[\Lambda - \tilde{\Lambda}] = [\Omega^2 - \tilde{\Omega}^2]$);
3. obtain the modal parameters modeling error matrices (Δm and Δk) using equation (3.46);
4. vectorize Δm and Δk (upper triangular elements only) to get the modeling error vector Δp (Eq. 3.49).

Then the covariance matrix of the modeling errors is obtained using equation (3.50) reproduced here

$$\Sigma_{pp} = E[\Delta p \Delta p^T] = \frac{1}{N} \sum_{i=1}^N [\Delta p \Delta p^T]_i \quad (6.27)$$

where N is the number of samples. For this example, we do not need the frequency normalized modal stiffness errors $\Delta \hat{k}$ as we would, if we were to propagate these uncertainties to the model of a different system. The database resulting from this exercise is the following

$$\Sigma_{pp} = \begin{bmatrix} 0.31579 & -0.089355 & 0.24968 & 0.030676 & -0.013382 & 0.043698 \\ -0.089355 & 0.20218 & 0.05938 & 0.030336 & 0.005591 & 0.036106 \\ 0.24968 & 0.05938 & 0.29661 & 0.008316 & 0.010168 & 0.016757 \\ 0.030676 & 0.030336 & 0.008316 & 0.13294 & 0.031466 & 0.10934 \\ -0.013382 & 0.005591 & 0.010168 & 0.031466 & 0.12176 & -0.049742 \\ 0.043698 & 0.036106 & 0.016757 & 0.10934 & -0.049742 & 0.14229 \end{bmatrix} \times 10^{-2} \quad (6.28)$$

Needless to say that the more samples used in the estimation of Σ_{pp} , the more accurate the database would be. Although, this is not the only factor affecting the accuracy of the estimation. Because of the linear approximation made to obtain the expressions for Δm and Δk (second and third order terms neglected), the covariance matrix will also be affected

by the size of the errors. That means that for large modeling errors (or large variability in the distribution of the components values) the approximation will fail and the error in the estimation of Σ_{pp} will increase. Therefore, it is important to keep in mind that this methodology is only valid if we assume that the analytical model is reasonably good.

In steps 1 through 4, we obtained the covariance matrix for the ensemble of the sampled oscillators. The components of these units were generated randomly based on the standard deviation of their respective distribution. To illustrate the accuracy of the estimation of Σ_{pp} dependence on the error sizes, we have repeated the exercise many times for different values of the components standard deviations. The standard deviations were all modified simultaneously by applying the same multiplicative factor to all of them at the same time. As the standard deviations are increased, the approximate values for Δm and Δk , computed with equation (3.46), become less and less accurate as the linear assumption is violated. We can see in Figure 6.7 that the error in the estimation of Σ_{pp} increases drastically for multiplicative factor values greater than ~ 1.3 . We are also happy to see that for our database, (multiplicative factor equal to one), the estimation error is small.

The estimation error is defined as the maximum singular value of the difference between the real and the approximate covariance matrices:

$$\text{Error}_{\Sigma} = \max(\text{SVD}[\Sigma_{pp} - \Sigma_{pp\text{APPROX}}]) \quad (6.29)$$

where $\Sigma_{pp\text{APPROX}}$ corresponds to the covariance matrix obtained as described above. The real covariance matrix is obtained using the following exact expressions as defined in Eq. 3.24, instead of using Eq. 3.46, to compute the Δm and Δk

$$\begin{aligned} \Delta m &= \tilde{\Phi}^T \Delta M \tilde{\Phi} = \tilde{\Phi}^T (M - \tilde{M}) \tilde{\Phi} = m - I \\ \Delta k &= \tilde{\Phi}^T \Delta K \tilde{\Phi} = \tilde{\Phi}^T (K - \tilde{K}) \tilde{\Phi} = k - \tilde{\Lambda} \end{aligned} \quad (6.30)$$

The reason why we do not always use the expressions of (6.30) to generate the database is that in real life, the actual modal mass and modal stiffness are not available. Only the

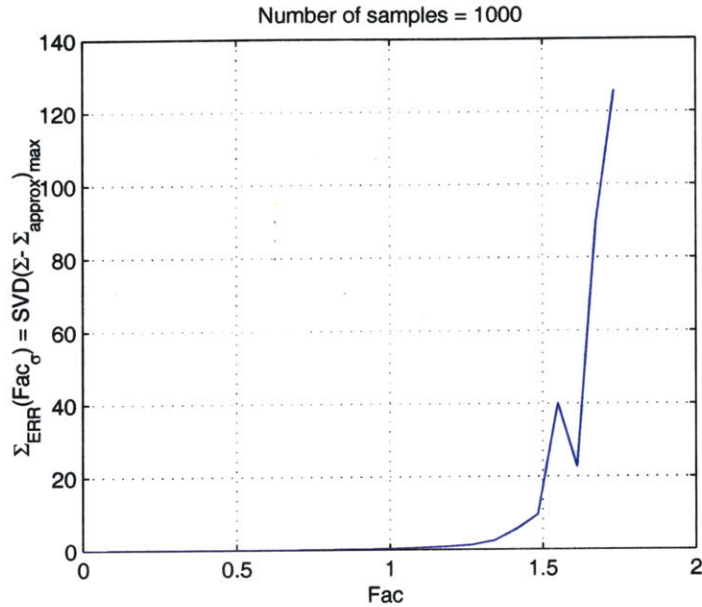


Figure 6.7 Covariance matrix estimation error vs. standard derivative multiplicative factor.

actual mode shapes and eigenvalues are made available from modal testing. This explains why equation (3.46) is so important.

6.3.2 Damping Database

Assuming that the modal damping ratios are independent, the damping database can be obtained directly using equation (3.70) and the transformed damping distribution parameters given in Table 6.1 as follows

$$\Sigma_{\gamma\gamma} = \begin{bmatrix} (0.70335)^2 & 0 \\ 0 & (0.70335)^2 \end{bmatrix} \quad (6.31)$$

We get the global database as shown in equation (3.69) by appending the damping database (Eq. 6.31) to the structural element database (Eq. 6.28).

$$\Sigma_{\hat{p}\hat{p}} = \begin{bmatrix} \Sigma_{mm} & \Sigma_{m\hat{k}} & 0 \\ \Sigma_{\hat{k}m} & \Sigma_{\hat{k}\hat{k}} & 0 \\ 0 & 0 & \Sigma_{\gamma\gamma} \end{bmatrix} = \begin{bmatrix} \begin{bmatrix} 1.0165 & 0.41675 & 0.80857 & 1.4543 & 0.42911 & 1.1012 \\ 0.41675 & 0.26572 & 0.5989 & 0.75004 & 0.23642 & 0.81279 \\ 0.80857 & 0.5989 & 1.4849 & 1.6605 & 0.51631 & 2.0396 \\ 1.4543 & 0.75004 & 1.6605 & 2.4237 & 0.73796 & 2.3116 \\ 0.42911 & 0.23642 & 0.51631 & 0.73796 & 0.25817 & 0.71622 \\ 1.1012 & 0.81279 & 2.0396 & 2.3116 & 0.71622 & 2.8449 \end{bmatrix} & 0 \\ 0 & \begin{bmatrix} (0.70335)^2 & 0 \\ 0 & (0.70335)^2 \end{bmatrix} \end{bmatrix} \quad (6.32)$$

With the uncertainty database compiled, the next step before we can actually perform the uncertainty analysis, is to compute the sensitivity.

6.4 Sensitivity Analysis

The sensitivity expressions for the performance RMS and the FRF with respect to the database parameters were obtained in equations (4.101) and (4.70) respectively. In this section, to demonstrate validity of linear approximation, we will derive explicitly sensitivities with respect to physical parameters (referred to as the r parameters) for our specific example. The vector of physical parameters is defined as follows

$$r = [M_1, M_2, K_1, K_2, \gamma_1, \gamma_2] \quad (6.33)$$

For brevity, we will only derive the sensitivity expressions with respect to three of these parameters, namely M_1 , K_1 and γ_1 .

6.4.1 Performance RMS Sensitivity

In equation (6.26) we have obtained an analytical expression for the performance RMS which is reproduced here

$$\tilde{\sigma}_z = \frac{1}{2} \sqrt{\frac{(\tilde{\Phi}_{21})^4}{\tilde{\zeta}_1 \tilde{\lambda}_1^{3/2}} + \frac{(\tilde{\Phi}_{22})^4}{\tilde{\zeta}_2 \tilde{\lambda}_2^{3/2}}} = \frac{1}{2} \sqrt{\frac{(\tilde{\Phi}_{21})^4}{e^{\tilde{\gamma}_1} \tilde{\lambda}_1^{3/2}} + \frac{(\tilde{\Phi}_{22})^4}{e^{\tilde{\gamma}_2} \tilde{\lambda}_2^{3/2}}} \quad (6.34)$$

where the eigenvalues and modes shapes are obtained from equation (6.6) and (6.7).

First Order Derivatives

The derivative with respect to γ_1 can be obtained directly as follows

$$\frac{\partial \sigma_z}{\partial \gamma_1} = \frac{1}{4} \left(\frac{(\tilde{\Phi}_{21})^4}{e^{\tilde{\gamma}_1 \tilde{\lambda}_1^{3/2}} + \frac{(\tilde{\Phi}_{22})^4}{e^{\tilde{\gamma}_2 \tilde{\lambda}_2^{3/2}}} \right)^{-\frac{1}{2}} \left(\frac{-3(\tilde{\Phi}_{21})^4}{e^{\tilde{\gamma}_1 \tilde{\lambda}_1^{5/2}}} \right) \quad (6.35)$$

while for the derivatives with respect to M_1 and K_1 , we need to apply the chain rule

$$\begin{aligned} \frac{\partial \sigma_z}{\partial M_1} &= \frac{\partial \sigma_z}{\partial \lambda_1} \frac{\partial \lambda_1}{\partial M_1} + \frac{\partial \sigma_z}{\partial \lambda_2} \frac{\partial \lambda_2}{\partial M_1} + \frac{\partial \sigma_z}{\partial \phi_{21}} \frac{\partial \phi_{21}}{\partial M_1} + \frac{\partial \sigma_z}{\partial \phi_{22}} \frac{\partial \phi_{22}}{\partial M_1} \\ \frac{\partial \sigma_z}{\partial K_1} &= \frac{\partial \sigma_z}{\partial \lambda_1} \frac{\partial \lambda_1}{\partial K_1} + \frac{\partial \sigma_z}{\partial \lambda_2} \frac{\partial \lambda_2}{\partial K_1} + \frac{\partial \sigma_z}{\partial \phi_{21}} \frac{\partial \phi_{21}}{\partial K_1} + \frac{\partial \sigma_z}{\partial \phi_{22}} \frac{\partial \phi_{22}}{\partial K_1} \end{aligned} \quad (6.36)$$

The needed derivatives to evaluate the two expressions above will be obtained in the following. First, the derivatives of the RMS with respect to the eigenvalues

$$\begin{aligned} \frac{\partial \sigma_z}{\partial \lambda_1} &= \frac{1}{4} \left(\frac{(\tilde{\Phi}_{21})^4}{e^{\tilde{\gamma}_1 \tilde{\lambda}_1^{3/2}} + \frac{(\tilde{\Phi}_{22})^4}{e^{\tilde{\gamma}_2 \tilde{\lambda}_2^{3/2}}} \right)^{-\frac{1}{2}} \left(\frac{-3(\tilde{\Phi}_{21})^4}{2 e^{\tilde{\gamma}_1 \tilde{\lambda}_1^{5/2}}} \right) \\ \frac{\partial \sigma_z}{\partial \lambda_2} &= \frac{1}{4} \left(\frac{(\tilde{\Phi}_{21})^4}{e^{\tilde{\gamma}_1 \tilde{\lambda}_1^{3/2}} + \frac{(\tilde{\Phi}_{22})^4}{e^{\tilde{\gamma}_2 \tilde{\lambda}_2^{3/2}}} \right)^{-\frac{1}{2}} \left(\frac{-3(\tilde{\Phi}_{22})^4}{2 e^{\tilde{\gamma}_2 \tilde{\lambda}_2^{5/2}}} \right) \end{aligned} \quad (6.37)$$

Then, the derivative with respect to the eigenvector elements

$$\begin{aligned} \frac{\partial \sigma_z}{\partial \phi_{21}} &= \frac{1}{4} \left(\frac{(\tilde{\Phi}_{21})^4}{e^{\tilde{\gamma}_1 \tilde{\lambda}_1^{3/2}} + \frac{(\tilde{\Phi}_{22})^4}{e^{\tilde{\gamma}_2 \tilde{\lambda}_2^{3/2}}} \right)^{-\frac{1}{2}} \left(4 \frac{(\tilde{\Phi}_{21})^3}{e^{\tilde{\gamma}_1 \tilde{\lambda}_1^{3/2}}} \right) \\ \frac{\partial \sigma_z}{\partial \phi_{22}} &= \frac{1}{4} \left(\frac{(\tilde{\Phi}_{21})^4}{e^{\tilde{\gamma}_1 \tilde{\lambda}_1^{3/2}} + \frac{(\tilde{\Phi}_{22})^4}{e^{\tilde{\gamma}_2 \tilde{\lambda}_2^{3/2}}} \right)^{-\frac{1}{2}} \left(4 \frac{(\tilde{\Phi}_{22})^3}{e^{\tilde{\gamma}_2 \tilde{\lambda}_2^{3/2}}} \right) \end{aligned} \quad (6.38)$$

Then we also have to get the eigenvalues and eigenvector elements derivative with respect to M_1 and K_1 . First, the eigenvalue derivatives

$$\frac{\partial \lambda_{1,2}}{\partial M_1} = \frac{1}{2} \left\{ \frac{-K_1}{M_1^2} - \frac{K_2}{M_1^2} \mp \frac{1}{2} \left[\left(\frac{K_1}{M_1} + \frac{K_2}{M_2} \left(1 + \frac{M_2}{M_1} \right) \right)^2 - \frac{4K_1K_2}{M_1M_2} \right]^{\frac{1}{2}} \left[2 \left(\frac{K_1}{M_1} + \frac{K_2}{M_2} \left(1 + \frac{M_2}{M_1} \right) \right) \left(\frac{-K_1}{M_1^2} - \frac{K_2}{M_1^2} \right) + \frac{4K_1K_2}{M_1^2M_2} \right] \right\} \quad (6.39)$$

$$\frac{\partial \lambda_{1,2}}{\partial K_1} = \frac{1}{2} \left\{ \frac{1}{M_1} \mp \frac{1}{2} \left[\left(\frac{K_1}{M_1} + \frac{K_2}{M_2} \left(1 + \frac{M_2}{M_1} \right) \right)^2 - \frac{4K_1K_2}{M_1M_2} \right]^{\frac{1}{2}} \left[2 \left(\frac{K_1}{M_1} + \frac{K_2}{M_2} \left(1 + \frac{M_2}{M_1} \right) \right) \frac{1}{M_1} - \frac{4K_2}{M_1M_2} \right] \right\}$$

and finally the eigenvector element derivative

$$\frac{\partial \phi_{21}}{\partial M_1} = \frac{-\lambda_1}{(M_1K_2^2 + M_2(K_1 + K_2 - \lambda_1M_1)^2)^{1/2}} + \frac{(K_1 + K_2 - \lambda_1M_1) \left(-\frac{1}{2} \right) [K_2^2 + 2M_2(K_1 + K_2 - \lambda_1M_1)(-\lambda_1)]}{(M_1K_2^2 + M_2(K_1 + K_2 - \lambda_1M_1)^2)^{3/2}}$$

$$\frac{\partial \phi_{22}}{\partial M_1} = \frac{-\lambda_2}{(M_1K_2^2 + M_2(K_1 + K_2 - \lambda_1M_1)^2)^{1/2}} \quad (6.40)$$

$$\frac{\partial \phi_{21,22}}{\partial K_1} = \frac{1}{(M_1K_2^2 + M_2(K_1 + K_2 - \lambda_1M_1)^2)^{1/2}} + \frac{(K_1 + K_2 - \lambda_1M_1) \left(-\frac{1}{2} \right) [2M_2(K_1 + K_2 - \lambda_1M_1)]}{(M_1K_2^2 + M_2(K_1 + K_2 - \lambda_1M_1)^2)^{3/2}}$$

Solving for equations (6.37) to (6.40) and substituting into (6.36) gives us the RMS sensitivity with respect to M_1 and K_1 . We have already obtained the sensitivity with respect to γ_1 in (6.35). Figure 6.8 shows an example of sensitivities computed with respect to the modal mass and stiffness elements, and the transformed modal damping.

Range of Validity of the Linear Approximation

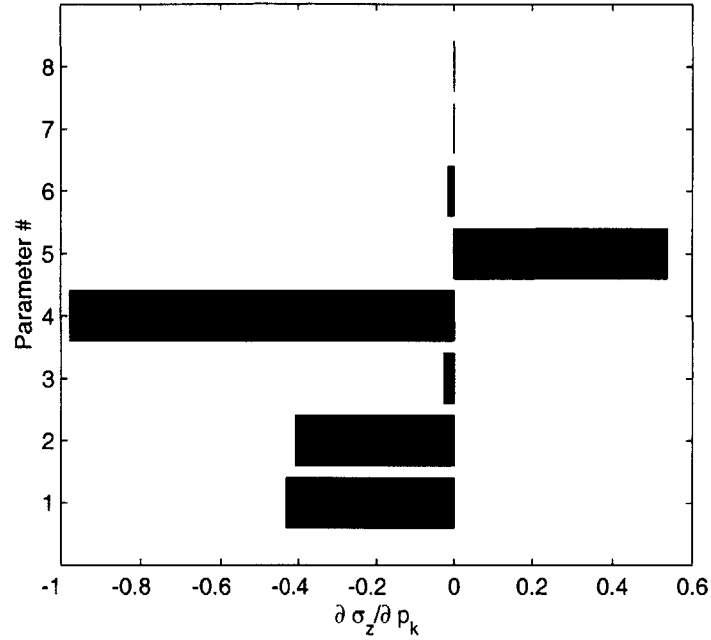
In order to evaluate the range of validity of the linear approximation as described in Chapter 4, we must first determine the second order derivatives.

The second derivative of the RMS with respect to γ_1 is obtained by differentiating equation (6.35)

$$\frac{\partial \sigma_z}{\partial \gamma_1} = \frac{1}{4} \left[\frac{1}{2} \left(\frac{(\tilde{\Phi}_{21})^4}{e^{\tilde{\gamma}_1 \tilde{\lambda}_1^{3/2}} + \frac{(\tilde{\Phi}_{22})^4}{e^{\tilde{\gamma}_2 \tilde{\lambda}_2^{3/2}}} \right)^{\frac{3}{2}} \left(\frac{-(\tilde{\Phi}_{21})^4}{e^{\tilde{\gamma}_1 \tilde{\lambda}_1^{3/2}}} \right)^2 + \left(\frac{(\tilde{\Phi}_{21})^4}{e^{\tilde{\gamma}_1 \tilde{\lambda}_1^{3/2}} + \frac{(\tilde{\Phi}_{22})^4}{e^{\tilde{\gamma}_2 \tilde{\lambda}_2^{3/2}}} \right)^{\frac{1}{2}} \left(\frac{(\tilde{\Phi}_{21})^4}{e^{\tilde{\gamma}_1 \tilde{\lambda}_1^{3/2}}} \right) \right] \quad (6.41)$$

Differentiating Eq. (6.36) gives the second derivatives for M_1 and K_1

Sensitivities of Tip Displacement, x RMS value with respect to database paramete

**Figure 6.8** Parameters sensitivities

$$\frac{\partial^2 \sigma_z}{\partial M_1^2} = \frac{\partial^2 \sigma_z}{\partial \lambda_1^2} \frac{\partial \lambda_1}{\partial M_1} + \frac{\partial \sigma_z}{\partial \lambda_1} \frac{\partial \lambda_1^2}{\partial M_1^2} + \frac{\partial^2 \sigma_z}{\partial \lambda_2^2} \frac{\partial \lambda_2}{\partial M_1} + \frac{\partial \sigma_z}{\partial \lambda_2} \frac{\partial \lambda_2^2}{\partial M_1^2} + \frac{\partial^2 \sigma_z}{\partial \phi_{21}^2} \frac{\partial \phi_{21}}{\partial M_1} + \frac{\partial \sigma_z}{\partial \phi_{21}} \frac{\partial \phi_{21}^2}{\partial M_1^2} + \frac{\partial^2 \sigma_z}{\partial \phi_{22}^2} \frac{\partial \phi_{22}}{\partial M_1} + \frac{\partial \sigma_z}{\partial \phi_{22}} \frac{\partial \phi_{22}^2}{\partial M_1^2} \quad (6.42)$$

$$\frac{\partial^2 \sigma_z}{\partial K_1^2} = \frac{\partial^2 \sigma_z}{\partial \lambda_1^2} \frac{\partial \lambda_1}{\partial K_1} + \frac{\partial \sigma_z}{\partial \lambda_1} \frac{\partial \lambda_1^2}{\partial K_1^2} + \frac{\partial^2 \sigma_z}{\partial \lambda_2^2} \frac{\partial \lambda_2}{\partial K_1} + \frac{\partial \sigma_z}{\partial \lambda_2} \frac{\partial \lambda_2^2}{\partial K_1^2} + \frac{\partial^2 \sigma_z}{\partial \phi_{21}^2} \frac{\partial \phi_{21}}{\partial K_1} + \frac{\partial \sigma_z}{\partial \phi_{21}} \frac{\partial \phi_{21}^2}{\partial K_1^2} + \frac{\partial^2 \sigma_z}{\partial \phi_{22}^2} \frac{\partial \phi_{22}}{\partial K_1} + \frac{\partial \sigma_z}{\partial \phi_{22}} \frac{\partial \phi_{22}^2}{\partial K_1^2}$$

We have already obtained the first order derivatives needed in the above expression, but we also need the second order derivatives for all the parameters. First, the second order derivatives of the RMS with respect to the eigenvalues

$$\frac{\partial^2 \sigma_z}{\partial \lambda_1^2} = \frac{1}{4} \left[-\frac{1}{2} \left(\frac{(\tilde{\Phi}_{21})^4}{e^{\tilde{\gamma}_1 \tilde{\lambda}_1^{3/2}} + \frac{(\tilde{\Phi}_{22})^4}{e^{\tilde{\gamma}_2 \tilde{\lambda}_2^{3/2}}} \right)^{-3/2} \left(\frac{-3 (\tilde{\Phi}_{21})^4}{2 e^{\tilde{\gamma}_1 \tilde{\lambda}_1^{5/2}}} \right)^2 + \left(\frac{(\tilde{\Phi}_{21})^4}{e^{\tilde{\gamma}_1 \tilde{\lambda}_1^{3/2}} + \frac{(\tilde{\Phi}_{22})^4}{e^{\tilde{\gamma}_2 \tilde{\lambda}_2^{3/2}}} \right)^{-1/2} \left(\frac{15 (\tilde{\Phi}_{21})^4}{4 e^{\tilde{\gamma}_1 \tilde{\lambda}_1^{7/2}}} \right) \right] \quad (6.43)$$

$$\frac{\partial^2 \sigma_z}{\partial \lambda_2^2} = \frac{1}{4} \left[-\frac{1}{2} \left(\frac{(\tilde{\Phi}_{21})^4}{e^{\tilde{\gamma}_1 \tilde{\lambda}_1^{3/2}} + \frac{(\tilde{\Phi}_{22})^4}{e^{\tilde{\gamma}_2 \tilde{\lambda}_2^{3/2}}} \right)^{-3/2} \left(\frac{-3 (\tilde{\Phi}_{22})^4}{2 e^{\tilde{\gamma}_2 \tilde{\lambda}_2^{5/2}}} \right)^2 + \left(\frac{(\tilde{\Phi}_{21})^4}{e^{\tilde{\gamma}_1 \tilde{\lambda}_1^{3/2}} + \frac{(\tilde{\Phi}_{22})^4}{e^{\tilde{\gamma}_2 \tilde{\lambda}_2^{3/2}}} \right)^{-1/2} \left(\frac{15 (\tilde{\Phi}_{22})^4}{4 e^{\tilde{\gamma}_2 \tilde{\lambda}_2^{7/2}}} \right) \right]$$

Then, the derivative with respect to the eigenvector elements

$$\begin{aligned}\frac{\partial^2 \sigma_z}{\partial \phi_{21}^2} &= \frac{1}{4} \left[-\frac{1}{2} \left(\frac{(\tilde{\Phi}_{21})^4}{e^{\tilde{\gamma}_1 \tilde{\lambda}_1^{3/2}} + \frac{(\tilde{\Phi}_{22})^4}{e^{\tilde{\gamma}_2 \tilde{\lambda}_2^{3/2}}} \right)^{-\frac{3}{2}} \left(4 \frac{(\tilde{\Phi}_{21})^3}{e^{\tilde{\gamma}_1 \tilde{\lambda}_1^{3/2}}} \right)^2 + \left(\frac{(\tilde{\Phi}_{21})^4}{e^{\tilde{\gamma}_1 \tilde{\lambda}_1^{3/2}} + \frac{(\tilde{\Phi}_{22})^4}{e^{\tilde{\gamma}_2 \tilde{\lambda}_2^{3/2}}} \right)^{-\frac{1}{2}} \left(12 \frac{(\tilde{\Phi}_{21})^2}{e^{\tilde{\gamma}_1 \tilde{\lambda}_1^{3/2}}} \right) \right] \\ \frac{\partial^2 \sigma_z}{\partial \phi_{21}^2} &= \frac{1}{4} \left[-\frac{1}{2} \left(\frac{(\tilde{\Phi}_{21})^4}{e^{\tilde{\gamma}_1 \tilde{\lambda}_1^{3/2}} + \frac{(\tilde{\Phi}_{22})^4}{e^{\tilde{\gamma}_2 \tilde{\lambda}_2^{3/2}}} \right)^{-\frac{3}{2}} \left(4 \frac{(\tilde{\Phi}_{22})^3}{e^{\tilde{\gamma}_2 \tilde{\lambda}_2^{3/2}}} \right)^2 + \left(\frac{(\tilde{\Phi}_{21})^4}{e^{\tilde{\gamma}_1 \tilde{\lambda}_1^{3/2}} + \frac{(\tilde{\Phi}_{22})^4}{e^{\tilde{\gamma}_2 \tilde{\lambda}_2^{3/2}}} \right)^{-\frac{1}{2}} \left(12 \frac{(\tilde{\Phi}_{22})^2}{e^{\tilde{\gamma}_2 \tilde{\lambda}_2^{3/2}}} \right) \right]\end{aligned}\quad (6.44)$$

Then we also have to get the second derivatives of the eigenvalues and eigenvector elements with respect to M_1 and K_1 . First, the eigenvalue second derivatives

$$\begin{aligned}\frac{\partial^2 \lambda_{1,2}}{\partial M_1^2} &= \frac{1}{2} \left[\frac{2K_1}{M_1^3} + \frac{2K_2}{M_1^3} \mp \frac{1}{2} \left(\left(-\frac{1}{2} \left(\frac{K_1}{M_1} + \frac{K_2}{M_2} \left(1 + \frac{M_2}{M_1} \right) \right)^2 - \frac{4K_1 K_2}{M_1 M_2} \right) \right)^{-\frac{3}{2}} \left[2 \left(\frac{K_1}{M_1} + \frac{K_2}{M_2} \left(1 + \frac{M_2}{M_1} \right) \right) \left(\frac{-K_1}{M_1^2} - \frac{K_2}{M_1^2} \right) + \frac{4K_1 K_2}{M_1^2 M_2} \right] \right] \\ &+ \left(\left(\frac{K_1}{M_1} + \frac{K_2}{M_2} \left(1 + \frac{M_2}{M_1} \right) \right)^2 - \frac{4K_1 K_2}{M_1 M_2} \right)^{-\frac{1}{2}} \left[2 \left(\frac{-K_1}{M_1^2} - \frac{K_2}{M_1^2} \right)^2 + 2 \left(\frac{K_1}{M_1} + \frac{K_2}{M_2} \left(1 + \frac{M_2}{M_1} \right) \right) \left(\frac{2K_1}{M_1^3} + \frac{2K_2}{M_1^3} - \frac{8K_1 K_2}{M_1^3 M_2} \right) \right]\end{aligned}\quad (6.45)$$

$$\frac{\partial \lambda_{1,2}}{\partial M_1} = \frac{1}{2} \left\{ \frac{-K_1}{M_1^2} - \frac{K_2}{M_1^2} \mp \frac{1}{2} \left(\left(\frac{K_1}{M_1} + \frac{K_2}{M_2} \left(1 + \frac{M_2}{M_1} \right) \right)^2 - \frac{4K_1 K_2}{M_1 M_2} \right)^{-\frac{1}{2}} \left[2 \left(\frac{K_1}{M_1} + \frac{K_2}{M_2} \left(1 + \frac{M_2}{M_1} \right) \right) \left(\frac{-K_1}{M_1^2} - \frac{K_2}{M_1^2} \right) + \frac{4K_1 K_2}{M_1^2 M_2} \right] \right\}\quad (6.46)$$

$$\frac{\partial \lambda_{1,2}}{\partial K_1} = \frac{1}{2} \left\{ \frac{1}{M_1} \mp \frac{1}{2} \left(\left(\frac{K_1}{M_1} + \frac{K_2}{M_2} \left(1 + \frac{M_2}{M_1} \right) \right)^2 - \frac{4K_1 K_2}{M_1 M_2} \right)^{-\frac{1}{2}} \left[2 \left(\frac{K_1}{M_1} + \frac{K_2}{M_2} \left(1 + \frac{M_2}{M_1} \right) \right) \frac{1}{M_1} - \frac{4K_2}{M_1 M_2} \right] \right\}$$

and finally the eigenvector element derivative

$$\begin{aligned}\frac{\partial \phi_{21}}{\partial M_1} &= \frac{-\lambda_1}{(M_1 K_2^2 + M_2 (K_1 + K_2 - \lambda_1 M_1)^2)^{1/2}} + \frac{(K_1 + K_2 - \lambda_1 M_1) \left(-\frac{1}{2} \right) [K_2^2 + 2M_2 (K_1 + K_2 - \lambda_1 M_1) (-\lambda_1)]}{(M_1 K_2^2 + M_2 (K_1 + K_2 - \lambda_1 M_1)^2)^{3/2}} \\ \frac{\partial \phi_{22}}{\partial M_1} &= \frac{-\lambda_2}{(M_1 K_2^2 + M_2 (K_1 + K_2 - \lambda_1 M_1)^2)^{1/2}} \\ \frac{\partial \phi_{21,22}}{\partial K_1} &= \frac{1}{(M_1 K_2^2 + M_2 (K_1 + K_2 - \lambda_1 M_1)^2)^{1/2}} + \frac{(K_1 + K_2 - \lambda_{1,2} M_1) \left(-\frac{1}{2} \right) [2M_2 (K_1 + K_2 - \lambda_1 M_1)]}{(M_1 K_2^2 + M_2 (K_1 + K_2 - \lambda_1 M_1)^2)^{3/2}}\end{aligned}\quad (6.47)$$

Solving for equations (6.37) to (6.40) and substituting into (6.36) gives us the RMS sensitivity with respect to M_1 and K_1 . We have already obtained the sensitivity with respect to γ_1 in (6.35).

TABLE 6.2 Maximum allowable perturbation size

Parameters	Variability σ	Range $ \Delta p _{max}$
M_1	0.2	0.332
K_1	0.4	0.521
γ_1	0.70335	0.881

6.4.2 FRF Sensitivity

As suggested above, one of the reasons for using the structural modification method is to bring modify dynamic properties of the structure, perhaps by moving certain critical frequencies. Even on a relatively simple structure, there will be a large number of possible modifications which could be made and it is necessary to determine which of these would be the most effective for the desired change.

One way of selecting the parameter(s) to modify is to use a sensitivity analysis based on the modal model of the original structure. Using a form of perturbation theory, valid for small changes, it is possible to determine the rate of change of each natural frequency of the original structure with each of the system parameters. Those with the greatest “slope” are singled out as the most effective elements for bringing about specific changes and the same can also be used to assess the secondary effects which will also accrue - i.e. changes in the other natural frequencies - since it is important to avoid removing one problem and introducing a different one.

It should be noted that because of “small” differences assumed in the sensitivity analysis, it is possible to predict accurately the extent of the changes which will result from a specific (non-second order) change in one of the structure’s parameters. The analysis will indicate the direction of change in frequencies, and will rank them in order of extent of change, but generally will not predict the magnitude of that change reliably (see Gutierrez, 1999).

Range of Validity of the Linear Approximation

We could use equation (4.111) to determine the maximum allowable perturbation size at every frequency point in function of a specified ratio ε like we have done in the previous section for the performance RMS derivatives. Although this would be very useful since we already have found these values for the RMS case (Table 6.2). A useful thing to do, is to determine the frequency range for which the linear approximation hold for the FRF.

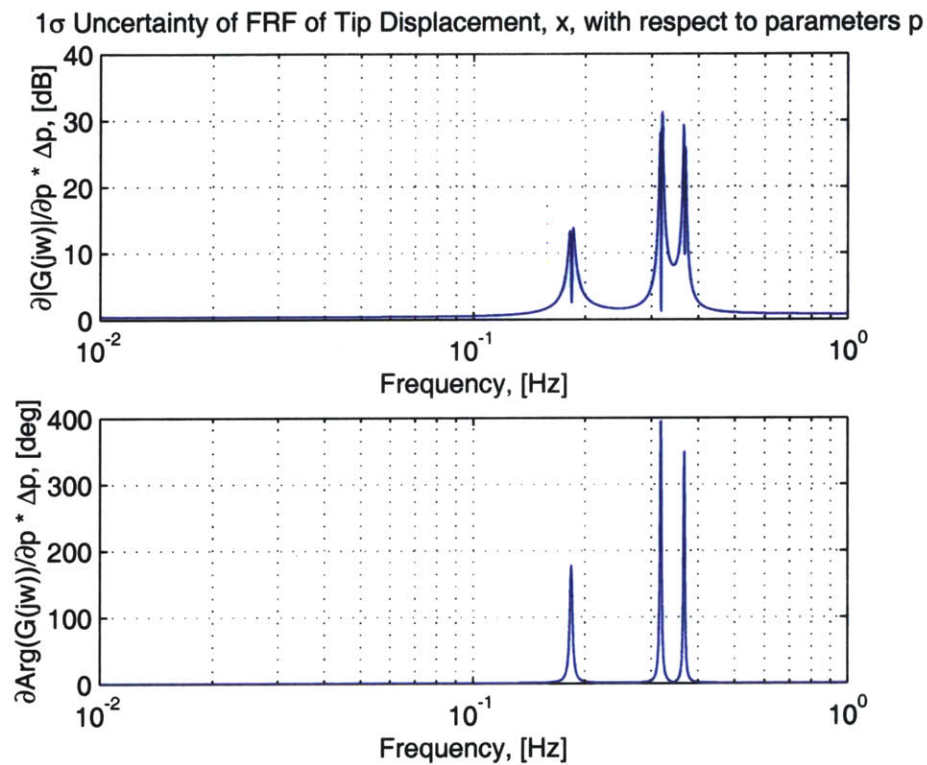


Figure 6.9 Frequency response derivatives (1st and order) evaluated at $|\Delta p|_{max}$

These range of validity of the linear approximation correspond to the range of validity of the linear covariance propagation technique as we will discuss later.

TABLE 6.3 Frequency range of validity of the linear approximation.

Parameters	Frequency Range ω
M_1	0-0.13, 0.21-0.24, 0.42-...
K_1	0-0.12, 0.22-0.26, 0.44-...
γ_1	0-0.11, 0.225-0.21, 0.45-...

6.5 Uncertainty Analysis

In this section, we will demonstrate all of the uncertainty propagation techniques presented in Chapter 5 firstly on the RMS performance predictions (Section 6.5.1), and then on the FRF (magnitude and phase) (Section 6.5.2). For the RMS uncertainty, we will compare the accuracy of the results with the results obtained analytically. We will discuss the advantages and inconveniences each methods as well.

6.5.1 Performance RMS Uncertainty

Analytical /Numerical Evaluation

To evaluate the standard deviation of the performance RMS we apply Eq. A.7 to get

$$\sigma_{RMS} = \sigma_{\sigma_z} = \sqrt{E[(\sigma_z - E(\sigma_z))^2]} = \sqrt{E(\sigma_z^2) - (E(\sigma_z))^2} \quad (6.48)$$

Hence, we will have to compute the $E(\sigma_z^2)$ and $E(\sigma_z)$ terms.

Computation of the RMS expectation

Let us start first with the RMS expectation, $E(\sigma_z)$. If the linearity is preserved, it should be equal to our nominal performance RMS prediction. Applying Eq. A.10, with the expression that have obtained for σ_z in (6.26) yields

$$\begin{aligned}
E[\sigma_z(r)] &= \int_{-\infty}^{\infty} \int_{-\infty}^{\infty} \int_{-\infty}^{\infty} \int_{-\infty}^{\infty} \int_{-\infty}^{\infty} \int_{-\infty}^{\infty} \sigma_z(r_0) f_{M_1 M_2 K_1 K_2 \gamma_1 \gamma_2}(M_{1_0}, M_{2_0}, K_{1_0}, K_{2_0}, \gamma_{1_0}, \gamma_{2_0}) dM_{1_0} dM_{2_0} dK_{1_0} dK_{2_0} d\gamma_{1_0} d\gamma_{2_0} \\
&= \int_{-\infty}^{\infty} \int_{-\infty}^{\infty} \int_{-\infty}^{\infty} \int_{-\infty}^{\infty} \int_{-\infty}^{\infty} \int_{-\infty}^{\infty} \frac{1}{2} \sqrt{\frac{\Phi_{21}^4}{e^{\gamma_1 \lambda_1^{3/2}} + \frac{\Phi_{22}^4}{e^{\gamma_2 \lambda_2^{3/2}}}} f_{M_1 \dots \gamma_2}(M_{1_0}, \dots, \gamma_{2_0}) dM_{1_0} \dots d\gamma_{2_0}
\end{aligned} \tag{6.49}$$

where we recall that r is the vector of physical parameters (Eq. 6.33). In our assembly plant, the way the spring and mass elements were picked from their respective batch to make an oscillator was completely independent. Hence, assuming independence, and using Eq. A.13, the above expression is rewritten as follows

$$E[\sigma_z(r)] = \int_{-\infty}^{\infty} \int_{-\infty}^{\infty} \int_{-\infty}^{\infty} \int_{-\infty}^{\infty} \int_{-\infty}^{\infty} \int_{-\infty}^{\infty} \frac{1}{2} \sqrt{\frac{\Phi_{21}^4}{e^{\gamma_1 \lambda_1^{3/2}} + \frac{\Phi_{22}^4}{e^{\gamma_2 \lambda_2^{3/2}}}} f_{M_1}(M_{1_0}) dM_{1_0} \dots f_{\gamma_2}(\gamma_{2_0}) d\gamma_{2_0} \tag{6.50}$$

where the explicit expressions for the eigenvalues and the necessary eigenvector elements were given in equation (6.6) and (6.7) respectively. Notice that on a real structure, it is generally not possible to separate the compound distribution of the mass and stiffness for they are not independent. In explicit, it is very difficult to change the mass of a structure without affecting its stiffness and vice-versa. For example, a stiffer beam is often heavier than a flexible beam. This is why space structures, which are generally optimized for lightness are sometimes very flexible.

All the parameter PDF's in equation (6.50) are Gaussian and are expressed as follows (Eq. A.31)

$$f_{r_k}(r_{k_0}) = \frac{1}{\sqrt{2\pi}\sigma_{r_k}} e^{-\frac{(r_{k_0} - \mu_{r_k})^2}{2\sigma_{r_k}^2}} \tag{6.51}$$

which substituted into (6.50) yields

$$E[\sigma_z(r)] = \frac{1}{16\pi^3 \sigma_{M_1} \dots \sigma_{\gamma_2}} \int_{-\infty}^{\infty} \int_{-\infty}^{\infty} \int_{-\infty}^{\infty} \int_{-\infty}^{\infty} \int_{-\infty}^{\infty} \int_{-\infty}^{\infty} \sqrt{\frac{\Phi_{21}^4}{e^{\gamma_1 \lambda_1^{3/2}} + \frac{\Phi_{22}^4}{e^{\gamma_2 \lambda_2^{3/2}}}} e^{-\frac{(M_{1_0} - \bar{M}_1)^2}{2\sigma_{M_1}^2}} e^{-\frac{(\gamma_{2_0} - \bar{\gamma}_2)^2}{2\sigma_{\gamma_2}^2}} dM_{1_0} \dots d\gamma_{2_0} \tag{6.52}$$

The above expression can only be evaluated numerically. The obtained computation result is

$$E(\sigma_z) = 1.8462 \text{ [m rms]} \quad (6.53)$$

which compared to the nominal value prediction, gives an error of only 0.005%.

$$\frac{E(\sigma_z) - \tilde{\sigma}_z}{E(\sigma_z)} \times 100 = \frac{1.8462 - 1.8461}{1.8462} \times 100 = 0.005\% \quad (6.54)$$

This small error in the performance RMS estimation confirms again that, for our system, the linearity is preserved which means that we can use this fact to say that the Gaussian-ness is also preserved.

Computation of the performance variance (MS) expectation

Now that we have computed $E(\sigma_z)$, we need to evaluate $E(\sigma_z^2)$ in Eq. 6.48. From Eq. 6.26, we deduce the expression for σ_z^2

$$\sigma_z^2 = \frac{1}{4} \left(\frac{\Phi_{21}^4}{e^{\gamma_1 \lambda_1^{3/2}} + \frac{\Phi_{22}^4}{e^{\gamma_2 \lambda_2^{3/2}}} \right) \quad (6.55)$$

Therefore, $E(\sigma_z^2)$ is given by

$$E[\sigma_z^2(r)] = \int_{-\infty}^{\infty} \int_{-\infty}^{\infty} \int_{-\infty}^{\infty} \int_{-\infty}^{\infty} \int_{-\infty}^{\infty} \int_{-\infty}^{\infty} \frac{1}{4} \left(\frac{\Phi_{21}^4}{e^{\gamma_1 \lambda_1^{3/2}} + \frac{\Phi_{22}^4}{e^{\gamma_2 \lambda_2^{3/2}}} \right) f_{M_1}(M_{1_0}) dM_{1_0} \dots f_{\gamma_2}(\gamma_{2_0}) d\gamma_{2_0} \quad (6.56)$$

which can be evaluated numerically.

$$E(\sigma_z^2) = 3.5181 \text{ [m}^2 \text{ rms]} \quad (6.57)$$

If we plug the values of (6.57) and (6.62) in Eq. 6.48 we get

$$\sigma_{RMS} = \sigma_{\sigma_z} = \sqrt{3.5181 - (1.8462)^2} = 0.31 \text{ [m rms]} \quad (6.58)$$

Monte Carlo Simulation

In this section we will perform a numerical simulation of the 2-DOF oscillator assembly plant. One hundred plant were sampled randomly (see the Database Generation, Section 6.3) from the production line for which their components characteristics were known for the purpose of this example. Figure 6.10 shows the sampled physical masses and physical stiffnesses with their corresponding gaussian distribution for which the parameters μ and σ were evaluated statistically.

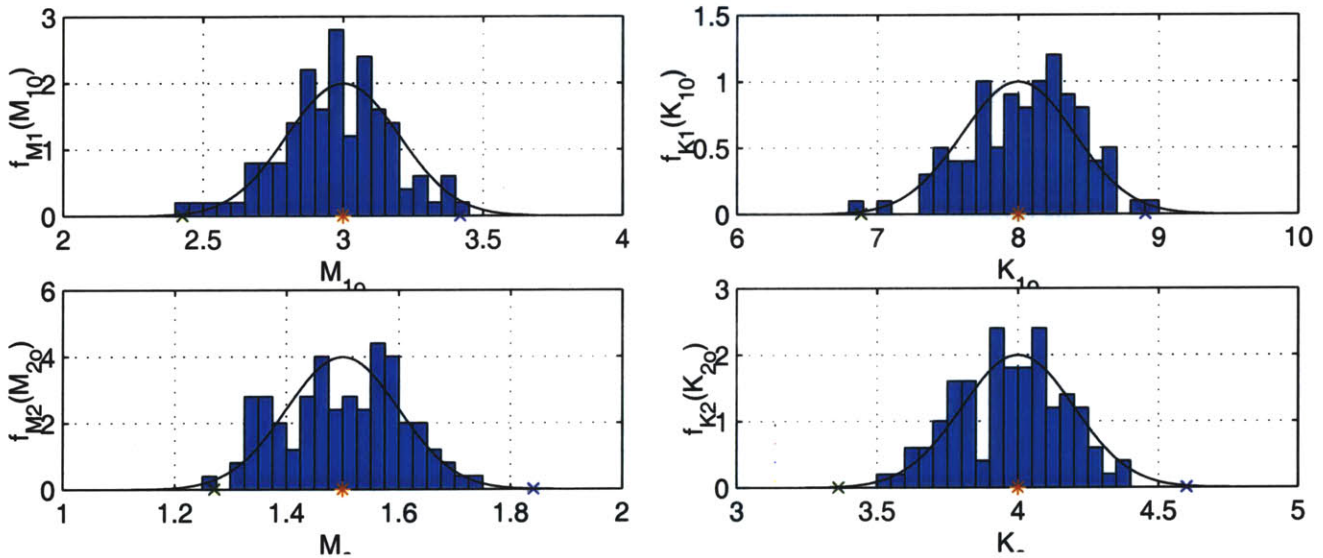


Figure 6.10 Histograms of the sampled physical mass (left) and stiffness (right) elements distributions with their corresponding Gaussian PDF's.

Figure 6.11 shows the sampled transformed damping parameters also represented with their corresponding Gaussian distribution.

It is very relieving that as we predicted, the distribution of the output RMS is also Gaussian in Figure 6.12. This result is extremely satisfying as it support the methodology that we count on implementing to predict the performance uncertainty range for large models.

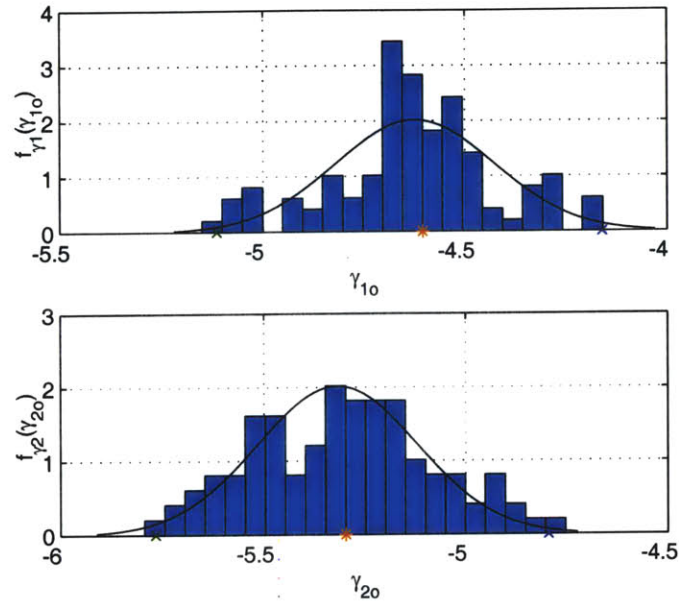


Figure 6.11 Histogram of the “sampled” transformed modal damping parameters with their corresponding Gaussian PDF’s.

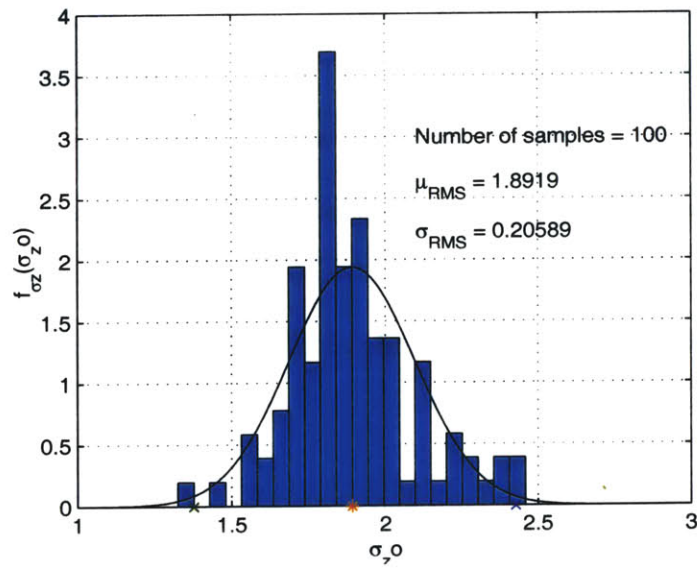


Figure 6.12 Histogram of the performance RMS distribution from the Monte Carlo simulation

Vertex Method

Although we mentioned in the previous chapter, it is generally not sufficient to only search the vertices to predict the worst case performance this the technique implemented for this example. Since the modes of our system are well separated and since that the disturbance input is a flat white noise, we have good confidence that the predictions will be accurate. In this example, we did performed the vertex method on the performance RMS, but we have demonstrated the technique on the FRF Bode plot in the next section.

Linear Covariance Method

As described in Chapter 5 this method is straight forward to use once we have the parameters sensitivities from the sensitivity analysis. It consist in propagating the uncertainty covariance matrix by pre- and post-multiplying it by the sensitivity matrix. Now, suppose we wish to analyze a modified system, whose difference from the nominal system are contained in the matrices ΔM and ΔK . (Note: It is assumed that the same coordinate are used in both cases.) The equation of motion for the unforced, undamped modified system may be written as:

$$[M + \Delta M]\ddot{x} + [K + \Delta K]x = 0 \quad (6.59)$$

or, using the original system modal transformation 6.8 (noting that the eigenvector and eigenvalue are NOT those of the new system), as:

$$[1 + \tilde{\Phi}^T \Delta M \tilde{\Phi}]\ddot{\eta} + [\tilde{\Lambda} + \tilde{\Phi}^T \Delta K \tilde{\Phi}]\eta = 0 \quad (6.60)$$

Using this equation we have established a new equation of motion with a new mass matrix (m) and stiffness matrix (k), both of which can be defined using the modal data available on the analytical system together with a description of the perturbations in mass and stiffness which are to constitute the actual system mass and stiffness matrices expressed in the modal coordinates of the analytical model.

$$\begin{aligned}
 m &= 1 + \tilde{\Phi}^T \Delta M \tilde{\Phi} = 1 + \Delta m \\
 k &= \tilde{\Lambda} + \tilde{\Phi}^T \Delta K \tilde{\Phi} = \tilde{\Lambda} + \Delta k
 \end{aligned}
 \tag{6.61}$$

The eigenvalue and eigenvector of these new mass and stiffness matrices can be determined in the usual way, thereby providing the natural frequency and mode shape of the actual structure.

These all stem from the fact that it is much easier to specify changing individual elements in a mass or stiffness matrix than it is to realize such changes in practice. For example, if we wish to add a mass at some point on the structure, it is inevitable that this will change the elements in the mass matrix which relate to the x , y , and z directions at the point in question and will also have an effect on the rotational motions as well since any real mass is likely to have rotary inertia as well. This means that it is seldom possible or realistic to consider changing elements individually, and also that it may be necessary to include rotational coordinates in the original modal model. This last consideration is seldom made, thanks to the difficulty of measuring rotations, but should be if reliable modification predictions are to be made. Similar comments apply to the stiffness matrix: the attachment of any stiffener, such as a beam or strut, will influence the stiffness in several directions simultaneously, including rotational ones. Lastly, it must be noted that this method, in common with all which rely on a modal data base that may not include all the structure's modes, is vulnerable to errors incurred if the effects of the modes omitted from the modal model are (a) not negligible and (b) ignored. This point will be discussed further in the next section.

Interpretations

In conclusion we are very happy to see that the distribution output of a 2-DOF system is Gaussian if the the uncertain parameters also have normal distribution, and as long as the linearity assumption is preserved.

TABLE 6.4 RMS Uncertainty Analysis Results

Evaluation Method	Mean prediction μ_{RMS}	Uncertainty prediction σ_{RMS}	Comments
Deterministic (nominal predictions)	1.8461	---	Not too hard to obtain if size of the model is reasonable.
Analytical/ Numerical	1,8462	0.26	Gets very complicated for any system that has more than one mode, but the solution is exact
Monte Carlo	1.9243	0.24	Useful to determine the shape of an unknown distribution
Vertex Method	Not predicted	Not predicted (gives worst-case predictions)	Becomes very costly for large model, even more so for the FRF. Provide a measure of the worst-case.
Linear Covariance Propagation	Assumed nominal	0.32	Very efficient and necessitate few computations. Can be used to obtain the probability of success as described in Chapter 5

6.5.2 FRF Uncertainty

Monte Carlo Simulation

The Monte Carlo simulation provides us with the envelope inside which all the possible plants will lay, Figure 6.13. It is always a good thing to start an analysis with a Monte Carlo simulation as it gives insight on the shape of the unknown distribution of the response. It also helps us validate the uncertainty propagation techniques we are assured that any predictions should never get out of the envelope. Otherwise, it indicates a serious problem in our theory.

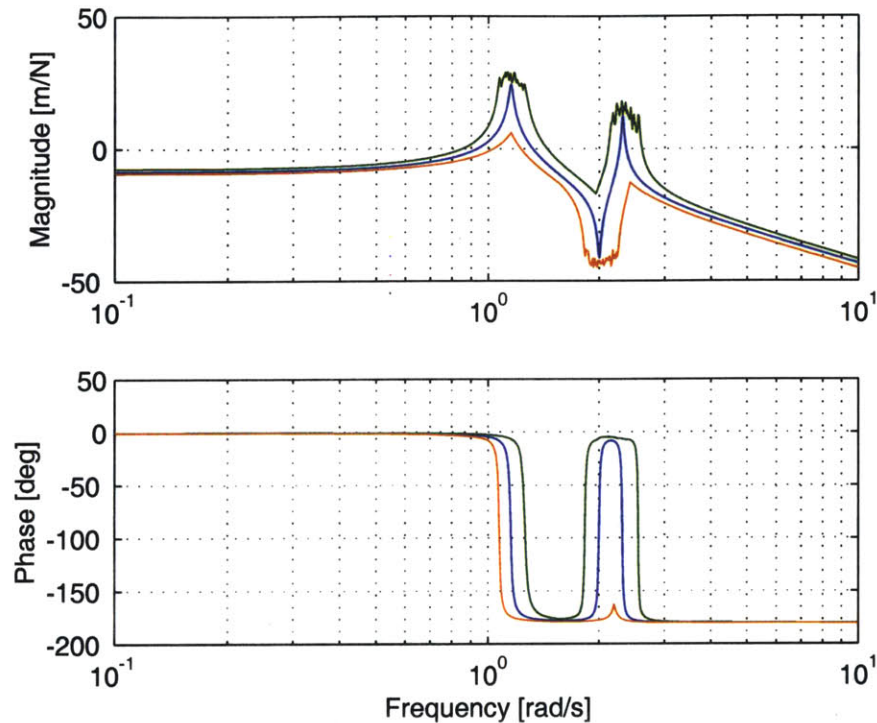


Figure 6.13 Monte Carlo simulation envelope for 100 random plants.

Vertex Method

In the context of evaluating the uncertainty on the FRF magnitude and phase, the vertex method must be used around the poles and zeros as all the method based on linear approximation fail. Near resonance, and antiresonance (zeros) the second and higher order terms become much important than the slopes, and therefore the linearity assumption is no longer valid. This is why, the linear covariance propagation does not work around the poles and zeros. Since the vertex method necessitate a lot of computations at every frequency point, we will use it in combination with the covariance propagation method to limit the computation costs,.

Linear Covariance Method

Figure 6.14 shown the prediction of the 1 sigma bound on the bode plot of the FRF

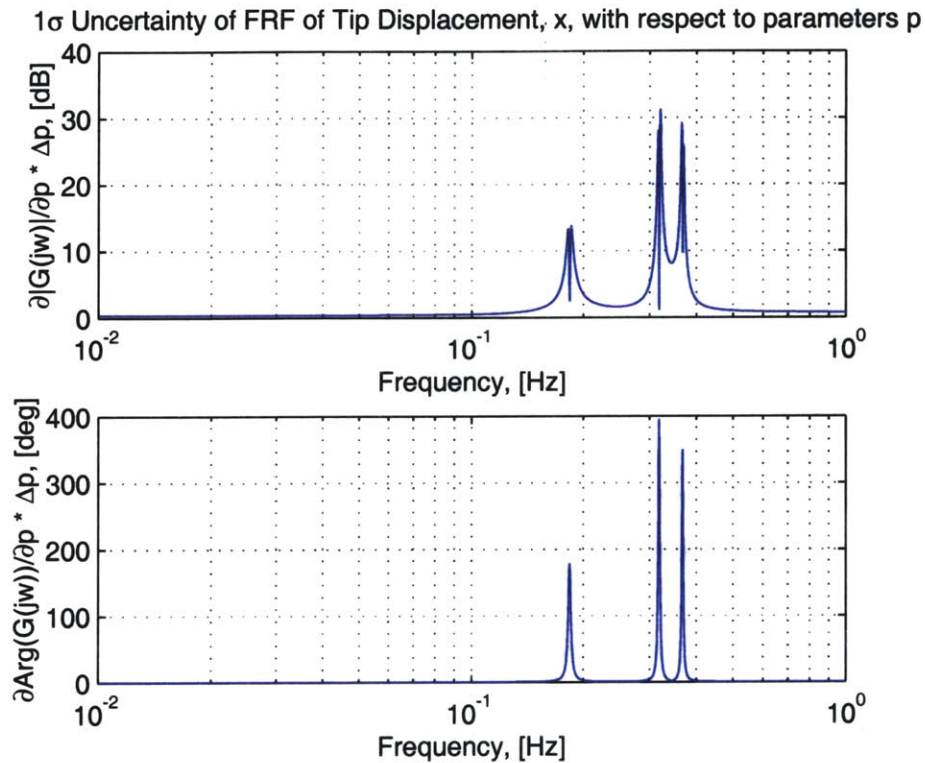


Figure 6.14 One sigma uncertainty for the FRF magnitude (top) and phase (bottom)

obtained by linear covariance propagation method. We can see very well that near the poles and zeros, the derivatives completely blow up. Nevertheless, the Covariance propagation method is very good at predicting the uncertainty bounds on the modal frequencies, or corresponding eigenvalues as shown Figure 6.15

It is clear from this simple example that the linear covariance propagation breaks down near the poles and zeros of the system where the second order derivatives become very

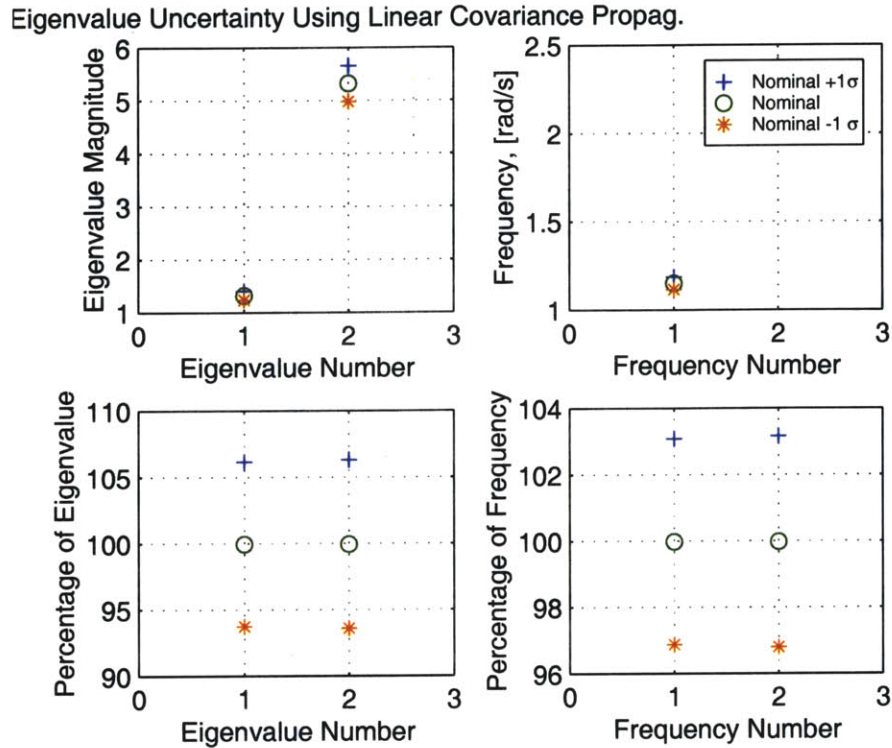


Figure 6.15 One sigma uncertainty bounds on the eigenvalues (left) and the corresponding modal frequencies in [rad/s] (right).

large. Away from these critical frequencies though the uncertainty intervals computed are valid as the linearity is preserved for these frequency range. In order to bound the uncertainty intervals near the singularities, we will use a vertex method approach. Figure 6.16 shows the results from the application of the linear covariance propagation technique on the bode plot of the FRF. We really see the effects of the non-linearities near the poles and zeros. Therefore, this technique will be applied complementary with the vertex method.

Hybrid Method

Figure 6.17 shows the composite plot of the covariance propagation method bounded by the vertex method near the poles and zeros. We can see that there is no more extravagant amplification of the bounds at poles and zeros. This is also shown in Figure 6.19 where on

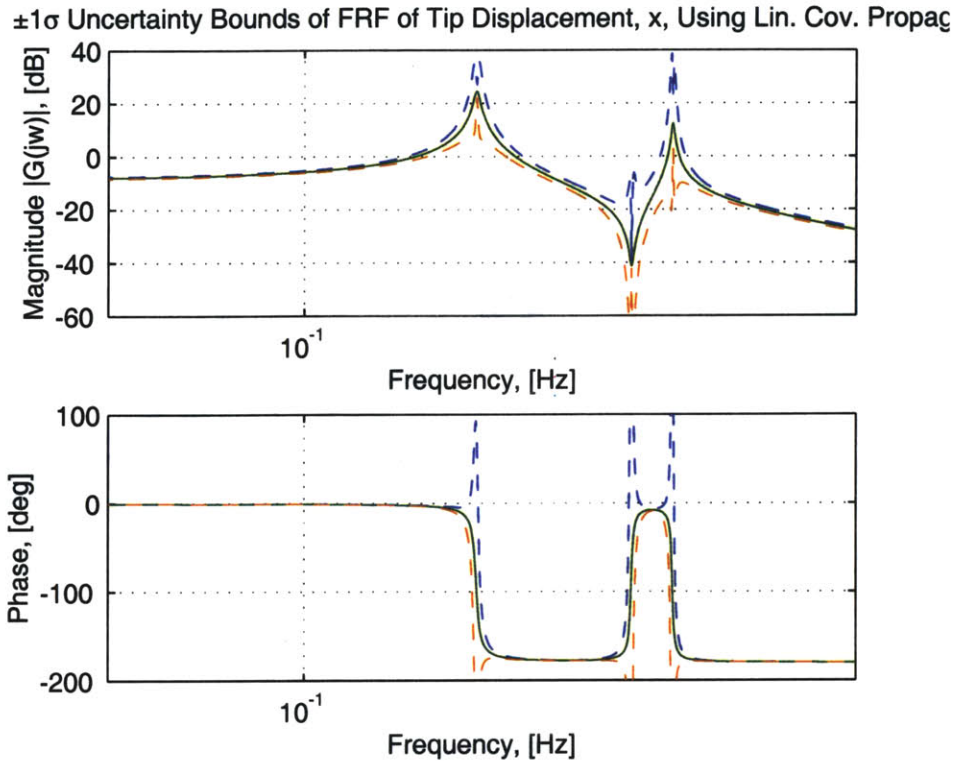


Figure 6.16 1 sigma bounds around the nominal FRF

the top figure we show that the linear covariance bounds are going out of the allowable envelope provided by the Monte-Carlo simulation.

On Figure 6.18 we also confirm the usefulness of bounding the covariance propagation method results. Not doing so would give enormous uncertainty bounds while integrating under the PSD curve to get the cumulative RMS plot. Even though the resulting bounds are less conservative, they are still large, This tells us that integrating under the PSD curve to get the uncertainty on the performance RMS might not be the best choice. In fact, if we compare the hybrid bounds on Figure 6.20, we see that they are far larger than the extreme bounds obtained from the monte carlo simulation. This tells us that we should in fact apply the linear propagation directly to the global performance RMS using the sensitivities as calculated in Chapter 4. In fact doing so, as shown on the Figure 6.20 gives the sigma bounds that correspond very well to the standard deviation obtained statistically from the

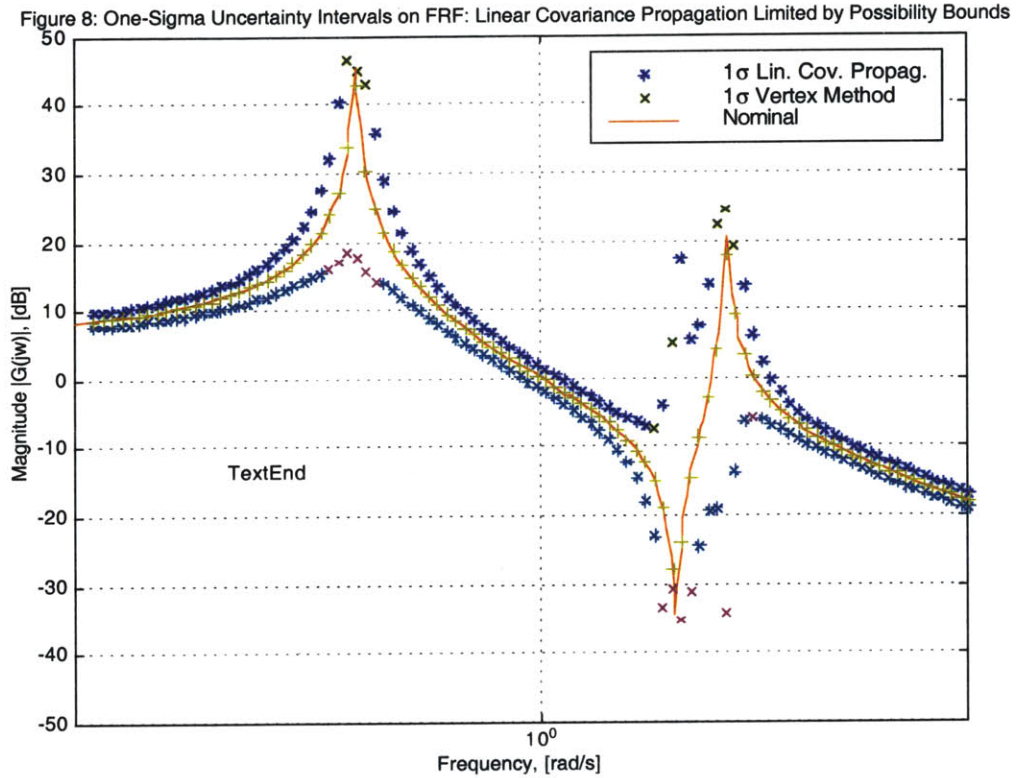


Figure 6.17 One sigma bounds on the FRF magnitude obtained by the hybrid method.

random simulation. This is very encouraging since it validates the approach we intend to implement on the large models of spacecraft missions such as SIM and NGST. An even more promising fact shown on Figure 6.20, is that the Monte Carlo maximum and minimum predictions on the RMS correspond almost perfectly to the 3sigma bounds of the linear covariance propagation applied directly to the RMS predictions. This also confirms that the linear approximation is valid for the performance RMS.

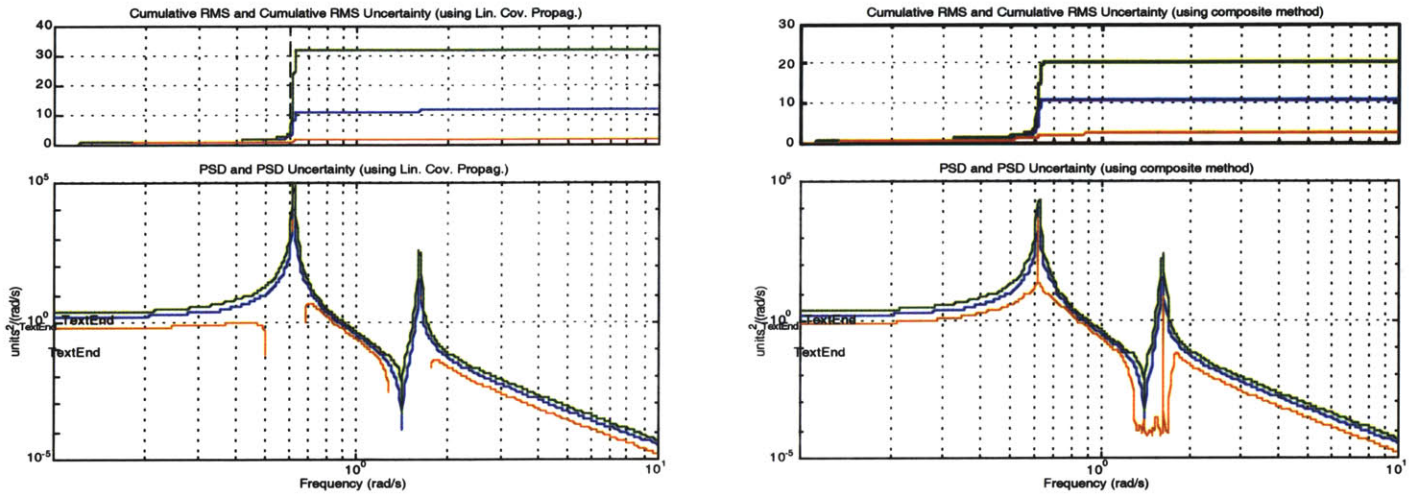


Figure 6.18 Comparison of the nominal and $\pm 1\sigma$ interval response computation for the PSD and cumulative RMS (using LSS data-base) from Linear Covariance Propagation (left) and hybrid method (right).

6.6 Summary

In this chapter, we have applied different method of propagating uncertainties from a data-base. We have demonstrated a way to get the uncertainty bounds around the FRF, but more interesting is the propagation of the uncertainty to the performance predictions as it is the quintessential question of structural design – will the systems meet the requirements? We have identified that in order to evaluate the uncertainty on the performance RMS, it is best to do it using the RMS sensitivities as oppose to try to integrate under the uncertain PSD curve.

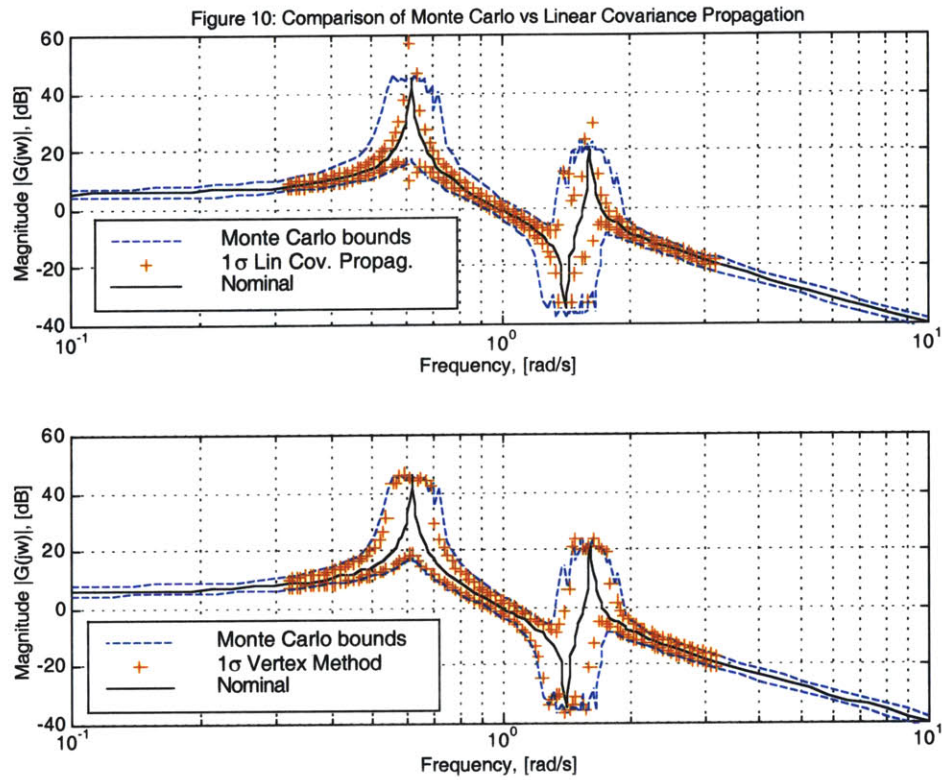


Figure 6.19
envelope

Comparison of the linear covariance method, and the vertex method with the Monte-Carlo simulation

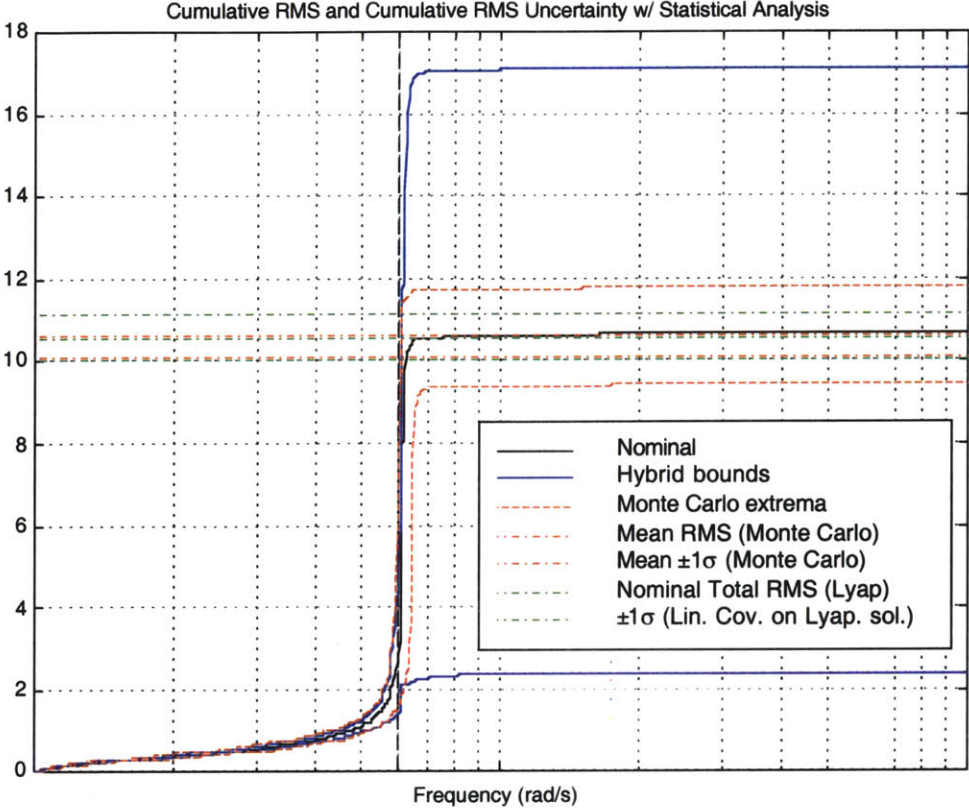


Figure 6.20 Cumulative RMS bounds comparison between the hybrid method, Monte Carlo, statistics on Monte Carlo, and first order approximation

Chapter 7

CONCLUSIONS

7.1 Thesis Summary and Contributions

To summarize the work done in this thesis, we first described the basic modeling tools and notation for performing integrated modeling and assessing the performance of precision controlled structures. We have established that it is not enough to evaluate only the nominal performance of the system based on the preliminary design models since these preliminary models can be quite crude in early design phase. Although they can provide great qualitative assessment of the performances, their quantitative predictions are not necessarily very accurate. Therefore, in order for the designer to make sure that, once it is built, the system will meet the requirements with a certain degree of confidence, it is a necessity to evaluate the uncertainty range around the performance outputs of the system. The tools to evaluate the uncertainty range around the nominal performances will be presented in the following chapters.

We have also presented a way to generate statistical structural database for performance analysis of space missions. For the near future, these techniques will be of utmost importance since direct system structure test data will not be available for large space systems. We have also introduced an innovative way of including the damping uncertainty into the system. As it was assumed to have lognormal distribution, we transform the modal damping parameters into the Gaussian space in order to propagate the uncertainty through linear

systems. It was also shown how the data obtained from a survey of spacecraft damping measurements could be utilized to probabilistically assess electro-optic jitter problems.

We have presented methodologies for computing uncertainties for the modal mass, stiffness and transformed damping. Modal mass and stiffness uncertainties for a structural model are expressed as a function of the error in the eigenvalue and mode shape predictions (cross-orthogonality). The methodology for obtaining modal mass and stiffness uncertainties is based on linear perturbation analysis of the eigen-problem. A database consisting of a covariance matrix of the normalized modal parameters (m and k), constructed from statistical analysis of families of structure/model pairs was presented [Hasselmann & Chrostowski, 1991]. The main limitations of the database are the limited sources of data available for statistical validity, and the limited number of modes documented for each sampled structure. Damping uncertainty for a structural model is defined in terms of the variability in experimental modal damping estimates. A methodology for obtaining damping uncertainties was outlined, assuming lognormal distributions for the modal damping data. The damping parameters were transformed from the lognormal space to the Gaussian space, in order to propagate their corresponding uncertainties. Three methods for generating damping uncertainty database were introduced, corresponding to different levels of accuracy (from model generation) in the uncertainty predictions.

The derivation of first order and second order derivatives of the frequency response function (FRF) matrix and the performance RMS, for a linear time invariant system, with respect to modal parameters $p = [m, k, \gamma]$ was presented. The second order derivatives are used to establish parameter uncertainty bounds Δp_i within which linearity is preserved. This is essential since the assumed normally distributed uncertainty parameters will lead to a Gaussian distribution of the performance RMS and FRF magnitude and phase. Expressions for second order derivatives for the eigenvalues and mode shapes with respect to the modal mass and stiffness matrix elements have still to be obtained.

Different methods that we use to propagate the uncertainties and evaluate the error bounds around the nominal performance predictions were presented. One contribution of this research work was to obtain the probability distribution of the response and hence evaluate the probability of success of the design given a certain error budget. We have also obtained the complementary probability of failure of the design given an error budget. This is an important result in the context of high profile spacecraft mission such as SIM or NGST as it help the engineer build confidence that a particular architecture is suitable to meet its specific tight requirements in presence of modeling uncertainties. An other contribution was to provide the constrained optimization technique, use to evaluate the worst-case performance, with the necessary bounds on the parameters. These bounds were obtained from the past experience database.

7.2 Recommendations for Future Work

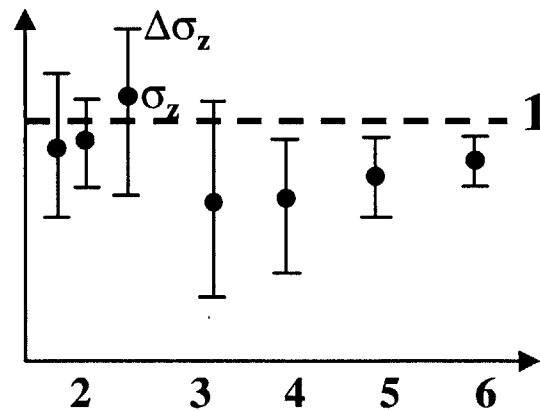
Still a lot of work needs to be done in order to characterize statistical structural uncertainties. Also, the characterization of the disturbance uncertainties would be most useful in order to evaluate the overall uncertainty of the integrated system.

The tools and methods developed in this thesis could be used in populating an uncertainty management for a flight program such as SIM or NGST. Such an uncertainty management plan could involve the following steps:

Flight Program Uncertainty Roadmap

1. Start: Define science and engineering requirements (WFT, DPL, BS, LOS Jitter)
2. Conceptual Design: Selection between competing designs using nominal performance $\tilde{\sigma}_z$ and level of uncertainty $\Delta\sigma_z$.
3. Preliminary Design: Design for small sensitivity to uncertainty, i.e. reduce sensitivity of performance to parametric uncertainty.
4. Detail Design: Optimization of design based on uncertainty bounds. Ensure that worst-case bound remains within requirements.

5. Testing and Integration: Establish testing requirements, focusing on the uncertain parameters p , which most affect performance uncertainty. Reduce Δp as much as possible.
6. Launch: At the time of launch the only remaining uncertainty should be in the environmental (disturbance) influences.



This plot shows the evolution of the error bars with respect to the nominal performance. The numbering corresponds to the flight program steps mentioned above.



Room 14-0551
77 Massachusetts Avenue
Cambridge, MA 02139
Ph: 617.253.2800
Email: docs@mit.edu
<http://libraries.mit.edu/docs>

DISCLAIMER

MISSING PAGE(S)

Chapter 8 (pages 181-184) has been omitted from both the Library, and Archives copy due to pagination error. The "Conclusions" section is included in Chapter 7.

REFERENCES

- [Balas, 1982] Balas, M.J., "Trends in Large Space Structures Control Theory: Fondest Hopes — Wildest Dreams", *IEEE Transactions on Automatic Control*, **AC-27**, No. 3, pp. 522-535, June 1982.
- [Balas & al., 1994] Balas, G.J., Doyle, J.C., Glover, K., Packard, A., and Smith, R., " μ -Analysis and Synthesis Toolbox", Version 3.0.3, MUSYN, Minneapolis, MN, 1994.
- [Barlow, 1992] Barlow, M. S., *The Dynamics of Deployable Truss Structures in Zero-gravity: The MODE STA Results*, MIT Master's Thesis in Aeronautics and Astronautics, Space Systems Lab., January 1992. SSL Report #1-92.
- [Bond & Laurenson, 1989] Bond, N. C., Laurenson, R. M., "Constrained Layer Damping for a Space-Based Optical System", WRDC-TR-89-3116, In *Proceedings of Damping '89*, Vol. I, 8-10 February 1989, West Palm Beach, Fl.
- [Bourgault & Ubelhart, 1999] Bourgault, F., Ubelhart, S., "Modeling Uncertainty and Error Management", MIT Space Systems Laboratory, Slide Presentation to JPL SIM/MPI Contract Review, April 23, 1999.
- [Campbell, 1996] Campbell, M.E., *Uncertainty Modeling for Structural Control Analysis and Synthesis*, MIT Ph.D. Thesis in Aeronautics and Astronautics, Space Systems Lab., January 1996. SSL Report #***
- [Campbell, 1997] Campbell, M.E., and Crawley, E.F., "Development of Structural Uncertainty Models", *Journal of Intelligent Guidance, Control, and Dynamics*, **20**, pp. 841-849, 1997.
- [Chen, 1985] Chen, S., Liu, Y., and Huang, D., "A Matrix Perturbation of Vibration Modal Analysis", In *Proceedings IMAC 3*, pp. 757-762, Orlando, FL, 1985.
- [Crawley & O'Donnell, 1987] Crawley, E.F., and O'Donnell, K.J., "A Procedure for Calculating the Damping in Multi-Element Space Structures", *Acta Astronautica*, **15**, No. 12, pp. 987-996, 1987.
- [Crawley, Sigler & van Schoor, 1988] Crawley, E.F., Sigler, J.L., and van Schoor, M.C., *Prediction and Measurement of Damping in Hybrid Scaled Space Structure Models*, MIT Space Systems Laboratory, July 1988. SSL Report #7-88.
- [Davis, Schmitt & See, 1989] Davis, P., Schmitt, F., See, C., "A Viscous Isolator for Shuttle Hubble Space Telescope Resupply", WRDC-TR-89-3116, In *Proceedings of*

- Damping '89*, Vol. I, 8-10 February 1989, West Palm Beach, FL.
- [Doyle, 1982] Doyle, J.C., "Analysis of feedback systems with structured uncertainties", *IEEE Proc.*, **129**, Part D(6), pp. 242-250, 1982.
- [de Weck, 1999] de Weck, O.L., *Integrated Modeling and Dynamics Simulation for the Next Generation Space Telescope*, MIT Master's Thesis in Aeronautics and Astronautics, Space Systems Lab., June 1999. SSL Report #5-99.
- [Dong & Shah, 1987] Dong, W., and Shah, H., "Vertex Method for Computing Function of Fuzzy Variables", *International Journal of Fuzzy Sets and Systems*, **24**, pp. 65-78, 1987.
- [Drake, 1967] Drake, Alvin, W., *Fundamentals of Applied Probability Theory*, Classic Textbook Reissue Series, McGraw-Hill, 1967, (Reissued 1988).
- [DMK/DPK, 1984] DMK/DPK, *Formeln und Tafeln: Mathematik—Physik*, 3rd ed., Orell Fussli, Zurich, 1984.
- [Ewins, 1984] Ewins, D.J., *Modal Testing: Theory and Practice*, Research Studies Press, John Wiley & Sons, 1984.
- [Fan, Tits & Doyle, 1990] Fan, M., Tits, A., and Doyle, J.C., "Robustness in the presence of joint parametric uncertainty and unmodeled dynamics", *IEEE Transactions on Automatic Control*, **36**, no.1, pp. 25-38, January 1991.
- [Garnek, 1997] Garnek, M., *EOS Orbital Damping Study*, EOS-Study 282, MA93-EOS-002, GE Astro-Space, Astro-Space Division, March 31, 1997.
- [Gehling, 1987] Gehling, R. N., "Large Space Structure Damping Treatment Performance: Analytic and Test Results", *The Role of Damping in Vibration and Noise Control*, ASME Publication, DE-Vol. 5, pp. 93-100, September 1987.
- [Gehling, 1991] Gehling, R. N., "Active Vibration Suppression via LQG/LTR; Analytic and Experimental Results for the PACOSS Dynamic Test Article", WL-TR-91-3078, In *Proceedings of Damping '91*, Vol. I, 13-14 February 1991, San Diego, Ca.
- [Gelb & al., 1974] *Applied Optimal Estimation*, written by the Technical Staff of The Analytic Sciences Corporation, edited by Arthur Gelb, The M.I.T. Press, Cambridge, MA, 1974.
- [Gilheany, 1989] Gehling, J.J., "Optimum Selection of Dampers for Freely Vibrating Multidegree of Freedom Systems", WRDC-TR-89-3116, In *Proceedings of Damping '89*, Vol. III, 8-10 February 1989, West Palm Beach, Fa.
- [Glurk, 1966] Glurk, R., "Material Damping of the OGO EP-5, EP-6 Blooms", TRW

Memorandum No. 66-3343.3-199, December 7th, 1966.

- [Grocott, 1994] Grocott, S.C.O., *Comparison of Control Techniques for Robust Performance on Uncertain Systems*, MIT Master's Thesis in Aeronautics and Astronautics, Space Engineering Research Center, January 1994. SSL Report #2-94.
- [Gutierrez, 1999] Gutierrez, H.L., *Performance Assessment and Enhancement of Precision Controlled Structured During Conceptual Design*, MIT Ph.D. Thesis in Aeronautics and Astronautics, Space Systems Lab., February 1999. SSL Report #1-99.
- [Gutierrez, Bourgault & Miller, 1999] Gutierrez, H.L., Bourgault, F., and Miller, D.W., "Development and Validation of Performance Sensitivities with Respect to Structural Parameters", To be submitted to the *Journal of Sound and Vibration*, July 1999.
- [Hagood, 1988] Hagood, N.W., and Crawley, E.F., *Development and Experimental Verification of Damping Enhancement Methodologies for Space Structures*, MIT Space Systems Laboratory, September 1988. SSL Report #18-88.
- [Hagood, 1989] Hagood, N.W., and von Flotow, A., "Damping of Structural Vibrations with Piezoelectric Materials and Passive Electrical Networks", WRDC-TR-89-3116, In *Proceedings of Damping '89*, Vol. III, 8-10 February 1989, West Palm Beach, Fl.
- [Hagood, 1991] Hagood, N.W., *Cost Averaging Techniques for Robust Control of Parametrically Uncertain Systems*, MIT Ph.D. Thesis in Aeronautics and Astronautics, June 1991. SSL Report #9-91.
- [Hasselmann, 1972] Hasselmann, T. K., "Method for Constructing a Full Modal Damping Matrix from Experimental Measurements", *AIAA Journal*, 4, no.10, pp.526-527, April 1972.
- [Hasselmann, 1976] Hasselmann, T. K., "Modal Coupling in Lightly Damped Structures", *AIAA Journal*, 14, no.11, November 1976.
- [Hasselmann & Simonian, 1980] Hasselmann, T. K., and Simonian, S. S., "Structural Uncertainty in Seismic Risk Analysis", J. H. Wiggins Co., Technical Report, Publication No. 80-1380, March 1980. Also: U.S. Nuclear Regulatory Commission Technical Report NUREG/CR-1560, UCLR-15218.
- [Hasselmann, 1981] Hasselmann, T. K., "Structural Uncertainty in Dynamic Analysis", Technical Paper No. 811049, *SAE Transactions*, 1981.
- [Hasselmann & Chrostowski, 1991] Hasselmann, T. K., Chrostowski, J. D., "Methods for Evaluating the Predictive Accuracy of Structural Dynamic Models", Final Report

No. NASA-CR-191337, December 1991.

- [Hasselmann, Chrostowski & Ross, 1992] Hasselmann, T. K., Chrostowski, J. D., and Ross, T. J. "Interval Prediction in Structural Dynamic Analysis", AIAA-92-2215-CP, *Proceedings, AIAA Structures, Structural Dynamics, and Materials Conference*, Dallas, TX, April 1992, pp. 1272-1284.
- [Hasselmann, Chrostowski & Ross, 1994] Hasselmann, T. K., Chrostowski, J. D., and Ross, T. J. "Propagation of Modeling Uncertainty through Structural Dynamic Models", AIAA-94-1316, *Proceedings, AIAA Structures, Structural Dynamics, and Materials Conference*, Hilton Head, SC, April 1994, pp. 72-83.
- [Haviland, 1976] Haviland, R., "A Study of the Uncertainties in the Fundamental Translational Periods and Damping Values for Real Buildings", Technical Report, Publication No. R76-12, Department of Civil Engineering, MIT, February 1976.
- [How, 1993] How, J.P., *Robust Control Design with Real Parameter Uncertainty using Absolute Stability Theory*, MIT Ph.D. Thesis in Aeronautics and Astronautics, Space Systems Lab., January 1993. SSL Report #1-93.
- [Huang, 1986] Huang, E.G., Choi, K.K., and Komkov, V., *Design Sensitivity Analysis of Structural Systems*, Academic Press, Inc., Orlando, 1986.
- [HST and Beyond Committee] Alan Dressler, Chair, *Exploration and the Search for Origins: A Vision for UV-Optical-IR Space Astronomy*, Report from the "HST and Beyond Committee". Also in Jet Propulsion Laboratory, *Origins Missions*, URL <<http://origins.jpl.nasa.gov/library/programdocs.html>>. Accessed March 20, 2000.
- [Ingham, 1998] Ingham, M.D., *Microdynamics and Thermal Snap Response of Deployable Space Structures*, MIT Masters Thesis in Aeronautics and Astronautics, Space Systems Lab., May 1998. SSL Report #2-98.
- [Jacques, 1994] Jacques, R.N., *On-line System Identification and Control Design for Flexible Structures*, MIT Ph.D. Thesis in Aeronautics and Astronautics, Space Systems Lab., May 1994. SSL Report #11-94.
- [Johnson & Kienholz, 1982] Johnson, C. D., and Kienholz, D. A., "Finite Element Prediction of Damping in Structures with Constrained Viscoelastic Layers", *AIAA Journal*, **20**, no.9, pp. 1284-1290, September 1982.
- [Johnson, 1985] Johnson, C. D., "Design and Analysis of Damped Structures using Finite Element Techniques", ASME Paper No. 85-DET-131, *ASME Conference on Mechanical Vibration and Noise*, Cincinnati, OH, September 1985.
- [Joshi, 1999] Joshi, S.S., "****???", *IEEE Control Systems*, **2??**, no. ???, pp. ???-63,

December 1999.

- [Kaplan, 1991] Kaplan, Wilfred, *Advanced Calculus*, Addison-Wesley Publishing Company, Fourth Edition, 1991.
- [Kato, 1966] Kato, T., *Perturbation Theory for Linear Operators*, Springer-Verlag, New York, 1966.
- [Lim & Giesy, 2000] Lim, K.B., and Giesy, D.P., "Parametrization of Model Validating Sets for Uncertainty Bound Optimizations", *Journal of Guidance, Control, and Dynamics*, **23**, no. 2, pp. 222-230, March-April 2000.
- [Lutes & Sarkani, 1997] Lutes, L.D., and Sarkani, S., *Stochastic Analysis of Structural and Mechanical Vibrations*, Prentice-Hall, NJ, 1997.
- [Mallory, 2000] Mallory, G.J.W., *Development and Experimental Validation of Direct Controller Tuning for Spaceborn Telescopes*, MIT Ph.D. Thesis in Aeronautics and Astronautics, Space Systems Lab., April 2000. SSL Report #1-2000.
- [Manning, 1991] Manning, R. A., "An Optimum Design Methodology for Passively Damped Truss Structures", WL-TR-91-3078, In *Proceedings of Damping '91*, Vol. I, 13-14 February 1991, San Diego, Ca.
- [Masterson, 1999] Masterson, R. A., *Development and Validation of Empirical and Analytical Reaction Wheel Disturbance Models*, MIT Master's Thesis in Mechanical Engineering, Space Systems Lab., June 1999. SSL Report #4-99.
- [Meirovitch, 1986] Meirovitch, L., *Elements of Vibration Analysis*, McGraw-Hill, 2nd edition, 1986.
- [Molnar, Hill & Stahle 1991] Molnar, J., Hill, D., and Stahle, C., "Statistical and Worst Case Evaluation of Orbital Jitter Reduction Using Passive Damping", WL-TR-91-3078, In *Proceedings of Damping '91*, 13-14 February 1991, San Diego, Ca.
- [Mosier & al., 1998] Mosier, G., Femiano, M., and Ha, K. (NASA, Goddard Space Flight Center), Redding, D., (JPL), "An Integrated Modeling Environment for System-level Performance Analysis of the Next Generation Space Telescope", *SPIE Conference*, Kona, 1998.
- [Nelson, 1976] Nelson, R. B., "Simplified Calculations of Eigenvector Derivatives", *AIAA Journal*, **14**, pp.1201-1205, 1976.
- [Packard & Doyle, 1993] Packard, A., and Doyle, J.C., "The complex structured singular value", *Automatica*, **29**, no.1, pp. 71-110, 1993.
- [Pandit, 1989] Pandit, S.M., "An Alternative To FFT For Precise Damping Estimates", WRDC-TR-89-3116, Text CBB, In *Proceedings of Damping '89*, 8-10 February

1989, West Palm Beach, Fl.

[Rellich, 1969] Rellich, F., *Perturbation Theory of Eigenvalue Problems*, Grodon Beach Science Publishers, Inc., New York, 1969.

[Simonian, 1987] Simonian, S. S., "Survey of Spacecraft Damping Measurements: Applications to Electro-Optic Jitter Problems", *The Role of Damping in Vibration and Noise Control, ASME Publication, DE-Vol. 5*, pp. 287-292, September 1987.

[Simonian, 1991] Simonian, S. S., "A Three Element Viscoelastic Isolator", WL-TR-91-3078, In *Proceedings of Damping '91*, 13-14 February 1991, San Diego, Ca.

[Skelton, 1989] Skelton, R. E., "Model error concepts in control design", *International Journal of Control*, **49**, no.5, pp. 1725-1753, May 1989.

[Slater, 1991] Slater, J. C., Inman, D. J., Belvin, W. K., "Modeling of Constrained Layer Damping in Trusses", WL-TR-91-3078, In *Proceedings of Damping '91*, Vol. II, 13-14 February 1991, San Diego, Ca.

[Smith & al., 1997 ***Idonhaveit] Smith, R..S., Dullerud, G., Rangan, S., and Poolla, K., "Model Validation for Dynamically Uncertain Systems", *Mathematical Modeling of Systems*, **3**, no. 1, pp. 43-58, 1997.

[Taguchi, 1995] Taguchi, G., "Quality Engineering (Taguchi Methods) For the Development of Electronic Circuit Technology", *IEEE Transactions*, **44**, no.2, pp. 225-229, June1995.

[Ting, 1989] Ting, J. M., Kim, C. K, Crawley, E. F., "Investigation of Structural Damping Combining Linear and Non-linear Contrained Viscoelastic Mechanisms", WRDC-TR-89-3116, In *Proceedings of Damping '89*, Vol. III, 8-10 February 1989, West Palm Beach, Fl.

[von Flotow & Vos, 1991] von Flotow, A. H., Vos, D. W. "The Need for Passive Damping in Feedback Controlled Flexible Structures", WL-TR-91-3078, In *Proceedings of Damping '91*, Vol. II, 13-14 February 1991, San Diego, Ca.

[Voth & Stoughton, 1991] Voth, C. T., and Stoughton, R. M., " H_{∞} Control for the PACOSS DTA", WL-TR-91-3078, In *Proceedings of Damping '91*, Vol. I, 13-14 February 1991, San Diego, Ca.

[Wada, 1988] Wada, B., Panel discussion at the USAF/NASA Workshop on Model Determination for Large SPace Structures, Passadena, Ca, March 1988.

[Wirsching, 1995] Wirsching, P.H., Paez, T.L., and Ortiz, K., *Random Vibrations: Theory and Practice*, Wiley-Interscience, John Wiley & Sons, 1995.

[Yang, 1997] Yang, K.Y.-L., *Efficient Design of Robust Controllers for H_2 Performance*,

- MIT Ph.D. Thesis in Aeronautics and Astronautics, Space Systems Lab., February 1997. SSL Report #8-96.
- [Young, Newlin & Doyle, 1991] Young, P.M., Newlin, M.P., Doyle, J.C., “ μ analysis with real parametric uncertainty”, In *Proceedings of the 30th IEEE Conference on Decision and Control*, Brighton, England, pp. 1251-1256, December 1991.
- [Zhou, 1996] Zhou, K., Doyle, J. C., and Glover, K, *Robust and Optimal Control*, Prentice-Hall, Inc., 1996.
- [Hagood, 1990] Hagood, N., Chung, W., and von Flotow, A., “Modeling of Piezoelectric Actuator Dynamics for Active Structural Control”, *J. Intelligent Materials, Systems, and Structures* **1**, pp. 327-354, July 1990.
- [Hagood, 1993] Hagood, N., and McFarland, A. J., “Modeling of a Piezoelectric Rotary Ultrasonic Motor”, *SPIE Conf. Proceedings* **2190**, Nesbitt Hagood, editor, pp. 814-818, 1993.
- [Kato, 1989] Kato, K., “Friction Between a Rotor and Stator”, *Ultrasonic Electronics: New Applications of Piezoelectricity*, 25th Tohoku University Communications Research Symposium III-5, pp. 101-106, 1989.
- [Kawai, 1995] Kawai, Y., Asai, K., Naito, S., Fukui, T., Adachi, Y., Handa, N., Ikeda, K., and Tsuda, K., “High Power Travelling-Wave Type Ultrasonic Motor”, *Jpn. J. Appl. Phys* **34**, pp. 2711-2714, May 1995.
- [Kumada, 1985] Kumada, A., “A Piezoelectric Ultrasonic Motor”, *Japanese Journal of Applied Physics* **24**, Supplement 24-2, pp. 739-741, 1985.
- [MacFarland, 1995] McFarland, A.J., Modeling, Design, Development, and Testing of a Piezoelectric Rotary Ultrasonic Motor, MIT S.M. Thesis in Aeronautical and Astronautical Engineering, June 1995
- [Sashida, 1993] Sashida, T., and Kenjo, T., *An Introduction to Ultrasonic Motors*, Clarendon Press, Oxford, 1993.
- [Ueha, 1993] Ueha, S., and Tomikawa, Y., *Ultrasonic Motors: Theory and Applications*, Clarendon Press, Oxford, 1993.

Appendix A

SOME PROBABILITY AND RANDOM VARIABLES FUNDAMENTALS

In this Appendix, we will briefly review some some of the basic and pertinent fundamentals of probability and random variables that are useful in this thesis. For a more detailed discussion on probability theory the reader is referred to [Drake, 1967].

A.1 Probability for continuous Random Variables

A random variable (RV) x is, in simplest terms, a variable which takes on values at random; and may be thought of as a function of the outcomes of some random experiment. The manner of specifying the probability with which different values are taken by the RV is by the *Cumulative Distribution Function* (CDF), also called the probability distribution function $F_x(x_0)$ which is defined by:

$$F_x(x_0) = p_{x \leq (x_0)} = P(x \leq x_0) = \int_{-\infty}^{x_0} f_x(x_0) dx_0 \quad (\text{A.1})$$

or by the *Probability Density Function* (PDF) $f_x(x_0)$ which is defined by:

$$F_x(x_0) = \frac{d}{dx_0} p_{x \leq (x_0)} = f_x(x_0) \quad (\text{A.2})$$

where

$$F_x(\infty) = \int_{-\infty}^{\infty} f_x(x_0) dx_0 = 1 \quad (\text{A.3})$$

The *expectation* of a RV x is defined as the sum of all values the RV may take, each weighted by the probability with which the value is taken. For a continuous RV, it is given by

$$E(x) = \int_{-\infty}^{\infty} x_0 f_x(x_0) dx_0 = \bar{x} \quad (\text{A.4})$$

This is also called the *mean value* of x , or the *first moment* of x . The notation $\overline{(\cdot)}$ can be used interchangeably for the expectation operator.

The expectation of a function of RV can be computed directly from the distribution of x by the integral

$$E(g(x)) = \int_{-\infty}^{\infty} g(x_0) f_x(x_0) dx_0 \quad (\text{A.5})$$

Note that it is not necessary to derive the PDF of a function of RV ($f_g(g_0)$) to get its mean ($E(g(x))$) or its variance (σ_g^2).

To derive the PDF for g , a function of one or multiple RV's, we need to perform only two steps in the event space of the original random variables (see Chapter 2 of [de Weck, 1999]):

Step 1) Determine the probability of the event $g \leq g_0$ for all values of g_0 . In other words, get the CDF, $p_{g \leq}(g_0)$.

Step 2) Differentiate this quantity with respect to g_0 to obtain $f_g(g_0)$.

An important statistical parameter descriptive of the distribution of x is its *mean-squared value*. Using Eq. A.5, the expectation of the square of x is written

$$E(x^2) = \int_{-\infty}^{\infty} x_0^2 f_x(x_0) dx_0 \quad (\text{A.6})$$

This quantity is also called the *second moment* of x . The root-mean squared (RMS) value of x is the square root of $E(x^2)$. The *variance* of a RV is the mean squared deviation of the RV from its mean; it is denoted by σ_x^2 where

$$\sigma_x^2 = E[(x - E(x))^2] = \int_{-\infty}^{\infty} (x_0 - E(x))^2 f_x(x_0) dx_0 = E(x^2) - (E(x))^2 \quad (\text{A.7})$$

The square root of the variance, or σ_x , is the standard deviation of the RV x . The RMS value and the standard deviation are equal only for a zero-mean RV.

The probability that x is comprised between a and b is then given by

$$P(a < x \leq b) = \int_a^b f_x(x_0) dx_0 = P_{x \leq b} - P_{x \leq a} \quad (\text{A.8})$$

In the two-dimensional event space for the possible experimental values of RV's x and y , we have the compound, or joint, PDF, $f_{x,y}(x_0, y_0)$, and the probability of an event A is given by the integral over its surface:

$$P(A) = \iint_{S_A} f_{xy}(x_0, y_0) dx_0 dy_0 \quad (\text{A.9})$$

The expectation of a function of two RV's can be computed directly from the compound distribution of x and y by the integral

$$E(g(x, y)) = \int_{-\infty}^{\infty} \int_{-\infty}^{\infty} g(x_0, y_0) f_{xy}(x_0, y_0) dx_0 dy_0 \quad (\text{A.10})$$

Conditional probability of RV x given the event that RV $y = y_0$:

$$f_{x|y}(x_0|y_0) = \frac{f_{xy}(x_0, y_0)}{f_y(y_0)} \quad (\text{A.11})$$

Two continuous RV's x and y are defined to be independent (or statistically independent) if and only if

$$f_{x|y}(x_0|y_0) = f_x(x_0) \quad \text{for all } x_0, y_0 \quad (\text{A.12})$$

This means that for independent RV's, the compound PDF is given by

$$f_{xy}(x_0, y_0) = f_x(x_0)f_y(y_0) \quad \text{for all } x_0, y_0 \quad (\text{A.13})$$

We say that any number of RV's are mutually independent if their compound PDF factors into the product of their marginal PDF's for all possible experimental values of the RV's.

Of greatest interest, is the second order moment of RV's x and y about their centroid, that is, the expected value of $g(x, y) = (x - \mu_x)(y - \mu_y)$. This moment is known as the *covariance* and denoted σ_{xy} :

$$\sigma_{xy} = E[(x - \mu_x)(y - \mu_y)] = \int_{-\infty}^{\infty} \int_{-\infty}^{\infty} (x_0 - \mu_x)(y_0 - \mu_y) f_{xy}(x_0, y_0) dx_0 dy_0 \quad (\text{A.14})$$

In the mechanical analogy, the covariance is the product of inertia of the joint density function. By expanding the product and simplifying, it can be shown that

$$\sigma_{xy} = E[xy] - \mu_x \mu_y \quad (\text{A.15})$$

This equation is the most useful way to compute the covariance. The expected value of the product, $E[xy]$, is known as the correlation of x and y and is of cardinal importance in the study of random processes. Just as the variance measures the deviations of x from its centroid, the covariance measures deviations of x and y together from their centroid. Relatively large absolute values of σ_{xy} indicate that x and y tend to vary from the centroid together; for example, if x is large, then y will also be large. Values of σ_{xy} near zero indicate that they tend not to vary together.

To speak of "relatively" large or small values of σ_{xy} , we must normalize the covariance to eliminate units of measurements and to account for the marginal dispersion of x and y . A nondimensional measure is given by the ratio known as the correlation coefficient ρ_{xy} :

$$\rho_{xy} = \frac{\sigma_{xy}}{\sigma_x \sigma_y} \quad (\text{A.16})$$

where the ratio ranges between +1 and -1. Note that ρ_{xy} can also be written as

$$\rho_{xy} = E \left[\frac{(x - \mu_x)(y - \mu_y)}{\sigma_x \sigma_y} \right] \quad (\text{A.17})$$

which is to say that the correlation coefficient is equal to the expected value of the product of the standardized variables for x and y .

The correlation coefficient is a measure of the linear dependence of two RV's. If random variable y is a linear function of x , where for example $y = ax + b$, the correlation coefficient is equal to ± 1 . If x and y are independent, the correlation coefficient is equal to zero. If y is partially linearly related to x , the correlation coefficient is in the range -1 to +1 depending on the strength of the linear relation. If x and y are nonlinearly related, the correlation coefficient can tell us nothing about that relationship.

Example 1: x and y are linearly related by $y = ax + b$, where a and b are constants.

$$\begin{aligned} \rho_{xy} &= E \left[\frac{(x - \mu_x)(y - \mu_y)}{\sigma_x \sigma_y} \right] \\ &= E \left[\frac{(x - \mu_x)(ax + b - (a\mu_x + b))}{\sigma_x |a| \sigma_x} \right] = \frac{a}{|a|} E \left[\left(\frac{x - \mu_x}{\sigma_x} \right)^2 \right] \\ &= \frac{a}{|a|} = 1 \end{aligned} \quad (\text{A.18})$$

Thus, if y is perfectly linearly dependent on x , $\rho_{xy} = \pm 1$, depending on the sign of the constant a .

Example 2: x and y are independent. Then their correlation, $E(xy)$, is just the product of the marginal expected values because the joint PDF may be factored into the product of the marginal density functions (see A.13):

$$\begin{aligned}
E(xy) &= \int_{-\infty}^{\infty} \int_{-\infty}^{\infty} x_0 y_0 f_{xy}(x_0, y_0) dx_0 dy_0 = \int_{-\infty}^{\infty} x_0 f_x(x_0) dx_0 \int_{-\infty}^{\infty} y_0 f_y(y_0) dy_0 \\
&= \mu_x \mu_y
\end{aligned} \tag{A.19}$$

It follows immediately that their covariance, $\sigma_{xy} = E[xy] - \mu_x \mu_y$, and hence their correlation coefficient are equal to zero. The converse of the above is not necessarily true. That is, if the covariance of x and y is equal to zero, it is not necessarily true that x and y are independent as shown in the following example.

Example 3: Let the PDF of x be symmetric about the origin, that is, $f_x(-x_0) = f_x(x_0)$. By symmetry, the expected value of x is equal to zero, $\mu_x = 0$. Let y be related to x by a symmetric, nonlinear function such as $y = x^2$. The covariance is shown to be equal to zero as follows:

$$\begin{aligned}
\sigma_{xy} &= E[xy] - \mu_x \mu_y = E[x \cdot x^2] = E[x^3] = \int_{-\infty}^{\infty} x_0^3 f_x(x_0) dx_0 \\
&= 0
\end{aligned} \tag{A.20}$$

The integral in the last step is equal to zero because $x_0^3 f_x(x_0)$ is antisymmetric; for each function evaluation at $+x$, there is a canceling evaluation at $-x$. Hence, if the dependence between x and y is nonlinear, their covariance might be equal to zero. The fact that $\sigma_{xy} = 0$, or $\rho_{xy} = 0$, does not mean that x and y are independent. If $\sigma_{xy} = 0$, we say that x and y are uncorrelated. If the correlation between x and y is equal to zero, $E[xy] = 0$, we say that x and y are orthogonal.

Covariance Matrix:

The cross-covariance matrix of two vectors \mathbf{r} and \mathbf{s} is defined in terms of the outer products:

$$\Sigma_{rs} = E[(\mathbf{r} - E(\mathbf{r}))(\mathbf{s} - E(\mathbf{s}))^T] = E[\mathbf{r}\mathbf{s}^T] - E[\mathbf{r}]E[\mathbf{s}^T] \tag{A.21}$$

When $r = s$, Eq. A.21 defines the covariance of r ; it is simply a matrix whose elements are the second moments of the random components r_1, r_2, \dots, r_n . In the following, we define the error Δp in the estimate of a parameter vector to be the difference between the actual p and the estimated (nominal) \tilde{p} values:

$$\Delta p \equiv p - \tilde{p} \quad (\text{A.22})$$

The covariance of Δp , designated Σ_{pp} is given by

$$\Sigma_{pp} = E[\Delta p \Delta p^T] \quad (\text{A.23})$$

It provides a statistical measure of the uncertainty in p . The notation permits us to discuss the properties of the covariance matrix independently of the mean value of the parameters.

Some features of the covariance matrix can be seen by treating the error in the knowledge of two uncertain parameters,

$$\Delta p = \begin{bmatrix} \Delta p_1 \\ \Delta p_2 \end{bmatrix} \quad (\text{A.24})$$

The covariance matrix of Δp is

$$\Sigma_{pp} = E \left\{ \begin{bmatrix} \Delta p_1^2 & \Delta p_1 \Delta p_2 \\ \Delta p_1 \Delta p_2 & \Delta p_2^2 \end{bmatrix} \right\} = \begin{bmatrix} E[\Delta p_1^2] & E[\Delta p_1 \Delta p_2] \\ E[\Delta p_1 \Delta p_2] & E[\Delta p_2^2] \end{bmatrix} \quad (\text{A.25})$$

Notice that the covariance matrix of an n -parameter vector is an $(n \times n)$ *symmetric* matrix. The diagonal of this covariance matrix are the mean square errors in knowledge of the uncertain parameters. Also, the trace of Σ_{pp} is the mean square length of the vector Δp . The off-diagonal terms of Σ_{pp} are indicators of cross-correlation between the elements of Δp . Specifically, they are related to the linear correlation coefficient $\rho(\Delta p_1, \Delta p_2)$ by

$$\rho(\Delta p_1, \Delta p_2) = \frac{E[\Delta p_1 \Delta p_2]}{\sigma_1 \sigma_2} \quad (\text{A.26})$$

where σ_i indicates the standard deviation of Δp_i .

A.2 Probability Density Function (PDF)

Two important specific forms of probability distribution are the uniform and normal distributions.

A.2.1 Uniform Probability Density Function

The *uniform distribution* is characterized by a uniform (constant) probability density, over some finite interval. The magnitude of the PDF in this interval is the reciprocal of the interval height as required to make the integral of the function unity. This function is shown in Figure A.1.

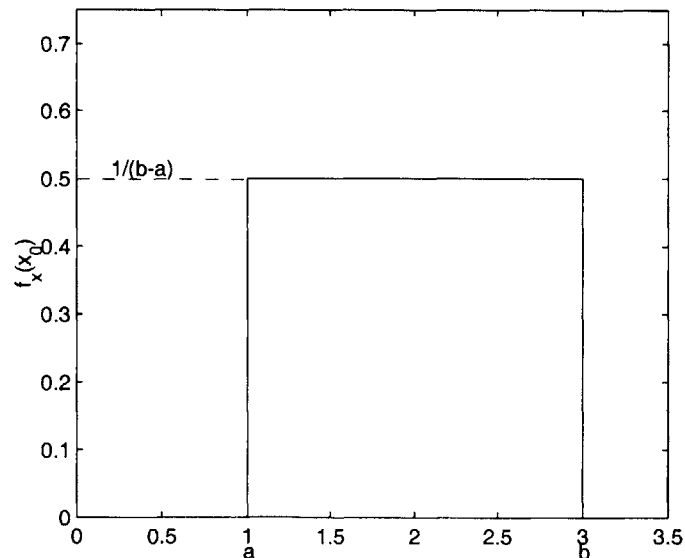


Figure A.1 Uniform Probability Density Function

The standard deviation for a uniform distribution can be found using the square root of Eq. A.7

$$\sigma_x = \sqrt{E[(x - E(x))^2]} = \sqrt{E(x^2) - (E(x))^2} \quad (\text{A.27})$$

where $E(x)$ is given by

$$E(x) = \frac{a + b}{2} \quad (\text{A.28})$$

and $E(x^2)$ is given by

$$E(x^2) = \int_a^b x_0^2 \frac{1}{b-a} dx_0 = \frac{x^3}{3(b-a)} \Big|_a^b = \frac{b^3 - a^3}{3(b-a)} = \frac{b^2 + ab + a^2}{3} \quad (\text{A.29})$$

plugged in A.27, we get

$$\sigma_x = \sqrt{\frac{b^2 + ab + a^2}{3} - \left(\frac{a+b}{2}\right)^2} = \sqrt{\frac{b^2 - 2ab + a^2}{12}} = \frac{(b-a)}{\sqrt{12}} \quad (\text{A.30})$$

A.2.2 Gaussian Probability Density Function

The *Gaussian* (or *normal*) PDF, shown in Figure A.2, has the following analytic form:

$$f_x(x_0) = \frac{1}{\sqrt{2\pi}\sigma_x} e^{-(x_0 - \mu_x)^2 / 2\sigma_x^2} \quad -\infty \leq x_0 \leq \infty \quad (\text{A.31})$$

where the two parameters that define the distribution are μ_x , the mean, and σ_x , the standard deviation. The s transform of the normal distribution is given by

$$f_x^T(s) = e^{((s^2\sigma_x^2)/e) - sE(x)} \quad (\text{A.32})$$

The integral of the function, or area under the curve, is unity. The area within $\pm 1\sigma$ bounds centered about the mean is approximately 0.68. Within the $\pm 2\sigma$ bounds, the area is 0.95.

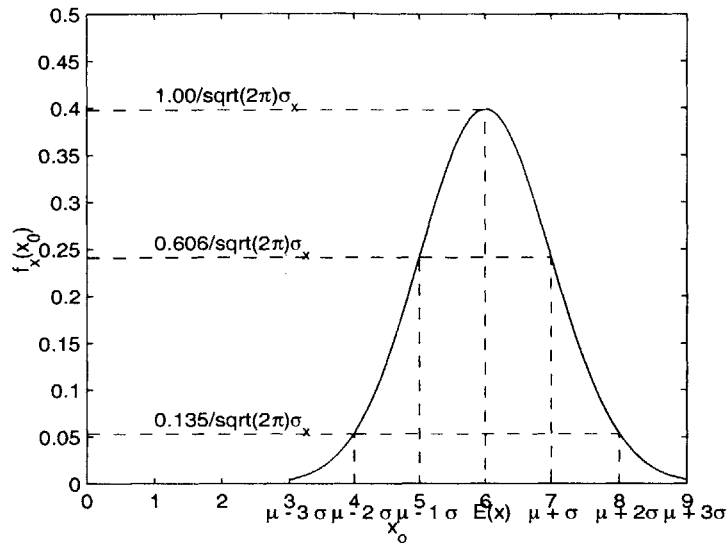


Figure A.2 Normal Probability Density Function

As an interpretation of the meaning of these values, the probability that a normally distributed random value is outside the $\pm 2\sigma$ bounds is approximately 0.05. The normality of the Gaussian distribution is preserved under sums of independent random variables and linear transformations.

ex.: -if α and β are scalars, then $y = \alpha x + \beta$ is also normal.

$$\begin{aligned}\bar{y} &= \alpha \bar{x} + \beta \\ \sigma_y^2 &= \alpha^2 \sigma_x^2\end{aligned}\tag{A.33}$$

-if x and y are normal (indep.) RV's, then $z = x + y$ is also normal.

$$\begin{aligned}\bar{z} &= \bar{x} + \bar{y} \\ \sigma_z^2 &= \sigma_x^2 + \sigma_y^2\end{aligned}\tag{A.34}$$

Since a Gaussian PDF is symmetrical about its expected values, the CDF may be fully described by tabulating it only for values above (or below) its expected value. The following is a four-place table of $\Phi(x_0^\circ)$, the CDF for a unit normal random variable:

TABLE A.1 CDF for the unit normal PDF

x_0°	$\Phi(x_0^\circ)$	x_0°	$\Phi(x_0^\circ)$	x_0°	$\Phi(x_0^\circ)$	x_0°	$\Phi(x_0^\circ)$
0.00	0.5000	1.00	0.8413	2.00	0.9772	3.00	0.9987
0.10	0.5398	1.10	0.8643	2.10	0.9821	3.10	0.9990
0.20	0.5793	1.20	0.8849	2.20	0.9861	3.20	0.9993
0.30	0.6179	1.30	0.9032	2.30	0.9893	3.30	0.9995
0.40	0.6554	1.40	0.9192	2.40	0.9918	3.40	0.9997
0.50	0.6915	1.50	0.9332	2.50	0.9938	3.60	0.9998
0.60	0.7257	1.60	0.9452	2.60	0.9953		
0.70	0.7580	1.70	0.9554	2.70	0.9965		
0.80	0.7881	1.80	0.9641	2.80	0.9974		
0.90	0.8159	1.90	0.9713	2.90	0.9981		

A more complete table of the cumulative distribution function of a standard normal RV can be found in Section E.1 of [Skelton, 1989].

Given a normal distribution $\mathcal{N}(\mu, \sigma)$, how do we get its CDF?

$$P_{x \leq}(x_0) = P(x \leq x_0) = P\left(\frac{x - \mu}{\sigma} \leq \frac{x_0 - \mu}{\sigma}\right) = \Phi\left(\frac{x_0 - \mu}{\sigma}\right) = \Phi(x_0^\circ) \quad (\text{A.35})$$

where

$$\Phi(x_0^\circ) = \frac{1}{\sqrt{2\pi}} \int_{-\infty}^{x_0^\circ} e^{-x^2/2} dx^\circ \quad (\text{A.36})$$

Values of the cumulative distribution function for negative argument can be calculated using the relation

$$\Phi(-x_0^\circ) = 1 - \Phi(x_0^\circ) \quad x_0^\circ \geq 0 \quad (\text{A.37})$$

Joint Normal Distribution

The *bivariate normal distribution* is given by

$$f_{xy}(x_0, y_0) = \frac{1}{2\pi\sigma_x\sigma_y\sqrt{1-\rho_{xy}^2}} e^{-\frac{1}{2(1-\rho_{xy}^2)}\left[\left(\frac{x_0-\mu_x}{\sigma_x}\right)^2 - 2\rho_{xy}\left(\frac{x_0-\mu_x}{\sigma_x}\right)\left(\frac{y_0-\mu_y}{\sigma_y}\right) + \left(\frac{y_0-\mu_y}{\sigma_y}\right)^2\right]}$$

$$-\infty \leq x_0 \leq \infty$$

$$-\infty \leq y_0 \leq \infty$$
(A.38)

If the correlation coefficient between x and y is equal to zero, $\rho_{xy} = 0$, the bivariate density can be factored into the product of two marginal PDF's. This means that if x and y are jointly normally distributed, a correlation coefficient equal to zero implies that x and y are independent. Recall that this is not generally true.

The bivariate density function can be easily generalized to more than two dimensions. Let there be n jointly distributed normal RV's x_i with mean values μ_i , variances σ_i^2 , and covariance σ_{ij} . The general *multidimensional* or *multivariate normal distribution* is

$$f_{x_1x_2\dots x_n}(x_{1_0}, x_{2_0}, \dots, x_{n_0}) = \frac{1}{(2\pi)^{n/2}|\Sigma|^{1/2}} e^{-\frac{1}{2}(\mathbf{x}-\mathbf{m})^T\Sigma^{-1}(\mathbf{x}-\mathbf{m})}$$
(A.39)

where Σ is the symmetric covariance matrix:

$$\Sigma = \Sigma_{xx} = E[(\mathbf{x}-\mathbf{m})(\mathbf{x}-\mathbf{m})^T] = \begin{bmatrix} \sigma_1^2 & \sigma_{12} & \dots & \sigma_{1n} \\ \sigma_{21} & \sigma_2^2 & \dots & \sigma_{2n} \\ \dots & \dots & \dots & \dots \\ \sigma_{n1} & \sigma_{n2} & \dots & \sigma_n^2 \end{bmatrix}$$
(A.40)

and $\mathbf{x}-\mathbf{m}$ is the vector

$$\mathbf{x}-\mathbf{m} = \begin{bmatrix} x_1 - \mu_1 \\ x_2 - \mu_2 \\ \dots \\ x_n - \mu_n \end{bmatrix}$$
(A.41)

Since all the statistical properties of a gaussian random process are defined by the first and second moment of the distribution, it is appropriate to introduce a shorthand notation like the following

$$\mathbf{x} \sim \mathfrak{N}(\mathbf{m}, \Sigma) \quad (\text{A.42})$$

which indicates that \mathbf{x} is a gaussian (normal) random vector with mean \mathbf{m} and covariance Σ . By way of example, for a one-dimensional random process x with mean μ and standard deviation σ , we would write

$$x \sim \mathfrak{N}(\mu, \sigma^2) \quad (\text{A.43})$$

A.2.3 Lognormal Probability Density Function

The *Lognormal* PDF, shown in Figure A.3, has the following analytic form:

$$f_x(x_0) = \frac{1}{\sqrt{2\pi}x_0d} e^{-(\ln(x_0) - c)^2/2d^2} \quad x_0 > 0 \quad (\text{A.44})$$

where the two parameters that define the distribution are c and d , defined in function of the statistical mean, μ_x , and standard deviation, σ_x , of the data as follows:

$$c = \left(\frac{\mu_x}{\sqrt{\rho_x^2 + 1}} \right), \quad d = \sqrt{\ln(\rho_x^2 + 1)}, \quad \rho_x = \frac{\sigma_x}{\mu_x} \quad (\text{A.45})$$

where the mean and variance can also be obtained by the following

$$\begin{aligned} E(x_0) &= \mu_x = e^{c + \frac{1}{2}d^2} \\ \sigma_x^2 &= e^{2c + d^2} (e^{d^2} - 1) \end{aligned} \quad (\text{A.46})$$

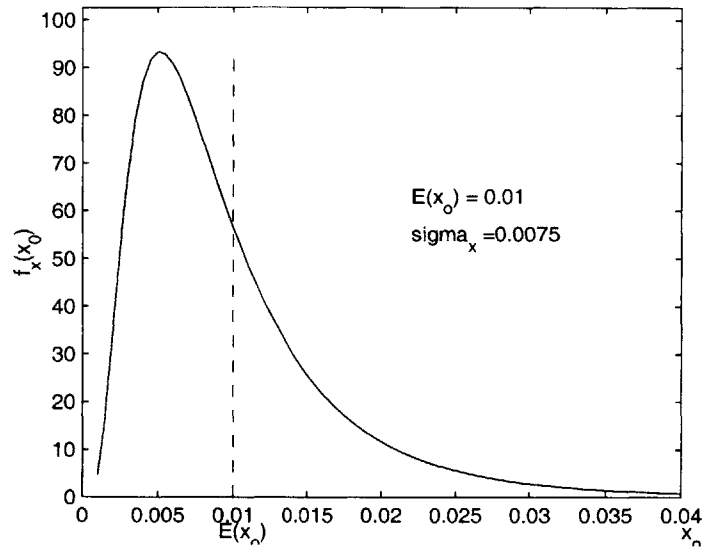


Figure A.3 Lognormal Probability Density Function

A.3 Random Processes

The subsequent review of random processes theory was presented in [Gutierrez, 1999]. For a more detailed discussion of the fundamentals of random processes, the reader should refer to [Wirsching, 1995], [Lutes & Sarkani, 1997], or [Gelb & al., 1974].

Suppose $w(t)$ is a random process, its *correlation function* is defined as

$$R_{ww}(t_1, t_2) = E[w(t_1)w^T(t_2)] \quad (\text{A.47})$$

For a stationary process, meaning a process for which the statistics do not change, the correlation function can be written more simply as

$$R_{ww}(\tau) = E[w(t)w^T(t + \tau)] \quad (\text{A.48})$$

where the variable τ is called the time-lag. This is a useful expression since the covariance matrix for a zero-mean process can be obtained by evaluating the correlation matrix at $\tau = 0$.

$$\Sigma_w = R_{ww}(0) = \begin{bmatrix} E[w_1^2] & E[w_1 w_2] & \dots & E[w_1 w_n] \\ E[w_2 w_1] & E[w_2^2] & \dots & E[w_2 w_n] \\ \dots & \dots & \dots & \dots \\ E[w_n w_1] & E[w_n w_2] & \dots & E[w_n^2] \end{bmatrix} = \begin{bmatrix} \sigma_1^2 & \sigma_{12} & \dots & \sigma_{1n} \\ \sigma_{21} & \sigma_2^2 & \dots & \sigma_{2n} \\ \dots & \dots & \dots & \dots \\ \sigma_{n1} & \sigma_{n2} & \dots & \sigma_n^2 \end{bmatrix} \quad (\text{A.49})$$

where n is the total number of elements in the vector w . The above simplification is possible for zero-mean processes since, from the covariance definition

$$\begin{aligned} \sigma_{w_i w_j} &= E[(w_i - \bar{w}_i)(w_j - \bar{w}_j)] \\ &= E[w_i w_j] - E[w_i \bar{w}_j] - E[\bar{w}_i w_j] + E[\bar{w}_i \bar{w}_j] \\ &= \overline{w_i w_j} - \bar{w}_i \bar{w}_j - \bar{w}_i \bar{w}_j + \bar{w}_i \bar{w}_j \\ &= \overline{w_i w_j} + \bar{w}_i \bar{w}_j - \bar{w}_i \bar{w}_j = \overline{w_i w_j} + 0 \\ &= \overline{w_i w_j} \end{aligned} \quad (\text{A.50})$$

Hence, the diagonal entries in the covariance matrix are simply the mean-square values of the elements of w .

$$(\Sigma_w)_{i,i} = E[w_i^2(t)] = \overline{w_i^2} \quad (\text{A.51})$$

Zero-mean processes have the nice characteristic to have their mean-square values identical to their variances.

$$\sigma_{w_i}^2 = E[w_i^2(t)] - \underbrace{(E[w_i])^2}_0 = \overline{w_i^2} \quad (\text{A.52})$$

The *spectral density function* (for zero-mean processes) is obtained by taking the Fourier transform of the correlation function (Eq. A.48).

$$S_{ww}(\omega) = \mathfrak{F}[R_{ww}(\tau)] = \int_{-\infty}^{\infty} R_{ww}(\tau) e^{-j\omega\tau} d\tau \quad (\text{A.53})$$

Conversely, the inverse Fourier transform recovers the correlation function.

$$R_{ww}(\tau) = \mathfrak{F}^{-1}[S_{ww}(\omega)] \equiv \frac{1}{2\pi} \int_{-\infty}^{\infty} S_{ww}(\omega) e^{j\omega\tau} d\omega \quad (\text{A.54})$$

As we mentioned earlier, evaluating the correlation function at $\tau = 0$ gives us the covariance matrix. Therefore, by setting $\tau = 0$ in (A.54), we get the covariance matrix of w .

$$\Sigma_w = \frac{1}{2\pi} \int_{-\infty}^{\infty} S_{ww}(\omega) d\omega \quad (\text{A.55})$$

Likewise, when the spectral density functions are available, Eq. A.55 provides us with an alternative way of calculating the mean-square values of w , as follow

$$\sigma_{w_i}^2 = (\Sigma_{ww})_{i,i} = \frac{1}{2\pi} \int_{-\infty}^{\infty} [S_{ww}(\omega)]_{i,i} d\omega \quad (\text{A.56})$$

where the diagonal elements of the spectral density function matrix ($[S_{ww}(\omega)]_{i,i}$) are referred to as the *power spectral densities* (PSD's). For the frequency expressed in Hz, the equivalent expression is given by

$$\sigma_{w_i}^2 = \int_{-\infty}^{\infty} [S_{ww}(f)]_{i,i} df \quad (\text{A.57})$$

where $\omega = 2\pi f$. The interpretation of the above expression is that the variance of a random signal is equal to the area under the PSD curve. This is a powerful result that is used a lot in frequency-domain analysis.

Appendix B

HASSELMAN'S DATABASES

The following databases, as described in Chapter 3, were reproduced from [Hasselmann & Chrostowski, 1991]. They represent two types of generically similar structures, namely large space structures in launch configuration (LSS, Section B.1), and conventional space structures (CSS, Section B.2) as well as a combined set of structures from LSS and CSS (COMB, Section B.3). The singular values for these four databases are listed in Table B.3 (Section B.4).

The databases are presented in the form of the correlation matrix of the modal mass matrix elements, ρ_{mm} , the correlation matrix of the normalized modal stiffness matrix elements, $\rho_{\hat{k}\hat{k}}$, and the cross-correlation matrix of modal mass and normalized modal stiffness matrix elements, $\rho_{m\hat{k}}$.

$$\rho_{\hat{p}\hat{p}} = \begin{bmatrix} \rho_{mm} & \rho_{m\hat{k}} \\ \rho_{m\hat{k}}^T & \rho_{\hat{k}\hat{k}} \end{bmatrix} \quad (\text{B.1})$$

The covariance matrix, $\Sigma_{\hat{p}\hat{p}}$, of the modal mass and normalized modal stiffness matrix elements can be obtained by constructing the correlation matrix $\rho_{\hat{p}\hat{p}}$ as follows

$$\Sigma_{\hat{p}\hat{p}} = \sigma_{\hat{p}} \rho_{\hat{p}\hat{p}} \sigma_{\hat{p}} \quad (\text{B.2})$$

where the standard deviations form the elements of the diagonal (square) matrix $\sigma_{\hat{p}}$.

B.1 LSS database (research models)

The seven structures from which the data sets were obtained to compile the LSS database are listed in Table B.1.

TABLE B.1 Structures in LSS Database.

Structure No.	Description	Source	No. Modes	Frequency Range (HZ)
LSS 1	LaRC Minimast 3-Longeron Deployable Truss Beam	NASA Langley Research Center	5	0.85 - 6.11
LSS 2	LaRC Ten Bay 4-Longeron Cantilever Erectable Truss Beam	NASA Langley Research Center	9	18.05 - 200.20
LSS 3	JPL 4-Longeron Cantilever Precision Truss Structure	Jet Propulsion Laboratory	4	8.31 - 35.53
LSS 4	JPL 3-Longeron Cantilever Tetrahedral Bay Truss Beam	Jet Propulsion Laboratory	5	10.61 - 71.83
LSS 5	JPL 3-Longeron Pre-Free Tetrahedral Bay Truss Beam	Jet Propulsion Laboratory	6	17.94 - 69.17
LSS 6	PACOSS Free-Free Dynamic Test Article (DTA)	Martin Marietta Corporation	22	1.03 - 9.26
LSS 7	PACOSS Cantilevered Solar Array (Substructure of DTA)	Martin Marietta Corporation	9	0.93 - 16.6

The number of modes indicated are the number of analysis-test mode pairs in the frequency range indicated, beginning with fundamental mode.

Standard Deviation Vectors:

$$\sigma_m =$$

0.185 0.183 0.248 0.214 0.104 0.140 0.136 0.235 0.269 0.151 0.191 0.100 0.330 0.143 0.290

$$\sigma_{\hat{k}} =$$

0.271 0.175 0.353 0.098 0.230 0.214 0.204 0.159 0.316 0.165 0.194 0.123 0.296 0.142 0.230

Correlation Matrices: $\rho_{mm} =$

1.000	-.327	-.339	-.119	0.483	0.841	-.108	-.181	0.152	0.187	0.127	0.282	0.295	-.095	0.315
-.327	1.000	-.427	0.162	-.631	0.189	-.438	0.349	-.374	0.328	0.318	-.113	-.113	-.685	-.337
-.339	-.427	1.000	0.047	0.109	-.647	0.734	0.005	0.262	-.869	-.733	-.264	0.050	0.078	0.164
-.119	0.162	0.047	1.000	-.789	-.227	0.453	0.963	-.936	-.483	-.660	0.246	-.831	0.201	-.848
0.483	-.631	0.109	-.789	1.000	0.272	-.045	-.872	0.880	0.167	0.282	0.134	0.768	0.070	0.789
0.841	0.189	-.647	-.227	0.272	1.000	-.515	-.174	0.103	0.530	0.493	0.134	0.341	-.447	0.268
-.108	-.438	0.734	0.453	-.045	-.515	1.000	0.289	-.142	-.871	-.923	0.341	-.097	0.189	-.116
-.181	0.349	0.005	0.963	-.872	-.174	0.289	1.000	-.938	-.428	-.561	0.102	-.854	0.044	-.889
0.152	-.374	0.262	-.936	0.880	0.103	-.142	-.938	1.000	0.160	0.358	-.203	0.861	-.167	0.894
0.187	0.328	-.869	-.483	0.167	0.530	-.871	-.428	0.160	1.000	0.959	-.009	0.260	-.079	0.223
0.127	0.318	-.733	-.660	0.282	0.493	-.923	-.561	0.358	0.959	1.000	-.163	0.377	-.171	0.348
0.282	-.113	-.264	0.246	0.134	0.134	0.341	0.102	-.203	-.009	-.163	1.000	0.056	0.083	-.262
0.295	-.113	0.050	-.831	0.768	0.341	-.097	-.854	0.861	0.260	0.377	0.056	1.000	-.470	0.895
-.095	-.685	0.078	0.201	0.070	-.447	0.189	0.044	-.167	-.079	-.171	0.083	-.470	1.000	-.225
0.315	-.337	0.164	-.848	0.789	0.268	-.116	-.889	0.894	0.223	0.348	-.262	0.895	-.225	1.000

 $\rho_{\hat{k}\hat{k}} =$

1.000	-.372	-.652	0.381	0.843	0.912	0.390	-.670	0.001	0.049	0.220	0.298	0.407	-.082	0.398
-.372	1.000	0.060	-.146	-.239	-.262	-.489	0.302	-.057	0.455	0.106	-.186	-.110	-.729	-.450
-.652	0.060	1.000	-.321	-.575	-.602	0.255	0.740	0.122	-.509	-.739	-.273	-.036	0.064	0.022
0.381	-.146	-.321	1.000	0.502	0.307	0.596	0.119	-.432	-.518	-.360	0.446	-.611	0.232	-.608;
0.843	-.239	-.575	0.502	1.000	0.812	0.451	-.632	0.024	-.149	0.121	0.283	0.228	-.272	0.174
0.912	-.262	-.602	0.307	0.812	1.000	0.398	-.554	-.289	0.133	0.191	0.584	0.532	-.292	0.420
0.390	-.489	0.255	0.596	0.451	0.398	1.000	0.240	-.283	-.827	-.772	0.432	-.036	0.199	0.044
-.670	0.302	0.740	0.119	-.632	-.554	0.240	1.000	-.426	-.413	-.759	0.131	-.449	0.096	-.507
0.001	-.057	0.122	-.432	0.024	-.289	-.283	-.426	1.000	0.026	0.237	-.923	0.188	0.026	0.348
0.049	0.455	-.509	-.518	-.149	0.133	-.827	-.413	0.026	1.000	0.842	-.063	0.399	-.423	0.209
0.220	0.106	-.739	-.360	0.121	0.191	-.772	-.759	0.237	0.842	1.000	-.153	0.273	-.160	0.234
0.298	-.186	-.273	0.446	0.283	0.584	0.432	0.131	-.923	-.063	-.153	1.000	0.044	-.043	-.079
0.407	-.110	-.036	-.611	0.228	0.532	-.036	-.449	0.188	0.399	0.273	0.044	1.000	-.450	0.914
-.082	-.729	0.064	0.232	-.272	-.292	0.199	0.096	0.026	-.423	-.160	-.043	-.450	1.000	-.080
0.398	-.450	0.022	-.608	0.174	0.420	0.044	-.507	0.348	0.209	0.234	-.079	0.914	-.080	1.000

$$\rho_{m\hat{k}} =$$

0.945	-.393	-.605	0.489	0.959	0.847	0.479	-.677	0.074	-.142	0.137	0.248	0.273	-.093	0.286
-.263	0.956	-.190	-.150	-.196	-.147	-.630	0.127	-.126	0.657	0.349	-.092	-.074	-.691	-.416
-.438	-.166	0.944	-.242	-.315	-.421	0.452	0.550	0.225	-.666	-.768	-.257	0.066	0.130	0.181
-.134	0.256	0.165	0.735	-.111	-.169	0.408	0.691	-.486	-.450	-.621	0.259	-.717	0.163	-.788
0.432	-.685	-.153	-.293	0.453	0.471	0.200	-.647	0.248	-.051	0.244	0.104	0.639	0.072	0.798
0.826	0.061	-.801	0.279	0.858	0.767	-.003	-.784	0.133	0.334	0.514	0.106	0.314	-.436	0.177
-.115	-.242	0.697	0.222	-.125	0.002	0.794	0.693	-.391	-.717	-.929	0.366	-.007	0.151	0.024
-.234	0.452	0.148	0.674	-.124	-.277	0.239	0.657	-.366	-.355	-.521	0.106	-.767	0.016	-.884
0.122	-.383	0.086	-.683	0.153	0.175	-.113	-.541	0.477	0.149	0.311	-.218	0.749	-.133	0.854
0.317	0.056	-.824	-.225	0.131	0.284	-.697	-.718	0.082	0.841	0.970	-.009	0.223	-.070	0.184
0.205	0.080	-.713	-.396	0.110	0.175	-.773	-.767	0.266	0.831	0.998	-.174	0.294	-.148	0.268
0.307	-.206	-.297	0.479	0.331	0.587	0.443	0.097	-.905	-.094	-.143	0.996	0.014	-.038	-.100
0.361	-.159	-.086	-.612	0.300	0.515	-.071	-.541	0.203	0.374	0.349	0.064	0.961	-.457	0.892
-.089	-.732	0.044	0.284	-.258	-.255	0.233	0.132	-.094	-.435	-.180	0.070	-.475	0.991	-.122
0.388	-.359	-.007	-.641	0.228	0.366	-.049	-.600	0.523	0.242	0.312	-.254	0.896	-.165	0.973

B.2 CSS database (for pretest and posttest models)

Table B.2 lists the eleven conventional space structures from which the data were extracted to compute the CSS the databases. Neither the structures nor the source of data are identified at the request of the contributors who considered the data proprietary.

The number of modes indicated are the number of analysis-test mode pairs in the frequency range indicated, beginning with fundamental mode. In this case case, some of the analysis modes were omitted because a test mode was not found to correlate with it. For the most part, the frequency range for the paired modes, where no analysis modes were skipped, represents the range of paired modes having cross-orthogonality of at least 0.50. The resulting databases for the the pretest modesI (CSS-I), and the posttest models (CSS-II) are reproduced in the following two subsections.

TABLE B.2 Structures in CSS Database.

Structure No.	No. Modes Pretest Model	Frequency Range (HZ)	No. Modes Posttest Model	Frequency Range (HZ)
CSS 1	9	13.71 - 23.58	N/A	
CSS 2	5	16.27 - 52.70	5	16.27 - 52.70
CSS 3	6	14.49 - 49.97	6	14.49 - 49.97
CSS 4	6	14.45 - 50.29	N/A	
CSS 5	9	29.38 - 95.99	9	29.38 - 95.99
CSS 6	5	15.11 - 27.35	N/A	
CSS 7	N/A		34	7.04 - 46.50
CSS 8	N/A		4	41.64 - 93.77
CSS 9	N/A		14	5.84 - 24.51
CSS 10	N/A		12	12.50 - 35.67
CSS 11	16	16.15 - 46.60	27	16.15 - 50.76

B.2.1 Pretest Models Database (CSS I)

Standard Deviation Vectors:

$$\sigma_m = [];$$

0.097 0.084 0.137 0.096 0.134 0.117 0.131 0.116 0.062 0.383 0.094 0.109 0.467 0.177 0.278

$$\sigma_{\hat{k}} = [];$$

0.193 0.104 0.196 0.072 0.072 0.287 0.133 0.122 0.073 0.634 0.096 0.125 0.407 0.175 0.320

Correlation Matrices:

$$\rho_{mm} = [];$$

1.000	-.707	-.256	0.288	0.046	0.953	0.821	-.644	-.376	0.792	0.724	0.625	0.874	0.120	0.429
-.707	1.000	0.140	-.533	-.179	-.608	-.834	0.739	0.500	-.386	-.526	-.798	-.751	-.287	-.284
-.256	0.140	1.000	0.305	0.482	-.249	-.043	0.004	-.368	-.109	-.585	0.013	-.330	0.465	-.514
0.288	-.533	0.305	1.000	0.699	0.139	0.661	-.624	-.937	0.002	-.131	0.851	0.153	0.766	-.631
0.046	-.179	0.482	0.699	1.000	0.000	0.254	-.508	-.867	0.138	-.609	0.417	0.044	0.987	-.683
0.953	-.608	-.249	0.139	0.000	1.000	0.634	-.434	-.264	0.919	0.656	0.416	0.780	0.032	0.530
0.821	-.834	-.043	0.661	0.254	0.634	1.000	-.878	-.643	0.381	0.566	0.941	0.781	0.383	0.049
-.644	0.739	0.004	-.624	-.508	-.434	-.878	1.000	0.702	-.274	-.284	-.859	-.766	-.625	0.090
-.376	0.500	-.368	-.937	-.867	-.264	-.643	0.702	1.000	-.224	0.223	-.782	-.265	-.911	0.597
0.792	-.386	-.109	0.002	0.138	0.919	0.381	-.274	-.224	1.000	0.378	0.164	0.651	0.115	0.477
0.724	-.526	-.585	-.131	-.609	0.656	0.566	-.284	0.223	0.378	1.000	0.351	0.686	-.515	0.721
0.625	-.798	0.013	0.851	0.417	0.416	0.941	-.859	-.782	0.164	0.351	1.000	0.586	0.540	-.221
0.874	-.751	-.330	0.153	0.044	0.780	0.781	-.766	-.265	0.651	0.686	0.586	1.000	0.136	0.526
0.120	-.287	0.465	0.766	0.987	0.032	0.383	-.625	-.911	0.115	-.515	0.540	0.136	1.000	-.669
0.429	-.284	-.514	-.631	-.683	0.530	0.049	0.090	0.597	0.477	0.721	-.221	0.526	-.669	1.000

$$\rho_{\hat{k}\hat{k}} = [];$$

1.000	-.453	0.025	0.005	0.089	0.675	0.402	-.124	-.259	0.700	0.436	0.261	0.437	0.022	0.562
-.453	1.000	0.040	-.579	-.555	-.077	-.898	0.390	0.293	-.366	-.591	-.744	-.712	-.294	-.015
0.025	0.040	1.000	-.033	0.042	-.188	-.160	0.172	-.304	0.024	-.362	0.274	-.223	0.299	-.263
0.005	-.579	-.033	1.000	0.840	-.077	0.595	0.157	-.600	0.021	-.029	0.761	0.295	0.765	-.404
0.089	-.555	0.042	0.840	1.000	-.065	0.630	-.276	-.630	-.042	-.119	0.834	0.304	0.919	-.443
0.675	-.077	-.188	-.077	-.065	1.000	-.098	0.109	0.238	0.889	-.039	-.257	0.488	-.059	0.868
0.402	-.898	-.160	0.595	0.630	-.098	1.000	-.487	-.413	0.127	0.688	0.817	0.613	0.334	-.156
-.124	0.390	0.172	0.157	-.276	0.109	-.487	1.000	-.159	0.049	-.386	-.249	-.427	-.025	-.003
-.259	0.293	-.304	-.600	-.630	0.238	-.413	-.159	1.000	0.264	0.066	-.776	0.288	-.717	0.603
0.700	-.366	0.024	0.021	-.042	0.889	0.127	0.049	0.264	1.000	0.173	-.062	0.716	-.090	0.850
0.436	-.591	-.362	-.029	-.119	-.039	0.688	-.386	0.066	0.173	1.000	0.231	0.486	-.440	0.228
0.261	-.744	0.274	0.761	0.834	-.257	0.817	-.249	-.776	-.062	0.231	1.000	0.267	0.734	-.512
0.437	-.712	-.223	0.295	0.304	0.488	0.613	-.427	0.288	0.716	0.486	0.267	1.000	0.031	0.535
0.022	-.294	0.299	0.765	0.919	-.059	0.334	-.025	-.717	-.090	-.440	0.734	0.031	1.000	-.510
0.562	-.015	-.263	-.404	-.443	0.868	-.156	-.003	0.603	0.850	0.228	-.512	0.535	-.510	1.000

$$\rho_{m\hat{k}} = [];$$

0.654	-0.762	-0.409	0.444	0.408	0.411	0.825	-0.329	-0.122	0.541	0.703	0.473	0.813	0.106	0.368
-0.440	0.989	0.016	-0.539	-0.493	-0.118	-0.831	0.333	0.271	-0.404	-0.556	-0.691	-0.679	-0.253	-0.057
0.310	0.146	0.847	0.015	0.193	0.171	-0.194	0.194	-0.434	0.197	-0.495	0.255	-0.196	0.483	-0.080
0.180	-0.571	0.298	0.764	0.788	-0.334	0.658	-0.037	-0.919	-0.220	0.079	0.951	-0.011	0.772	-0.647
-0.038	-0.213	0.287	0.759	0.883	-0.018	0.234	0.061	-0.658	-0.072	-0.533	0.649	0.007	0.991	-0.478
0.702	-0.636	-0.469	0.395	0.278	0.616	0.638	-0.111	-0.045	0.682	0.593	0.286	0.774	0.029	0.546
0.482	-0.901	-0.019	0.563	0.622	-0.038	0.984	-0.482	-0.418	0.219	0.659	0.836	0.648	0.356	-0.103
-0.210	0.813	-0.005	-0.627	-0.822	0.086	-0.869	0.633	0.326	-0.118	-0.328	-0.819	-0.651	-0.584	0.226
-0.227	0.550	-0.229	-0.854	-0.927	0.103	-0.629	0.055	0.850	0.046	0.073	-0.920	-0.148	-0.915	0.504
0.592	-0.407	-0.409	0.417	0.264	0.768	0.369	0.115	0.043	0.766	0.264	0.116	0.715	0.117	0.623
0.418	-0.553	-0.473	-0.104	-0.197	0.126	0.596	-0.408	0.294	0.320	0.963	0.059	0.614	-0.539	0.427
0.298	-0.856	0.094	0.678	0.723	-0.273	0.943	-0.384	-0.625	-0.031	0.503	0.951	0.407	0.519	-0.406
0.355	-0.804	-0.313	0.424	0.416	0.281	0.779	-0.488	0.156	0.521	0.605	0.419	0.959	0.088	0.330
-0.001	-0.329	0.307	0.774	0.931	-0.074	0.359	-0.061	-0.682	-0.079	-0.424	0.747	0.078	0.997	-0.509
0.293	-0.243	-0.440	-0.336	-0.484	0.531	0.056	-0.145	0.741	0.648	0.526	-0.450	0.631	-0.697	0.833

B.2.2 Posttest Models Database (CSS II)

Standard Deviation Vectors:

$$\sigma_m = [];$$

0.125	0.143	0.042	0.044	0.048	0.132	0.036	0.043	0.030	0.153	0.061	0.105	0.336	0.096	0.297
-------	-------	-------	-------	-------	-------	-------	-------	-------	-------	-------	-------	-------	-------	-------

$$\sigma_{\hat{k}} = [];$$

0.163	0.142	0.040	0.049	0.100	0.175	0.023	0.023	0.047	0.233	0.074	0.096	0.383	0.111	0.316
-------	-------	-------	-------	-------	-------	-------	-------	-------	-------	-------	-------	-------	-------	-------

Correlation Matrices:

$$\rho_{mm} = [];$$

1.000	-.167	0.043	0.426	-.631	0.905	0.161	0.118	-.233	0.868	-.902	-.951	0.653	-.700	0.846
-.167	1.000	-.793	-.101	-.296	-.427	-.968	0.374	-.491	-.514	0.069	0.088	-.086	0.518	-.131
0.043	-.793	1.000	-.016	0.423	0.317	0.777	-.293	0.492	0.412	0.072	0.116	0.145	-.661	0.175
0.426	-.101	-.016	1.000	-.813	0.585	0.119	0.713	0.511	0.356	-.243	-.597	0.498	-.327	0.468
-.631	-.296	0.423	-.813	1.000	-.604	0.301	-.766	-.081	-.386	0.451	0.767	-.659	0.235	-.654
0.905	-.427	0.317	0.585	-.604	1.000	0.412	0.232	0.190	0.942	-.676	-.860	0.798	-.849	0.911
0.161	-.968	0.777	0.119	0.301	0.412	1.000	-.450	0.489	0.467	-.112	-.122	0.036	-.550	0.097
0.118	0.374	-.293	0.713	-.766	0.232	-.450	1.000	0.396	0.035	0.160	-.220	0.563	0.014	0.398
-.233	-.491	0.492	0.511	-.081	0.190	0.489	0.396	1.000	0.070	0.518	0.157	0.323	-.262	0.114
0.868	-.514	0.412	0.356	-.386	0.942	0.467	0.035	0.070	1.000	-.666	-.743	0.689	-.821	0.847
-.902	0.069	0.072	-.243	0.451	-.676	-.112	0.160	0.518	-.666	1.000	0.880	-.282	0.509	-.553
-.951	0.088	0.116	-.597	0.767	-.860	-.122	-.220	0.157	-.743	0.880	1.000	-.599	0.589	-.764
0.653	-.086	0.145	0.498	-.659	0.798	0.036	0.563	0.323	0.689	-.282	-.599	1.000	-.692	0.946
-.700	0.518	-.661	-.327	0.235	-.849	-.550	0.014	-.262	-.821	0.509	0.589	-.692	1.000	-.794
0.846	-.131	0.175	0.468	-.654	0.911	0.097	0.398	0.114	0.847	-.553	-.764	0.946	-.794	1.000

$$\rho_{\hat{k}\hat{k}} = [];$$

1.000	-.048	-.088	-.113	-.376	0.849	-.393	-.419	-.090	0.783	-.558	-.622	0.732	-.809	0.764
-.048	1.000	-.819	-.009	-.111	-.270	-.141	0.548	-.494	-.285	0.087	0.013	-.124	0.289	-.128
-.088	-.819	1.000	-.345	0.342	0.158	-.035	-.524	0.555	0.268	0.450	0.464	0.130	-.204	-.029
-.113	-.009	-.345	1.000	-.459	0.115	0.786	0.281	-.757	0.114	-.367	-.639	0.231	0.331	0.345
-.376	-.111	0.342	-.459	1.000	-.345	-.247	-.133	0.522	-.322	0.360	0.574	-.382	-.204	-.282
0.849	-.270	0.158	0.115	-.345	1.000	-.139	-.414	-.233	0.971	-.388	-.600	0.920	-.725	0.938
-.393	-.141	-.035	0.786	-.247	-.139	1.000	-.072	-.538	-.085	-.012	-.223	-.016	0.492	0.029
-.419	0.548	-.524	0.281	-.133	-.414	-.072	1.000	-.382	-.399	0.157	0.055	-.233	0.595	-.278
-.090	-.494	0.555	-.757	0.522	-.233	-.538	-.382	1.000	-.282	0.101	0.505	-.471	-.285	-.457
0.783	-.285	0.268	0.114	-.322	0.971	-.085	-.399	-.282	1.000	-.201	-.482	0.973	-.649	0.912
-.558	0.087	0.450	-.367	0.360	-.388	-.012	0.157	0.101	-.201	1.000	0.879	-.155	0.452	-.448
-.622	0.013	0.464	-.639	0.574	-.600	-.223	0.055	0.505	-.482	0.879	1.000	-.508	0.365	-.714
0.732	-.124	0.130	0.231	-.382	0.920	-.016	-.233	-.471	0.973	-.155	-.508	1.000	-.528	0.917
-.809	0.289	-.204	0.331	-.204	-.725	0.492	0.595	-.285	-.649	0.452	0.365	-.528	1.000	-.660
0.764	-.128	-.029	0.345	-.282	0.938	0.029	-.278	-.457	0.912	-.448	-.714	0.917	-.660	1.000

$$\rho_{m\hat{k}} = [];$$

0.784	-.139	-.306	0.422	-.558	0.743	0.016	-.211	-.308	0.612	-.883	-.955	0.585	-.556	0.767
-.083	0.992	-.786	0.058	-.124	-.253	-.058	0.561	-.574	-.246	0.152	0.024	-.069	0.335	-.095
0.121	-.796	0.764	-.202	0.558	0.326	-.175	-.462	0.530	0.346	0.003	0.091	0.205	-.579	0.269
-.090	-.170	-.177	0.956	-.427	0.196	0.666	0.334	-.661	0.210	-.320	-.604	0.313	0.270	0.390
-.272	-.247	0.539	-.848	0.743	-.384	-.464	-.360	0.879	-.369	0.444	0.780	-.511	-.162	-.549
0.670	-.440	0.041	0.515	-.473	0.832	0.192	-.311	-.301	0.761	-.689	-.855	0.718	-.531	0.847
0.026	-.963	0.727	0.018	0.204	0.194	0.206	-.649	0.530	0.176	-.202	-.056	0.001	-.330	0.088
-.064	0.284	-.259	0.647	-.441	0.192	0.326	0.638	-.820	0.293	0.159	-.269	0.478	0.383	0.348
-.356	-.596	0.668	0.386	0.115	0.093	0.555	-.099	-.142	0.248	0.435	0.179	0.258	0.220	0.131
0.717	-.500	0.142	0.257	-.377	0.863	-.051	-.384	-.049	0.756	-.670	-.736	0.656	-.652	0.793
-.645	0.002	0.495	-.304	0.405	-.440	0.053	0.177	0.131	-.255	0.989	0.883	-.214	0.494	-.485
-.604	0.077	0.417	-.642	0.642	-.580	-.284	0.123	0.472	-.463	0.878	0.988	-.475	0.319	-.665
0.666	-.149	0.063	0.432	-.489	0.888	0.165	-.182	-.583	0.933	-.241	-.621	0.975	-.416	0.920
-.650	0.530	-.272	-.247	-.020	-.802	-.049	0.535	0.061	-.763	0.526	0.619	-.686	0.791	-.842
0.789	-.161	-.060	0.414	-.482	0.942	0.064	-.232	-.485	0.910	-.516	-.791	0.917	-.576	0.972

B.3 Combined LSS and CSS Database (COMB)

The database reproduced below was obtained by combining the data from the three databases describe precedently (LSS, CSS-I, and CSS-II).

Standard Deviation Vectors:

$$\sigma_m = [];$$

0.138	0.140	0.160	0.133	0.102	0.129	0.109	0.148	0.153	0.257	0.124	0.105	0.386	0.142	0.289
-------	-------	-------	-------	-------	-------	-------	-------	-------	-------	-------	-------	-------	-------	-------

$$\sigma_{\hat{k}} = [];$$

0.211	0.142	0.227	0.075	0.145	0.231	0.137	0.114	0.181	0.410	0.128	0.115	0.368	0.145	0.294
-------	-------	-------	-------	-------	-------	-------	-------	-------	-------	-------	-------	-------	-------	-------

Correlation Matrices:

$$\rho_{mm} = [];$$

1.000	-.330	-.262	0.019	0.119	0.870	0.204	-.229	0.056	0.497	0.074	-.033	0.543	-.152	0.505
-.330	1.000	-.309	0.009	-.351	-.190	-.534	0.377	-.250	-.153	0.121	-.185	-.255	-.219	-.238
-.262	-.309	1.000	0.101	0.261	-.361	0.431	-.003	0.178	-.262	-.655	-.102	-.088	0.168	-.055
0.019	0.009	0.101	1.000	-.197	-.017	0.477	0.638	-.881	-.111	-.530	0.269	-.246	0.313	-.511
0.119	-.351	0.261	-.197	1.000	-.012	0.140	-.643	0.308	0.087	-.044	0.366	0.131	0.614	-.173
0.870	-.190	-.361	-.017	-.012	1.000	0.081	-.173	0.038	0.733	0.285	-.129	0.642	-.338	0.584
0.204	-.534	0.431	0.477	0.140	0.081	1.000	-.131	-.191	0.079	-.357	0.517	0.369	0.227	-.012
-.229	0.377	-.003	0.638	-.643	-.173	-.131	1.000	-.701	-.229	-.464	-.220	-.553	-.191	-.361
0.056	-.250	0.178	-.881	0.308	0.038	-.191	-.701	1.000	0.005	0.333	-.207	0.363	-.261	0.564
0.497	-.153	-.262	-.111	0.087	0.733	0.079	-.229	0.005	1.000	0.341	-.067	0.575	-.055	0.460
0.074	0.121	-.655	-.530	-.044	0.285	-.357	-.464	0.333	0.341	1.000	0.176	0.329	-.190	0.249
-.033	-.185	-.102	0.269	0.366	-.129	0.517	-.220	-.207	-.067	0.176	1.000	0.090	0.407	-.428
0.543	-.255	-.088	-.246	0.131	0.642	0.369	-.553	0.363	0.575	0.329	0.090	1.000	-.192	0.743
-.152	-.219	0.168	0.313	0.614	-.338	0.227	-.191	-.261	-.055	-.190	0.407	-.192	1.000	-.541
0.505	-.238	-.055	-.511	-.173	0.584	-.012	-.361	0.564	0.460	0.249	-.428	0.743	-.541	1.000

$$\rho_{\hat{k}\hat{k}} = [];$$

1.000	-.292	-.389	0.175	0.457	0.770	0.331	-.426	-.039	0.475	0.146	0.072	0.488	-.190	0.538
-.292	1.000	-.008	-.218	-.238	-.187	-.502	0.303	-.051	-.135	-.036	-.278	-.281	-.278	-.183
-.389	-.008	1.000	-.221	-.403	-.324	0.129	0.531	0.071	-.075	-.589	-.022	-.080	0.129	-.080
0.175	-.218	-.221	1.000	0.382	0.100	0.575	0.136	-.427	-.057	-.272	0.345	-.029	0.460	-.251
0.457	-.238	-.403	0.382	1.000	0.279	0.414	-.475	0.008	-.084	0.121	0.417	0.049	0.029	-.093
0.770	-.187	-.324	0.100	0.279	1.000	0.117	-.187	-.114	0.760	0.009	-.082	0.608	-.258	0.769
0.331	-.502	0.129	0.575	0.414	0.117	1.000	-.029	-.285	-.084	-.347	0.496	0.216	0.245	-.041
-.426	0.303	0.531	0.136	-.475	-.187	-.029	1.000	-.344	-.057	-.583	-.039	-.345	0.061	-.188
-.039	-.051	0.071	-.427	0.008	-.114	-.285	-.344	1.000	0.049	0.201	-.599	0.080	-.129	0.191
0.475	-.135	-.075	-.057	-.084	0.760	-.084	-.057	0.049	1.000	0.201	-.125	0.669	-.208	0.715
0.146	-.036	-.589	-.272	0.121	0.009	-.347	-.583	0.201	0.201	1.000	0.139	0.208	-.140	0.051
0.072	-.278	-.022	0.345	0.417	-.082	0.496	-.039	-.599	-.125	0.139	1.000	-.031	0.404	-.456
0.488	-.281	-.080	-.029	0.049	0.608	0.216	-.345	0.080	0.669	0.208	-.301	1.000	-.239	0.756
-.190	-.278	0.129	0.460	0.029	-.258	0.245	0.061	-.129	-.208	-.140	0.404	-.239	1.000	-.442
0.538	-.183	-.080	-.251	-.093	0.769	-.041	-.188	0.191	0.715	0.051	-.456	0.756	-.442	1.000

$$\rho_{m\hat{k}} = [1];$$

0.829	-0.378	-0.483	0.453	0.537	0.620	0.484	-0.481	0.015	0.293	0.052	-0.021	0.502	-0.140	0.449
-0.239	0.970	-0.163	-0.173	-0.203	-0.152	-0.539	0.185	-0.116	-0.077	0.152	-0.188	-0.206	-0.238	-0.177
-0.168	-0.137	0.914	-0.156	-0.167	-0.094	0.252	0.410	0.143	-0.015	-0.651	-0.037	-0.021	0.180	0.066
-0.049	0.026	0.186	0.728	-0.019	-0.164	0.468	0.463	-0.525	-0.161	-0.462	0.338	-0.244	0.337	-0.428
0.119	-0.372	0.058	0.129	0.506	0.075	0.183	-0.258	0.046	-0.092	-0.029	0.467	0.073	0.553	-0.147
0.733	-0.282	-0.529	0.361	0.366	0.698	0.206	-0.414	0.042	0.533	0.250	-0.121	0.620	-0.272	0.558
0.132	-0.499	0.412	0.338	0.072	-0.002	0.843	0.129	-0.311	0.046	-0.332	0.520	0.297	0.206	-0.029
-0.201	0.458	0.104	0.300	-0.236	-0.078	-0.056	0.635	-0.291	-0.101	-0.434	-0.212	-0.441	-0.155	-0.224
0.035	-0.233	0.051	-0.575	0.068	0.108	-0.169	-0.392	0.488	0.051	0.274	-0.254	0.313	-0.214	0.439
0.469	-0.248	-0.404	0.193	0.051	0.679	0.003	-0.128	0.032	0.765	0.281	-0.064	0.585	-0.042	0.554
0.138	-0.062	-0.607	-0.303	0.102	0.059	-0.376	-0.605	0.253	0.262	0.989	0.058	0.252	-0.175	0.131
0.048	-0.275	-0.077	0.272	0.435	-0.122	0.505	-0.102	-0.502	-0.121	0.251	0.969	-0.006	0.302	-0.433
0.415	-0.347	-0.146	0.053	0.107	0.476	0.302	-0.427	0.072	0.543	0.285	0.052	0.957	-0.167	0.632
-0.154	-0.251	0.125	0.399	0.076	-0.255	0.253	0.053	-0.166	-0.208	-0.148	0.499	-0.246	0.956	-0.483
0.462	-0.252	-0.135	-0.266	-0.092	0.582	0.000	-0.322	0.333	0.554	0.168	-0.484	0.796	-0.491	0.911

B.4 Database comparison

Table B.3 compares the eigenvalues of the four covariance matrices obtained by singular values decomposition (SVD) of the covariance matrices. The rank of the matrices in general equals the number of structures in the database, as confirmed by the number of non-zero eigenvalues.

TABLE B.3 Eigenvalues of Covariance Matrices.

LSS Research Models	CSS Pretest Models	CSS Posttest Models	Combined LSS and CSS
Matrix Rank = 6	Matrix Rank = 7	Matrix Rank = 7	Matrix Rank = 20
s.v.#1 = 0.569675	s.v.#1 = 0.933333	s.v.#1 = 0.582411	s.v.#1 = 0.599062
s.v.#2 = 0.337463	s.v.#2 = 0.293328	s.v.#2 = 0.0590164	s.v.#2 = 0.125285
s.v.#3 = 0.226366	s.v.#3 = 0.170940	s.v.#3 = 0.0466032	s.v.#3 = 0.120427
s.v.#4 = 0.125469	s.v.#4 = 0.0752265	s.v.#4 = 0.0279430	s.v.#4 = 0.110258
s.v.#5 = 0.0888634	s.v.#5 = 0.0427559	s.v.#5 = 0.0136299	s.v.#5 = 0.0693005
s.v.#6 = 0.0303972	s.v.#6 = 0.0219202	s.v.#6 = 0.00339969	s.v.#6 = 0.0581739
0.0	s.v.#7 = 0.0102209	s.v.#7 = 0.00122147	s.v.#7 = 0.0324544
0.0	0.0	0.0	s.v.#8 = 0.0239023
0.0	0.0	0.0	s.v.#9 = 0.0236756
0.0	0.0	0.0	s.v.#10 = 0.0157983
0.0	0.0	0.0	s.v.#11 = 0.0103530
0.0	0.0	0.0	s.v.#12 = 0.00622819
0.0	0.0	0.0	s.v.#13 = 0.00535949
0.0	0.0	0.0	s.v.#14 = 0.00414099
0.0	0.0	0.0	s.v.#15 = 0.00365832
0.0	0.0	0.0	s.v.#16 = 0.00239505
0.0	0.0	0.0	s.v.#17 = 0.00091741
0.0	0.0	0.0	s.v.#18 = 0.00037091
0.0	0.0	0.0	s.v.#19 = 0.00026105
0.0	0.0	0.0	s.v.#20 = 0.00013077
0.0	0.0	0.0	0.0
Trace = 1.377	Trace = 1.547	Trace = 0.734	Trace = 1.210

Appendix C

SIMONIAN'S DAMPING COMPILATION

The following compilation of damping data as described in Chapter 3, was taken from [Simonian, 1987]. Table C.1 lists the twenty-three spacecrafts from which the data was collected.

TABLE C.1 Satellites Surveyed^a

Vehicle		
Intelsat IV (in-orbit data)	HERMES (in-orbit data)	M35 Phase II upgrade
Space Teles. Metering Truss	Intelsat IV-A	M35 Phase I
Ranger III STM	Skylab	M35 Phase II
SEASAT	Apollo-Saturn V, 1/10 scale	FLTSATCOM
Hughes Satellite	Nimbus	OGO-3 (in-orbit data)
Hughes Satellite	ATS-F	OSO-8 (in-orbit data)
Hughes Satellite	777 Redesign	FRUSA (in-orbit data)
Scatha Satellite	777	

a. From [Simonian, 1987]

The computed statistical damping parameters are summarized in Table C.2. It appears that the damping ratios, ζ_r 's, distributions fit well to a lognormal and/or gamma probability density function. The statistical analysis was performed for various combinations of the data, grouped by frequency bandwidth (identified by letter, A through G in the table).

TABLE C.2 Summary of Spacecraft Measured Damping Statistics^a

Frequency Interval (Hz)	μ_{ζ} Mean (% critical)	σ_{ζ} Standard Deviation (% critical)	ρ_{ζ} COV (%)	Gamma ^b			Lognormal ^c		Number of samples
				a (%)	b	$\Gamma(b)$	c	d	
A: 0.14 - 195	1.20	0.92	76.7	0.705	1.701	0.909	-0.0488	0.680	290
B: 0.14 - 9.99	1.90	1.58	83.2	1.314	1.446	0.886	0.379	0.725	39
C: 10.00 - 19.99	0.94	0.57	60.6	0.346	2.800	1.569	-0.218	0.560	85
D: 20.00 - 29.99	1.18	0.86	72.9	0.627	1.883	0.956	-0.0475	0.653	56
E: 30.00 - 39.99	1.09	0.75	68.8	0.516	2.112	1.053	-0.108	0.623	51
F: 40.00 - 49.99	1.27	0.79	62.2	0.491	2.584	1.413	0.0755	0.572	29
G: 50.00 - 195	1.16	0.50	43.1	0.216	5.382	43.369	0.0632	0.413	30

a. From [Simonian, 1987]

b. $p(\zeta) = \frac{1}{a\Gamma(b)} \left(\frac{\zeta}{a}\right)^{b-1} \text{EXP}\left(-\frac{\zeta}{a}\right)$, $a = (\sigma_{\zeta}^2/\bar{\zeta})$, $b = (\bar{\zeta}/\sigma_{\zeta})^2$, $\Gamma(b) = \int_0^{\infty} y^{b-1} e^{-y} dy$

c. $p(\zeta) = \left(\frac{1}{\zeta d \sqrt{2\pi}}\right) \text{EXP}\left[-\frac{1}{2}\left(\frac{\ln \zeta - c}{d}\right)^2\right]$, $c = \ln(\bar{\zeta}/\sqrt{\rho_{\zeta}^2 + 1})$, $d = \sqrt{\ln(\rho_{\zeta}^2 + 1)}$, $\rho_{\zeta} = \sigma_{\zeta}/\bar{\zeta}$

Appendix D

CHAIN RULES

All the development of the next two sections can be found in [Johnson, 1985].

D.1 Derivatives and Differentials of Composite Functions

The functions to be considered in the following will be assumed to be defined in appropriate domains and to have continuous first partial derivatives, so that the corresponding differentials can be formed.

THEOREM If $z = f(x, y)$ and $x = g(t)$, $y = h(t)$, then

$$\frac{dz}{dt} = \frac{dz}{dx} \frac{dx}{dt} + \frac{dz}{dy} \frac{dy}{dt}. \quad (\text{D.1})$$

If $z = f(x, y)$ and $x = g(u, v)$, $y = h(u, v)$, then

$$\frac{dz}{du} = \frac{dz}{dx} \frac{dx}{du} + \frac{dz}{dy} \frac{dy}{du}, \quad \frac{dz}{dv} = \frac{dz}{dx} \frac{dx}{dv} + \frac{dz}{dy} \frac{dy}{dv}. \quad (\text{D.2})$$

In general, if $z = f(x, y, t, \dots)$ and $x = g(u, v, w, \dots)$, $y = h(u, v, w, \dots)$, $t = h(u, v, w, \dots)$, ..., then

$$\begin{aligned}
\frac{dz}{du} &= \frac{dz}{dx} \frac{dx}{du} + \frac{dz}{dy} \frac{dy}{du} + \frac{dz}{dt} \frac{dt}{du} + \dots, \\
\frac{dz}{dv} &= \frac{dz}{dx} \frac{dx}{dv} + \frac{dz}{dy} \frac{dy}{dv} + \frac{dz}{dt} \frac{dt}{dv} + \dots, \\
\frac{dz}{dw} &= \frac{dz}{dx} \frac{dx}{dw} + \frac{dz}{dy} \frac{dy}{dw} + \frac{dz}{dt} \frac{dt}{dw} + \dots, \\
&\dots
\end{aligned}
\tag{D.3}$$

These rules, known as "chain rules", are basic for computation of derivatives of composite functions. Equations (D.1), (D.2), and (D.3) are concise statements of the relations between the derivatives involved. Thus in (D.1),

$$z = f[g(t), h(t)]$$

is the function of t whose derivative is denoted by dz/dt , while dx/dt and dy/dt stand for $g'(t)$ and $h'(t)$, respectively. The derivatives dz/dx and dz/dy , which could be written $(dz/dx)_y$ and $(dz/dy)_x$, stand for $f_x(x, y)$ and $f_y(x, y)$. In (D.2),

$$z = f[g(u, v), h(u, v)]$$

is a function whose derivatives with respect to u is denoted by dz/du , which should be understood as $(dz/du)_v$. A more precise statement of the first equation in (D.2) would be as follows:

$$\left(\frac{dz}{du}\right)_v = \left(\frac{dz}{dx}\right)_y \left(\frac{dx}{du}\right)_v + \left(\frac{dz}{dy}\right)_x \left(\frac{dy}{du}\right)_v,$$

and similar remarks apply to the other equations.

The proof of (D.1) will be given as a sample; the other rules are proved in the same way. Let t be a fixed value and let x , y , z be the corresponding values of the functions g , h , and f . Then, for given Δt , Δx and Δy are determined as

$$\Delta x = g(t + \Delta t) - g(t), \quad \Delta y = h(t + \Delta t) - h(t),$$

while Δz is then determined as

$$\Delta z = f(x + \Delta x, y + \Delta y) - f(x, y).$$

FUNDAMENTAL LEMMA If $z = f(x,y)$ has continuous first partial derivatives in its domain D , then z has a differential

$$dz = \frac{\partial z}{\partial x} \Delta x + \frac{\partial z}{\partial y} \Delta y \quad (\text{D.4})$$

at every point (x,y) of D .

By the Fundamental Lemma, one has

$$\Delta z = \frac{\partial z}{\partial x} \Delta x + \frac{\partial z}{\partial y} \Delta y + \varepsilon_1 \Delta x + \varepsilon_2 \Delta y.$$

Hence

$$\frac{\Delta z}{\Delta t} = \frac{\partial z}{\partial x} \frac{\Delta x}{\Delta t} + \frac{\partial z}{\partial y} \frac{\Delta y}{\Delta t} + \varepsilon_1 \frac{\Delta x}{\Delta t} + \varepsilon_2 \frac{\Delta y}{\Delta t}.$$

As Δt approaches 0, $\Delta x/\Delta t$ and $\Delta y/\Delta t$ approach the derivatives dx/dt and dy/dt , respectively, while ε_1 and ε_2 approach 0, since Δx and Δy approach 0. Hence

$$\lim_{\Delta t \rightarrow 0} \frac{\Delta z}{\Delta t} = \frac{\partial z}{\partial x} \cdot \frac{dx}{dt} + \frac{\partial z}{\partial y} \cdot \frac{dy}{dt} + 0 \cdot \frac{dx}{dt} + 0 \cdot \frac{dy}{dt}$$

that is,

$$\frac{dz}{dt} = \frac{\partial z}{\partial x} \frac{dx}{dt} + \frac{\partial z}{\partial y} \frac{dy}{dt},$$

as was to be proved.

The three functions of t considered here ($x = g(t)$, $y = h(t)$ and $z = f[g(t),h(t)]$) have differentials

$$dx = \frac{dx}{dt} \Delta t, \quad dy = \frac{dy}{dt} \Delta t, \quad dz = \frac{dz}{dt} \Delta t.$$

From (D.1), one concludes that

$$\frac{dz}{dt} \Delta t = \frac{\partial z}{\partial x} \left(\frac{dx}{dt} \Delta t \right) + \frac{\partial z}{\partial y} \left(\frac{dy}{dt} \Delta t \right),$$

that is, that

$$dz = \frac{\partial z}{\partial x} dx + \frac{\partial z}{\partial y} dy. \quad (\text{D.5})$$

This is the same as (D.4) since Δx and Δy can be replaced by dx and dy , for being arbitrary increments of independent variables, in the Fundamental Lemma. Thus (D.5) holds

whether x and y are independent and dz is the corresponding differential or whether x and y , and hence dz , depend on t , so that dx , dy , dz are differentials of these variables in terms of t .

Similar reasoning applies to (D.2). Here u and v are independent variables on which x , y , and z depend. The corresponding differentials are

$$dx = \frac{\partial x}{\partial u}\Delta u + \frac{\partial x}{\partial v}\Delta v, \quad dy = \frac{\partial y}{\partial u}\Delta u + \frac{\partial y}{\partial v}\Delta v, \quad dz = \frac{\partial z}{\partial u}\Delta u + \frac{\partial z}{\partial v}\Delta v.$$

But (D.2) gives

$$\begin{aligned} dz &= \left(\frac{\partial z}{\partial x} \frac{\partial x}{\partial u} + \frac{\partial z}{\partial y} \frac{\partial y}{\partial u} \right) \Delta u + \left(\frac{\partial z}{\partial x} \frac{\partial x}{\partial v} + \frac{\partial z}{\partial y} \frac{\partial y}{\partial v} \right) \Delta v \\ &= \frac{\partial z}{\partial x} \left(\frac{\partial x}{\partial u} \Delta u + \frac{\partial x}{\partial v} \Delta v \right) + \frac{\partial z}{\partial y} \left(\frac{\partial y}{\partial u} \Delta u + \frac{\partial y}{\partial v} \Delta v \right) \\ &= \frac{\partial z}{\partial x} dx + \frac{\partial z}{\partial y} dy. \end{aligned}$$

Again (D.5) holds. Generalization of this to (D.3) permits one to conclude:

THEOREM The differential formula

$$dz = \frac{\partial z}{\partial x} dx + \frac{\partial z}{\partial y} dy + \frac{\partial z}{\partial t} dt + \dots, \quad (\text{D.6})$$

which holds when $z = f(x, y, t, \dots)$ and $dx = \Delta x$, $dy = \Delta y$, $dt = \Delta t$, ..., remain-true when x , y , t , ..., and hence z , are all functions of other independent variables and dx , dy , dt , ..., dz are the corresponding differentials.

As a consequence of this theorem, one can conclude: *Any equation in differentials that is correct for one choice of independent and dependant variables remains true for any other choice.* Another way of saying this is that any equation in differentials treats all variables on an equal basis. This if

$$dz = 2dx - 3dy$$

at a giveb point, then

$$dx = \frac{1}{2}dz + \frac{3}{2}dy$$

is the corresponding differential of x in terms of y and z .

An important practical application of the theorem is that in order to compute partial derivatives, one can first compute differentials, pretending that all variables are functions of a hypothetical single variable (for example, t), so that *all the rules of ordinary differential calculus apply*. From the resulting differential formula, one can obtain all partial derivatives desired.

EXAMPLE 1 If $z = \frac{x^2 - 1}{y}$, then

$$dz = \frac{2xydx - (x^2 - 1)dy}{y^2}$$

by the quotient rule. Hence

$$\frac{\partial z}{\partial x} = \frac{2x}{y}, \quad \frac{\partial z}{\partial y} = \frac{1 - x^2}{y^2}.$$

EXAMPLE 2 If $r^2 = x^2 + y^2$, then $rdr = xdx + ydy$, whence

$$\left(\frac{\partial r}{\partial x}\right)_y = \frac{x}{r}, \quad \left(\frac{\partial r}{\partial y}\right)_x = \frac{y}{r}, \quad \left(\frac{\partial x}{\partial r}\right)_y = \frac{r}{x}, \quad \text{and so on.}$$

EXAMPLE 3 If $z = \text{atan} y/x$, ($x \neq 0$), then

$$dz = \frac{1}{1 + \left(\frac{y}{x}\right)^2} d\left(\frac{y}{x}\right) = \frac{xdy - ydx}{x^2 + y^2}$$

and hence

$$\frac{\partial z}{\partial x} = \frac{-y}{x^2 + y^2}, \quad \frac{\partial z}{\partial y} = \frac{x}{x^2 + y^2}.$$

D.2 The General Chain Rule

On occasion, one deals with two sets of functions:

$$\begin{aligned}
 y_1 &= f_1(u_1, \dots, u_p) \\
 \dots &\quad \dots \\
 y_m &= f_m(u_1, \dots, u_p)
 \end{aligned}
 \tag{D.7}$$

and

$$\begin{aligned}
 u_1 &= g_1(x_1, \dots, x_n) \\
 \dots &\quad \dots \\
 u_p &= g_p(x_1, \dots, x_n)
 \end{aligned}
 \tag{D.8}$$

If one substitutes the functions (D.8) in the functions (D.7), one obtains composite functions

$$\begin{aligned}
 y_1 &= f_1(g_1(x_1, \dots, x_n), \dots, g_p(x_1, \dots, x_n)) = F_1(x_1, \dots, x_n) \\
 \dots &\quad \dots \quad \dots \\
 y_m &= f_m(g_1(x_1, \dots, x_n), \dots, g_p(x_1, \dots, x_n)) = F_m(x_1, \dots, x_n)
 \end{aligned}
 \tag{D.9}$$

Under the appropriate hypotheses, one can obtain the partial derivatives of these composite functions by chain rules, as in the previous section:

$$\frac{\partial y_i}{\partial x_j} = \frac{\partial y_i}{\partial u_1} \frac{\partial u_1}{\partial x_j} + \dots + \frac{\partial y_i}{\partial u_p} \frac{\partial u_p}{\partial x_j} \quad (i = 1, \dots, m, \quad j = 1, \dots, n). \tag{D.10}$$

The formulas (D.10) can be expressed concisely in matrix language. The partial derivatives $\partial y_i / \partial x_j$ are the entries in the $m \times n$ matrix

$$\left(\frac{\partial y_i}{\partial x_j} \right) = \begin{bmatrix} \frac{\partial y_1}{\partial x_1} & \frac{\partial y_1}{\partial x_2} & \dots & \frac{\partial y_1}{\partial x_n} \\ \dots & \dots & \dots & \dots \\ \frac{\partial y_m}{\partial x_1} & \frac{\partial y_m}{\partial x_2} & \dots & \frac{\partial y_m}{\partial x_n} \end{bmatrix}. \tag{D.11}$$

This is the Jacobian matrix of the mapping (D.9). The formulas (D.10) involve two other Jacobian matrices:

$$\left(\frac{\partial y_i}{\partial u_j}\right) = \begin{bmatrix} \frac{\partial y_1}{\partial u_1} & \cdots & \frac{\partial y_1}{\partial u_p} \\ \cdots & \cdots & \cdots \\ \frac{\partial y_m}{\partial u_1} & \cdots & \frac{\partial y_m}{\partial u_p} \end{bmatrix} \quad \left(\frac{\partial u_i}{\partial x_j}\right) = \begin{bmatrix} \frac{\partial u_1}{\partial x_1} & \cdots & \frac{\partial u_1}{\partial x_n} \\ \cdots & \cdots & \cdots \\ \frac{\partial u_p}{\partial x_1} & \cdots & \frac{\partial u_p}{\partial x_n} \end{bmatrix}. \quad (\text{D.12})$$

The chain rules (D.10) state that the product of the last two Jacobian matrices equals the previous one:

$$\left(\frac{\partial y_i}{\partial x_j}\right) = \left(\frac{\partial y_i}{\partial u_j}\right)\left(\frac{\partial u_i}{\partial x_j}\right). \quad (\text{D.13})$$

This equation is called the *general chain rule*. It includes all the rules of the previous section.

EXAMPLE 1 Let $y_1 = u_1 u_2 - u_1 u_3$, $y_2 = u_1 u_3 + u_2^2$, $u_1 = x_1 \cos x_2 + (x_1 - x_2)^2$, $u_2 = x_1 \sin x_2 + x_1 x_2$, $u_3 = x_1^2 - x_1 x_2 + x_2^2$. Then, by (D.13),

$$\left(\frac{\partial y_i}{\partial x_j}\right) = \begin{bmatrix} u_2 - u_3 & u_1 & -u_1 \\ u_3 & 2u_2 & u_1 \end{bmatrix} \cdot \begin{bmatrix} \cos x_2 + 2(x_1 - x_2) & -x_1 \sin x_2 - 2(x_1 - x_2) \\ \sin x_2 + x_2 & x_1 \cos x_2 + x_1 \\ 2x_1 - x_2 & 2x_2 - x_1 \end{bmatrix}.$$

On the right-hand side, u_1 , u_2 , u_3 can be expressed in terms of x_1 , x_2 , and the two matrices can be multiplied. However, for many purposes it is sufficient to leave the result in indicated form. In particular, to obtain numerical values, one can substitute the appropriate values and multiply the matrices only as a last step. For example, for $x_1 = 1$, $x_2 = 0$, we obtain $u_1 = 2$, $u_2 = 0$, $u_3 = 1$ and hence

$$\left(\frac{\partial y_i}{\partial x_j}\right) = \begin{bmatrix} -1 & 2 & -2 \\ 1 & 0 & 2 \end{bmatrix} \begin{bmatrix} 3 & -2 \\ 0 & 2 \\ 2 & -1 \end{bmatrix} = \begin{bmatrix} -7 & 8 \\ 7 & -4 \end{bmatrix};$$

that is to say, $\partial y_1 / \partial x_1 = -7$, $\partial y_1 / \partial x_2 = 8$, $\partial y_2 / \partial x_1 = 7$, and $\partial y_2 / \partial x_2 = -4$.

Differentials and the chain rule. If we take differentials in Eqs. (D.7) and (D.8), we obtain the equations

$$\begin{aligned} dy_1 &= \frac{\partial y_1}{\partial u_1} du_1 + \dots + \frac{\partial y_1}{\partial u_p} du_p, \\ &\dots \qquad \dots \\ dy_m &= \frac{\partial y_m}{\partial u_1} du_1 + \dots + \frac{\partial y_m}{\partial u_p} du_p, \end{aligned} \tag{D.14}$$

and

$$\begin{aligned} du_1 &= \frac{\partial u_1}{\partial x_1} dx_1 + \dots + \frac{\partial u_1}{\partial x_n} dx_n, \\ &\dots \qquad \dots \\ du_p &= \frac{\partial u_p}{\partial x_1} dx_1 + \dots + \frac{\partial u_p}{\partial x_n} dx_n. \end{aligned} \tag{D.15}$$

In (D.14), du_1, \dots, du_p are arbitrary increments $\Delta u_1, \dots, \Delta u_p$, whereas in (D.15) they are functions of the arbitrary increments $dx_1 (= \Delta x_1), \dots, dx_n (= \Delta x_n)$. However, we know from Section D.1 that the relationships are the same no matter how we interpret the differentials. We can write these equations in matrix form:

$$\begin{bmatrix} dy_1 \\ \dots \\ dy_m \end{bmatrix} = \begin{pmatrix} \partial y_i \\ \partial u_j \end{pmatrix} \begin{bmatrix} du_1 \\ \dots \\ du_p \end{bmatrix} \qquad \begin{bmatrix} du_1 \\ \dots \\ du_p \end{bmatrix} = \begin{pmatrix} \partial u_i \\ \partial x_j \end{pmatrix} \begin{bmatrix} dx_1 \\ \dots \\ dx_n \end{bmatrix}. \tag{D.16}$$

If we eliminate the vector $\text{col}(du_1, \dots, du_p)$ in these equations, we obtain

$$\begin{bmatrix} dy_1 \\ \dots \\ dy_m \end{bmatrix} = \begin{pmatrix} \partial y_i \\ \partial u_j \end{pmatrix} \begin{pmatrix} \partial u_i \\ \partial x_j \end{pmatrix} \begin{bmatrix} dx_1 \\ \dots \\ dx_n \end{bmatrix} \tag{D.17}$$

or

$$dy_1 = \left(\frac{\partial y_1}{\partial u_1} \frac{\partial u_1}{\partial x_1} + \dots + \frac{\partial y_1}{\partial u_p} \frac{\partial u_p}{\partial x_1} \right) dx_1 + \left(\frac{\partial y_1}{\partial u_1} \frac{\partial u_1}{\partial x_2} + \dots \right) dx_2 + \dots$$

and so on. From these equations we can read off $\partial y_1 / \partial x_1$, $\partial y_1 / \partial x_2$, Clearly, the results are the same as (D.10) or (D.13). Thus (D.17) can be termed the *general chain rule in differential form*.

Appendix E

INTEGRAL OF TRANSFER FUNCTIONS¹

For stable linear systems with transfer functions $H_n(\omega)$ of the form

$$H_n(\omega) = \frac{b_0 + (i\omega)b_1 + (i\omega)^2 b_2 + \dots + (i\omega)^{n-1} b_{n-1}}{a_0 + (i\omega)a_1 + (i\omega)^2 a_2 + \dots + (i\omega)^n a_n} \quad (\text{E.1})$$

The integral I_n of the complex modulus squared, $|H_n(\omega)|^2$,

$$I_n = \int_{-\infty}^{\infty} |H_n(\omega)|^2 d\omega \quad (\text{E.2})$$

is given by

$$I_1 = \pi \frac{b_0^2}{a_0 a_1} \quad n = 1 \quad (\text{E.3})$$

$$I_2 = \pi \frac{a_0 b_1^2 + a_2 b_0^2}{a_0 a_1 a_2} \quad n = 2 \quad (\text{E.4})$$

$$I_3 = \pi \frac{a_0 a_3 (2b_0 b_2 - b_1^2) - a_0 a_1 b_2^2 + a_2 a_3 b_0^2}{a_0 a_3 (a_0 a_3 - a_1 a_2)} \quad n = 3 \quad (\text{E.5})$$

1. From James, Nichols and Phillips (1947). Also found in [Skelton, 1989].

$$I_4 = \pi \left\{ \left[\frac{a_0 b_3^2 (a_0 a_3 - a_1 a_2) + a_0 a_1 a_4 (2b_1 b_3 - b_2^2)}{a_0 a_4 (a_0 a_3^2 + a_1^2 a_4 - a_1 a_2 a_3)} \right] \right. \\ \left. + \left[\frac{-a_0 a_3 a_4 (b_1^2 - 2b_0 b_2) + a_4 b_0^2 (a_1 a_4 - a_2 a_3)}{a_0 a_4 (a_0 a_3^2 + a_1^2 a_4 - a_1 a_2 a_3)} \right] \right\} \quad n = 4 \quad (\text{E.6})$$